MASTER THESIS IN ENVIRONMENTAL CHEMISTRY AND RENEWABLE ENERGY

Hydrothermal liquefaction of *Nannochloropsis Gaditana* and *Phaeodactylum Tricornutum* in mixture: a systematic study of process variables and analysis of the product fractions

By
Kristine Lauve Irgens

Institute of Chemistry
University of Bergen
June 2022

ABSTRACT

Nowadays, we see a global shift toward cleaner energy from green energy sources, due to the environmental concerns regarding the use of fossil fuels and GHG emissions [1]. The production of biofuels for the substitution of conventional motor fuels has received much attention in this context. Microalgae have been identified as a feasible feedstock for HTL biofuel production as they do not require high-quality agricultural conditions to grow or any of the other disadvantages associated with the use of first and second-generation biofuels, including having greater photosynthetic efficiency, greater CO_2 fixation potential, higher growth rate, and greater biomass productivity [2], [3]. This allows for a greater yield of renewable, sustainable, and carbon-neutral sources of biofuels, capable of meeting the global demand for transport fuels [4]. Various types of biomass have shown promising results in terms of energy densities, chemical compositions, and combustion performances, similar to that of petroleum liquid fuels [4], [5]. However, the production of biofuels that can be directly applicable for transport fuels has yet to be found [6]. Consequently, an upgrading of bio-oils is necessary to produce a liquid product that can be used as liquid fuel or chemical feedstocks in various applications [7].

This thesis highlights the production of renewable biofuels by hydrothermal liquefaction (HTL) of algal biomass and evaluates the production of potential high-value platform chemicals for different industries to boost sustainability, reduce production costs and increase the industrial scale. The effects of the hydrothermal liquefaction (HTL) conditions, such as temperature, holding time, hydrogen-donor, and catalyst, on product yields were investigated for the two microalgae species, *Nannochloropsis gaditana*, and *Phaeodactylum tricornutum*, in mixture. Experiments were conducted using a non-stirred, 25 cm^3 volume batch reactor.

Fractional factorial designs were set up to explore the effect of selected experimental factors on the amount and composition of the products. In the first pilot series, Pilot series 1, HTL of the mixed algae culture was performed at different temperatures (280-380℃), holding times (2-6 hours), with or without catalyst (1 M, KOH), and with or without concentrated formic acid. The three experimental variables selected – based on the findings from Pilot series 1 – in Pilot series 2 were time (2-6 hours), temperature (220-280℃), and with or without concentrated formic acid. Pilot Series 3 was conducted, using the same experimental condition as in P1, but without catalyst. To assess the best strategy for utilization of the algal feedstock and HTL-products, quantitative and qualitative analysis methods are used such as elemental analysis, GC-MS, and IR.

Keywords: Algae biomass, hydrothermal liquefaction (HTL), biofuel, microalgae, algal lipid.

ACKNOWLEDGMENTS

First and foremost, I would like to thank my supervisor Tanja Barth for letting me take part in the construction of this project and for her invaluable guidance and support throughout this thought-provoking, inventive, and challenging journey.

I would like to give special gratitude to my co-supervisor, Stian Hersvik Hegdahl, who taught me about HTL of biomass and always being available whenever I needed help.

Thanks to Johanne Fjellanger for providing help with and around EA and thanks to Cecilie Sævdal Dybsland and Solmaz Ghoreishi for their help with the GC-MS apparatus. I would also like to thank the staff of the Department of Chemistry.

A special thank you to the research group and friends at the university for providing a nice and social working area, where help and support have been provided on both professional and personal levels whenever needed.

Lastly, I want to thank my beloved parents, my dearest Daniel, and his family, who have supported me along the way and never doubted my abilities. You all followed me through my highest and lowest points, and yet never doubted my abilities – not even when I doubted them myself. Without your love and support, this journey would never have been possible.

Thank you

Kristine Lauve Irgens

Bergen, June 2022

ABBREVIATION

BSTFA	Bis(trimethylsilyl)trifluoroacetamide
DAF	Dry ash free
DCM	Dichloromethane
EA	Elemental analysis
EtOAc	Ethyl acetate
FA	Formic acid
FT	Fourier Transform
GC	Gas chromatography
GHG	Greenhouse gas
HTL	Hydrothermal liquefaction
IR	Infrared spectroscopy
IS	Internal standard
MS	Mass spectrometry
NIST	National Institute of Standards and Technology
P1	Pilot Series 1
P2	Pilot Series 2
P3	Pilot Series 3
PCA	Principal component analysis
PLS	Partial Least-Square Regression
SE	Soxhlet extraction
TOC	Total Organic Carbon
TS	Total solid
VS	Volatile solid
Wv	Loss of ignition

CONTENTS

1.0 INTRODUCTION

This chapter gives an overview of the current and future global fuel and environmental situation, and the utilization situation of algal biomass at present, including relevant literature for HTL optimization of bio-oil from microalgae biomass.

1.1 CURRENT AND FUTURE ENERGY SITUATION

There is a consensus that high levels of atmospheric CO_2 cause greenhouse effects, due to the absorption and emission of radiation within the thermal infrared region [8]–[10]. Growth in anthropogenic greenhouse gas (GHG) emissions is one of the current greatest global challenges. By 2019, the largest growth in absolute emissions across all groups of GHGs occurred in CO_2 from the combustion of fossil fuels and industry (Figure 1.1-a) [11]. Almost 88% of the global primary energy used by humans currently derives from conventional fossil fuels (coal, petroleum, and natural gas), and the energy demand continues to increase, due to the rapid growth in human population and economic developments [4], [5], [12]. While the depletion of these finite unsustainable global resources is not a pressing issue in near future, their use is the leading cause of global warming and other major environmental problems [4], [12]. In an effort to stop the atmospheric CO_2 concentration from further increasing and to combat climate change, the Paris Agreement of the United Nations Framework Convention on Climate Change (UNFCC) was established in December 2015. This agreement was initially signed by 194 countries, wherein it was agreed to keep "global temperature rise this century well below 2 degrees Celsius above pre-industrial levels and to pursue efforts to limit the temperature increase even further to 1.5 degrees Celsius" [13], [14]. The global concern relating to the use of fossil fuels has urged the search for clean, sustainable, and renewable energy solutions, with the Paris Agreement as a foundation [5]. The global economy presently relies on carbon-based energy to operate, from generating plastics and fertilizers, to provide the energy required for lighting, heating, and commuting [15]. Renewable energy options, such as solar and wind power, play a key role in solving the global climate crisis, but cannot directly be used to produce carbon-based fuels and chemicals [16]. Therefore, biofuels from different types of biomass have attracted considerable interest worldwide as a viable substitution for fossil fuels concerning cost, renewability, and environmental issues [4], [12]. Biomass is considered an abundant and approximately carbon-neutral resource, as the carbon in biomass is obtained from atmospheric CO_2. By circulating carbon to and from the biosphere through energy generation systems in the form of biomass, the total atmospheric CO_2 inventory is close to neutral. Biomass is also an abundant energy source, available in most countries, and its application may diversify the fuel-supply in many situations [17]. Considering the ever-increasing need for carbon-based fuels and chemicals, biomass utilization is very important to allow a more secure energy supply and decarbonized sustainable future [1], [17].

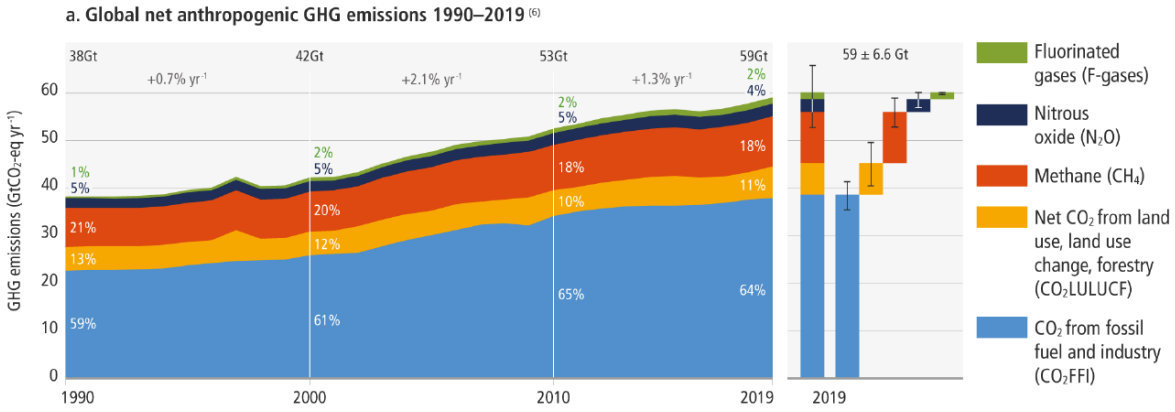

Figure 1.1-a: Global net anthropogenic GHG emissions [$GtCO_2$-eq yr^{-1}] 1990-2019. This figure is a panel from the IPCC Sixth Assessment Report (AR6) "Climate Change 2022 – Mitigation of Climate Change" [11].

1.2 BIOMASS AND CURRENT PRODUCTION OF BIOFUELS

1.2.1 BIOMASS

The term "biomass" is broadly defined as any organic material, produced by a living organism, that are available on a renewable basis. Biomass can be classified as primary and secondary biomass, where primary biomass comes directly from terrestrial plants, animals, and aquatic algae. Secondary biomass is organic waste produced from primary biomass, such as agricultural solid waste and wood residue [16]. Biomass is considered as a highly complex mixture of organic and inorganic (ash) materials. "Ash" is the general term for the inorganic residue remaining from biomass-combustion [16]. The degree of complexity of the bio-oils depends on the nature of the feedstock, which often varies by location and season [18].

Van Krevelen diagram has been used widely to classify the change of biomass composition to coal during thermochemical decomposition. This method is based solely on the change in atomic H/C vs. O/C ratios of the molecular compositions of solid fuels [1]. Classification according to its atomic ratio allows for interpretation of correlation of its energy density and heating value. A Van Krevelen diagram for various fuels is shown in Figure 1.2-a. Comparisons of biomass with coal shows a substantially higher proportion of oxygen and hydrogen, compared with carbon. This reduces the energy value of the fuel, owing to the lower energy obtained in C-O and C-H bonds, than in C-C bonds [17]. Hence, fuels with high O/C ratios have lower heat of combustion. Fuels with higher O/C ratios also obtain a higher CO_2 emission per amount of energy released, which is not in accordance with the Paris Agreement to reduce the CO_2 emissions [16]. Choosing a suitable type of biomass and conversion method are key factors to produce biofuels of good quality, in terms of energy density and heating value.

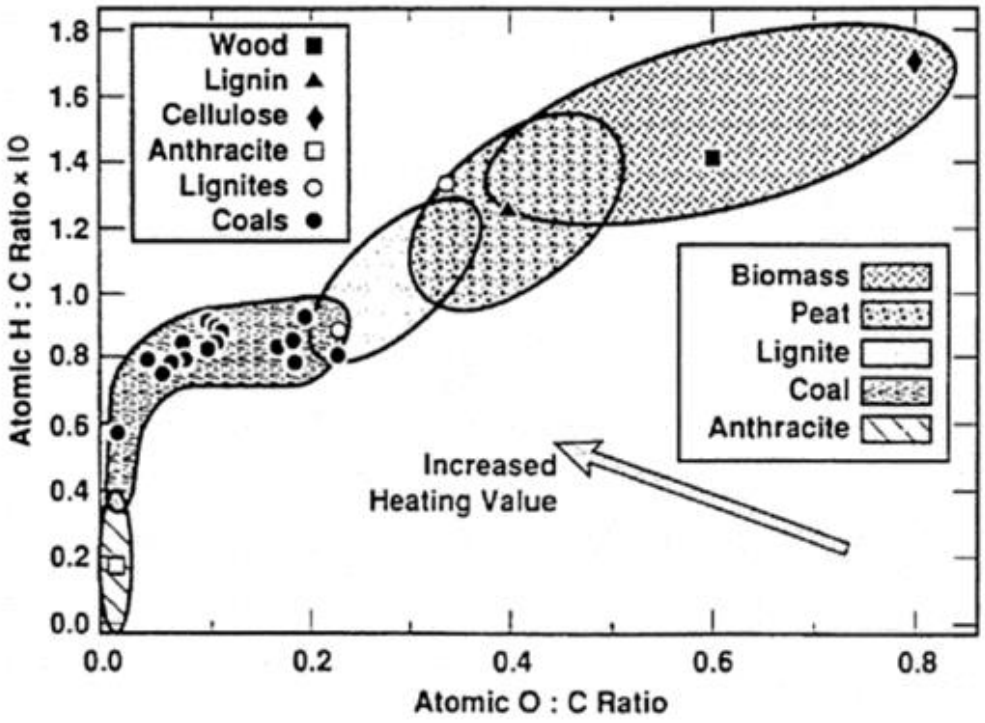

Figure 1.2-a: The Van Krevelen diagram for various solid fuels (van Loo S. and Koppejan J., 2012) [19], [20].

1.2.2 PRODUCTION OF BIOFUELS

Biofuels can be generated from numerous biodegradable and sustainable biomass feedstocks through biochemical and thermochemical processes, including biological digestion [16]. Biofuels are usually categorized into first-, second-, and third-generation biofuels relating to the type of biomass used. First-generation biofuels are largely based on edible food resources, such as corn and soybean, second-generation biomass are produced from non-edible food residues (e.g., wood processing wastes), while third generation biofuels derives from algae, sewage sludge, and municipal solid wastes [21]. Figure 1.2-b gives a summary of the current conversion techniques for utilizing and converting biomass into different types of renewable energy supplies [22]. The biomass moisture content is usually the dominant factor that dictates the most economically suited form of energy conversion process [17]. Biomass with high moisture content is generally used in aqueous conversion processes, such as fermentation and direct liquefaction, while low-moisture biomass (e.g., wood residues) is more suitable in gasification, pyrolysis, or combustion. A pre-drying step is sometimes included, to reduce the moisture content of biomass, allowing the use of initially high-moisture biomass in the latter conversion processes. However, aqueous processing is needed when the energy for drying are particularly large compared to the energy content of the biofuels produced [17].

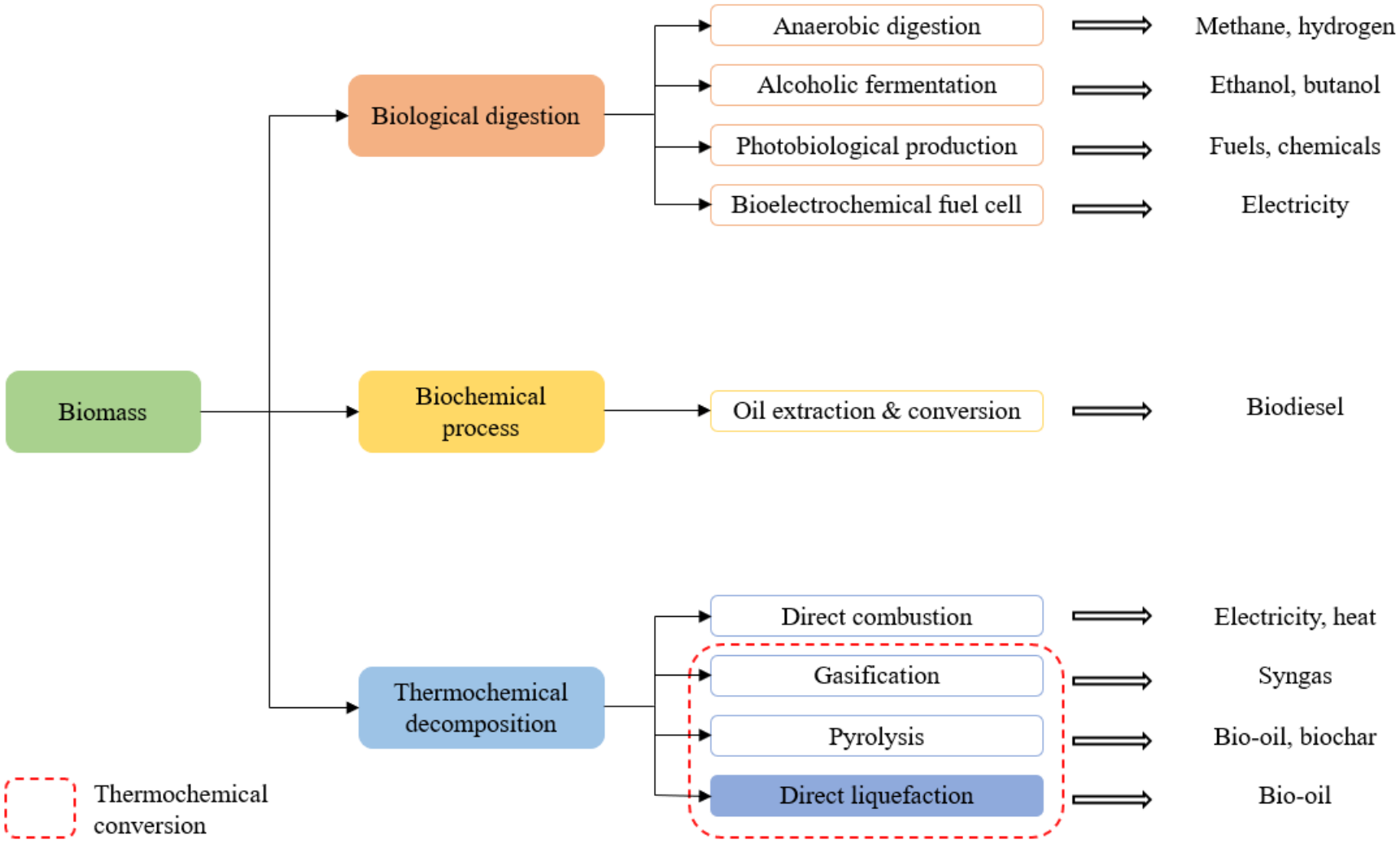

Figure 1.2-b: A schematic overview of current biomass conversion techniques and products. Adapted from ref. [22]. *Direct liquefaction is highlighted (blue color) in this figure, to show that hydrothermal liquefaction belongs to this thermochemical conversion technique.*

Various feedstocks have produced biofuels with similar energy densities, chemical compositions, and combustion performances as petroleum liquid fuels [4], [5]. However, current production of biofuels are not directly applicable as liquid fuel for transport and needs an upgrading [6], [7]. This upgrading of biofuels is often associated with high production costs. Moreover, the technological improvements in the exploration of fossil fuels have resulted in lower production costs over the past decades, and subsequently, negatively affected the growth of renewable energy resources, including biofuels [16].

1.2.3 ALGAE-BASED BIOFUELS

Several crucial criteria must be addressed for biofuels to be able to replace fossil fuels in near future. Firstly, the biofuels must be economically competitive with petroleum fuels. Secondly, the production of biofuels should require minimal water and land use. Thirdly, the biofuels need to be able to improve air quality (e.g., mitigate CO_2 emissions) [5]. The principal substitution of fossil fuels currently applied are of first- and second-generation biofuels but their sustainability has been questioned by their competition with edible products, including substantial consumption of arable land and water resources. For this reason, biofuels from feedstocks of non-edible products that do not compete with the cultivation of food crops, are highly desirable [16]. Third-generation biofuels derived from cultivated aquatic feedstocks, such as algae, have received much attention in this context. Aquatic algal feedstocks, avoids many of the restrictions related to the use of first- and second-generation feedstocks, since they do not directly compete with edible crops for arable land and consumes less water compared to land crops. Many species of algae are even capable of robust growth in wastewater, thereby reducing freshwater usage even further [23], [24]. The fact that they grow in aqueous mediums, makes them also easy to handle and harvest [25]. Another advantage of using these third-generation feedstocks is that the cultivation process is not seasonal and can be carried out nearly year-round [26]. In addition, these aquatic organisms exhibit greater photosynthetic efficiency, greater CO_2 fixation potential, higher growth rate and greater biomass productivity, compared with first- and second-generation feedstocks [2], [24]–[29]. This allows for a greater yield of products and bioactive compounds accumulation, such as carbohydrates, proteins, and lipids [8], [25], [28]. Algae biofuels are also non-toxic, highly biodegradable, and contain no sulfur [24]. These advantages make algae feedstocks especially suitable for the production of advanced liquid biofuels [5], [16]. However, there are some limitations and challenges regarding the production of algae biofuel that remains and must be overcome to upgrade the technology to an industrial level. The main challenges with current conversion methods used for the production of algae biofuels are that they are more intricate, and economically expensive, compared to fossil fuels and even biofuels from other feedstocks (e.g., lignocellulosic biomass) [1], [16]. Yet, there is a potential ground for optimism based on the sustainability of this feedstock and the greater likelihood of new applications and products due to its diversity [16].

1.2.4 TYPES OF ALGAE

The word “algae” is a collective term and can be broadly divided into subgroups based on their habitat, as freshwater algae and seawater algae; and by size, as macro- and microalgae [12], [30]. Macroalgae or seaweeds are multicellular, large-sized algae, with roots, stems, and

leaves, which grow around the sea beds [12], [16]. They are usually divided into different algal species, based on their pigmentation, e.g., Rhodophyta (red algae), Phaeophyceae (brown algae), and Chlorophyceae (green algae) (Figure 1.2-c) [12], [16]. Seaweeds are currently used in the production of food and the extraction of hydrocolloids for food applications (e.g., as thickeners, emulsifiers, and dietary fibers.) [31]. Microalgae (microphytes) consist of a wide variety of microscopic single cells that may either be prokaryotic or eukaryotic [12]. The majority of microalgae species are eukaryotic [16], [24]. There are currently over 3000 different breeds of microalgae registered worldwide, with diversity greatly exceeding that of the terrestrial plants [16], [24]. The three most important classes of microalgae in terms of abundance are the Chlorophyceae (green algae), Chrysophyceae (golden algae) and the diatoms Bacillariophytes (Figure 1.2-c) [12], [16]. Microalgae are considered very robust aquatic organisms as they can tolerate a wide range of temperatures, salinities, and pH-values, in addition to different light intensities [12], [16]. Thus, these microorganisms can grow in a variety of aquatic habitats, including oceans, lakes, ponds, rivers, and even wastewater, either alone in a colony or in symbiosis with other organisms [12].

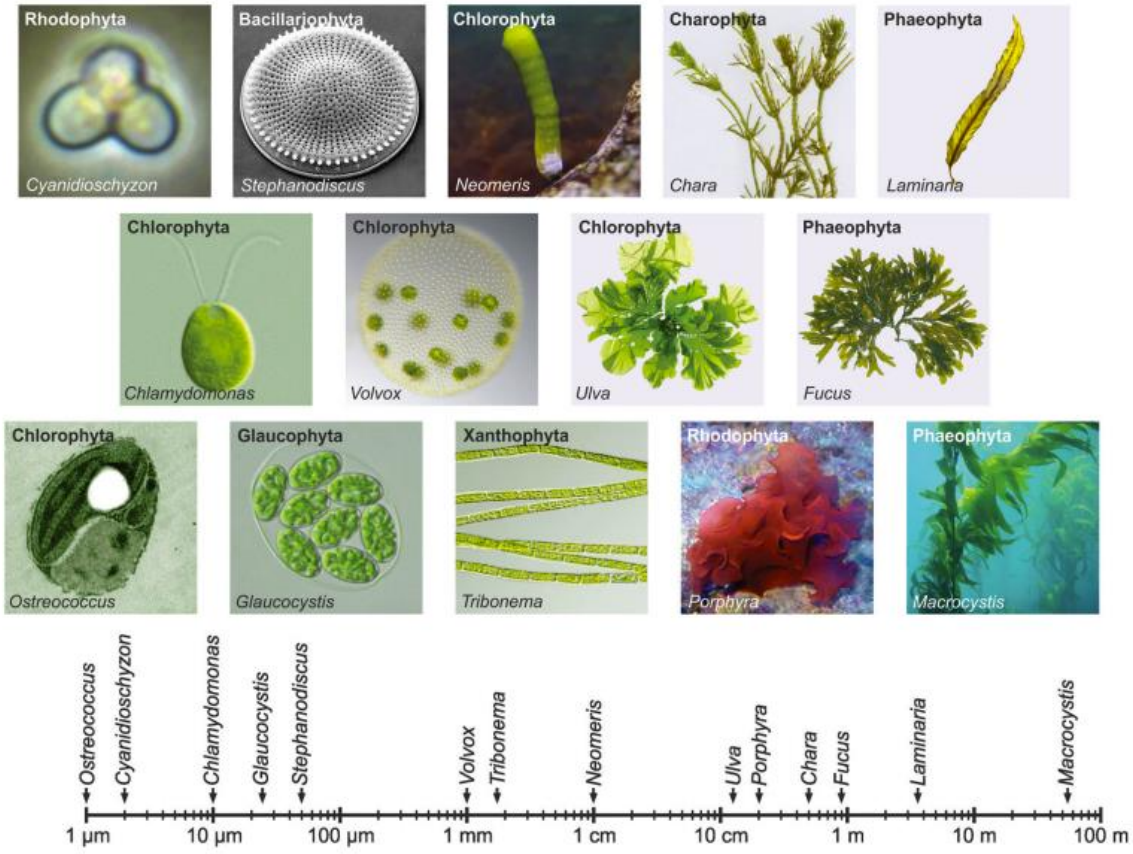

Figure 1.2-c: Spectrum of phenotypes and sizes of algal species (Hallmann A., 2015) [32] .

Microalgae are considered as “rich” raw materials, consisting of a wide range of bioproducts, including carbohydrates, lipids, proteins, pigments, vitamins, bioactive compounds, and antioxidants which can be utilized in various industries, including cosmetics, animal and human feed, and renewable energy [12], [33]. The main components of microalgae can be roughly classified into proteins, lipids, carbohydrates, and ash. The proportions of proteins, lipids and carbohydrates in these aqueous organisms are strongly dependent on the species of

algae [34]. Microalgae have starch, glycogen, and cellulose as sources of carbohydrates, where starch is one of the largest microalgal sources of carbon [26]. Many microalgae have been shown to produce more than 50% of their biomass as lipids, with much of this as triacylglycerols (TAGs) [28]. TAGs are the most common form of lipid in biological systems and can be hydrothermally cleaved into free fatty acids and glycerol [35]. TAGs are the starting material for high energy-dense biofuels such as biodiesel, green jet fuel, and green gasoline [28]. Biodiesel is currently produced from terrestrial and oleaginous crops and animal lipids and makes up just 3% of the global total diesel consumed [4]. A study done by Christi Y. (2007) showed that microalgae can obtain a 10-20 times higher average biodiesel production yield (in Lha^{-1}) compared to the yield obtained from oleaginous seeds and vegetable oils [29]. The production of biodiesel generally involves catalytic transesterification of extracted TAGs from lipids, with an alcohol to yield fatty acids methyl esters (FAMEs) [4]. About 50% of the required energy for this process is consumed during distillation and drying. If wet microalgal biomass can be directly used for the production of biofuels, without the need for drying, it will substantially reduce the energy demand and subsequently the cost of the process and development of the algae biofuel industry [4].

1.3 HYDROTHERMAL LIQUEFACTION

Hydrothermal liquefaction (HTL), also referred to as "hydrous pyrolysis", is one of the most promising thermochemical conversion techniques within direct liquefaction processes (Figure 1.2-b) for converting wet biomass into energy-dense liquid fuels, termed "biocrude" or "bio-oil". Together with the bio-oil product, HTL simultaneously generates an aqueous phase, a gaseous phase, and carbonaceous solids (coke) as co-products [2], [36]. A typical HTL process takes place in a closed reactor at moderate temperature (typically from 200-400℃) and high pressure (typically, 5-20 MPa), in the presence of water or water-containing solvents [37], [38]. Water is the most commonly used solvent in liquefaction as it is both cheap, eco-friendly, and in an abundant supply [4], [39], [40]. Water is also convenient as a solvent since a large number of raw materials naturally contains a substantial amount of water. During HTL, water is kept at a subcritical temperature and pressure, providing a single-phase environment for reactions that would otherwise occur in a multiphase system under conventional conditions [40]. This alters the physical and chemical properties of water such that it promotes both the degradation of the macromolecules – into smaller fragments of unstable molecules – and the repolymerization – into the larger compounds that make up bio-oils [4], [37], [41].

1.3.1 PROPOSED REACTION MECHANISM FOR HTL OF ALGAE

The compositional complexity of biomass feedstocks makes it difficult to determine the exact reaction mechanisms occurring during the HTL process. Considerable effort for understanding the HTL mechanism have been made through the years by many researchers [18]. As previously mentioned, the main components of algae can be roughly grouped into proteins, lipids, carbohydrates, and ash [34]. The high reactivity among the reaction intermediates, produced from the different components, makes the mechanism difficult to

predict. It has been suggested that the mechanism for HTL of algae takes place through a sequence of structural and chemical changes, which includes several reaction pathways[1]. A simplified reaction pathway scheme for HTL of algae is illustrated in Figure 1.3-a, and can in brief be described as followed [22], [42]:

In the first step, algae are depolymerized into fragments of lipids, proteins, and carbohydrates, then these fragments hydrolysis:

1) Lipid hydrolysis to produce fatty acids.
2) Protein hydrolysis to produce amino acids.
3) Carbohydrate hydrolysis to produce sugars.

In the next step, the fatty acids, amino acids, and sugars are decomposed:

4) Alkanes and alkenes are produced from fatty acids and organic acids through decarboxylation.
5) Oxygen removal from carboxyl groups in amino acids via decarboxylation to form carbon dioxide.
6) Deamination of amino acids to form ammonia.
7) Sugars are degraded to produce cyclic oxygenates.

In the following step, the reaction intermediates are recombined and decomposed:

8) Carboxyl group in amino acids or fatty acids reacts with the amine to produce N-heterocyclic compounds.
9) Amino acids react with reducing sugars to produce N, O-heterocyclic compounds via Maillard reaction.

Decarboxylation and deamination are two favorable reactions in HTL as they contribute to remove oxygen and nitrogen content from the biomass and thus improving the quality of the bio-oil products. However, deamination can also lead to the loss of hydrogen on the associated amine group [42].

[1] The order of the reaction steps described may vary, because the reactions in the hydrothermal liquefaction process of biomass is much more complex.

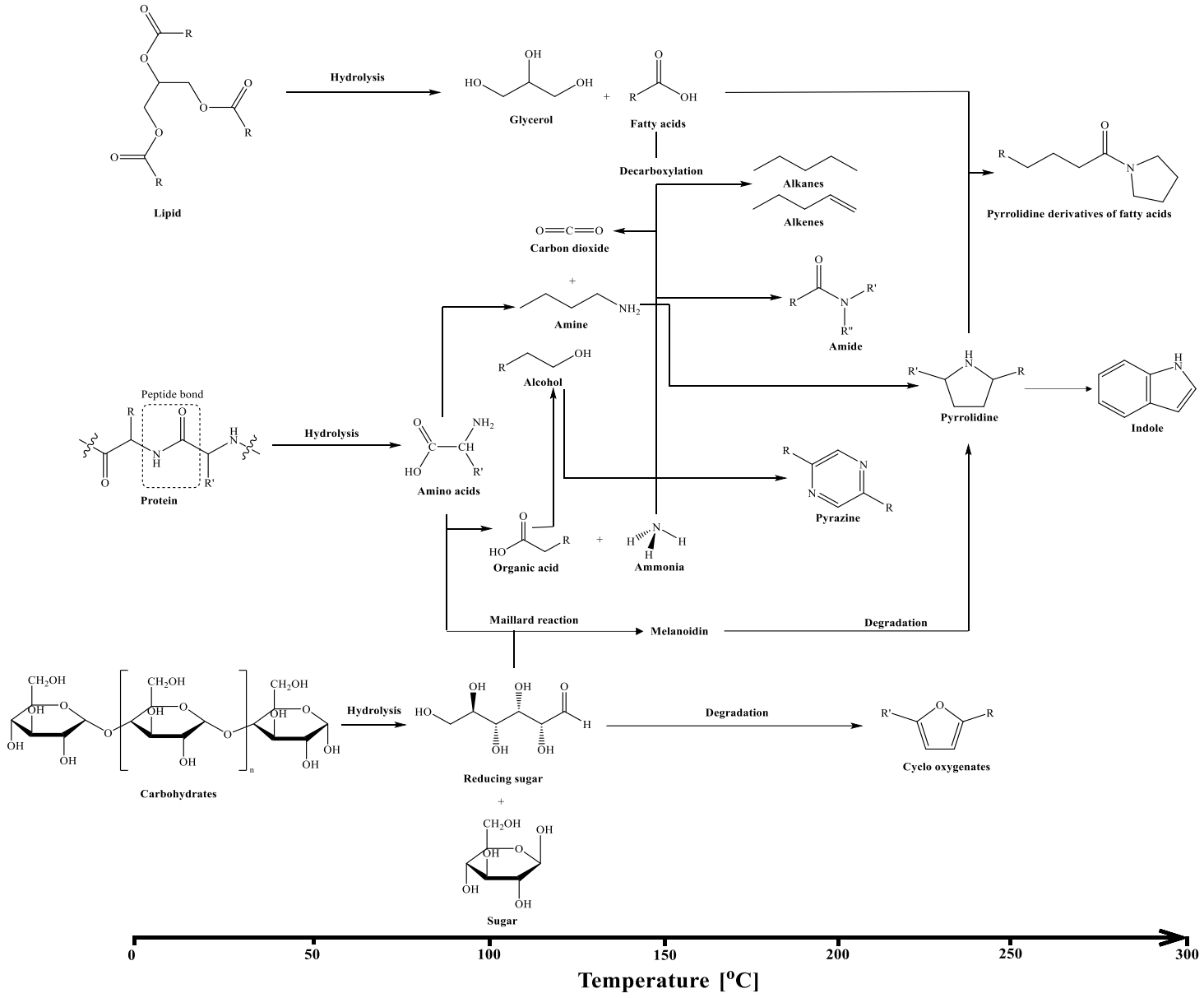

Figure 1.3-a: Schemtatic overview of proposed reaction pathway for HTL of microalgae. Adapted from ref. [22]*. The temperature axis represents the lowest temperature at which reactions take place.*

1.3.2 ADVANTAGES AND DISADVANTAGES FOR HTL OF ALGAE

Conversion of algae biomass into primary liquid fuels via HTL is a process with many advantages. First, wet biomass can be directly used in the liquefaction process, and thus, obviates energy and resource-intensive steps, such as drying and solvent extraction, that are common in other thermochemical conversion processes (e.g., pyrolysis and gasification) [2], [27], [41]. Second, the bio-oil yield from HTL is greater compared to biochemical processes for oil extraction and conversion methods because HTL utilizes the whole algae biomass, where not only lipids but also the proteins and carbohydrates in the algae are mostly converted into bio-oil [2]. Hence, HTL avoids the demand for promoting lipid accumulation, such as for the production of biodiesel from algal lipids [43]. Third, the nutrients in algae (such as nitrogen and phosphorus) are converted into the corresponding water-soluble salts

and acids in HTL, which can be reused for algae growth by aqueous phase recovery [2]. The energy-dense bio-oil product can potentially be used as a substitute for petroleum crudes. However, the direct substitution of HTL bio-oil for regular fossil fuels is severely limited due to quality drawbacks. A significant drawback with water as a solvent is that it yields a relatively viscous bio-oil with higher oxygen content compared to organic solvents such as ethanol, acetone, methanol, and toluene [41]. In addition to high water contents, other drawbacks that reduces the quality of the bio-oils are high content of heteroatoms (such as nitrogen and oxygen), high viscosity (caused by the abundance of long chain and complex molecules in the crude oil), low heating value, and high corrosiveness (high acidity) [7], [29], [43]. Consequently, an upgrading of bio-oil is generally necessary for improvements in bio-oil properties [7]. Studies have shown that the selection of feedstock, biomass loading, temperature, pressure, residence time (holding time), solvent, and catalysts are some of the main factors that affect the yield and quality of bio-oil [14], [37], [34]. In this thesis, the effect of some of these reaction parameters are investigated, including the addition of a hydrogen donor (formic acid), in an effort to enhance the performance and production of the HTL bio-oil from microalgae.

1.3.3 Relevant work on upgrading of bio-oil production

Kleinert and Barth (2008), established a novel conversion process of lignin to a high yield liquid biofuel with low oxygen content, called lignin-to-liquid (LtL) [45]. The LtL-process can be considered as a thermochemical solvolytic process, where both the depolymerization of lignin and oxygen removal by formation of water occurs in a single step. Formic acid was used for this process as a hydrogen donor. Several tests were conducted using a wide range of reaction conditions such as, temperature, duration (holding time), reactor size, and solvent combinations. They discovered that the formic acid, in addition to creating a reductive environment, assists in the depolymerization of the lignin structure, which results in higher oil yields [45]. The elemental composition and some physical properties of relevant products showed that the produced liquid biofuel obtained, among others, a high content of carbon (76-83 wt.%), relatively low oxygen content (5-10 wt.%), low ash content (0.05-0.1 wt.%), and high HHV values (35.5-44 MJ/kg). In addition, the LtL bio-oil are less polar and have solvent properties much like petroleum, making it fully miscible with petroleum-based fuels. Based on the elemental composition and physical properties of the LtL bio-oil, it was proposed that it would be suitable as a blending component for conventional motor fuels [45]. A report published in 2017, by Løhre et al. showed similar bio-oil yields (69.2-94.2 wt.%) from LtL conversion of lignin from spruce and pine, using different levels of formic acid as hydrogen donor and water as solvent under high temperatures (320-360℃) [46]. Temperature was shown to be the dominating reaction parameter for the structural composition of the LtL bio-oil, with a clear negative correlation with O/C ratio. The observations from the experiments showed that both experiments with high and low levels of formic acid did not achieve the highest bio-oil yields, which indicates that the amount of formic acid only needs to reach a sufficient level to induce depolymerization hand hydrogenation of the lignin. The study underlines the potential use of the LtL bio-oil as source of building blocks for the chemical and pharmaceutical industries [46].

Research has also been performed on feedstock that are more comparable to algae. Marrone et al. (2018) conducted HTL-conversion at 300-350℃ and 20 MPa of primary and secondary

sewage sludge, including digested solids [47]. The yields of bio-oil ranged from 25 to 37% on a dry, ash-free basis. The bio-oil composition and quality from primary and secondary sludge were similar to those generated from algae feedstocks (*Saccharina spp*. and *Nannochloropsis sp.*) and had about 80% of the HHV of petroleum crude [47]. Badrolnizam R.S et al. (2019) achieved bio-oil yield of 52% by HTL of sewage sludge at a temperature of 350℃ and holding time of 1 hour [47]. Paulsen M. (2019) and Ødegaard M. (2019) wrote two comparable theses on HTL of bio residues from sewage sludge, based on the LtL-method by Kleinert. M and Barth. T (2008) [45], [48], [49]. Both studies investigate the effects of water as reaction medium and how seasonal change of feedstock alters the yield and composition of the bio-oil and coke. In both studies, formic acid was used as both a hydrogen donor and reaction medium. The bio-oils generally had low H/C and low (O+N)/C ratios at high temperatures, where the latter indicates that better deoxygenation of the feedstock was achieved at higher temperatures. According to study by Paulsen M. the greatest bio-oil yield of 53.4% was achieved at 360℃ , with a 2-hour holding time, and with formic acid, while the greatest bio-oil yield (53.5%) by Ødegaard M. was obtained for the experiment run at 380℃, with a 2 hour holding time and with the addition of formic acid [48], [49]. Based on the results obtained from lignin and bio residues from sewage sludge, it is useful to investigate whether the LtL-method is suitable for the conversion of algae feedstock to bio-oil.

A study on decomposition of stearic acid (C_{17}-acid) (400℃, 25 MPa and 30 min) showed that decarboxylation of fatty acids could be enhanced in the presence of alkali hydroxide catalysts, such as NaOH and KOH [50]. The reaction conditions was compared to anhydrous pyrolysis of water-free stearic acid, where the it was revealed that hot compressed water helps to stabilize the fatty acids, and subsequently, suppresses the degradation process [50]. It is therefore worth investigating if catalytic decarboxylation of biomass will be favourable in alkaline conditions, during the HTL process of *Nannochloropsis Gaditana* and *Phaeodactylum Tricornutum*. KOH is chosen to represent the strong alkali being investigated for its catalytic effects on the bio-oils, in terms of yield and quality.

1.3.4 Relevant work on algal feedstock

This section addresses some of the relevant literature regarding the two microalgae species used in hydrothermal liquefaction in this thesis. The word “algae” will from here on, and throughout the rest of this thesis, refer to microalgae, unless otherwise specified.

Nannochloropsis Gaditana is a unicellular microalgal species, found in both marine and freshwater sources. The species is one of the six known members of the genus *Nannochloropsis* [26]. It is a microscopical spherical algae, with a cell diameter of about 2-5 μm [51]. Algae of *Nannochloropsis* differs from other microalgae in that they only contain chlorophyll *a* and completely lack chlorophyll *b* and chlorophyll *c*. This species is known for its ability to accumulate large amounts of lipids, specifically TAGs. On average, the lipid content ranges from 25-45 wt.%. Some studies have even reported lipid contents up to 54%, with a lipid productivity level of about 27.00 $mgL^{-1}day^{-1}$ [30]. For this reason, *Nannochloropsis sp.* is considered a suitable biomass for biofuel production [52].

Several studies on HTL of this genus have been investigated, especially in the last decade. Brown et al. (2010) performed hydrothermal liquefaction on *Nannochloropsis sp*., with a temperature range from 200 to 500℃ and a batch holding time of 1 hour. The highest bio-oil

yield of 43 wt.% was achieved at a moderate temperature of 350℃, with an estimated heating value close to petroleum crude oil of approximately 39 MJ/kg. The major components found in the bio-oils included phenol and its alkylated derivatives, heterocyclic N-containing compounds, long fatty acids, alkanes and alkenes, and derivatives of phytol and cholesterol [53]. Li et al. (2014) did a study on HTL-conversion, which focused on the effects of reaction temperature (220-300℃), retention time (30-90 min), and a total solid content (TS, 15-25% wt.) on the low-lipid high-protein microalgae *Nannochloropsis sp*. The highest biocrude yield was reported to 55 wt.% for *Nannochloropsis sp*. at 260℃, 60 min. The higher heating values (HHV) of the bio-oils were about 37 MJ/kg. The GC-MS revealed that the bio-oils mainly consisted of cyclic nitrogen compounds (C_5-C_{16}), straight and branched hydrocarbons (C_{15}-C_{33}), branched oxygenates, aromatic compounds, and heterocyclic compounds [54]. Sirong et al. (2020) did a study on the HTL-process of *Nannochloropsis sp.* and *Sargassum sp.*, under various reaction temperatures (260-340℃). The results showed that the highest bio-oil yield obtained from *Nannochloropsis sp*. were 54.11 wt.%, at 340℃. The maximum HHV was estimated to 37.88 MJ/kg. The GC-MS analysis of the bio-oils showed that Nannochloropsis sp. mainly contained N-heterocyclic compounds [55].

Phaeodactylum Tricornutum is the other microalgae species used in hydrothermal liquefaction in this thesis. *Phaeodactylum Tricornutum* is one of the most studied marine diatoms, because of its high biomass productivity (~235 $mgL^{-1}day^{-1}$). The typical compound biochemical composition of this microalgae is 30-70% proteins, 10-30% carbohydrates, and lipid contents from 20% to 30%. With this in mind, this species has a high scale-up potential to produce biofuels [56]. This diatom is also an atypical species because it is the only representative of the genus *Phaeodactylum* [57].

Only one relevant article was found on HTL conversion of this genus. Megía-Hervás et al. (2020) investigated the influence of reaction time on the production of bio-oil and elemental distribution, using a 1 L and 90 L bioreactor. The HTL production of biofuels were performed at temperature of 230℃ at three reaction times (0, 10, and 30 min) [56]. In this work, time 0 was considered when the photobioreactor reached the temperature setpoint. The highest yield of bio-oil (36.64% $\pm$ 4.93%) was obtained in the 1 L bioreactor at 10 min. However, the results showed that the bio-oil yields produced using the 1 L were significantly unaffected at different reaction times. The calculated HHV values of the bio-oils were about 38.27 MJ/kg. A significant decrease in the oxygen amount was observed in all of the bio-oils with respect to the biomass feedstock. The O/C ratios obtained (0.066-0.099) were lower than those obtained for biodiesel (0.11) and *N.gaditana*-derived bio-oil (0.28) [56].

2.0 SCOPE

Chapter 2 outlines the scope of this thesis, including problem definition, problem solution, and a brief review of related work.

2.1 PROBLEM DEFINITION

Currently, the greatest challenge in biofuel area is to produce renewable liquids that can directly be used as substitute or blend for petroleum fuels in motor fuels [45]. The

optimization of reaction conditions for the HTL process is important to obtain a high yield of biofuel with good quality. Currently, the production of algae-based biofuels generally involves catalytic transesterification of extracted lipids into biodiesel [4]. Compared to biodiesel production, which only extracts lipids from algae, hydrothermal liquefaction (HTL) utilizes the whole algae biomass – including the use of fast-growing species with low lipid content – and hence avoids the demand for promoting lipid growth [43]. This energy-dense bio-oil product can potentially be used as a substitute for petroleum crudes. Another possible approach could be to merge these two processes together for a broader exploitation/utilization of the algal feedstock, by extraction of lipids to produce biodiesel and production of other biofuels by HTL of the feedstock residues collected from the extraction.

To provide more information on the point presented above, this thesis investigates HTL of a microalgae feedstock, and the main objectives are listed below.

- Objective 1: Optimization of HTL conditions in terms of bio-oil yield and quality.
- Objective 2: Characterization of bio-oil produced by HTL.
- Objective 3: Comparison of bio-oil produced from feedstock residue and untreated feedstock.
- Objective 4: Evaluation of possible applications of feedstock and HTL-products.

2.2 PROBLEM SOLUTION

The objectives of this thesis are achieved by the following processes.

- A proximate analysis of the feedstock was performed prior to HTL-procedure for quality control.
- A pilot series, named Pilot Series 1, consisting of initial experiments was carried out to establish a HTL procedure with wet microalgae as feedstock.
- A second pilot series, Pilot Series 2, was constructed based on the results from Pilot Series 1 to further explore how the yield and quality of bio-oil changes in HTL conversion performed at lower temperatures and without catalyst present, compared to bio-oils from P1.
- Soxhlet extraction was performed for the extraction of lipids from the wet algal feedstock.
- A third pilot series, Pilot Series 3, was established to investigate if feedstock residues from lipid extraction is suitable for conversion to bio-oil by HTL. The reaction conditions for Pilot Series 3 were based on the experimental conditions in Pilot Series 1, but without the addition of catalyst, for comparison of bio-oil from treated and untreated feedstock.
- To assess the best strategy for utilization of the algal feedstock and HTL-products, quantitative and qualitative analysis methods are used such as elemental analysis, GC-MS, and IR.

2.2.1 EXPERIMENTAL DESIGN

Factorial designs allow the study of combined effect of the factors (or process/design parameters) on a response. A factorial design can either be full or fractional factorial, where a full factorial experiment consists of all possible combinations of levels for all factors. Fractional factorial designs consist only of the most important factors that influences critical quality characteristics of the responses, which allows for more efficient use of resources as it reduces the number of experimental tests [58]. The total number of experiments for k factors at n levels is n^k. In design for factors at 2-levels, the responses is assumed to be approximately linear over the range of the factor setting chosen [58].

A fractional factorial design was used in each of the pilot series to reduce the number of experiments to a fraction. In these designs, a high (+) and a low (-) level for each factor was selected, together with an intermediate center point (0).

For convenience, Pilot Series 1 is abbreviated to P1, Pilot Series 2 to P2, and Pilot Series 3 to P3 in most of the tables and other data collections. Each experiment is given a descriptive name code, based on the pilot series number and values of operational parameters. The name code is given in the following order: P.T.t.cat.FA., where P: Pilot series number; T: oven temperature in Celsius degrees; t: holding time in hours; cat.: with (KOH) or without (H2O) catalyst; FA: volume of formic acid added in milliliters. As an example, the name code for experiment "P1.280.2.H2O.0" implies that the experiment belongs to Pilot series 1 and that the experiment was run at 280℃ for 2 h, without (H2O) the addition of catalyst (i.e., just water) and without (0 mL) of formic acid.

3.0 METHODS AND EXPERIMENTAL PROCEDURES

Chapter 3 describes the algal feedstock, methods, instruments, and experimental procedures for this work. All laboratory work and data acquisition were conducted in laboratory facilities at the Department of Chemistry at the University of Bergen (UiB).

3.1 FEEDSTOCK

A large batch of frozen microalgae feedstock was provided by Dr. Dorinde Kleinegris, principal investigator of microalgae at NORCE (Norwegian Research Center AS). The feedstock is composed of the two species *Nannochloropsis Gaditana* and *Phaeodactylum tricornutum*, in unknown mixture ratio, collected from a cultivation done in 2019 at the National Algae pilot Mongstad (NAM). The cultivation had initially been done on *N. Gaditana* but was interrupted by contamination of *P. Tricornutumn*, which had started to take over the culture. The algal feedstock had been preserved in an airtight package in the freezer since the cultivation.

The feedstock was prepared by slow defrosting of the biomass in the fridge at 4℃ over two days and distributed into smaller batches of feedstock. Each batch of feedstock was then placed in the freezer for provisional preservation. Before the experimental workup, the

feedstocks were defrosted and stored in the refrigerator at 4℃ for 24 h prior to their use and were used within a two-month period.

3.2 PROXIMATE ANALYSIS: TS, VS, AND WV

3.2.1 DEFINITIONS AND FORMULAS

In this analysis, the quantity of total solids (TS), volatile solids (VS), and loss of ignition (Wv) in the algal feedstock was determined based on the weight differences in feedstock at elevated temperatures. Hence, TS, VS, and Wv are given by weight percentages (wt.%). TS is expressed as the dry matter (i.e., all inorganic and organic matter) in the wet feedstock sample and is calculated based on the weight ratio of the dried sample and the initial amount of the wet sample. VS represents the portion of volatiles (or organic matter) in the initial wet sample and is calculated as the weight difference between the amount of sample after drying and burning, and the initial amount of wet sample. Wv is an estimate of the total amount of dry organic matter that is burned in the sample and is measured as the weight difference between the dried sample and residue of ignition. The residue of ignition determines the proportion of inorganic material in the dry matter. The following equations are used to calculate the weight percentage of TS, VS and Wv, respectively:

$$TS\ [\%] = \frac{m_{Dry\ sample}}{m_{Wet\ sample}} \cdot 100\% \qquad (3.2\text{-}1)$$

$$VS\ [\%] = \frac{m_{Dry\ sample} - m_{Burned\ sample}}{m_{Wet\ sample}} \cdot 100\% \qquad (3.2\text{-}2)$$

$$Wv\ [\%] = \frac{m_{Dry\ sample} - m_{Burned\ sample}}{m_{Dry\ sample}} \cdot 100\% \qquad (3.2\text{-}3)$$

3.2.2 ABOUT

Proximate analysis of the feedstock was performed before HTL-procedure of Pilot series 1 (P1) for quality control. Proximate analysis of the feedstock was performed before the HTL-procedure of Pilot series 1 (P1) for quality control (Table….). Proximate analysis was done prior to Pilot Series 1 (P1), to determine the mass of total solids and moisture present in the wet raw material, together with the percentage of volatile solids on dry basis. The procedure was done with two parallels, using feedstock from two sample batches. The result from this analysis documents any inhomogeneity in the algae samples, in terms of the quantity of total solids (TS), volatile solids (VS), loss of ignition (Wv) and moisture. The procedure used in the proximate analysis of wet algal feedstock was based on standard protocol for TS and a calcination oven program elaborated by Erwan Le Roux – professor (Associate) at UiB – for VS and Wv. A sketch of the protocol done on the first batch (Feedstock 1) is shown in Figure 3.2-a.

3.2.3 EXPERIMENTAL PROCEDURE FOR DETERMINATION OF TS, VS, AND WV

This procedure briefly summarizes the method done for each batch of feedstock: Two crucibles were first washed with acetone and dried for 10 min at 100℃ to ensure that all the acetones had evaporated. The crucibles were numbered and weighed. Algae samples were

added to the crucibles and then weighed before heated. In the protocol, the algae samples were heated at 100℃ for 20 hours to remove all water content. Then, the samples were placed in a desiccator to cool to ambient temperature. The samples were weighed once again, and TS was calculated. After determining TS, the dry matter was heated to 540℃ for 10 hours in an ignition oven (5 hours heating time up to 540℃, 10 hours at 540℃ and 8 hours cooldown time). The samples were placed in a desiccator, before final weighing. VS was determined based on the weight difference between the amount of sample after drying and burning. The residues of ignition represent the inorganic material in the dry feedstock.

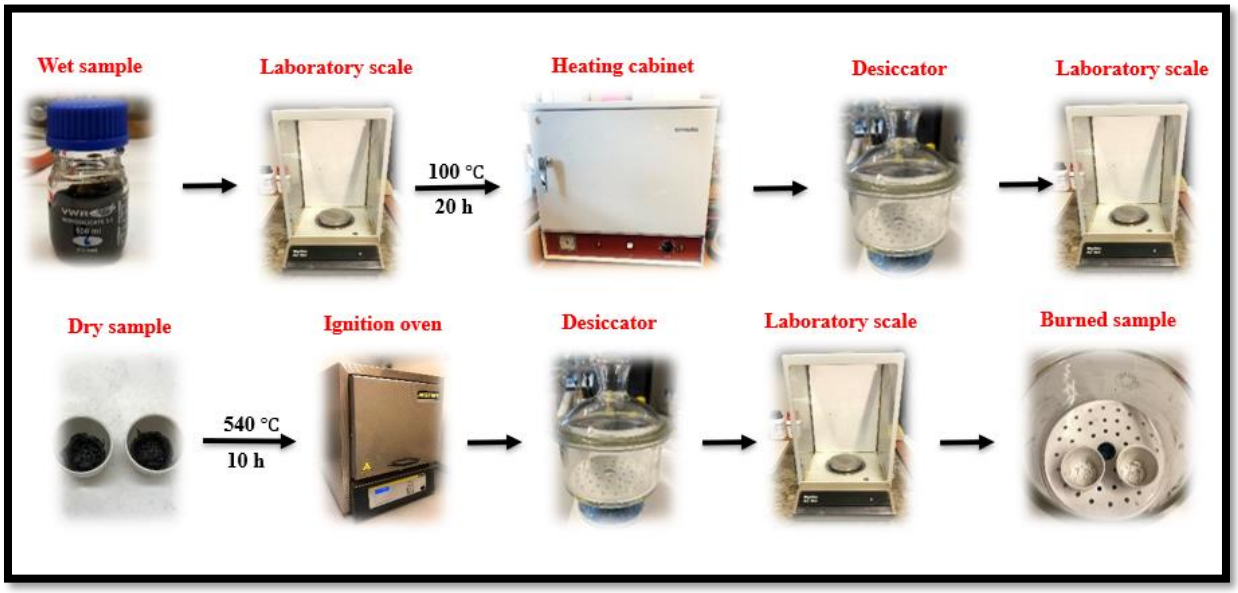

Figure 3.2-a: Procedure for determining TS, VS, and Wv of wet algal feedstock.

3.3 HTL APPARATUS AND PROCEDURE

3.3.1 DEFINITIONS AND FORMULAS

The yields of the HTL-products for the different experiments were calculated based on weight difference. The various calculations and concepts are defined here.

Coke is the term used for the solid phase that is recovered after HTL-process. This phase might also contain residues of unconverted feedstock, catalytic residues, ash and residues from batch reactor and filter after the experimental workup. The coke yield can be calculated based on the assumption that all inorganic material in feedstock ends up in the coke after HTL, in which the calculate of coke yield would be based on the proportion of dry organic matter in the feedstock [49], [59]. This assumption was shown to not agree with the results of calculate coke yields for the different pilot series as it resulted in negative yields of coke. Thus, the yield is calculated based on dry matter in the feedstock, shown in Eq. 3.3-3.

The liquid phase consists of two phases, an aquatic phase (Aq.ph.) and an organic phase (bio-oil). Water recycling is calculated as the amount of water collected in the HTL-process and is expressed as a percentage of water in the wet feedstock and the total amount of added water.

For comparison of coke yield, yield of bio-oil was calculated based on the proportion of dry matter in the feedstock (Eq. 3.3-4).

The quantity of gaseous products is both determined from the weight difference of the reactor before and after gas venting, and as a percentage of the total amount of formic acid (FA) added (Eq. 3.3-5).

The mass balance is expressed as the total amount of the weighed HTL-products (gas, coke, bio-oil, aq.ph.) as a percentage of the total amount of reactants added (Eq. 3.3-7).

$$TS\ [g] = \frac{m_{Feedstock} \cdot TS_{MV.}}{100\%} \quad (3.3\text{-}1)$$

$$Wv\ [g] = \frac{m_{Feedstock} \cdot Wv_{MV.}}{100\%} \quad (3.3\text{-}2)$$

$$Y_{Coke}[\%] = \frac{m_{Coke}}{m_{Dry\ matter}} \cdot 100\% \quad (3.3\text{-}3)$$

$$Y_{Oil}\ [\%] = \frac{m_{Oil}}{m_{Dry\ matter}} \cdot 100\% \quad (3.3\text{-}4)$$

$$Y_{Gas}\ [\%] = \frac{m_{Gas}}{m_{FA}} \cdot 100\% \quad (3.3\text{-}5)$$

$$Total\ [g] = m_{Feedstock} + m_{Water} + m_{Catalyst} + m_{FA} \quad (3.3\text{-}6)$$

$$Y_{Total}\ [\%] = \left(\frac{m_{Gas} + m_{Coke} + m_{Oil} + m_{Aq.ph}}{Total}\right) \cdot 100\% \quad (3.3\text{-}7)$$

3.3.2 MATERIALS AND REAGENTS

All the HTL experiments were conducted in a non-stirred, 25 mL volume batch reactor (Model 4742, Parr Instrument Company, Moline, USA) with self-sealing closures (Figure 3.3-a). The high-pressure vessel is made of type 316 stainless steel and has a maximum operating temperature of 350℃ and a maximum working pressure of 8500 psi (575 bar) [60]. The vessel comes with an alloy steel screw cap, which includes six cap screws to achieve the force needed for sealing on a flat, adaptable graphite gasket [60]. All the volumetric measurements were performed with mechanical pipettes (Eppendorf Research® Plus, Eppendorf).

Formic acid ((Sigma-Aldrich), puriss. p.a., ACS reagent, reag. Ph. Eur., ≥98%), together with catalyst, distilled water and wet algal feedstock, were used during the experimental workup of the HTL bio-oils. Formic acid was chosen due to its efficiency to act as a hydrogen donor [61]. The catalyst, a 1M KOH solution, was freshly prepared by dissolving KOH pellets (Sigma-Aldrich), puriss. p.a., reag. Ph. Eur., ≥85%) with deionized water. Ethyl acetate (EtOAc (Sigma-Aldrich), puriss. p.a., ACS reagent, reag. ISO, reag. Ph. Eur., ≥99.5% (GC)) was used as a solvent. Dry sodium sulfate (Na_2SO_4 (Sigma-Aldrich), ACS reagent, ≥99.0%, anhydrous, powder) was used as a drying agent.

Figure 3.3-a: Picture of the 25 mL volume batch reactor, both assembled (L) and dismantled (R).

3.3.3 HTL PROCEDURE FOR PRODUCTION OF BIO-OIL

The procedure is based on the established LtL-method as described in the report by Kleinert. and Barth (2008) [45]. The method have been investigated using different organic residues, such as lignocelluloses/lignin biomass and bio residues from wastewater in our research group at the University of Bergen [45], [48], [62], [63]. The workup protocol was the same for all the HTL experiments in order to ensure compatibility. For comparison between experiments, the biomass-loading and the total reactor volume was kept approximately constant in all the experimental series, by adjusting the volume of added solvent (water) to adjust for the absence of formic acid and/or catalyst. A flow diagram for the experimental workup of the HTL-procedure is given in Figure 3.3-b.

Briefly summarized, wet feedstock was loaded to a non-stirring reactor, with the addition of distilled water, formic acid and/or catalyst. The reactor was tightly sealed, keeping ambient air in the reactor headspace. Shortly after sealing, the reactor was heated in a preheated Carbolite Laboratory High-Temperature oven at a selected temperature. Holding time was set to start when the oven temperature had reached the selected temperature, after the reactor was placed in the oven. After heating, the reactor was slowly cooled down at ambient temperature for approximately 24 hours. The produced gas was vented via the top screw cap. The reactor was washed clean for solid and liquid products using ethyl acetate (EtOAc). The solid phase (coke) was separated from the liquid phases by two types of vacuum filtrations: first, with the use of a paper filter, through a Büchner funnel; second, using a glass filter. The coke collected from these two filtrations represents the total amount of coke in the sample. The coke was air-dried for approximately one hour before weighing. The coke was transferred from the filter papers to a sample glass and further air-dried for two days before final weighing. The aqueous phase was separated from the organic oil phase using a syringe and was stored in a sample glass, in the fridge. The organic phase was further dried over dry sodium sulfate (Na_2SO_4), under constant stirring, for one hour. The drying salt was shortly after removed by gravity filtration, using filter paper. The solvent fraction was evaporated (at ~ 40℃, ~ 200 mbar) on a rotary evaporator to recover the solvent-free bio-oil. The bio-oil was then extracted from the

rotary evaporating flask, using an additional solvent to wash clean the flask, to a sample glass. The diluted bio-oil sample was further dried under N_2 gas for ~24 h before final weighing. The percentage yield of oil and coke was determined by weighing.

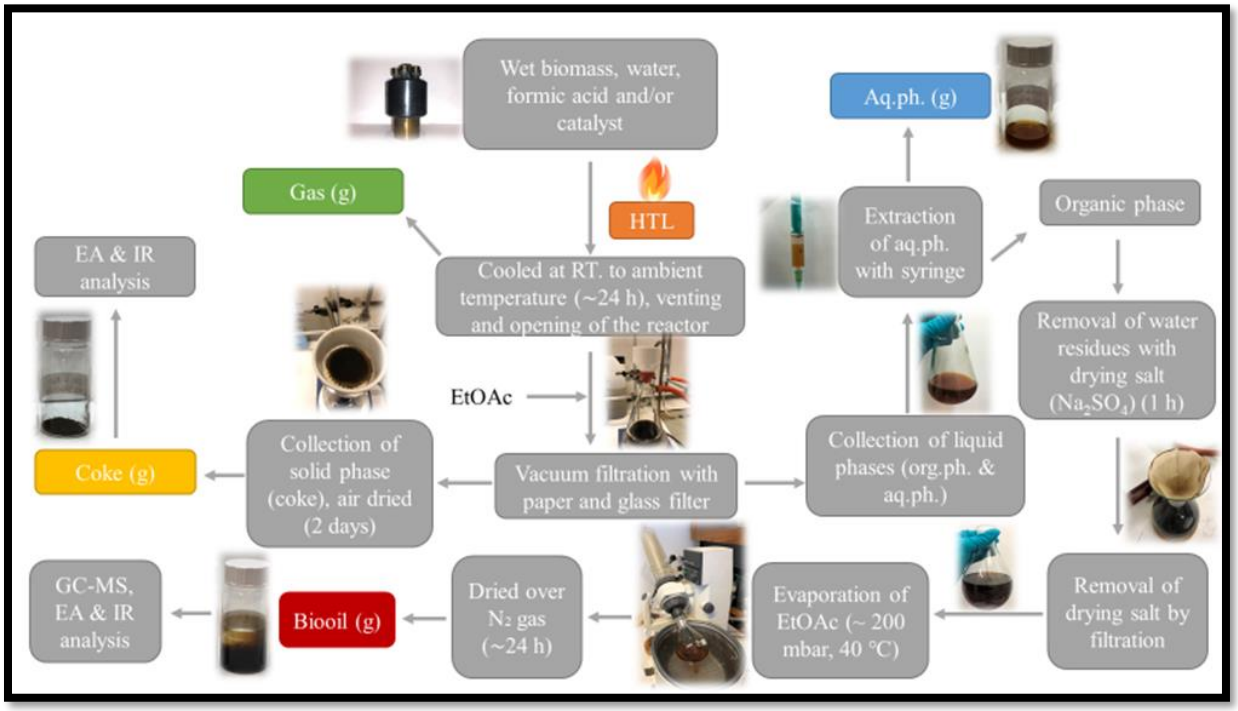

Figure 3.3-b: Flow diagram of experimental HTL procedure.

3.3.4 Pilot Series 1

This experimental series aimed to establish a baseline of experimental data on direct conversion of wet algal feedstock, under conditions used for optimalization of bio residues from the municipal biogas plant in Rådalen, at University of Bergen (UiB). The operational parameters being investigated in Pilot series 1, were temperature (280-380℃), holding time (2-6 hours), with or without a catalyst (1M KOH solution), and with or without the addition of concentrated formic acid (FA). A 2^{4-1} fractional factorial design was constructed for optimization of the operational conditions. Table 3.3-1 and Table 3.3-2 outlines the complete fractional design, including the experimental conditions, for Pilot Series 1.

Table 3.3-1: Operating parameters and values for Pilot Series 1 (P1)

Parameters	**Low value (-)**	**Center value (0)**	**High value (+)**
Temperature (T) [°C]	280	330	380
Holding time (t) [h]	2	4	6
1M KOH [mL]	0	n/a	1
Formic acid [mL]	0	0.5	1

Table 3.3-2: Outline of fractional factorial design for Pilot Series 1 (P1)

	Experiment	Temperature (T) [°C]	Holding time (t) [h]	KOH [mL]	Formic acid [mL]
Block 1: Without catalyst	**P1.280.2.H2O.0**	-	-	-	-
	P1.380.2.H2O.1	+	-	-	+
	P1.280.6.H2O.1	-	+	-	+
	P1.380.6.H2O.0	+	+	-	-
	P1.330.4.H2O.0,5	0	0	-	0
Block 2: With catalyst	**P1.280.2.KOH.1**	-	-	+	+
	P1.380.2.KOH.0	+	-	+	-
	P1.280.6.KOH.0	-	+	+	-
	P1.380.6.KOH.1	+	+	+	+
	P1.330.4.KOH.0,5	0	0	+	0

3.3.5 PILOT SERIE 2

The experimental setup for the second pilot series, Pilot Series 2, was based on the result from Pilot series 1. The purpose of Pilot Series 2 was to investigate whether a significant drop in temperature affects the bio-oil yield for the HTL-experiments. The following experimental parameters were used; time (2-6 hours); temperature (220-280℃), and with or without the addition of concentrated formic acid. The catalyst was excluded from this pilot series as it seemed to have a negative correlation with bio-oil yields. A 2^{4-1} fractional factorial design was constructed for optimization of the operational conditions. Table 3.3-3 and Table 3.3-4 presents the experimental conditions and fractional design for Pilot Series 2.

Table 3.3-3: Operating parameters and values for Pilot Series 2 (P2)

Parameters	Low value (-)	Center value (0)	High value (+)
Temperature (T) [°C]	220	250	280
Holding time (t) [h]	2	4	6
Formic acid [mL]	0	n/a	1

Table 3.3-4: Outline of fractional factorial design for Pilot Series 2 (P2)

Experiment	Temperature (T) [°C]	Holding time (t) [h]	Formic acid [mL]
P2.220.2.H2O.0	-	-	-
P2.280.2.H2O.1	+	-	+
P2.220.6.H2O.1	-	+	+
P2.280.6.H2O.0	+	+	-
P2.220.2.H2O.1	-	-	+
P2.280.2.H2O.0	+	-	-
P2.220.6.H2O.0	-	+	-
P2.280.6.H2O.1	+	+	+
P2.250.4.H2O.0	0	0	-
P2.250.4.H2O.1	0	0	+

3.3.6 PILOT SERIES 3

The feedstock residues collected after the Soxhlet extractions were used as feedstock in the HTL process for Pilot Series 3. The experimental parameters in Pilot Series 3 were based on the reaction conditions for Pilot series 1. This series had the following experimental parameters; time (2-6 hours); temperature (280-380℃), with the addition of water and or formic acid. Additional water was added to the microalgal extraction residue, during HTL-workup, to achieve comparable starting material and reaction medium with Pilot Series 1. The amount of additional water added to the dry feedstock, were determined based on the average TS (26.12%) from Pilot Series 1. This means that approximately 2.96 g of the 4.0 g of feedstock added to the reactor in each HTL-workup, is expected to consist of water. A 2^{3-1} fractional factorial design was constructed for optimization of the operational conditions. Table 3.3-5 and Table 3.3-5 displays the fractional factorial design and conditions, for Pilot Series 3.

Table 3.3-5: Operating parameters and values for Pilot Series 3 (P3)

Parameters	Low value (-)	Center value (0)	High value (+)
Temperature (T) [°C]	280	330	380
Holding time (t) [h]	2	4	6
Formic acid [mL]	0	0.5	1

Table 3.3-6: Outline of fractional factorial design for Pilot Series 3 (P3)

Experiment	Temperature (T) [°C]	Holding time (t) [h]	Formic acid [mL]
P3.280.2.H2O.0	-	-	-
P3.380.2.H2O.1	+	-	+
P3.280.6.H2O.1	-	+	+
P3.380.6.H2O.0	+	+	-
P3.330.4.H2O.0,5	0	0	0

3.4 MULTIVARIATE ANALYSIS

3.4.1 ABOUT

Principal component analysis (PCA) is a widely used statistical technique for reducing the dimensionality of large datasets that otherwise would be difficult to interpret [64]. Most of the statistical information (variables) in the data is preserved, by constructing principal components (PCs). PCs are new variables that are constructed as linear combinations of the initial variables. A tradeoff with this method is that reducing the number of variables in the dataset also reduces the accuracy [64].

Prior to PCA, the initial variables are standardized so that the range of variances for each variable contributes equally to the analysis. A covariance matrix is computed to see how the standardized variables varies from the mean with respect to each other. That is, to see if there are any correlations between them. The sign of the covariance gives an indication of the correlation between the variables: If positive, the two variable positively correlates; if negative, the two variables anticorrelates [64], [65]. The first principal component (PC1) is a linear combination that explain the largest possible variance in the dataset, i.e., it has the maximum possible information that can be obtained in a PC. The second principal component (PC2), which is extracted by removing PC1, comprises the maximum of variance that cannot be explained by PC1, and the third principal component (PC3) includes the maximum remaining information that is not described in PC1 and PC2 and so forth [64], [65]. This way of compromising and organizing information in PCs, allows for reduction of dimensionality without losing much information, by discarding the components with low information.

Two principal components together define a model plane. By projecting all the information from a high-dimensional space into a lower-dimensional sub-space, it is possible to visualize the structure of the investigated dataset. The coordinate values of the observations on this

plane are called scores, and the plotting of such a projected configuration is known as a score plot. Loading plots shows how strongly each variable influences a principal component. When two vectors are close, forming a small angle, the two variables they represent are positively correlated. If they meet each other at 90^o, they are not likely to be correlated. When they diverge and form a large angle, close to 180^o, they are negatively correlated. Loadings of variables and PC scores of samples (objects) together form a biplot [51],[66].

Partial least square regression (PLSR) analysis is a versatile method for multivariate data analysis, which addresses the problem of making good predictions in multivariate problems. PLS is used to establish quantitative relations between two blocks of data for the prediction of expected responses for a new system [66],[67].

3.5 SOXHLET EXTRACTION OF LIPIDS

3.5.1 DEFINITIONS AND FORMULAS

In the following, extraction yields were calculated according to Eq 3.5-1.

$$Extraction\ yield\ [\%] = \left(\frac{A}{B}\right) \cdot 100 \qquad (3.5\text{-}1)$$

where, A is the weight of the total extract (Soxhlet extract (lipids), feedstock residue or water) collected by Soxhlet, determined by gravimetry, and B is the weight of the initial wet algal feedstock.

Eq 3.5-2 were used to calculate the lipid content in the Soxhlet extract.

$$Y_{Lipids}\ [\%] = \left(\frac{Soxhlet\ extract}{TS}\right) \cdot 100 \qquad (3.5\text{-}2)$$

where, *Soxhlet extract* is the weight of the total amount of dried Soxhlet extract collected by Soxhlet, and *TS* is the weight of dry matter in the initial wet algal feedstock.

3.5.2 ABOUT

Soxhlet extraction was chosen as the method for extracting lipids from the wet algal feedstock. The lipids extracted from the algal feedstock can potentially be converted into biodiesel through transesterification. Soxhlet extraction is a conventional and well-established technique for solvent extraction of lipids from a solid material, and it is often used as a reference for evaluating the performance of other solid-liquid extraction methods [68]. Conventional Soxhlet extraction is a very simple and nonlabor-intensive process, which is both cheap and scalable [69]. Another advantage of using this method is that the Soxhlet apparatus minimizes solvent consumption. However, one major drawback to this method is that it is very time-consuming. Another practical issue with Soxhlet extraction is choosing a suitable solvent as different solvents will extract different solutes and vary in yield productivity [5], [68]. The solvent used for lipid extraction should have a high solubility for all lipid compounds and be sufficiently polar to remove them from their binding sites with cell membranes, lipoproteins, and glycolipids [70].

An overview of a Soxhlet extraction system is given in the figure 3.5-a. The Soxhlet apparatus consists of a round-bottom flask containing the solvent, a Soxhlet extractor comprised of the

feedstock placed in an extraction thimble, a water separator, and a condenser. The water separator is only necessary if the feedstock is wet. When the solvent is heated, it begins to evaporate from the distillation flask, moving through the apparatus to the condenser. The condenser channels the condensate into the extractor and drips into the thimble. The thimble filter is filled with fresh solvent and prevents feedstock from being carried out of the extractor with the solvent. Once the level of solvent in the thimble reaches the overflow limit in the extractor, a siphon extracts the solution and unloads it back into the distillation flask, carrying extracted solutes into the bulk liquid. In the distillation flask, the solute is separated from the solvent using distillation. The solute is left in the flask and fresh solvent passes back into the extraction thimble. This cyclic process is repeated until the extraction is completed [5]. The extraction is classified as complete when the solvent in the Soxhlet extractor comes out without any trace of feedstock. By use of water separator, one must extract for 24 h after the separator have finished to separate water.

3.5.3 EXPERIMENTAL

The Soxhlet extraction apparatus was set up as shown in Figure 3.4-a. Initially, the plan was to use EtOAc as solvent. However, the design of the water separator that was available for use in the Soxhlet experiments only works with solvents with lower densities than water. Due to its availability at the laboratory and its similarity in polarity, with a polarity index (PI) of 3.1, dichloromethane (DCM) was decided to be used as solvent instead of EtOAc (PI=4.4)[71].

The solvent vapor tube and water extractor were partly covered with aluminum foil, to prevent potential heat loss and pre-condensation solvent vapor. In this procedure, approximately 40 g of wet algal feedstock was loaded into a 33 x 118 mm porous cellulose extraction thimble (Schleicher & Schuell). The extraction thimble, filled with the algal feedstock, was then placed inside the Soxhlet extractor. 400 mL $\pm$ 5 mL of DCM ((Sigma-Aldrich), puriss. p.a., ACS reagent, reag. ISO, $\geq$99.9%) was added to a round bottom flask, on an isomantle heater. The process was run, under reflux, for a total of 144 hours. Additional solvent (100 mL $\pm$ 5 mL) was added midway in the process to prevent the content in the distillation flask from drying out. Water was collected throughout the extraction process from the water extractor, to avoid being overfilled. The water samples were weighed after all the water had been extracted from the system. Once the process was finished, the solvent was removed using a rotary evaporator (at $\sim$ 40℃, $\sim$ 840 mbar). The lipid extract was extracted from the rotary evaporating flask, using an additional solvent to wash clean the flask, to a sample glass. The diluted sample was further dried under N_2 gas for 72 h before final weighing. The dry microalgal feedstock residue was dried for 24 h before final weighing. The feedstock residue was lightly pulverized into a coarse powder using a coffee grinder and stored in an airtight flask at ambient temperature for HTL. The percentage yield of lipids, water and feedstock residue was determined by weighing.

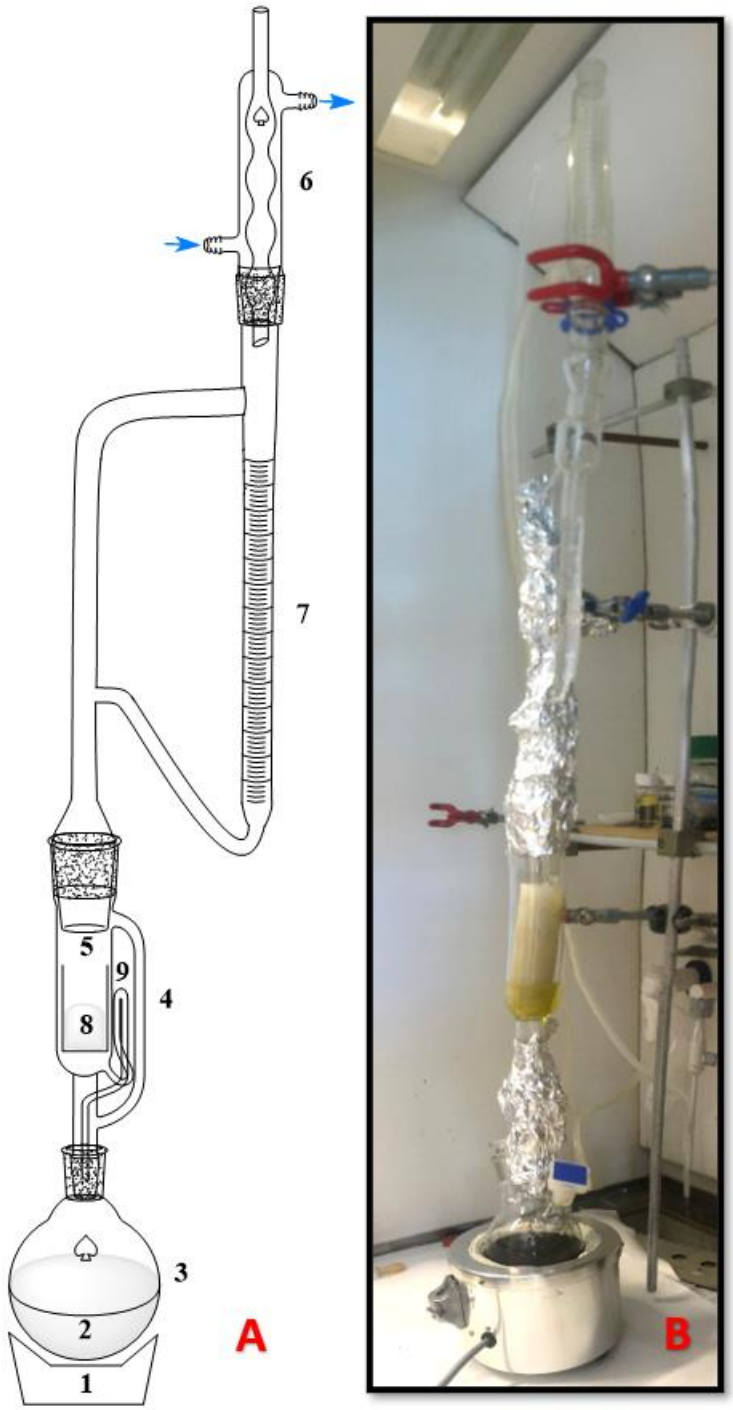

Figure 3.5-a: A) Sketch of the assembled experimental Soxhlet extraction apparatus, which includes (1) Isomantle (heat source); (2) Solvent (DCM); (3) Round bottom distillation flask; (4) Solvent vapor tube; (5) Soxhlet extractor; (6) Condenser with running water; (7) Water separator; (8) Extraction thimble (filled with raw material); (9) Siphon. B) Picture of the experimental Soxhlet extraction apparatus. Parts of the soxhlet extractor and water separator are isolated with aluminium foil to minimize the heat during the extraction process.

3.6 ELEMENTAL ANALYSIS

3.6.1 DEFINITIONS AND FORMULAS

In this thesis, the result data for the elemental analysis results were used to calculate the HHV of the bio-oils and the solids (Eq. 3.6-1). Higher heating value (HHV) defines the energy content of the fuel and is therefore an important fuel property. Estimation of HHV from the elemental composition of the fuel is widely used for performance modelling and calculations on thermal systems. Numerous correlations for calculations on HHV from elemental composition are available in the literature [72]. The higher heating values in this study were calculated using approach by Channiwala (2002) according to Eq 3.6-1 [72]:

$$HHV = 0.3491C + 1.1783H + 0.1005S - 0.1034O - 0.0151N - 0.0211A \quad (3.6\text{-}1)$$

where, *C, H, O, N, S* and *A* represents carbon, hydrogen, oxygen, nitrogen, sulphur and ash contents of the material, respectively, expressed mass percentage on dry basis. Note that carbon, hydrogen and sulfur add to the energy content, while oxygen, nitrogen and ash reduce the energy content. HHV is expressed in MJ/kg.

Energy recovery (ER) was calculated by the following equation:

$$ER\ [\%] = \frac{(HHV \cdot m)_{Oil}}{(HHV \cdot m)_{Feedstock}} \cdot 100\% \quad (3.6\text{-}2)$$

where, *HHV* and *m* represents the associated higher heating value and weight of a given material.

3.6.2 ABOUT

Elemental analysis (EA) is an established technique used to assess the elemental composition of organic liquid and solid samples. CHN(O)S elemental analysis determines the quantity of carbon (C), hydrogen (H), nitrogen (N), oxygen (O), and sulfur (S) present in an organic substance. This method is also known as combustion analysis because it is based on the complete combustion of the sample. Combustion analysis is often used for solid fuel characterization, such as coal, coke, biomass, and other solid carbon-based fuels, where an accurately weighed amount of substance is burned in oxygen to form combustion gases (CO_2, H_2O, and N_2) [73]. These elements are then selectively collected on specific and weighed adsorption columns (adsorbents). The weight difference of the adsorbents before and after elemental adsorption is determined with a thermal conductivity detector (TCD) [74], [75]. For organic samples, the oxygen content is indirectly determined as the residual mass from the quantities of the other elements (C, H, and N) [75], [76]. However, this is an assumption that will be incorrect if there are some inorganics present in the samples. Determining a fuel's elemental composition allows for the determination of its calorific value, i.e. its quality as a fuel [73].

3.6.3 EXPERIMENTAL

Compositional analysis of the gas and aqueous products was not performed since the main objectives of this thesis are to maximize and compare bio-oil products. Elemental analysis of the oil and coke products from each pilot series, including samples of feedstocks, were

performed on a Vario EL III analyzer (Elementar) in CHNS mode. In this case, the instrumentation was not calibrated for sulfur. Acetanilide and nitrile were used to calibrate the instrument. Helium was used for flushing and as carrier gas [74]. A replica was prepared for each sample that had an adequate amount of sample. A small part of the sample (approx. 4-8 mg) was packed in a pre-weighed tin capsule, weighed, and placed into the carousel of the automatic sample feeder. All analysis and data collection were performed by the head engineer at the Department of chemistry, Inger Johanne Fjellanger, at UiB.

3.7 GAS CHROMATOGRAPHY – MASS SPECTROSCOPY

3.7.1 ABOUT

Gas chromatography-mass spectroscopy (GC-MS) is an effective and relatively inexpensive analytical method used to distinguish and resolve the individual organic compounds in mixtures with high resolution. GC-MS is a hybrid of two instruments, where a gas chromatograph (GC) is coupled to a mass spectrometer (MS), using fused silica capillaries, to achieve high levels of chemical analysis, in terms of both capacity and precision [77, pp. 1–4]. Gas chromatography provides an easy method for separating and analyzing volatile organic compounds in complex mixtures, both quantitively and qualitatively [78]. The mass spectrometer, which serves as the GC detector, involves the ionization of molecules using various techniques [77, pp. 493–495]. In GC, the compounds being analyzed are passed through a column that contains a stationary phase, moved by a gaseous mobile phase (carrier gas) [77, pp. 1–4], [79]. The carrier gas is an inert gas, usually helium or nitrogen. The stationary phase consists of a thin, uniform liquid film applied either to the interior surface or to a thin layer of solid support lining the capillary column. In both cases, the center of the column is open for the passage of the carrier gas with the vaporized substances. The stationary phase is generally made of a polymer with a high boiling point (e.g., polysiloxanes), or other non-volatile liquids (e.g., Carbowax and diethylene glycol succinate). The sample mixture is injected through a septum into a heated injection port, where the components rapidly vaporize. The vaporized compounds are carried by the carrier gas through the column where they start to separate themselves between the two phases in an equilibrium that depends on temperature, rate of gas flow, and solubility of the components in the liquid phase [78]. A compound's ability to partition between the mobile and stationary phase relies on both its relative attraction to the liquid phase and its vapor pressure. A compound with high vapor pressure will have a greater tendency to go from the liquid phase into the gas phase, compared to a compound with lower vapor pressure, and vice versa. Generally, a low-boiling compound with high vapor pressure travels faster through the column than a high-boiling compound [78]. After the separation in the GC column, the vaporized molecules are fed into the mass spectrometer where they are ionized by electron impact to generate either cationic or anionic species. The reaction below displays the ionization of a general compound (M) into a radical cation by electron ionization [80]:

$$M + e^- \rightarrow M^{\cdot +} + 2e^-$$

This resulting radical cation will normally undergo fragmentations, and because it has an odd number of electrons, it can fragment either into a radical (R·) and an even-numbered ion (EE^+) or a new radical cation (OE^+) and a molecule (N). The primary ions products derived from the molecular ions can, in turn, undergo fragmentation, and so on [80]. All the ions are then

accelerated and passed into the mass analyzer, using magnetic or electric fields, where their mass-to-charge (m/z) ratio is determined [81]. At a given magnetic field strength, a beam of ions with a specific m/z ratio will reach the detector. Ions with a larger m/z ratio are not deflected enough to reach the detector. Likewise, ions with a smaller m/z ratio are deflected too much to strike the detector. A mass spectrum is generated of each compound eluting from the GC by the MS. The individual molecular structures obtained by the MS are compared to standards or extensive databases for molecular identities, such as the National Institute of Standards and Technology (NIST) database [77].

There are some restrictions to this analytical method. First, GC-MS is limited to substances that are volatile enough to be analyzed by GC [77]. Second, the GC-MS analysis using databases like NIST is limited by the selection of the standards databases. The interpretation of components can also be done manually, without the use of databases. For complex mixtures like bio-oil, comprised of a large variety of compounds, that are time consuming and difficult to analyze, NIST is a valuable tool for compound identification. Third, the closest match from the ranked "hit list" of compounds with similar mass spectra, does not necessarily prove the structure of a compound. Impurities can also produce additional peaks in the mass spectrum and provide false candidates [78].

Quantification of compounds should ideally be based on calibrations curves using standards for each compound. However, the unpredictable composition of bio-oils and lack of standards makes this approach difficult. Thus, other methods that allow semi-quantification of compounds are more applicable for complex sample mixtures. Semi-quantification based on internal standard abundance are one of the most common methods used in GC-MS [82]. In a GC chromatogram, the area under the peak of the associated component is proportional to the amount of the component reaching the detector. A suitable internal standard (IS) of known concentration is added to the sample to quantify the concentration of the analytes, based on the relationship between the peak area ratio and concentration ratio of the target component and IS in the GC chromatogram [83]. The ratio is determined with use of a response factor (RF). There are several advantages to this type of quantitative method. First, the quantity can be calculated as long as the target component and IS are detected. Second, the concentration ratio is independent of injection volume, and thus, compensates for sample injection volume errors in the results. Third, it is not sensitive to different sample densities caused by different sample compositions. However, there are some disadvantages and requirements to this method, regarding the use of RF and internal standards. In theory, the RF value for a substance (A) in a sample can be determined by calculating the RF-value in advance from GC analysis of the substance (A) in known concentration and IS in solution. As mentioned, this is only practical feasible for samples of low complexity. The use of internal standard requires that it separates sufficiently from all components in the sample, elutes close to the target component, has similar chemical properties to the target component, and is chemically stable [83].

3.7.2 Definitions, reaction equations and formulas

Silylation of the bio-oils and Soxhlet extracts is performed prior to the analysis to lower the volatility of any high boiling compounds, which may fail to properly vaporize upon injection to the GC-MS. Silylation is the substitution of active hydrogen on a heteroatom by a silyl

group, forming a silicon heteroatom bond (trialkyl group), without any additional alteration of the molecule. The general reaction equation for silylation of polar compound is given in below:

$$\boldsymbol{R-OH+(CH_3)_3SiX \rightarrow R-O-Si(CH_3)_3+HX}$$

The concentration of the analytes (C_A) was semi-quantitatively calculated, using Eq. 3.7-1. In this thesis, the response factor (RF) was set to be equal to 1, since it was not feasible to determine the RF value for each individual component in the bio-oil samples. This means that the RF value is the same as for the two internal standards, dodecane and benzoic acid.

$$C_A = \frac{A_A \cdot C_{IS}}{A_{IS} \cdot RF} \qquad (3.7\text{-}1)$$

Where A_A: area under analyte peak, C_{IS}: concentration of internal standard, A_{IS}: area under internal standard peak, RF: response factor.

3.6.3 EXPERIMENTAL

GC-MS was applied in the analysis of the different components present in the bio-oils and Soxhlet extracts. All the volumetric measurements were performed with a mechanical pipette (Eppendorf Research® Plus, Eppendorf). The same procedure was done on all samples in this thesis and is shown in Figure 3.6-a.

Preparation of stock solution for GC-MS samples

In the determination of the GC-MS samples, a stock solution of ethyl acetate with benzoic acid and dodecane as internal standards was prepared. In a 100 mL volumetric flask, approx. 0.23 g benzoic acid (Fluka Analytical, analytical standard) and add 0.30 mL dodecane (Fluka Analytical, analytical standard) were added with an auto pipette. EtOAc ((Sigma-Aldrich), puriss. p.a., ACS reagent, reag. ISO, reag. Ph. Eur., ≥99.5% (GC)) was added to the 100 mL-mark. As a matter of form, this solvent mixture is referred to as "Solvent A1". In another 100 mL volumetric flask, 3.5 mL of Solvent A1 was diluted with EtOAc to the 100 mL mark. This solvent is referred to as "Solvent A2".

Derivatization and preparation of oil samples

About 7.5 mg of an oil sample was added in a 20 mL volumetric sample glass along with 3 mL EtOAc. The oil mixture was stirred till the oil was completely dissolved in the solvent. 1 mL of the bio-oil solution was transferred to an Agilent 2 mL-glass sample (2 mL clear glass vial 12x32 mm, screw thread PTFE/Silicone septum (bonded), 9 mm, SupelCO®). Pyridine (150 μL) ((Fluka Analytical), puriss. p.a., for titration in nonaqueous solution, Assay (GC) ≥99.5%) and BSTFA (150 μL) ((Sigma-Aldrich), for GC derivatization, LiChropur™, contains 1% TMCS, 99% (excluding TMCS)) was added in the next step. The glass sample was then sealed with a cap and placed in a drying oven (Termaks, AS) at 70℃ for approximately 30 minutes. The sample was cooled down to ambient temperature. In another 2 mL-glass sample (Conv Pk 9mm Vial clear with PTFE/Silicone Septa), 0.7 mL of the oil-solution and 0.7 mL pentane ((Sigma-Aldrich), anhydrous, ≥99%) was added. The derivatized oil sample was stored in the fridge overnight and filtered the following day using a 0.5 μL syringe filter (Acrodisc, Pall Corporation, 13 mm with 0.2 μm nylon).

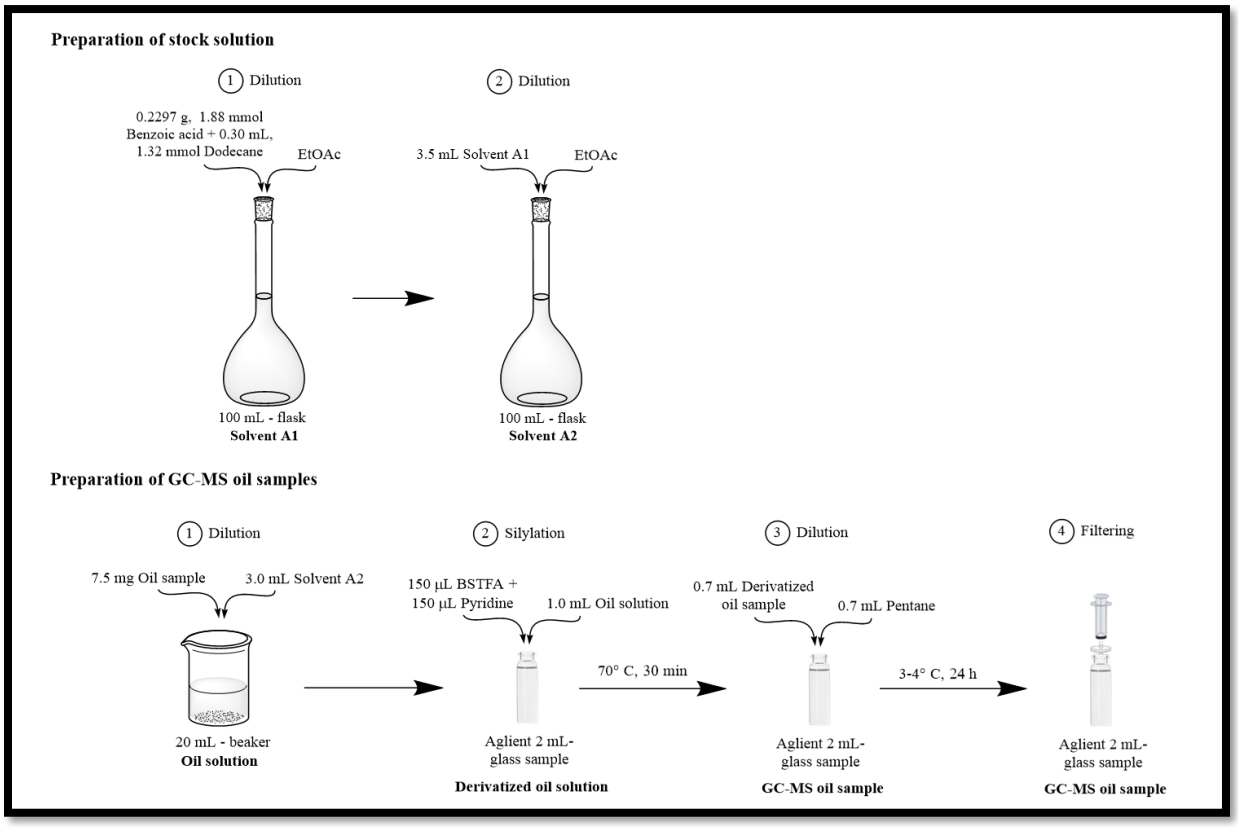

Figure 3.7-a.: Preparation of stock solution and GC-MS samples

GC-MS apparatus and temperature program

The instruments used are the Agilent 7890A gas chromatograph with split-splitless injector and automatic exchanger, and the Agilent 5977A MSD mass spectrometer. The GC-MS samples were diluted in EtOAc to a concentration of approximately 1.0 mg mL^{-1} from where 1 µL of the diluted solution was injected into the GC using a splitless injector. Helium was used as a carrier gas and introduced into the GC column at a constant gas flow rate of 1 mL min^{-1} (v = 36.7 cm s^{-1}). The temperature program used is displayed in Table 3.7-1.

The other chromatographic parameters were:

- GC column: (5% Phenyl)-methylpolysiloxane HP – 5 ms (Agilent)
- Column dimensions: L = 30 m, ID = 0.250 mm, stationary phase thickness = 0.25 µm
- Injector temperature: 280°C
- Detector temperature: 260°C
- Injected sample volume: 0.5 µL

Mass detection was operated in full scan mode (m/z ratio of range 25-400) at 3.8 s^{-1} for product identification. Ionization was electron impact at 70 eV. Ion source temperature was 230°C. Solvent delay was put on 5.5 min.

Table 3.7-1: GC-MS temperature program.

	Rate [°C/min]	Temperature [°C]	Holding time [min]
Start		50	2
Level 1	10	200	0
Level 2	20	300	5

Limit requirements for identification of compounds in GC-MS

MSD ChemStation Data Analysis software was used to examine the bio-oil samples. Due to the complexity of the bio-oils, the chromatograms of the oil samples contain a large number of peaks. Therefore, a limit requirement was set for how thoroughly each chromatogram should be examined. To focus on the peaks with the highest intensities, the initial threshold value was set to 22.5. Furthermore, a requirement of ≥50% probability was also set for the NIST library. With the two requirements, the analysis of the oil samples will provide an overview of the oil-components with the highest intensities and probability. However, this also discard a large part of the bio-oil composition that will not be identified. (X) marks unidentified peaks in the GC diagrams displayed in this thesis.

3.8 FOURIER TRANSFORM – INFRARED SPECTROSCOPY

3.8.1 ABOUT

Infrared (IR) spectroscopy provides an efficient technique for identifying the presence or absence of functional groups when determining the structures of organic molecules [78]. Infrared Spectroscopy is based on the interaction of electromagnetic radiation – in the form of infrared light – with the matter, when electromagnetic waves are passed through an organic sample [84]. Only molecules with either a permanent or induced (temporary) dipole moment vibrate, because of changes in the vibrational energy in the bonds during absorption of infrared radiation and are referred to as being "IR active". The type of vibration (stretching or bending) induced by the infrared radiation depends on the distinctive bond arrangement and functional groups within the molecule. Thus, the IR active molecule only absorbs frequencies of specific wavelengths that match the corresponding frequency which triggers vibrational motion. An absorption band (peak) appears in an IR spectrum at a frequency where a molecular vibration occurs in the molecule. The difference in the transmittance pattern makes it possible to characterize and identify the different functional groups within the molecules, as each frequency absorbed by a molecule corresponds to a specific molecular motion [85]. The IR spectrum shows the measured energy from the molecular vibrations of the individual molecules (along the horizontal axis as either frequency or wavelength) plotted against the intensity of the absorption (along the vertical axis) [78]. IR bands can be classified as strong (s), medium (m), or weak (w), depending on their relative intensities in the infrared spectrum. A strong band covers most of the y-axis, a medium band falls to about half of the y-axis, and a weak band falls to about 1/3 or less of the y-axis. The IR region of the electromagnetic spectrum covers the range from $7.8 \cdot 0^{-7}$m to approximately 10^{-4} m. In organic chemistry, we often focus on the midportion region from $2.5 \cdot 10^{-6}$ m to $2.5 \cdot 10^{-5}$ m, corresponding to wavenumbers of 4000 to 400 cm^{-1} [78].

Each peak corresponds with a functional group or bond present in the sample molecule. FT-IR (Fourier transform infrared) spectroscopy is the technique used for the analysis of the HTL-samples, due to its high precision, sensitivity, and effectiveness compared to other techniques. Another benefit of using the FTIR method is that it does not destroy the sample [85]. In addition to identifying the functional groups present in the HTL-samples, IR was used to investigate potential differences in products, concerning the changes in reaction conditions during the HTL process, by comparison of structural changes between the HTL-samples. Principal component analysis (PCA) was used to identify the main sources of variation in the IR spectra of the samples. FT-IR of a sample allows for the identification of functional groups. However, the identification of compounds in mixtures often fails in distinguishing compounds apart.

3.8.2 EXPERIMENTAL

The infrared spectrophotometer Nicolet Protege 460 FTIR (Thermo electron corporation) with OMNIC 7.3 software was used for recording IR spectra for both oil and coke products from the HTL-samples. The oil samples were analyzed in their liquid state as droplets on the ATR (Attenuated Total Reflection) – cell. Finely ground powders of solids (coke) were also directly analyzed on the cell. The spectrophotometer was measuring %-reflectance over a wavelength from 4000 to 650 cm^{-1}, collecting 32 scans per spectrum with a resolution of 4 wavenumbers. The ATR cell was cleaned with EtOAc between each sample analysis. Each IR-spectra were analyzed with a threshold value of approx. 0.95 and a sensitivity of 75 % for IR sensor. The peaks from IR-spectra were used to assign functional groups present in the sample, based on an infrared spectral correlation chart from *"Introduction to spectroscopy"* by Pavia et al. [86, p. 29].

4.0 RESULTS

This chapter summarizes the main results achieved within this thesis. The data are represented in tables and figures, through bar- and scatter plot diagrams, to illustrate and give a better overview of differences in results. Some of the representative chromatograms and IR-spectra are also presented here. The remaining collection of chromatograms and IR-spectra from the three series of experiments, along with supplementary and comprehensive data, can be found in Appendix A to C.

4.1 PROXIMATE ANALYSIS: TS, VS, AND WV

The results from proximate analysis of the two feedstock batches, named Feedstock 1 and 2, are represented in Table 4.1-1. Additional data are reported in Table A.1-1, Appendix A. The calculated values for total solid (TS), volatile solid (VS), and loss of ignition (Wv) of each feedstock sample are given as mean values on a mass percentage basis, based on two parallels.

Table 4.1-1: Proximate analysis results of TS, VS, and Wv.

	Feedstock 1		Feedstock 2	
Parallel no.	**1**	**2**	**1**	**2**
Moisture [%]	73.87	73.90	73.89	74.23
TS [%]	26.13	26.10	26.11	25.77
VS [%]	23.30	23.27	n/a	n/a
Wv [%]	89.18	89.13	n/a	n/a
TS MV. [%]	26.12		25.94	
VS MV. [%]	23.29		n/a	
Wv MV. [%]	89.16		n/a	

4.2 PILOT SERIES 1

4.2.1 HTL

The operational parameters being investigated in Pilot Series 1 (P1) are presented in Table 3.3-1. Two experimental tests (T) were performed prior to this pilot series for preparatory training for the experimental procedure. These tests are not included in the final HTL results, due to uncertainty in experimental errors which might affect the yield results in the experimental series. In this series, a total of 11 experiments were performed to establish the method. Replicas (R) of the two experiments with the highest bio-oil yields were performed to gain insight to the reproducibility of the reaction process.

Pictures from the HTL-workup of bio-oil and coke samples, from P1 are shown in Figure 4.2-a.

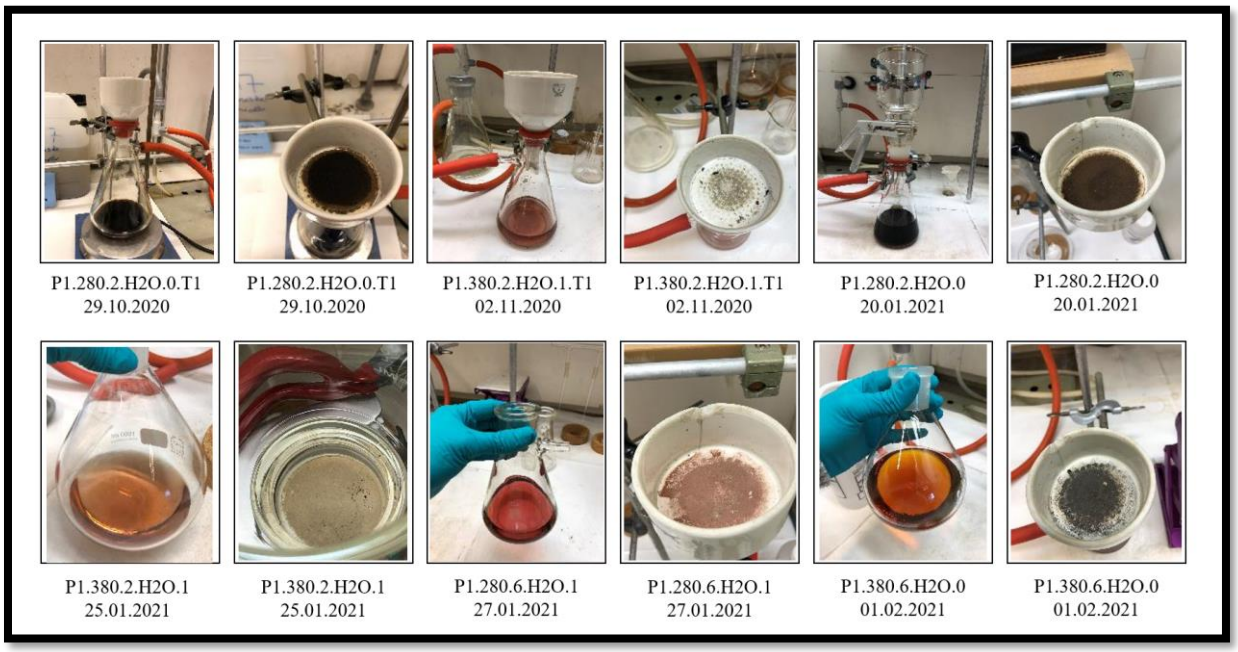

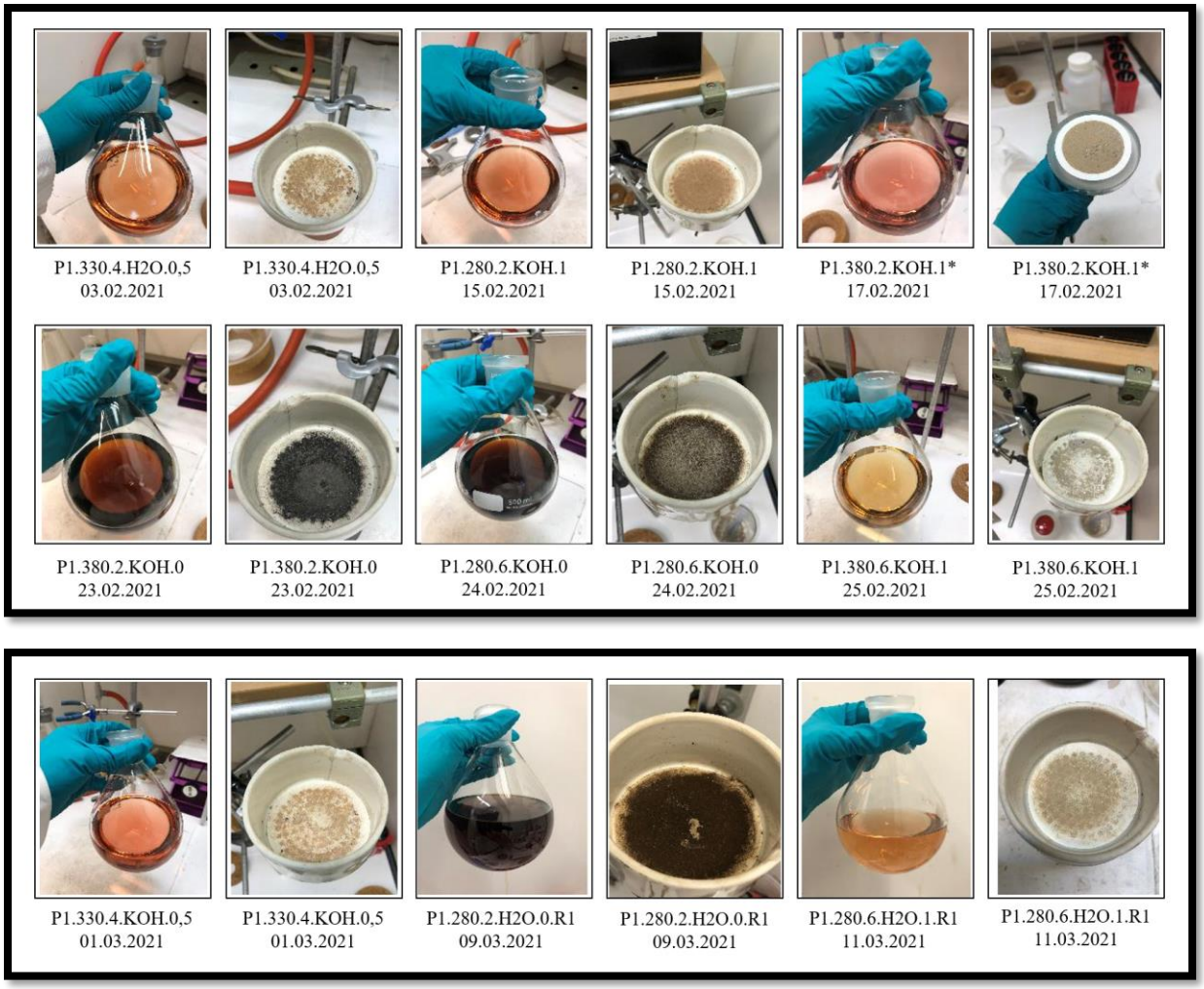

Figure 4.2-a: Pictures of the coke and bio-oil (diluted in solvent) samples from the HTL work-up from P1.

The products obtained in P1 from HTL of the microalgal feedstock consisted of gas, coke, bio-oil, and an aqueous phase. The collection of HTL products from the experimental series, including the two experimental tests, are shown in Figure 4.2-b to 4.2-d. HTL products from experiment P1.280.2.H2O.0.R2 are not included in these pictures, as this replica was made after these pictures were taken.

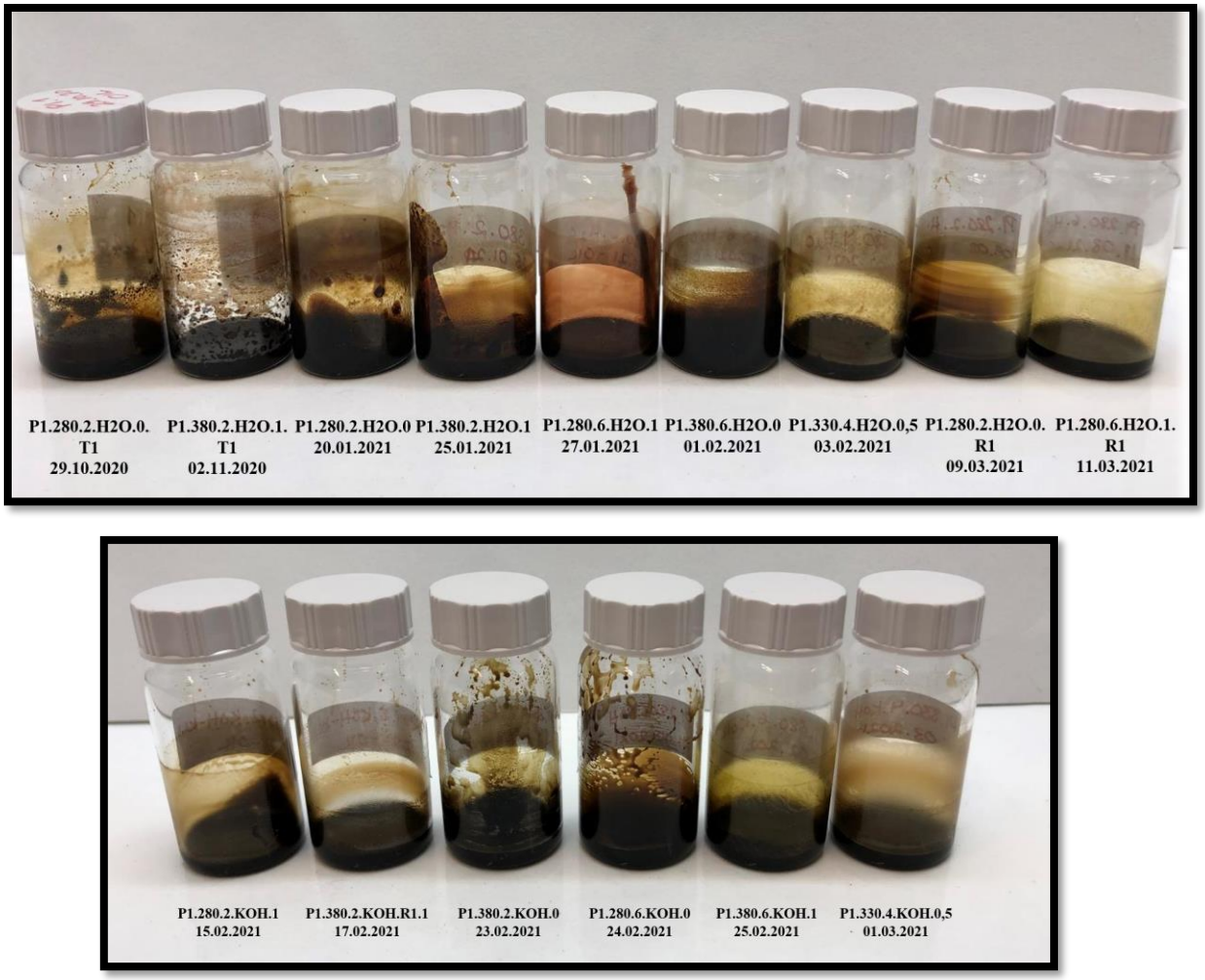

Figure 4.2-b: Pictures of the collected oil samples from P1.

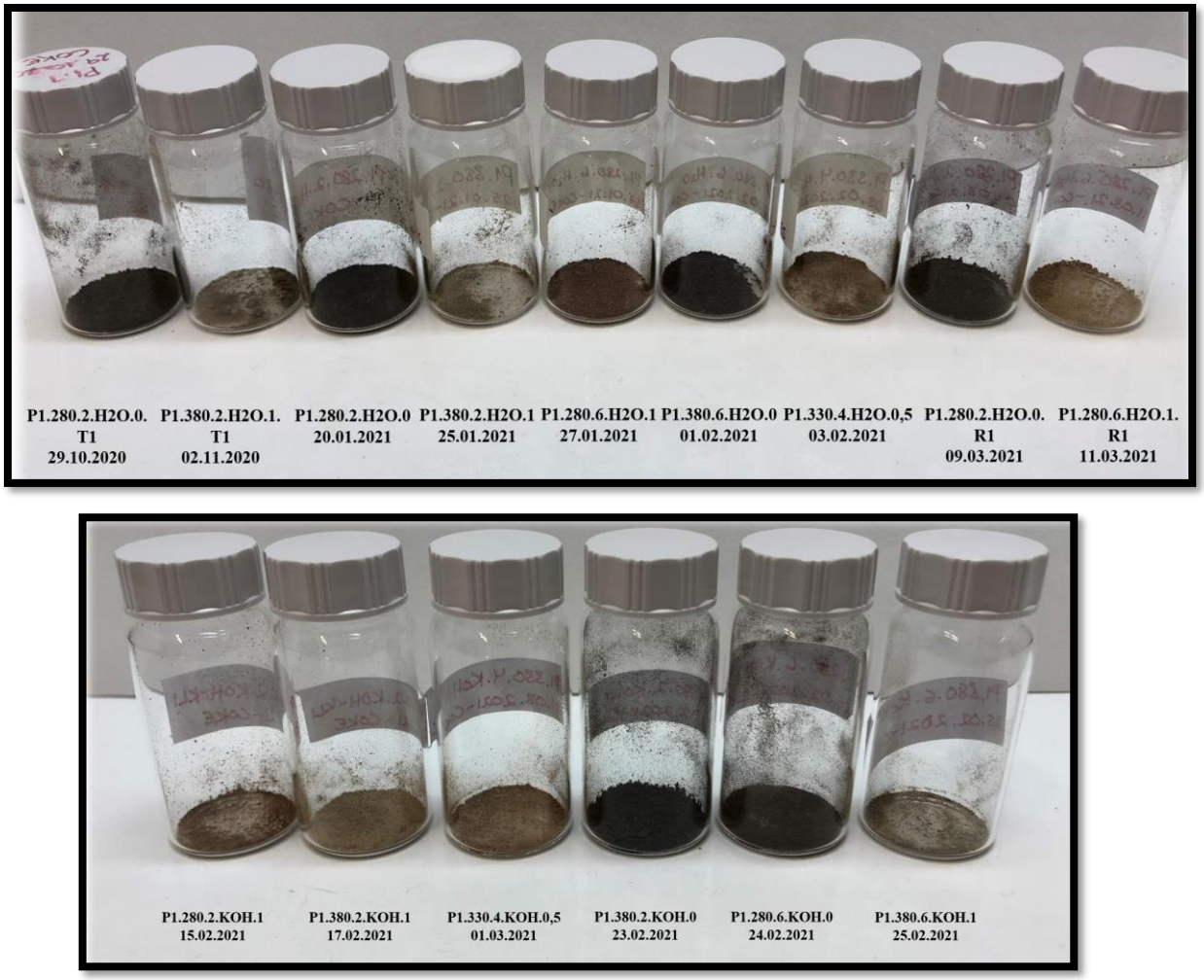

Figure 4.2-c: Pictures of the collected coke samples from P1.

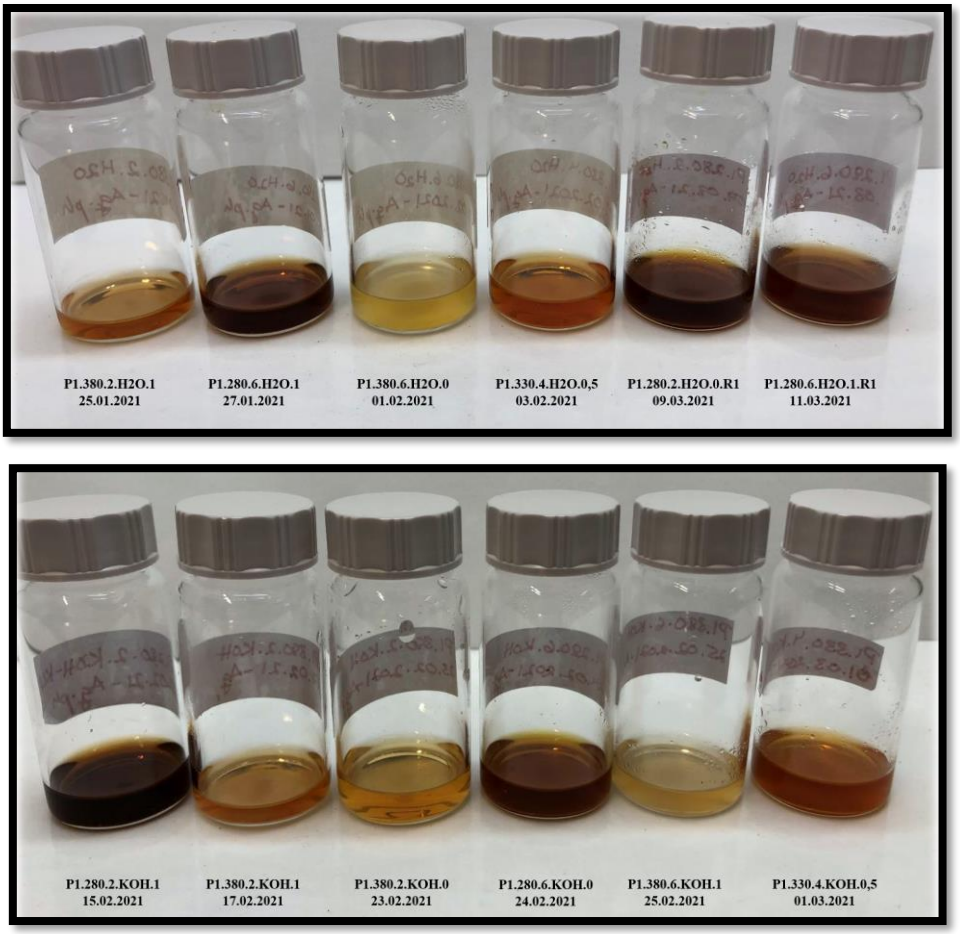

Figure 4.2-d: Pictures of the collected aqueous samples from P1.

The yields of bio-oil, including other HTL products, are presented in Table 4.2-1. The yields of gaseous products in this table are included for the experiments with formic acid added (Eq. 3.3.5). Otherwise, the yields are represented as the weight mass of gases produced. Experiment P1.280.2.H2O.0 is classified as an outlier, based on multivariate analysis, and is not included in any of the quantitative analyses for this pilot series. However, this experiment is included in the HTL results to show the full experimental series. Raw data from the HTL workup is presented in Table A.2-1 in Appendix A.

Table 4.2-1: Yields of HTL-products in Pilot Series 1.

Experiment	Aq.ph. [g]	Gas [g]	Coke [g]	Oil [g]	Y_{Gas} [%]	Y_{Coke} [%][a]	Y_{Oil} [%][a]	Y_{Total} [%]
P1.280.2.H2O.0	n/a	0.08	0.10	0.58	n/a	9.57	55.39	n/a
P1.280.2.H2O.0.R1	2.94	0.09	0.13	0.44	n/a	12.54 (-1.89)	42.01 (-1.59)	59.88
P1.280.2.H2O.0.R2	2.48	0.09	0.17	0.48	n/a	16.32 (+1.89)	45.20 (+1.59)	53.30
P1.380.2.H2O.1	1.48	1.19	0.05	0.43	97.54	4.78	40.69	50.37
P1.280.6.H2O.1	2.15	1.07	0.10	0.48	87.70	9.80 (+0.94)	45.97 (+1.23)	60.90
P1.280.6.H2O.1.R1	2.78	0.99	0.08	0.46	81.15	7.92 (-0.94)	43.51 (-1.23)	68.90
P1.380.6.H2O.0	2.79	0.19	0.12	0.42	n/a	11.07	40.50	58.74
P1.330.4.H2O.0,5	2.36	0.64	0.02	0.40	104.92	1.50	38.55	55.83
P1.280.2.KOH.1	2.55	0.92	0.07	0.44	75.41	6.27	42.36	63.45
P1.380.2.KOH.1	1.72	1.25	0.11	0.41	102.46	10.49	39.23	55.89
P1.380.2.KOH.0	2.45	0.13	0.08	0.44	n/a	7.55	42.05	51.16
P1.280.6.KOH.0	2.30	0.05	0.17	0.46	n/a	15.86	44.11	49.32
P1.380.6.KOH.1	1.75	1.26	0.13	0.41	103.28	12.61	39.57	57.07
P1.330.4.KOH.0,5	2.69	0.59	0.02	0.39	96.72	1.50	37.66	59.94

[a] Deviation from the mean for bio-oil and coke yields for each replica (R) in the experimental series was calculated.

The yields of bio-oil, coke, and gas obtained in Pilot Series 1 are illustrated in Figure 4.2-e.

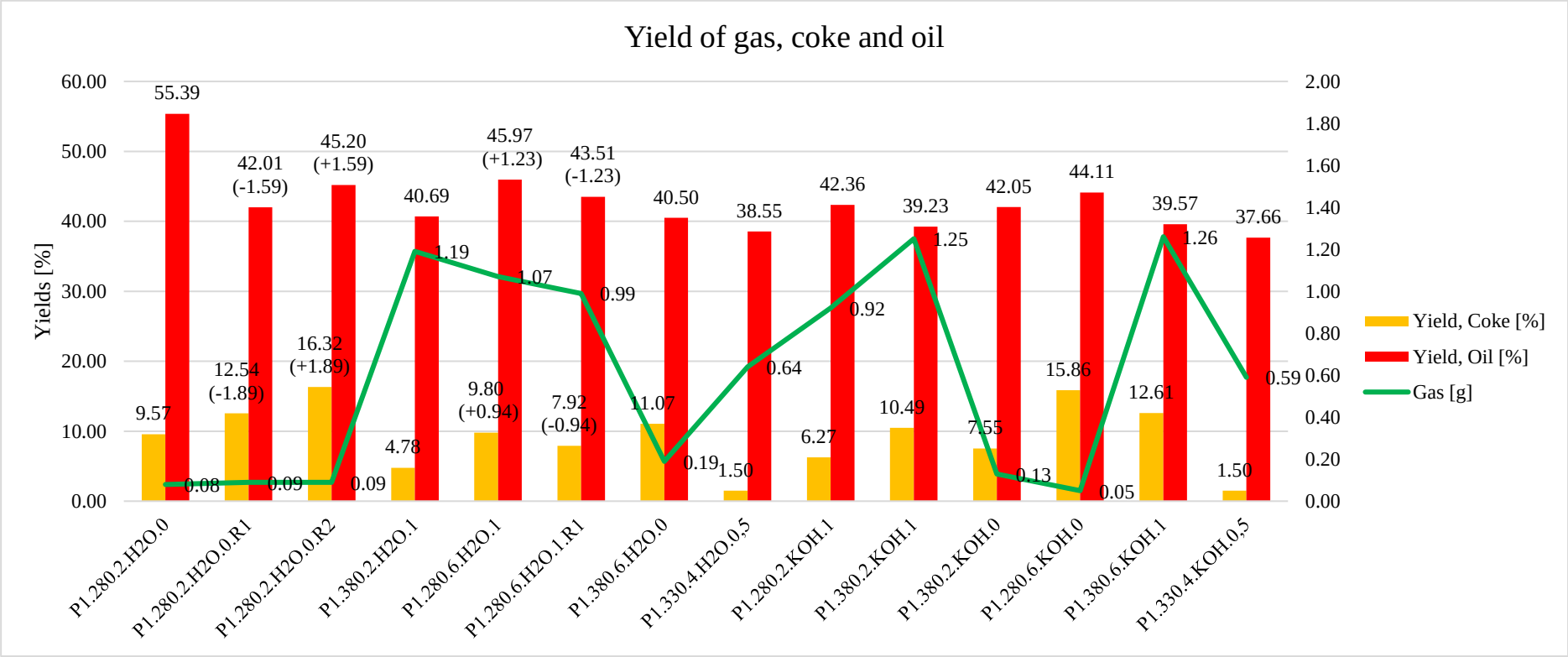

Figure 4.2-e: Yields of HTL products from Pilot Series 1. Experiment P1.280.2.H2O.0 is considered an outlier. Deviation from the mean for bio-oil and coke yields for each replica (R) are included, in brackets.

4.2.2 MULTIVARIATE ANALYSIS

The two types of multivariate analysis methods, principal component analysis (PCA) and partial least squares regression (PLSR), were used to determine correlations between variables or factors (T, t, Cat., and FA.), responses (yields of oil, coke and gas) and objects (experiments) from HTL of Pilot Series 1. Experiment P1.280.2.H2O.0 is detected as an outlier (Figure A.3-a, Appendix A). Figure 4.2-f shows a biplot from the PCA analysis of all objects (without outliers), variables, and responses in Pilot Series 1. In addition, the plot shows the effect of interaction between the variables in the form of cross-terms: Txt (temperature x time); TxFA (temperature x formic acid); txFA (time x formic acid); TxCat. (temperature x catalyst); txCat. (time x catalyst).

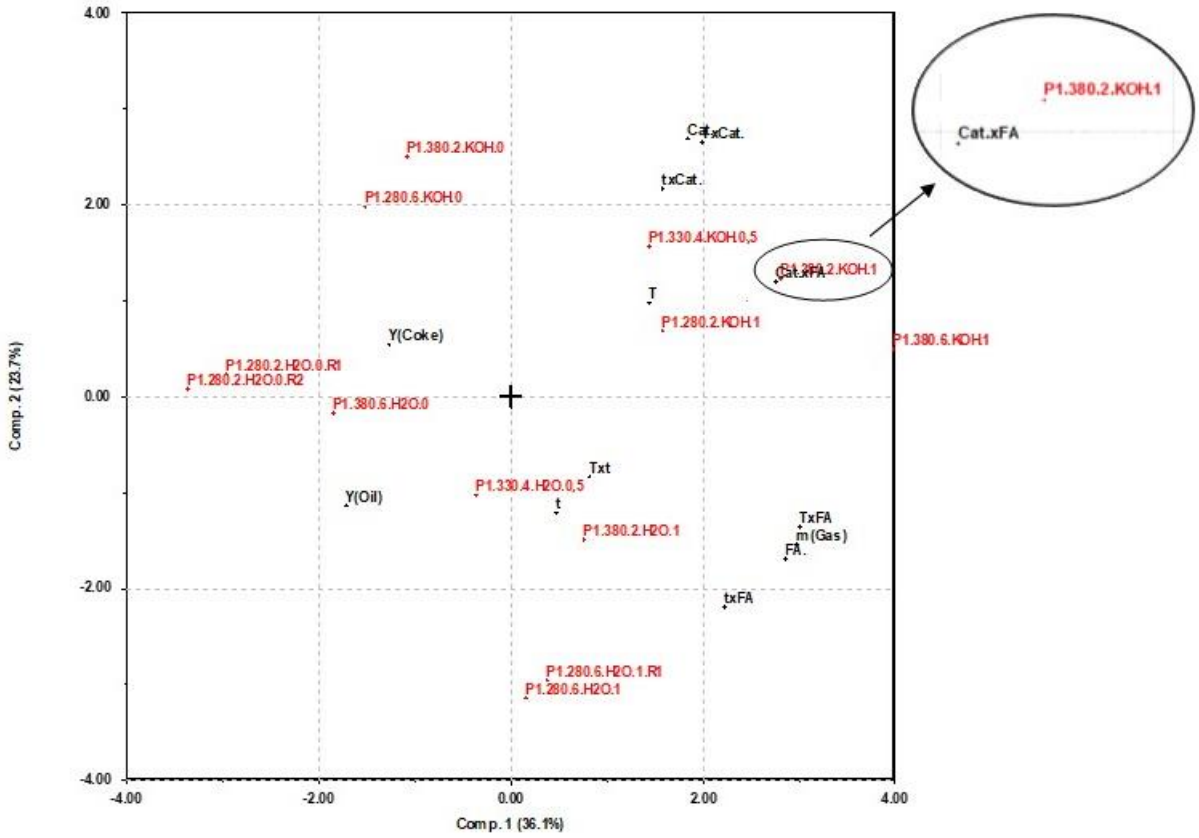

Figure 4.2-f: Biplot from the PCA analysis of all objects (without outliers), variables, and responses in Pilot Series 1, including cross-terms of the variables.

The PLS plot for predicted vs. measured values for bio-oil yields are shown in Figure 4.2-g. The PLS plots for coke and gas are presented in Figure A.3-b and Figure A.3-c, respectively, in Appendix A.

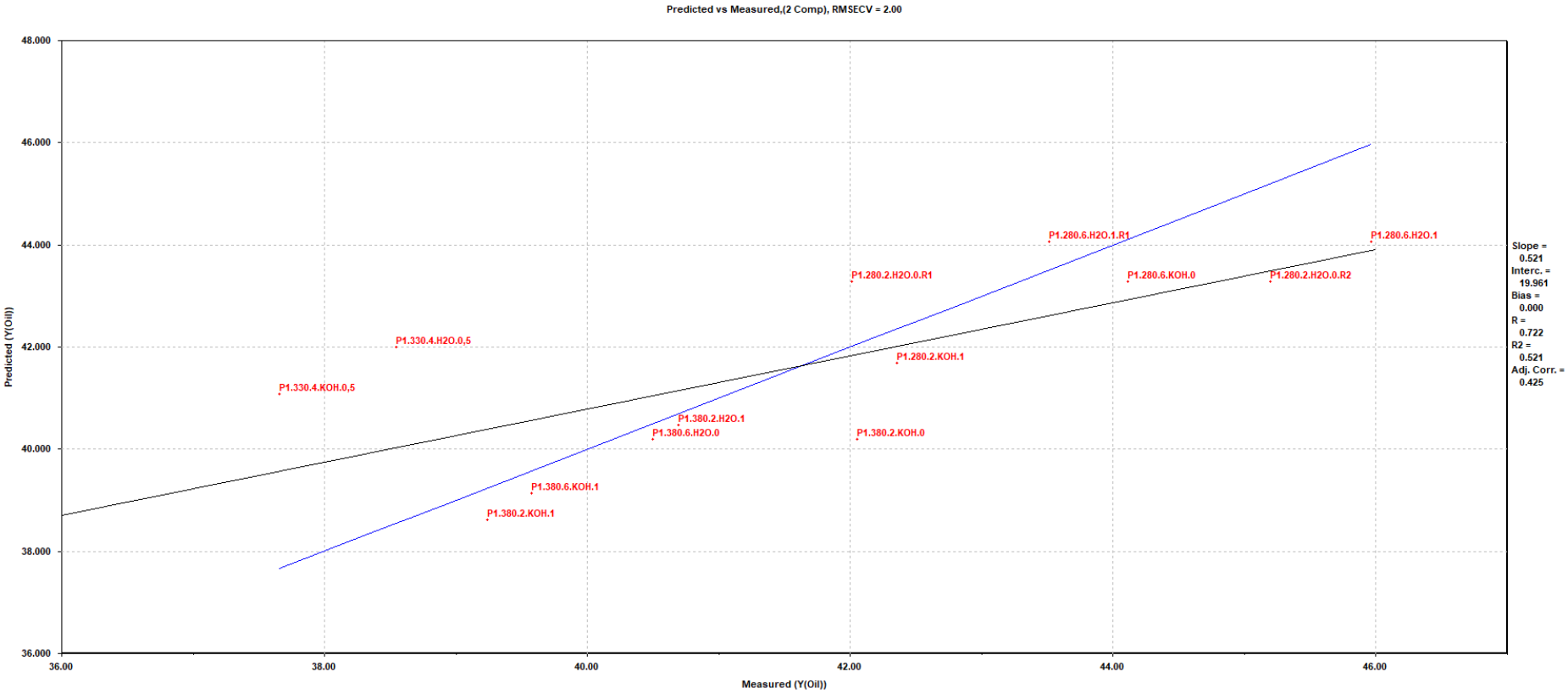

Figure 4.2-g: PLS plot of predicted vs. measured values for bio-oil yields in Pilot Series 1, without outlier.

Table 4.2-2 shows the correlation coefficients for the predicted regression equations from partial least square regression (PLSR) analysis, based on the PLS model for bio-oil, coke, and gas yields (Table 4.2-3).

Table 4.2-2: Correlation coefficients to the responses from PLSR analysis of Pilot Series 1.

Respons	R	R^2
Y_{Oil}	0.722	0.521
Y_{Coke}	0.562	0.316
m_{Gas}	0.993	0.987

Table 4.2-3: Equations to PLS model for the responses from PLSR analysis of Pilot Series 1.

Respons	Coeff.	T	t	Cat.	FA	Txt	TxCat.	TxFA	txCat.	txFA	Cat.xFA
Y_{Oil}	20.2	-0.57	-	-	-	-	-	-	-	0.12	-0.32
Y_{Coke}	2.54	-	-	-0.82	-0.61	-	-	-	0.6	-	0.53
m_{Gas}	0.22	-	-	-	0.5	-	-	0.5	-	-	-

4.2.3 Elemental analysis

EA was conducted on all the bio-oil and coke samples, including feedstock, from P1. The results for the oils and feedstock are included here since they are of main interest. For each sample, two parallels were prepared for analysis, with some exceptions where only one sample was prepared due to lack of sample or experimental errors. The results of the analysis were used to calculate moles of H, C, N, and O, and molar ratios for H/C, O/C, N/C and (O+N)/C, for the bio-oil samples (Table A.4-1 and Table A.4-2, Appendix A). The results for the elemental analysis of the oil and feedstock samples are presented in a Van Krevelen diagram, shown in Figure 4.2-f and 4.2-i. These figures illustrate how temperature and formic acid affects the bio-oil composition.

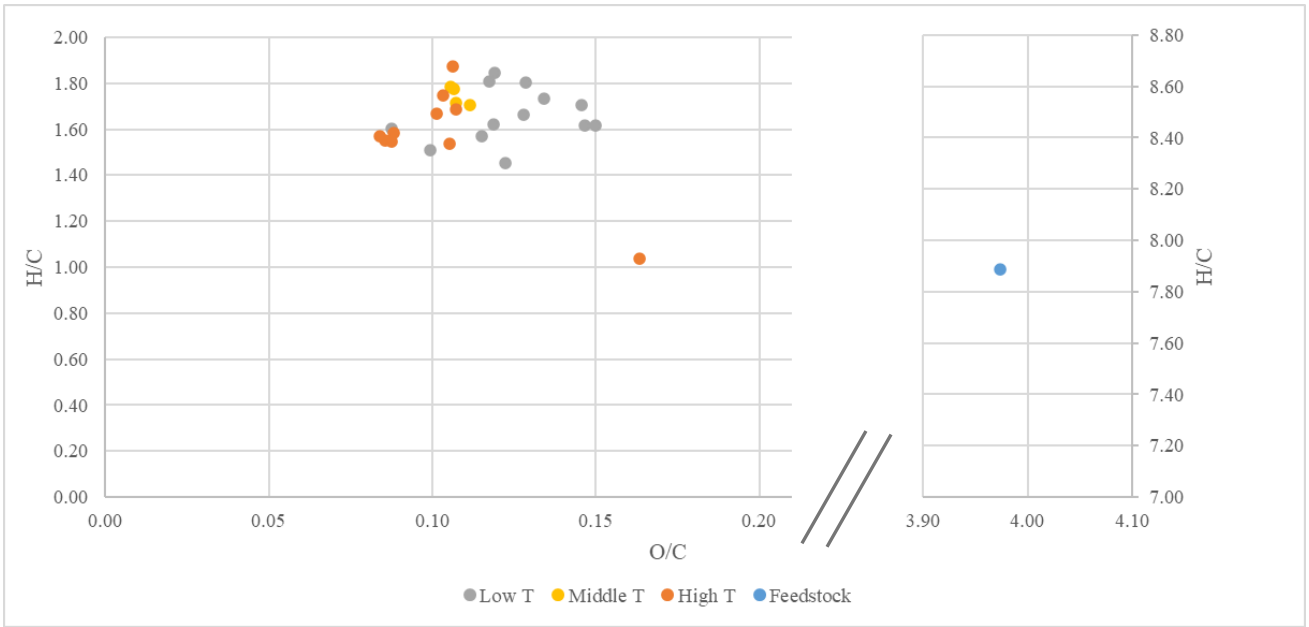

Figure 4.2-h: Van Krevelen diagram showing H/C and O/C ratios of the feedstock and bio-oil samples in Pilot Series 1. Color codings are used to illustrate how temperature affects the bio-oil composition.

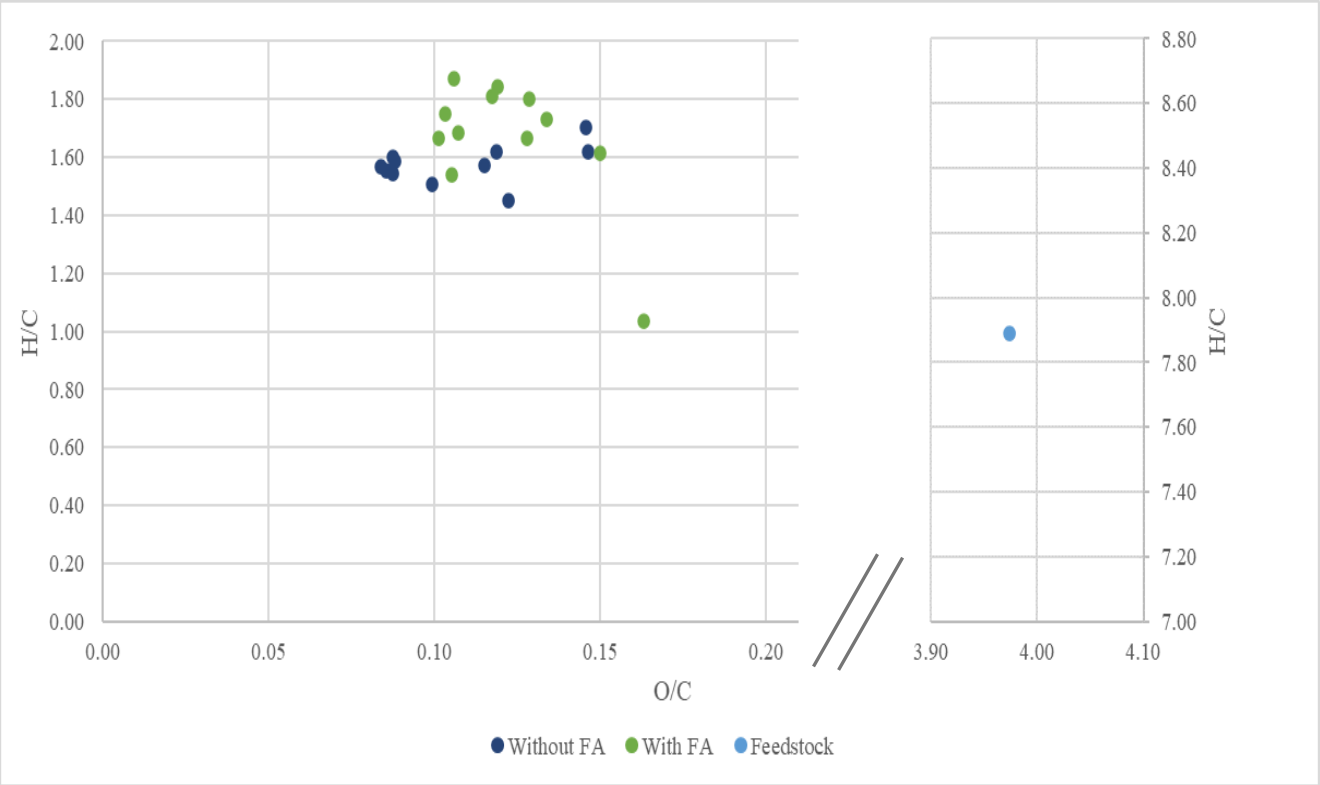

Figure 4.2-i: Van Krevelen diagram showing H/C and O/C ratios of the feedstock and bio-oil samples in Pilot Series 1. Color codings are used to illustrate how formic acid (FA) affects the bio-oil compositions.

Calculated higher heating value (HHV) and energy recovery (ER) for the feedstock and bio-oil samples in Pilot Series 1 are presented in Table 4.2-4.

Table 4.2-4: Calculated HHV and energy recovery for feedstock and bio-oil samples in Pilot Series 1.

Sample	HHV [MJ/kg]	Energy Recovery [%][a]
P1.280.2.H2O.0-oil	34.26	0.65
	33.86	0.64
P1.380.2.H2O.1-oil	31.19	0.43
	36.88	0.51
P1.280.6.H2O.1-oil	36.05	0.57
	35.88	0.56
P1.380.6.H2O.0-oil	36.66	0.51
	36.76	0.51
P1.330.4.H2O.0,5-oil	36.67	0.48
	36.25	0.48
P1.280.2.KOH.1-oil	34.20	0.49
	33.86	0.49
P1.380.2.KOH.1-oil	36.11	0.48
	36.55	0.49
P1.380.2.KOH.0-oil	36.41	0.52
	36.60	0.53
P1.280.6.KOH.0-oil	36.74	0.55
	35.00	0.53
P1.380.6.KOH.1-oil	36.09	0.49
	35.29	0.48
P1.330.4.KOH.0,5-oil	36.16	0.47
	36.63	0.47
P1.280.2.H2O.0.R1-oil	n/a	n/a
	33.82	0.49
P1.280.6.H2O.1.R1-oil	35.01	0.52
	35.45	0.53
P1.280.2.H2O.0.R2-oil	34.98	0.54
	34.97	0.54
P1 - Feedstock	7.65	n/a
	n/a	n/a

[a] Calculated using HHV value for feedstock from Table 4.2-4.

4.2.4 GC-MS

Several tests were performed, using the two experimental tests from the HTL procedure, for the purpose of finding a suited internal standard (IS) in appropriate concentration, that are easily distinguishable from the bio-oil components. These GC-MS tests are not included in the GC-results for this pilot series. Methyl nonadecanoate, in different concentrations were, examined as IS. The GC-chromatograms from these tests showed that methyl nonadecanoate functions poorly as IS for these oil samples, as its signal overlapped with other oil peaks in the chromatogram. New GC-MS samples were conducted using two different internal standards in different concentrations: one that is silylated – to see the effectiveness of the silylation; and one that is not silylated. Benzoic acid and dodecane were chosen as internal

standards for this purpose. The GC chromatograms obtained from these tests showed that both dodecane and benzoic acid were suitable as internal standards for semi-quantitative analysis of the oil-samples. An IS concentration of approximately 0.030 mg/mL for each IS was considered appropriate in the GC-MS analysis with approximately 1.0 mg/mL bio-oil concentration.

Table 4.2-5 gives an overview of the compounds identified in the chromatograms of the bio-oil experiments in P1. A cross (X) represents the presence of the associated compounds, identified by use of NIST database, based on GC-peak. Two crosses are used in the case of two peaks for isomeric compounds. For convenience, the isomers are illustrated in cis-configuration in all the GC-chromatograms.

Table 4.2-5: Overview of identified components for bio-oils produced from HTL in Pilot Series 1.

Designation	Formula	P1.280.2.H2O.0	P1.280.2.H2O.0.R1	P1.380.2.H2O.1	P1.280.6.H2O.1	P1.280.6.H2O.1.R1	P1.380.6.H2O.0	P1.330.4.H2O.0,5	P1.280.2.KOH.1	P1.380.2.KOH.1	P1.380.2.KOH.0	P1.280.6.KOH.0	P1.380.6.KOH.1	P1.330.4.KOH.0,5
3-Ethylphenol, trimethylsilyl ether	**C11H18OSi**			X				X			X		X	X
Glycerol, tris(trimethylsilyl) ether	**C12H32O3Si3**	X	X		X	X		X	X			X		X
Silane, (dodecyloxy) trimethyl-	**C15H34OSi**		X	X	X		X	X	X	X				
Tetradecanoic acid, trimethylsilyl ester	**C17H36O2Si**	X	X	X	X	X	X	X		X	X	X	X	X
9-Hexadecenoic acid, trimethylsilyl ester	**C19H38O2Si**	X,X	X,X	X,X		X,X		X,X	X,X	X,X	X,X	X,X	X	X,X
Hexadecanoic acid, trimethylsilyl ester	**C19H40O2Si**	X	X	X	X	X	X	X	X	X	X	X	X	X
Octadecanoic acid, trimethylsilyl ester	**C21H44O2Si**			X	X		X	X		X	X		X	X
***N,N*-Dimethyl dodecanamide**	**C14H29NO**			X				X		X	X	X	X	X
Octadecanamide, N-butyl-	**C22H45NO**											X		
Hexadecanoic acid, 2,3-bis[(trimethylsilyl) oxy] propyl ester	**C25H54O4Si2**	X												

Figure 4.2-j shows the GC-chromatogram for bio-oil experiment P1.280.2.H2O.0. The peaks analyzed are numbered with the associated compound inserted directly into the chromatogram. The compounds were sketched using ChemDraw 21.0.0. The semi-quantitative analysis of the GC-chromatograms for the oil-samples, based on area under the peaks, are shown in Table A.5-2, in Appendix A. The semi-quantitative analysis of the bio-oils samples, relative to dodecane and benzoic acid are illustrated in Figure 4.2-k and 4.2-l, respectively.

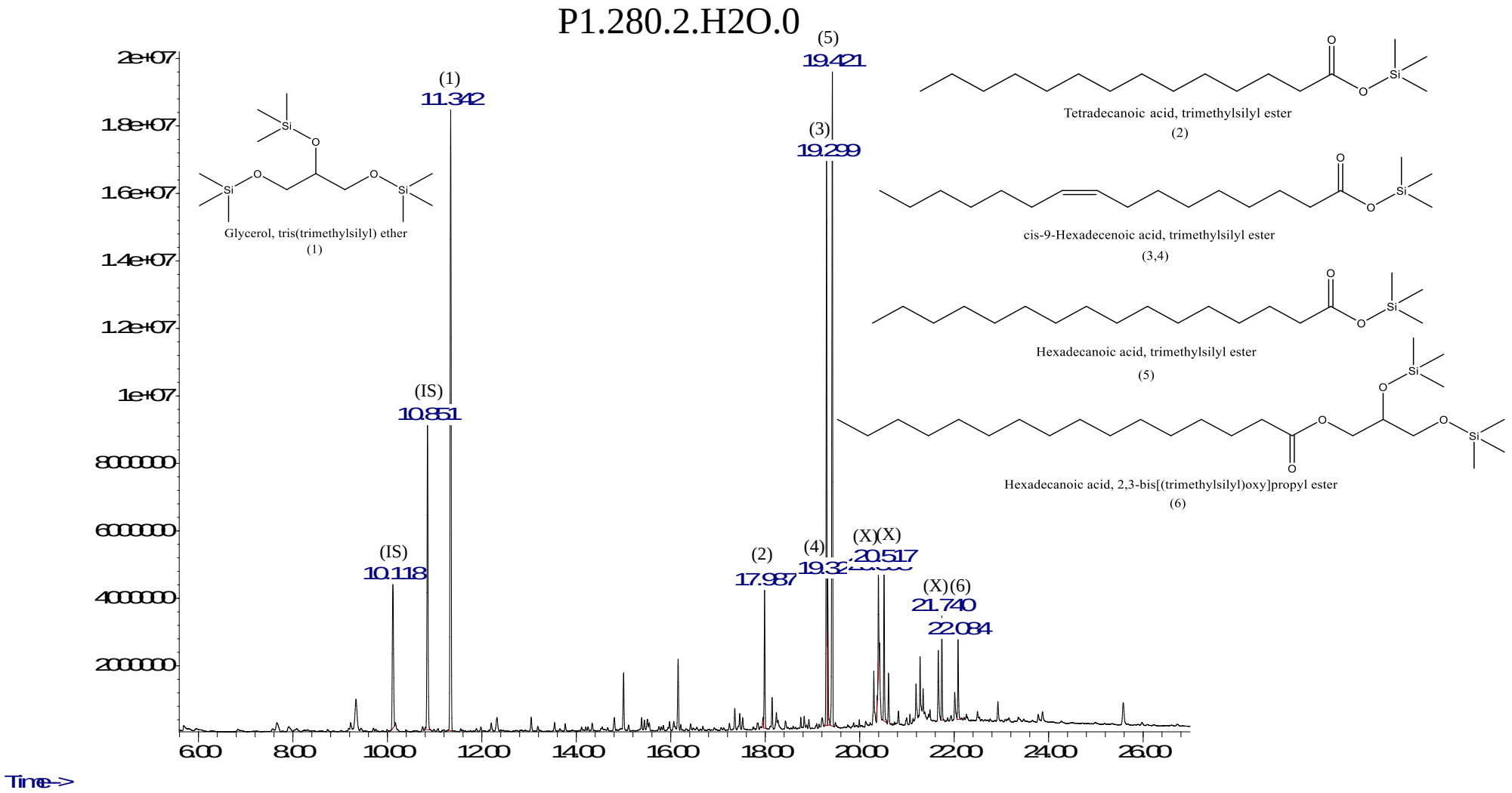

Figure 4.2-j: GC-MS chromatogram of bio-oil experiment P1.280.2.H2O.0. Dodecane and benzoic acid were used as internal standards (IS). (X) marks unidentified peaks.

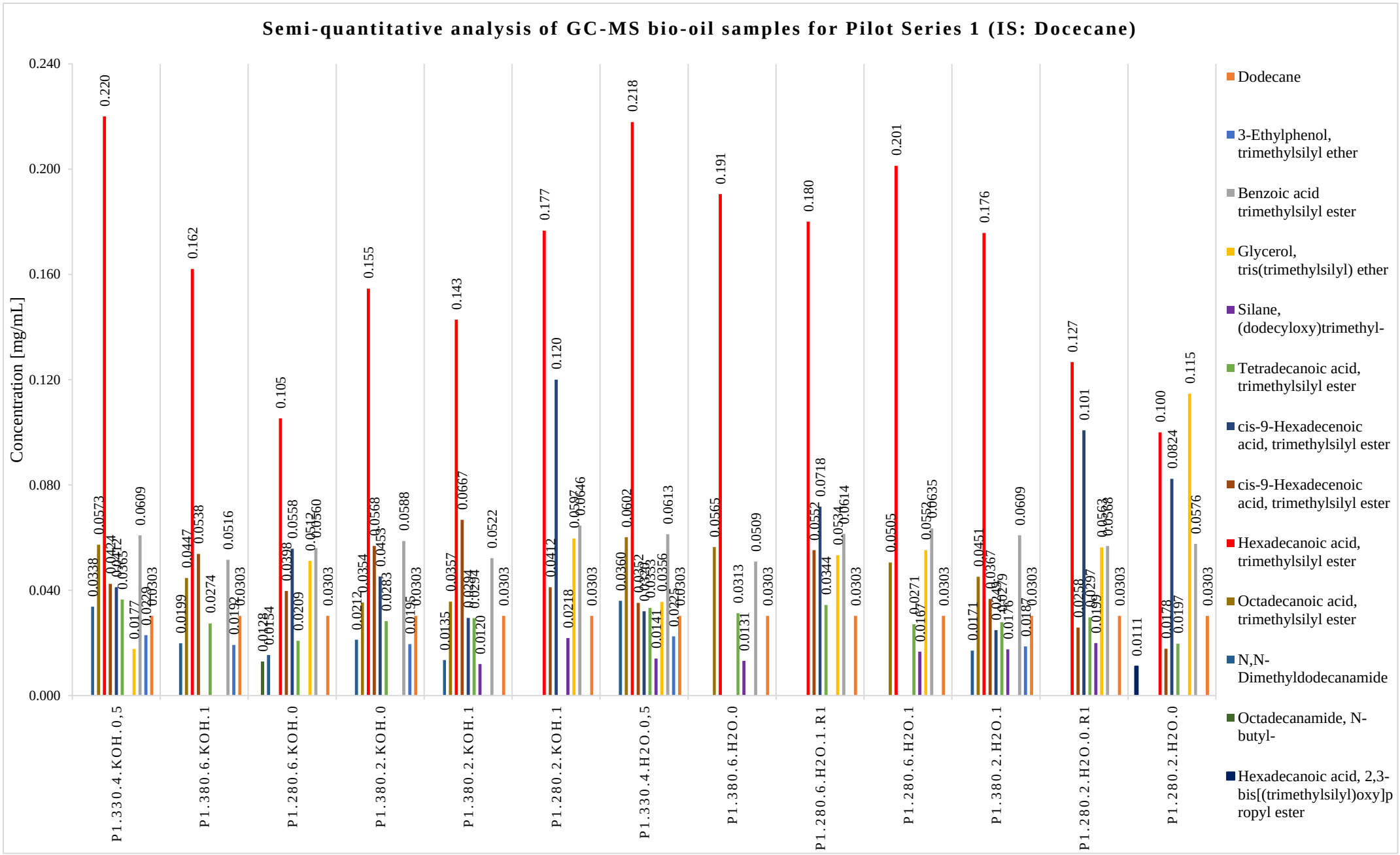

Figure 4.2-k: Semi-quantitative analysis of GC-MS bio-oil samples for Pilot Series 1, relative to dodecane as internal standard.

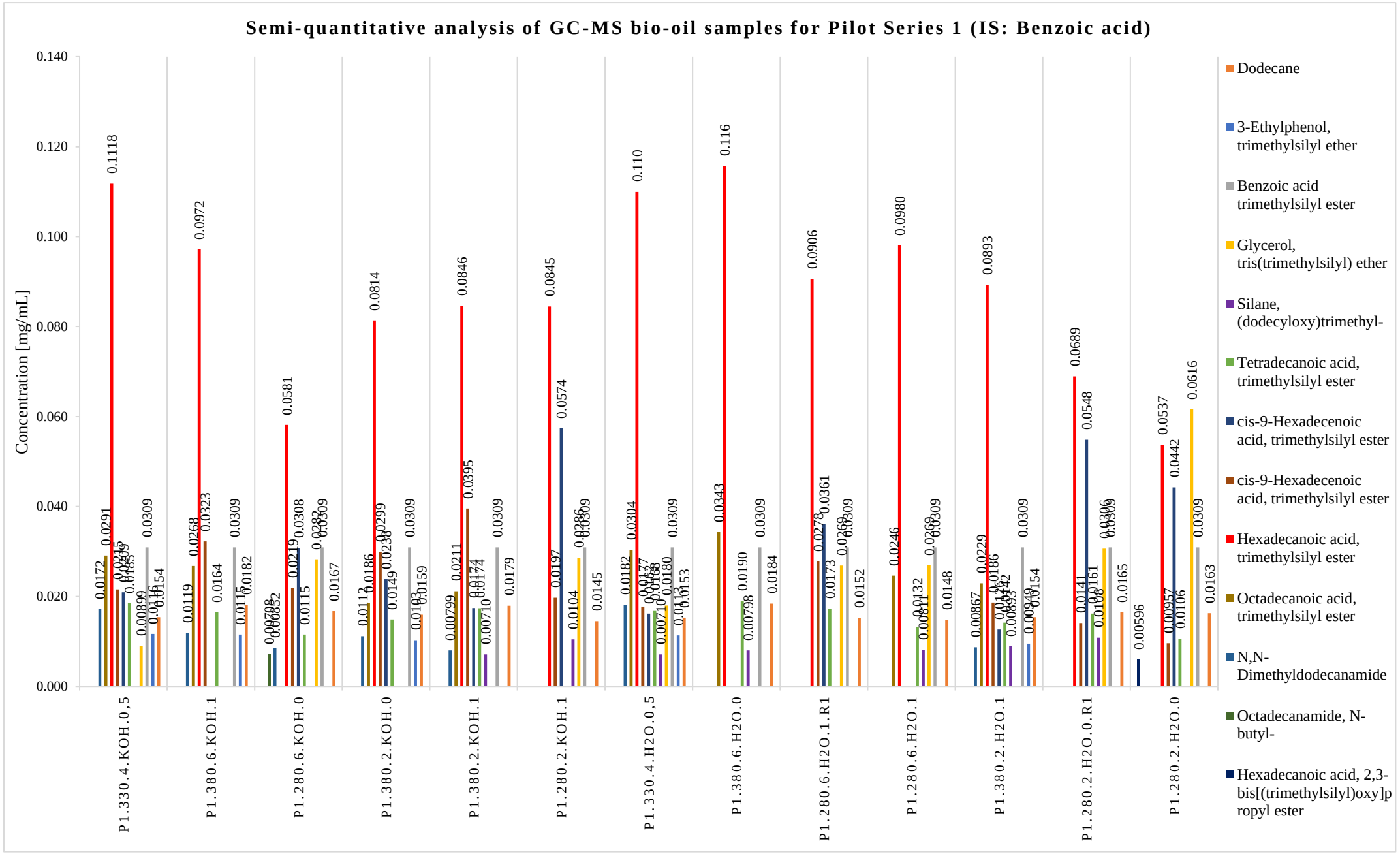

Figure 4.2-l: Semi-quantitative analysis of GC-MS bio-oil samples for Pilot Series 1, relative to benzoic acid as internal standard.

4.2.5 FT-IR

Qualitative analysis with IR was performed to determine the presence of some of the characteristic functional groups found for bio-oil samples in Pilot Series 1. IR-spectra of the coke samples are included in Appendix A for comparison of coke experiments. Table 4.2-6 shows theoretical and observed infrared absorption frequencies of functional groups from the IR-spectra for the bio-oils samples in Pilot Series 1. A comparison of the IR spectra for the oil experiment with all high vs. all low levels in terms of the selected operational parameters in HTL are shown in Figure 4.2-m. The collection of the IR spectra can be found in Appendix A.

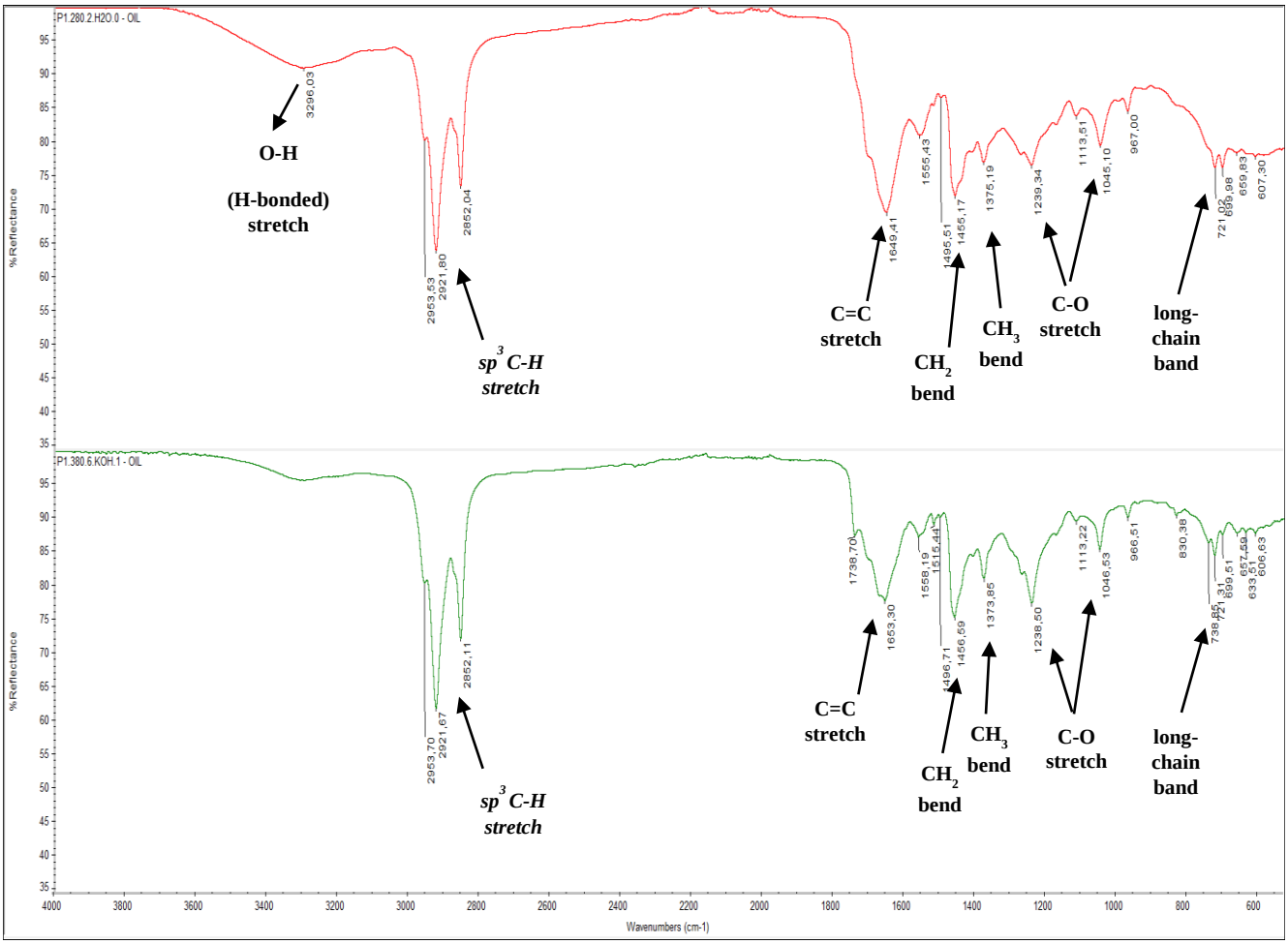

Figure 4.2-m: Comparison of the IR spectra for bio-oil sample with all high levels [(+)(+)(+)(+)] (green) and all low levels [(-)(-)(-)(-)](red).

Table 4.2-6: IR – analysis for bio-oils in Pilot Series 1

		Functional groups						
		Alkanes				**Alkenes**	**Alcohols**	
		***sp3* C-H stretch**	**-CH_2 bend**	**-CH_3 bend**	**Long-chain band**	**C=C stretch**	**C-O stretch**	**O-H stretch (H-bonded)**
Experiments	**Theoretic value[a] [cm^{-1}]**	3000-2850 (s)	1450 (m)	1375 (m)	720 (s)	1680-1600 (m-w)	1260-1000 (s)	3400-3200 (m)
P1.280.2.H2O.0	**Observed value [cm^{-1}]**	2921.80 (s) and 2852.04 (s)	1455.17 (w)	1375.19 (m)	721.02 (m)	1649.41 (s)	1239.34 (m) and 1045.10 (m)	3296.03 (w)
P1.280.2.H2O.0.R1	**Observed value [cm^{-1}]**	2920.45 (s) and 2851.22 (s)	1455.68 (s)	1375.96 (m)	719.57 (m)	1647.34 (s)	1240.91 (m) and 1045.38 (m)	3293.15 (w)
P1.380.2.H2O.1	**Observed value [cm^{-1}]**	2921.55 (s) and 2851.95 (s)	1456.19 (s)	1375.80 (m)	721.23 (m)	1654.55 (s)	1239.43 (m) and 1046.72 (m)	3295.96 (w)
P1.280.6.H2O.1	**Observed value [cm^{-1}]**	2921.45 (s) and 2851.84 (s)	1455.71 (s)	1373.86 (m)	721.12 (m)	1654.03 (s)	1238.83 (s) and 1046.14 (m)	3292.87 (w)
P1.280.6.H2O.1.R1	**Observed value [cm^{-1}]**	2921.75 (s) and 2852.07 (s)	1456.07 (s)	1376.72 (m)	721.42 (m)	1653.83 (s)	1240.07 (m) and 1046.57 (m)	3304.49 (w)
P1.380.6.H2O.0	**Observed value [cm^{-1}]**	2921.43 (s) and 2851.82 (s)	1456.49 (m)	1373.26 (m)	741.62 (m)	1669.23 (m)	1238.29 (s) and 1045.89 (m)	3202.75 (w)
P1.330.4.H2O.0,5	**Observed value [cm^{-1}]**	2921.30 (s) and 2851.80 (s)	1456.01 (s)	1376.74 (m)	721.30 (m)	1650.60 (s)	1268.72 (m) and 1048.38 (m)	3290.67 (w)
P1.280.2.KOH.1	**Observed value [cm^{-1}]**	2921.70 (s) and 2852.00 (s)	1455.40 (s)	1377.51 (m)	721.48 (m)	1654.79 (s)	1046.31 (m)	3269.36 (w)
P1.380.2.KOH.1	**Observed value [cm^{-1}]**	2921.55 (s) and 2851.96 (s)	1456.11 (s)	1376.84 (m)	721.51 (m)	1652.58 (s)	1268.78 (m) and 1049.34 (w)	3288.74 (w)
P1.380.2.KOH.0	**Observed value [cm^{-1}]**	2953.95 (s) and 2851.64 (s)	1456.01 (m)	1376.47 (m)	740.10 (m)	1651.92 (m)	1267.66 (m) and 1060.64 (w)	3279.32 (w)
P1.280.6.KOH.0	**Observed value [cm^{-1}]**	2953.63 (s) and 2851.34 (s)	1455.73 (2)	1376.34 (m)	720.66 (m)	1646.50 (s)	1269.11 (m) and 1047.08 (m)	3291.94 (w)
P1.380.6.KOH.1	**Observed value [cm^{-1}]**	2921.67 (s) and 2852.11 (s)	1456.59 (m)	1373.85 (m)	738.85 (m)	1653.30 (m)	1238.50 (m) and 1046.53 (m)	n/a
P1.330.4.KOH.0,5	**Observed value [cm^{-1}]**	2921.24 (s) and 2851.77 (s)	1456.31 (s)	1377.01 (m)	738.78 (m)	1652.42 (m)	1269.14 (m) and 1057.96 (m)	3292.30 (w)

[a] Based on an infrared spectral correlation chart from *"Introduction to spectroscopy"* by Pavia et al. [86, p. 29].

4.3 PILOT SERIES 2

4.3.1 HTL

The operational parameters being investigated in Pilot Series 2 (P2) are presented in Table 3.3-3. In this series, a total of 10 experiments, including two replicas (R) were conducted. Pictures from the HTL-workup of bio-oil and coke samples from P2 are shown in Figure 4.3-a.

Figure 4.3-a: Pictures of the oil (diluted in solvent) and coke samples from the experimental work-up from P2.

The HTL products obtained in P2 were gas, coke, bio-oil, and an aqueous phase. The yields of bio-oil and other products are presented in Table 4.3-1. Experiment P2.280.6.H2O.0 is considered an outlier but is included to show a full display of the pilot series. Like for P1, the yields of gas products, are represented as weight mass of the gaseous products in Figure 4.3-b. Raw data from the HTL workup is presented in Table B.1-1 in Appendix B.

Table 4.3-1: Yields for HTL-products in Pilot Series 2.

Experiment	**Aq. ph. [g]**	**Gas [g]**	**Coke [g]**	**Oil [g]**	**Y_{Gas} [%]**	**Y_{Coke} [%][a]**	**Y_{Oil} [%][a]**	**Y_{Total} [%]**
P2.220.2.H2O.0	2.10	0.06	0.31	0.38	n/a	29.73	36.36	47.30
P2.280.2.H2O.1	1.03	0.97	0.27	0.48	79.5	26.05	45.72	44.14
P2.220.6.H2O.1	1.21	0.79	0.16	0.49	64.8	15.50	47.26	42.52
P2.280.6.H2O.0	2.76	0.10	0.12	0.66	n/a	11.38 (-0.57)	62.75 (+8.58)	60.44
P2.280.6.H2O.0.R1	1.73	0.08	0.13	0.48	n/a	12.51 (+0.57)	45.59 (-8.58)	40.18
P2.220.2.H2O.1	1.58	0.46	0.24	0.52	37.7	22.65 (-0.60)	49.75 (-4.44)	44.72
P2.220.2.H2O.1.R1	1.22	0.50	0.25	0.61	41.0	23.86 (+0.60)	58.64 (+4.44)	41.45
P2.280.2.H2O.0	1.30	0.04	0.14	0.47	n/a	13.71	44.77	32.35
P2.220.6.H2O.0	1.45	0.07	0.23	0.43	n/a	22.19	41.25	36.40
P2.280.6.H2O.1	2.58	1.02	0.17	0.47	83.6	16.59	45.32	68.23
P2.250.4.H2O.0	1.13	0.08	0.17	0.47	n/a	16.08	44.95	30.80
P2.250.4.H2O.1	1.75	0.91	0.14	0.47	74.6	13.29	44.89	52.50

[a] Deviation from the mean for bio-oil and coke yields for each replica (R) in the experimental series was calculated.

The yields of bio-oil, coke, and gas obtained in Pilot Series 2 are illustrated in Figure 4.3-b.

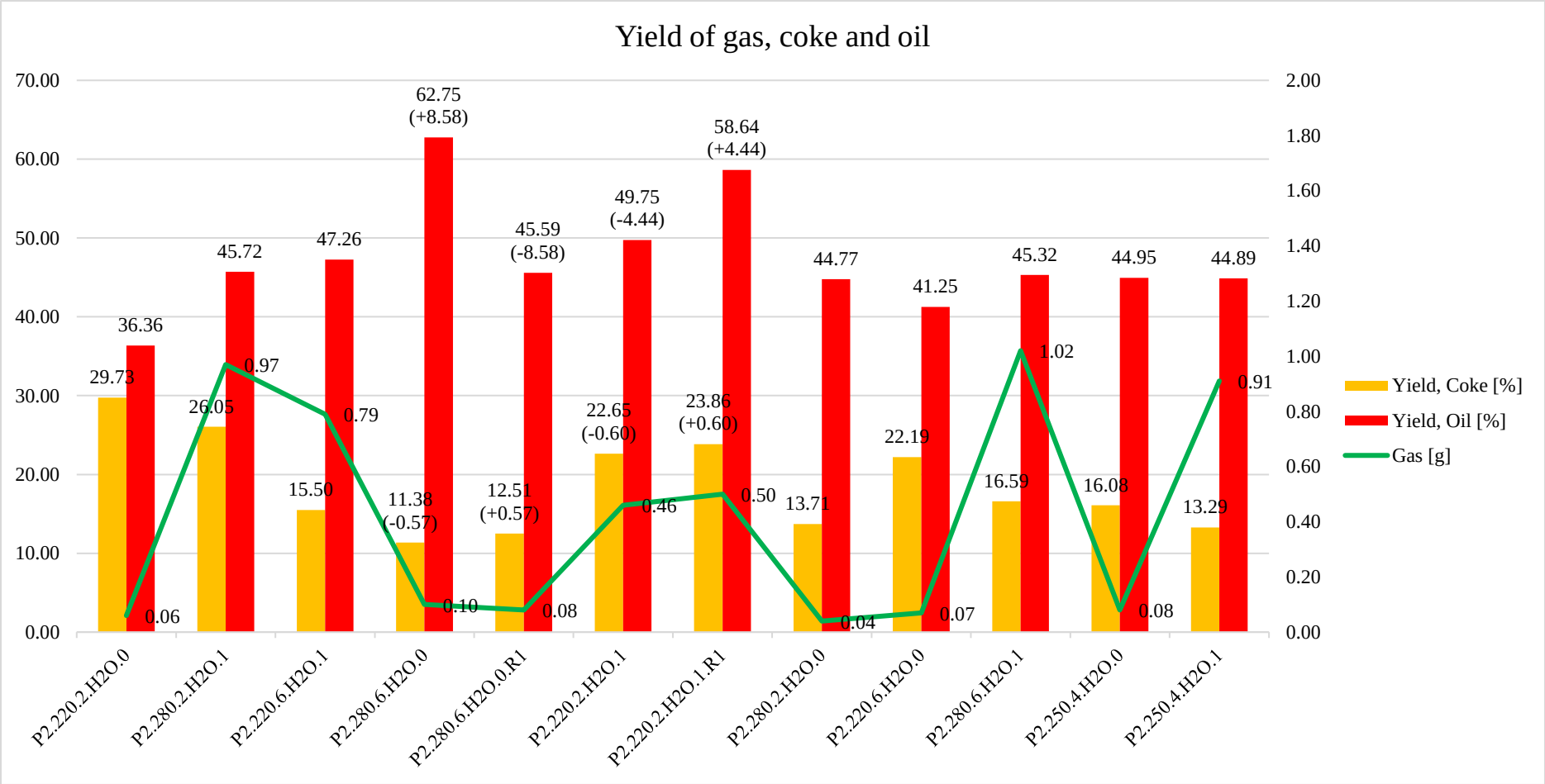

Figure 4.3-b: Yields of HTL products from Pilot Series 2. Experiment P2.280.6.H2O.0 is considered an outlier. Deviation from the mean for bio-oil and coke yields for each replica (R) are included, in brackets.

4.3.2 MULTIVARIATE ANALYSIS

Principal component analysis (PCA) and partial least squares regression (PLSR) were conducted on the HTL samples of gas, coke, and bio-oil from Pilot Series 2. Experiment P2.280.6.H2O.0 is classified as an outlier (Figure B.2-a, Appendix B). Figure 4.3-c shows a biplot from the PCA analysis of all objects (without outliers), variables, and responses in Pilot Series 2. In addition, the plot shows the effect of interaction between the variables in the form of cross-terms: Txt (temperature x time); TxFA (temperature x formic acid); txFA (time x formic acid).

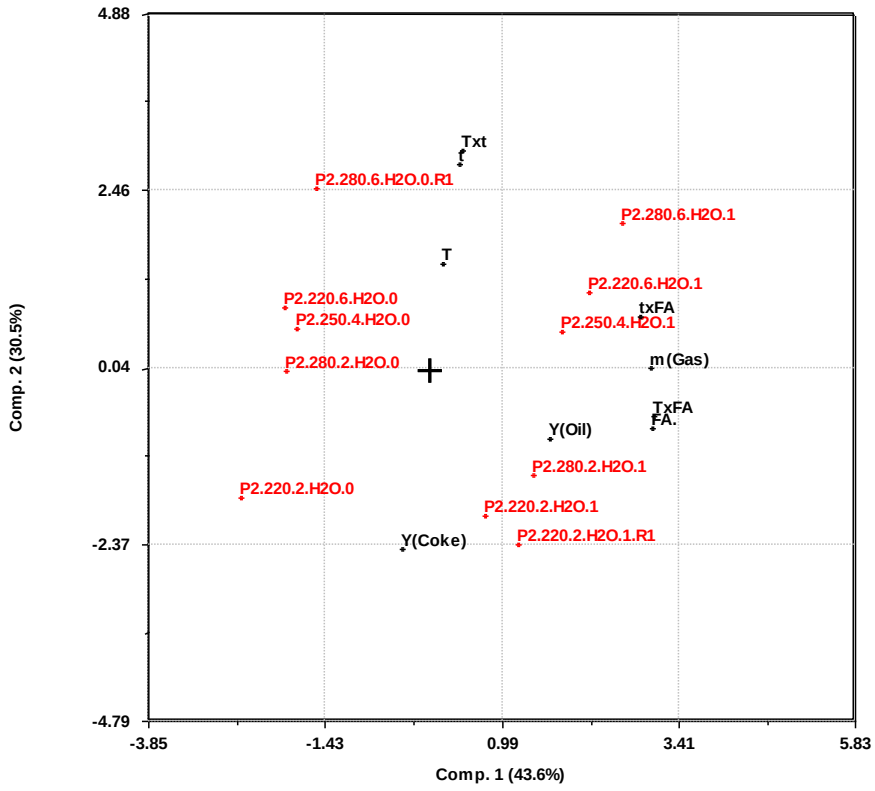

Figure 4.3-c:Biplot from the PCA analysis of all objects (without outliers), variables, and responses in Pilot Series 2, including cross-terms of the variables.

The PLS plot for predicted vs. measured values for bio-oil yields are shown in Figure 4.3-d. PLS plots for coke and gas are presented in Figure B.2-b and Figure B.2-c, respectively, in Appendix B.

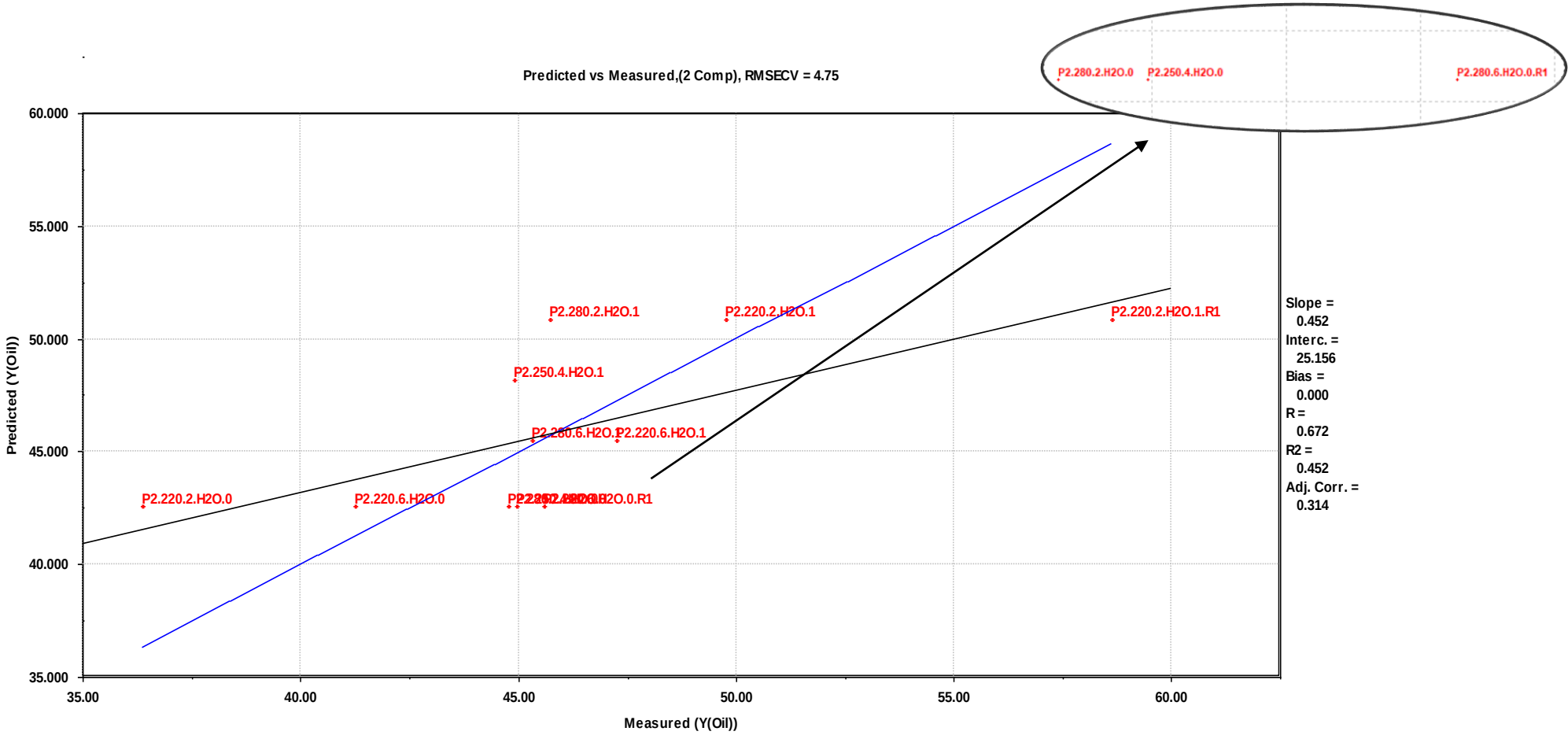

Figure 4.3-d: PLS plot of predicted vs. measured values for all bio-oil yields, without outliers, in Pilot Series 2.

Table 4.3-2 shows the correlation coefficients for the predicted regression equations from partial least square regression (PLSR) analysis, based on the PLS model for bio-oil, coke, and gas yields (Table 4.3-3).

Table 4.3-2: Correlation coefficients to the responses from PLS analysis of Pilot Series 2.

Respons	R	R^2
$\mathbf{Y_{Oil}}$	0.672	0.452
$\mathbf{Y_{Coke}}$	0.676	0.456
$\mathbf{m_{Gas}}$	0.991	0.982

Table 4.3-3: Equations to PLS model for the responses from PLS analysis of Pilot Series 2.

Respons	Coeff.	T	t	FA.	Txt	TxFA	txFA
$\mathbf{Y_{Oil}}$	7.87	-	-	1.05	-	-	-0.59
$\mathbf{Y_{Coke}}$	6.97	-0.31	-	-	-0.51	-	-
$\mathbf{m_{Gas}}$	0.16	-	-	-1.37	-	2.05	0.31

4.3.3 ELEMENTAL ANALYSIS

EA was conducted on all the bio-oil and coke samples from P2. The result for the bio-oils is included here. For each sample, two parallels were prepared for analysis, with some exceptions where only one sample was prepared due to lack of sample or experimental errors. The results of the analysis were used to calculate moles of H, C, N, and O, and molar ratios for H/C, O/C, N/C and (O+N)/C, for the bio-oil samples (Table B.3-1 and Table B.3-2, Appendix B). The results for the elemental analysis of the oil and feedstock samples are presented in a Van Krevelen diagram, shown in Figure 4.3-e and 4.3-f. These figures illustrate how temperature and formic acid affects the bio-oil composition.

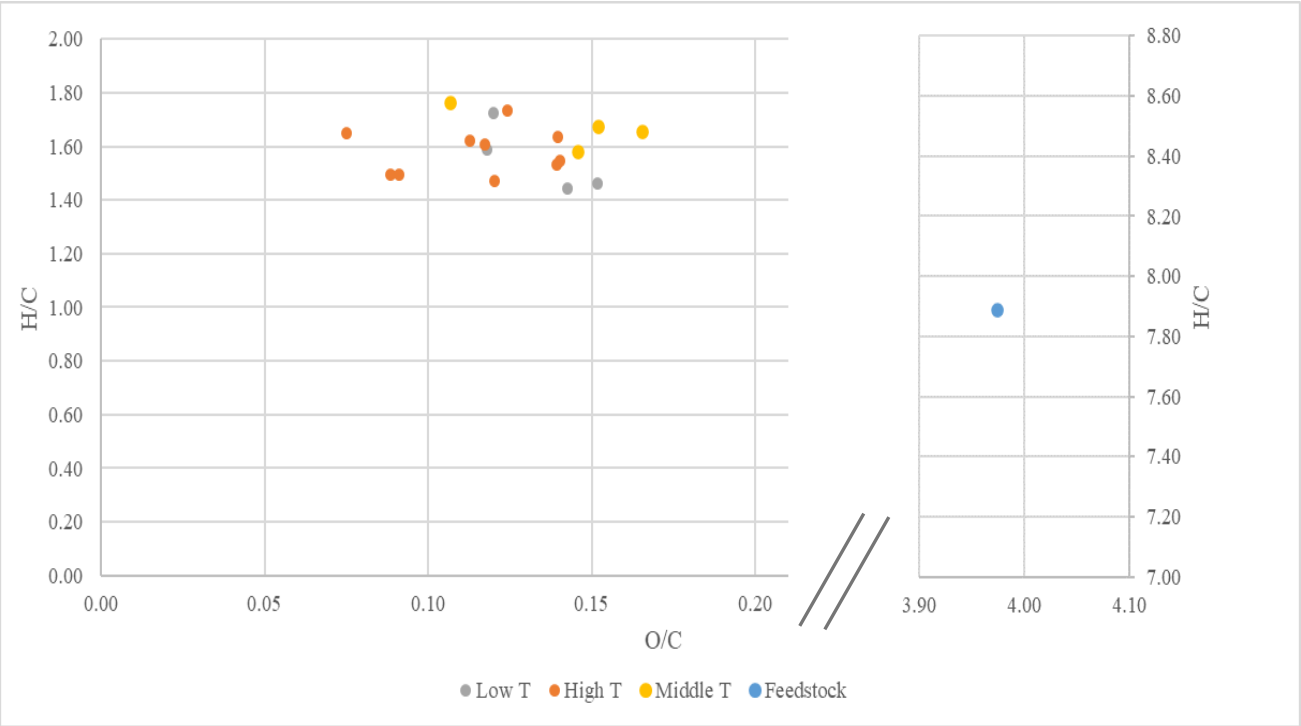

Figure 4.3-e: Van Krevelen diagram showing H/C and O/C ratios of the feedstock and bio-oil samples in Pilot Series 2. Color codings are used to illustrate how temperature affects the bio-oil composition.

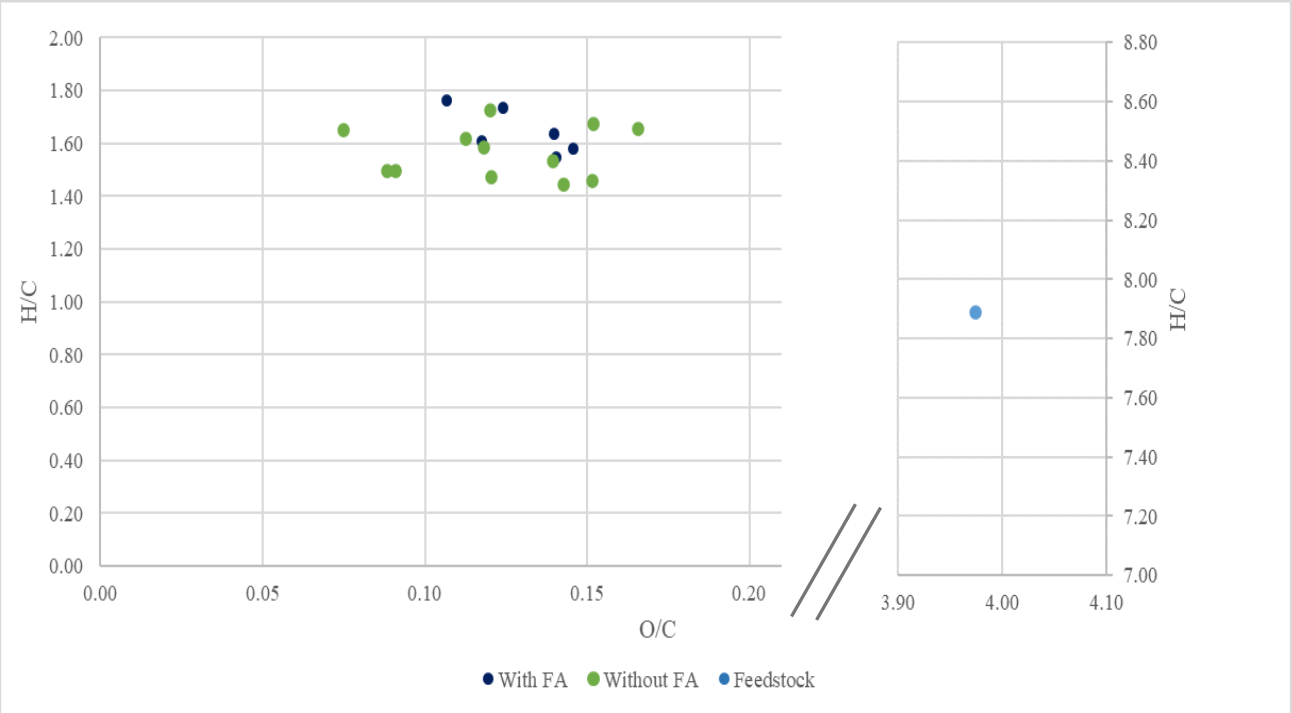

Figure 4.3-f: Van Krevelen diagram showing H/C and O/C ratios of the feedstock and bio-oil samples in Pilot Series 2. Color codings are used to illustrate how formic acid (FA) affects the bio-oil compositions.

Calculated higher heating value (HHV) and energy recovery (ER) for the bio-oil samples in Pilot Series 2 are presented in Table 4.3-4.

Table 4.3-4: Calculated HHV and energy recovery for bio-oil and feedstock samples in Pilot Series 2.

Sample	HHV [MJ/kg]	Energy Recovery [%][a]
P2.220.2.H2O.0	33.52	0.42
	33.17	0.41
P2.280.6.H2O.1	34.52	0.53
	35.55	0.55
P2.220.2.H2O.1	26.61	0.45
	25.83	0.44
P2.280.6.H2O.0	36.26	0.78
	35.64	0.76
P2.280.2.H2O.0	33.74	0.52
	35.46	0.54
P2.250.4.H2O.1	34.22	0.52
	36.73	0.56
P2.280.2.H2O.1	35.20	0.55
	34.83	0.54
P2.220.6.H2O.0	34.94	0.49
	35.58	0.50
P2.250.4.H2O.0	34.38	0.53
	33.15	0.51
P2.220.6.H2O.1	31.04	0.50
	31.40	0.51
P2.280.6.H2O.0.R1	35.85	0.56
	37.46	0.58
P2.220.2.H2O.1.R1	28.01	0.56
	21.91	0.44

[a] ER [%] for the bio-oil samples were calculated using HHV value for feedstock from Table 4.2-4.

4.3.4 GC-MS

Table 4.3-5 gives an overview of the compounds identified in the chromatograms of the bio-oil experiments in P2. A cross (X) represents the presence of the associated compounds, identified by use of NIST database, based on GC-peak. Two crosses are used in the case of two peaks for isomeric compounds. For convenience, the isomers are illustrated in cis-configuration in all the GC-chromatograms.

Table 4.3-5: Overview of identified components for bio-oils produced from HTL in Pilot Series 2.

Designation	Formula	P2.220.2. H2O.0	P2.280.2. H2O.1	P2.220.6. H2O.1	P2.280.6. H2O.0	P2.280.6. H2O.0.R1	P2.220.2. H2O.1	P2.220.2. H2O.1.R1	P2.280.2. H2O.0	P2.220.6. H2O.0	P2.280.6. H2O.1	P2.250.4. H2O.0	P2.250.4. H2O.1
Butanoic acid 2-(trimethylsilyl)oxy - trimethylsilyl ester	**C10H24O3Si2**			X			X	X					
Glycerol, tris(trimethylsilyl) ether	**C12H32O3Si3**	X	X	X	X	X	X	X	X	X	X	X	X
Butanedioic acid, bis(trimethylsilyl)ester	**C10H22O4Si2**			X			X	X					
Pyrimidine, 2,4-bis[(trimethylsilyl)oxy]-	**C10H20N2O2Si2**	X		X			X	X		X		X	
Silane, (1,2,4,5-cyclohexanetetrayltetraoxy)tetrakis[trimethyl-	**C18H44O4Si4**	X							X			X	
L-proline, 5-oxo-1-(trimethylsilyl)- ,trimethylsilyl ester	**C11H23NO3Si2**			X			X	X					
Tetradecanoic acid, trimethylsilyl ester	**C17H36O2Si**	X	X	X	X	X	X	X	X	X	X	X	X
9-Hexadecenoic acid, trimethylsilyl ester	**C19H38O2Si**	X	X,X	X,X	X,X	X,X	X	X	X,X	X	X,X	X	X,X
Hexadecanoic acid, trimethylsilyl ester	**C19H40O2Si**	X	X	X	X	X	X	X	X	X	X	X	X
9,12-Octadecadienoic acid *(Z,Z)*-, trimethylsilyl ester	**C21H40O2Si**	X			X								
Octadecanoic acid, trimethylsilyl ester	**C21H44O2Si**			X							X		
Dehydroabietic acid, trimethylsilyl ester	**C23H36O2Si**				X								
***N,N*-Dimethyldodecanamide**	**C14H29NO**					X							

Table 4.3-5: Overview of identified components for bio-oils produced from HTL in Pilot Series 2. Table continued.

Designation	Formula	P2.220.2. H2O.0	P2.280.2. H2O.1	P2.220.6. H2O.1	P2.280.6. H2O.0	P2.280.6. H2O.0.R1	P2.220.2. H2O.1	P2.220.2. H2O.1.R1	P2.280.2. H2O.0	P2.220.6. H2O.0	P2.280.6. H2O.1	P2.250.4. H2O.0	P2.250.4. H2O.1
Arachidonic acid, trimethylsilyl ester	**C23H40O2Si**	X					X						
Podocarp-8(14)-en-15-oic acid, 13-methyl-13-vinyl-, trimethylsilyl ester	**C23H38O2Si**				X								
***cis*-5,8,11,14,17-Eicosapentaenoic acid, trimethylsilyl ester**	**C23H38O2Si**	X					X	X		X			
Hexadecanoic acid, 2,3-bis[(trimethylsilyl)oxy]propyl ester	**C25H54O4Si2**	X											

The semi-quantitative analysis of the GC-chromatograms for the oil-samples, based on area under the peaks, are shown in Table B.5-2 (Appendix B) and illustrated in Figure 4.3-g and 4.3-h. Figure 4.3-i shows the chromatogram for the bio-oil experiment P2.220.2.H2O.0. The peaks analyzed are numbered with the corresponding compound inserted directly into the chromatogram. The compounds were sketched using ChemDraw 21.0.0.

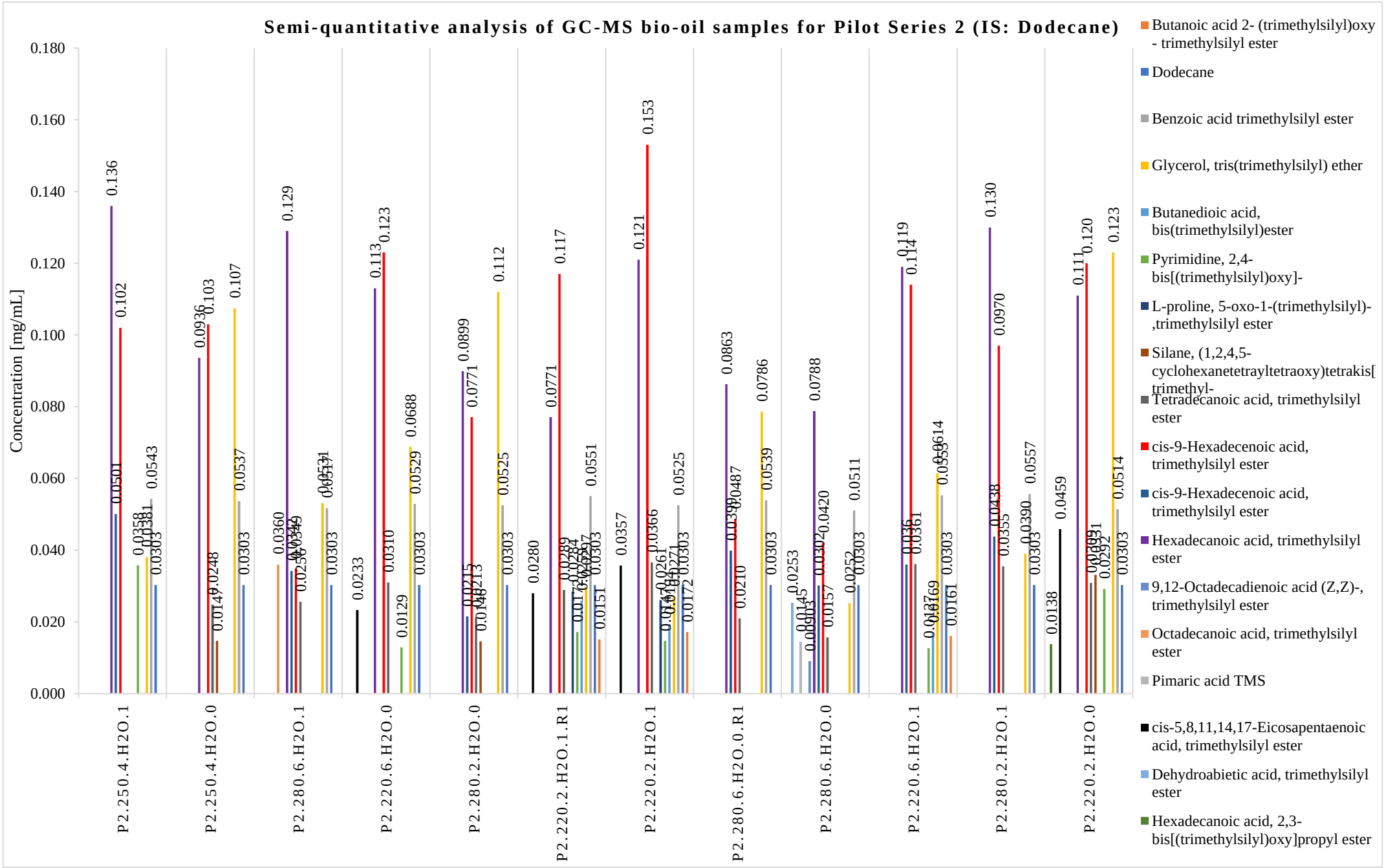

Figure 4.3-g: Semi-quantitative analysis of GC-MS bio-oil samples for Pilot Series 2, relative to dodecane as internal standard.

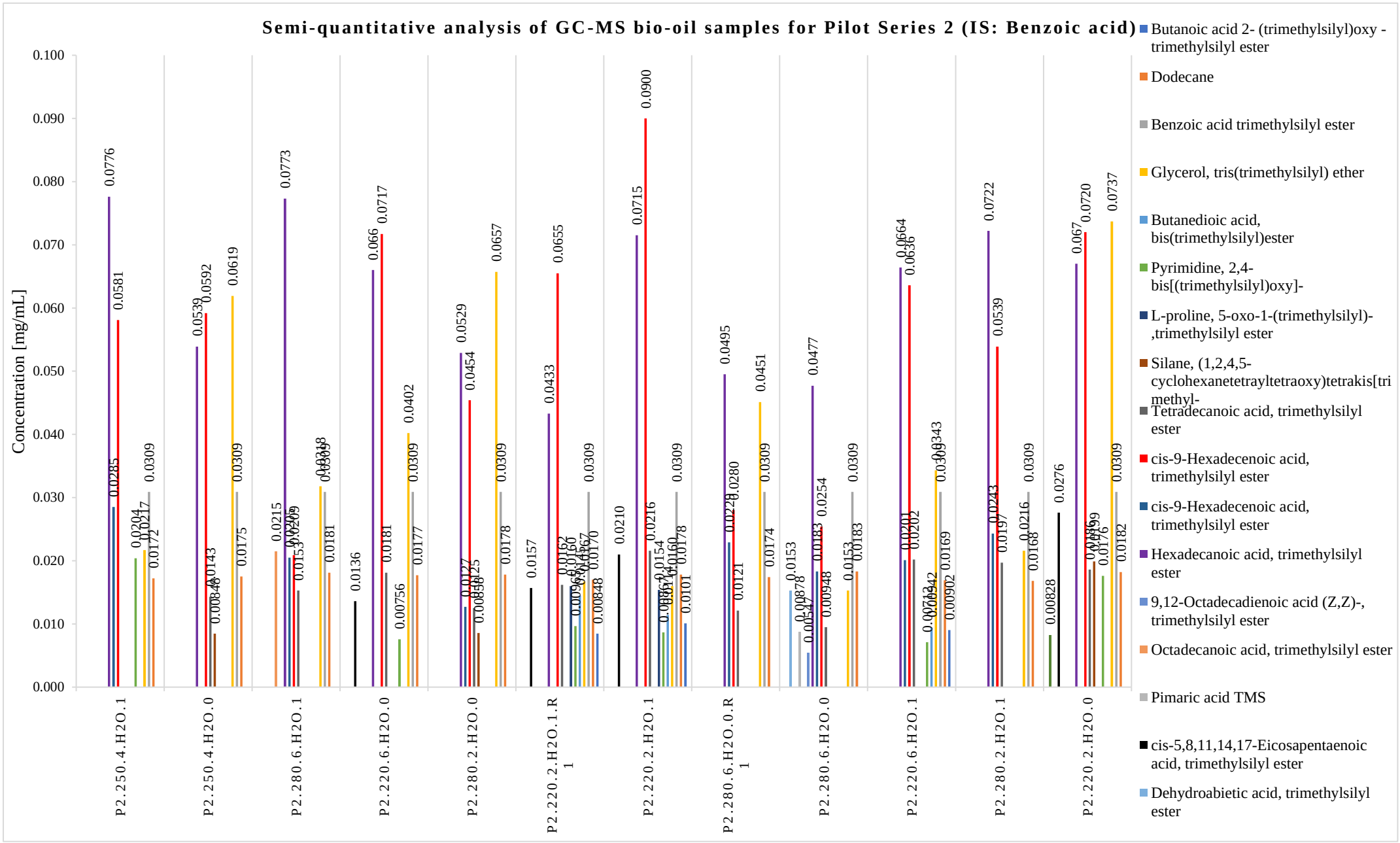

Figure 4.3-h: Semi-quantitative analysis of GC-MS bio-oil samples for Pilot Series 2, relative to benzoic acid as internal standard.

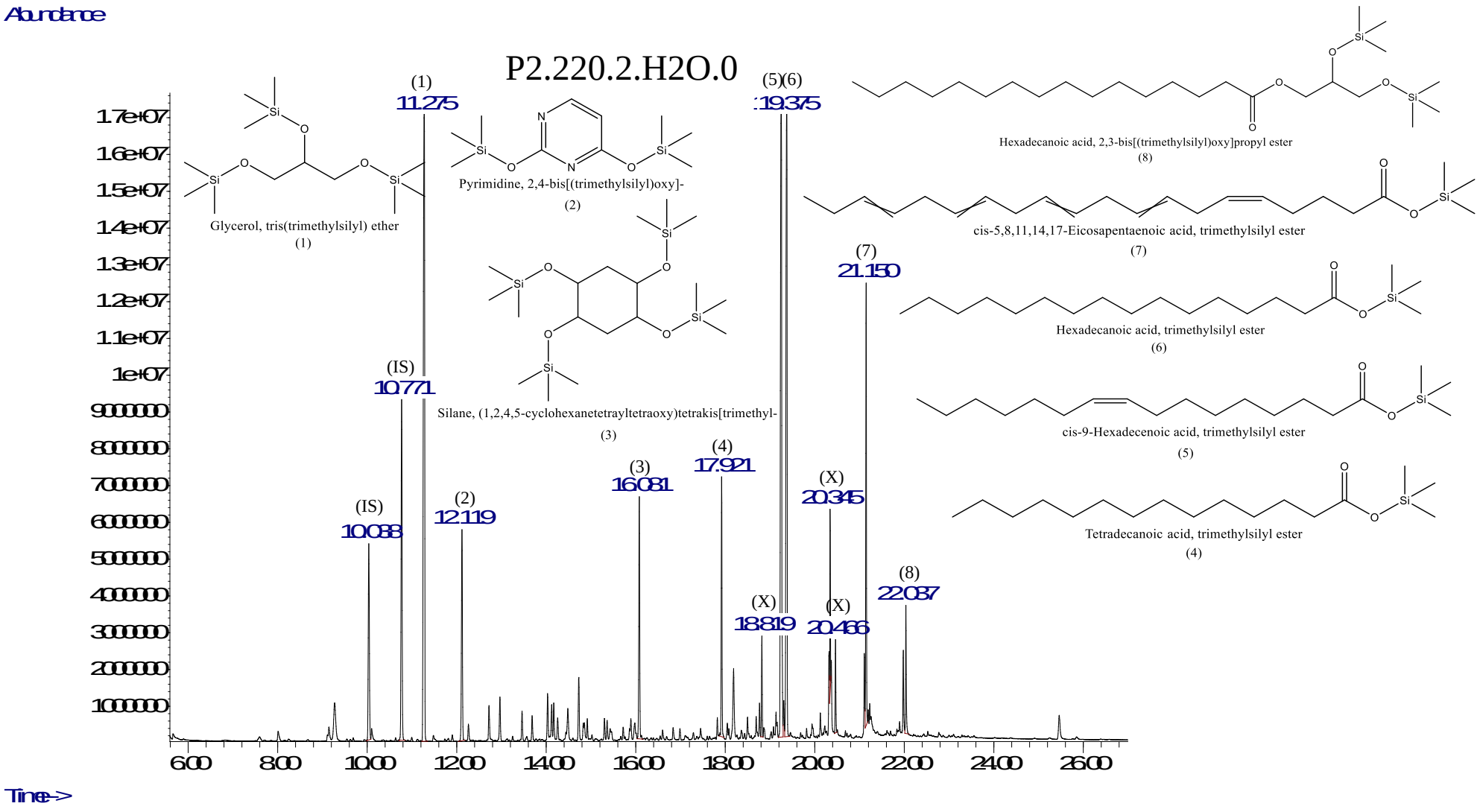

Figure 4.3-i: GC-MS chromatogram of bio-oil experiment P2.220.2.H2O.0. Dodecane and benzoic acid were used as internal standards (IS). (X) marks unidentified peaks.

4.3.5 FT-IR

IR analysis was performed to determine the presence of some of the characteristic functional groups found for bio-oil samples in Pilot Series 2. IR-spectra of the coke samples are included in Appendix B for comparison of coke experiments. Table 4.3-6 shows theoretical and observed infrared absorption frequencies of functional groups from the IR-spectra for the bio-oils samples in Pilot Series 2. The collection of the IR spectra can be found in Appendix B.

Table 4.3-6: IR – analysis for bio-oils in Pilot Series 2

		Functional groups								
		Alkanes				**Alkenes**		**Alcohols**		**Carboxylic acids**
		***sp*³ C-H stretch**	**-CH_2 bend**	**-CH_3 bend**	**Long-chain band**	***sp*² C-H stretch**	**C=C stretch**	**C-O stretch**	**O-H stretch (H-bonded)**	**C=O stretch**
Experiments	**Theoretic value[a] [cm^{-1}]**	3000-2850 (s)	1450 (m)	1375 (m)	720 (s)	3100-3000 (m)	1680-1600 (m-w)	1260-1000 (s)	3400-3200 (m)	1725-1700 (s)
P2.220.2.H2O.0	**Observed value [cm^{-1}]**	2922.50 (s) and 2852.64 (s)	1456.21 (s)	1377.54 (m)	721.22 (m)	3009.05 (w)	1668.45 (s)	1239.07 (m)	3218.13 (w)	1705.54 (s)
P2.280.2.H2O.1	**Observed value [cm^{-1}]**	2922.29 (s) and 2852.54 (s)	1456.02 (m)	1377.62 (m)	721.68 (m)		1656.14 (s)	1241.41 (m)	3294.89 (w)	
P2.220.6.H2O.1	**Observed value [cm^{-1}]**	2922.38 (s) and 2852.64 (s)	1456.63 (m)	1377.63 (m)	721.59 (m)		1651.79 (s)	1190.22 (m)		1707.99 (s)
P2.280.6.H2O.0	**Observed value [cm^{-1}]**	2921.65 (s) and 2851.96 (s)	1456.54 (m)	1377.17 (m)	721.55 (m)		1638.98 (m)	1269.78 (m)	3301.17 (w)	1704.79 (m)
P2.280.6.H2O.0.R1	**Observed value [cm-1]**	2921.14 (s) and 2851.58 (s)	1456.13 (s)	1376.81 (m)	719.57 (m)		1646.24 (s)	1269.38 (m)	3299.59 (w)	1701.08 (m)
P2.220.2.H2O.1	**Observed value [cm^{-1}]**	2922.49 (s) and 2852.77 (s)	1456.88 (m)	1377.34 (m)	721.19 (m)	3008.22 (w)	1652.13 (m)	1178.09 (s)		1708.43 (s)
P2.220.2.H2O.1.R1	**Observed value [cm^{-1}]**	2922.51 (s) and 2852.84 (s)	1457.15 (m)	1377.44 (m)	721.22 (m)	3008.31 (w)	1652.11 (m)	1181.00 (m)		1708.57 (s)
P2.280.2.H2O.0	**Observed value [cm^{-1}]**	2921.31 (s) and 2851.69 (s)	1455.78 (m)	1376.74 (m)	721.22 (m)		1648.33 (s)	1269.81 (m)	3299.74 (w)	
P2.220.6.H2O.0	**Observed value [cm^{-1}]**	2922.00 (s) and 2852.19 (m)	1455.25 (m)	1377.31 (m)	721.15 (m)		1656.25 (s)	1270.96 (m)	3279.18 (w)	1702.55 (m)
P2.280.6.H2O.1	**Observed value [cm^{-1}]**	2922.03 (s) and 2852.36 (s)	1456.13 (s)	1377.94 (m)	721.24 (m)		1652.14 (s)	1271.14 (m)	3296.58 (w)	
P2.250.4.H2O.0	**Observed value [cm^{-1}]**	2921.74 (s) and 2852.02 (m)	1455.85 (m)	1376.85 (m)	721.45 (m)		1650.49 (s)	1241.78 (m)	3299.81 (w)	
P2.250.4.H2O.1	**Observed value [cm^{-1}]**	2922.11 (s) and 2852.41 (s)	1456.23 (m)	1377.57 (m)	721.56 (m)		1655.58 (s)	1240.79 (m)	3263.43 (w)	

[a] Based on an infrared spectral correlation chart from *"Introduction to spectroscopy"* by Pavia et al. [86, p. 29].

4.4 SOXHLET EXTRACTION

Soxhlet extraction was conducted for lipid extraction of the wet algal feedstock. The extractions were conducted using the same batch of feedstock. In the first procedure, the experiment was complete after approximately 6 days. In the second procedure, the experiment was stopped after 13 days. This experiment was classified as uncomplete as the solvent in the Soxhlet extractor still showed colour traces of feedstock. Table 4.4-1 shows the yields obtained from the two Soxhlet extractions of Experiment 1 and 2. Picture of the Soxhlet products obtained from experiment 1 are presented in Figure 4.4-a. Additional data for Soxhlet extraction are included in Appendix C.

Table 4.4-1: Overview of yields from Soxhlet extractions performed on the algal feedstock.

	Experiment	**1**	**2**
Product	**Soxhlet extract [g]**	2.388	2.4156
	Feedstock residue [g]	15.8839	12.3126
	Water [g]	26.353	24.7544
Yield	**Soxhlet extract[a] [%]**	5.95	6.00
	Y_{Lipids}[b] [%]	22.78	22.97
	Feedstock residue [%]	39.58	30.58
	Water [%]	65.67	61.48
	Y_{Total} [%]	111.20	98.06

[a] Based on weight of wet feedstock.
[b] Expressed as mass percentage on dry basis.

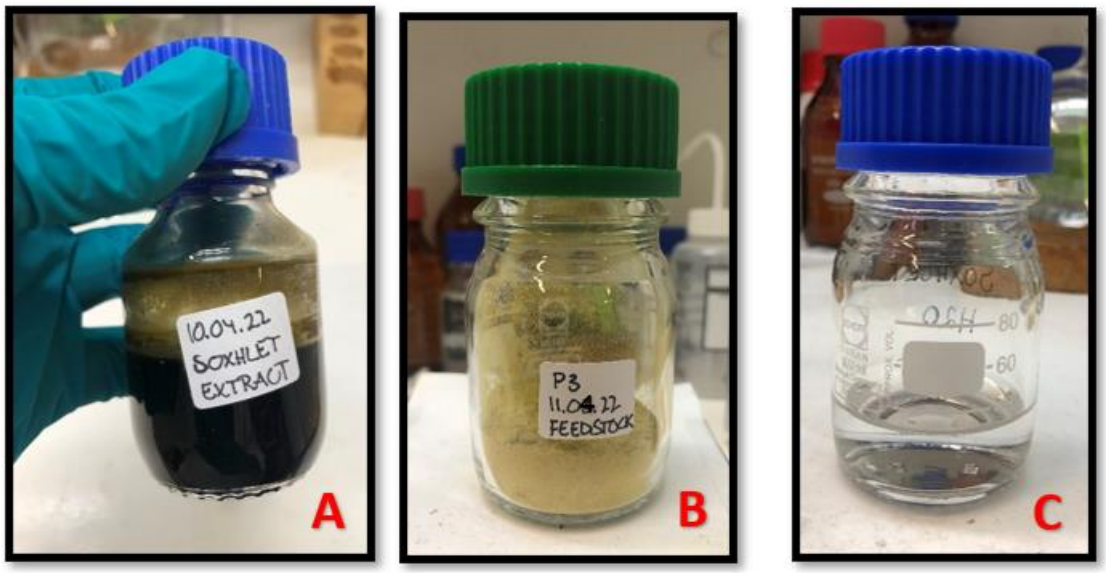

Figure 4.4-a: The Soxhlet products collected from Soxhlet extraction of Experiment 1; A) Soxhlet extract, B) Feedstock residue powder, C) Water collected from the water separator.

GC-chromatogram of Soxhlet extract from Feedstock 1, called Soxhlet extract 1, are included in the results to illustrate the main compounds that were identified, using NIST database.

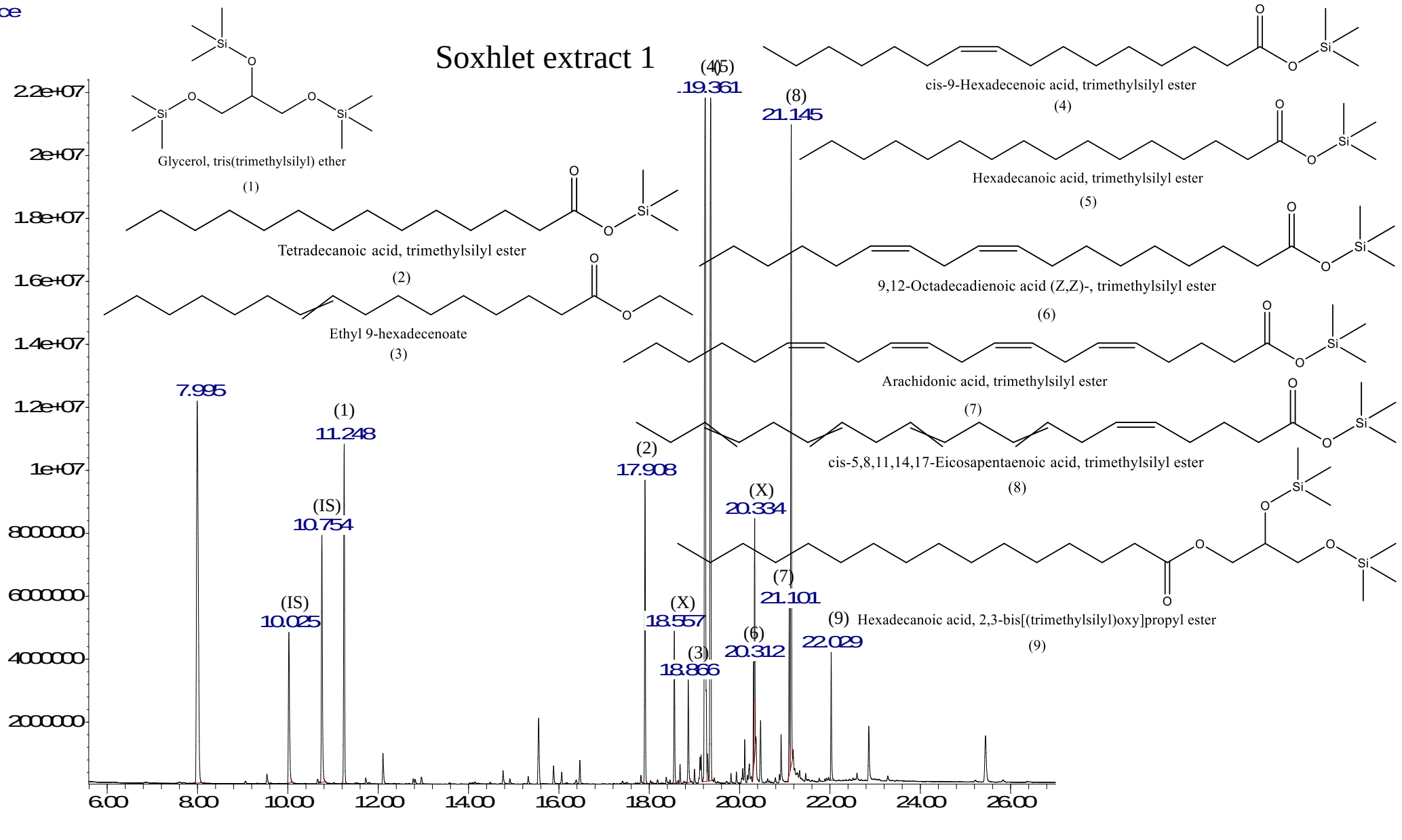

Figure 4.4-a: GC-MS chromatogram of Soxhlet extract 1, from Experiment 1.Dodecane and benzoic acid were used as internal standards (IS). (X) marks unidentified peaks.

4.5 PILOT SERIES 3

4.5.1 HTL

Pilot Series 3 was established to investigate if feedstock residues from lipid extraction is suitable for conversion to bio-oil by HTL. The reaction conditions for Pilot Series 3 were based on the experimental conditions in Pilot Series 1, but without the addition of catalyst, for comparison of bio-oil from treated and untreated feedstock. The operational parameters for Pilot Series 3 are presented in Table 3.3-5. In this pilot series, a total of 5 experiments, including a replica (R), were performed. Pictures from the HTL-workup of bio-oil and coke samples, from P1 are shown in Figures 4.5-b.

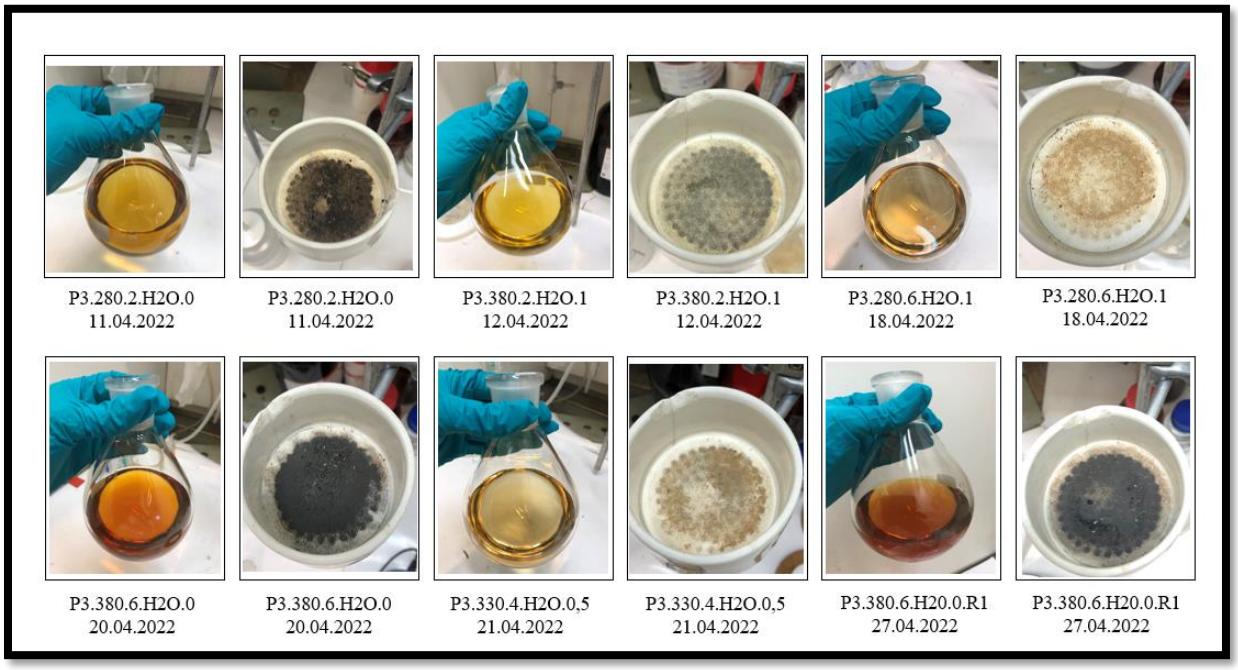

Figure 4.5-b: Pictures of the oil (diluted in solvent) and coke samples from the experimental work-up from P3.

The HTL products obtained in P3 consisted of gas, coke, bio-oil, and aqueous phase. The yields of bio-oil and other products are presented in Table 4.5-2. The yield of gas is presented as mass of gas produced in Figure 4.5-c. No outliers were detected in this pilot series. Raw data from the HTL workup is presented in Table C.2-1 in Appendix C.

Table 4.5-2: Yields for HTL-products in Pilot Series 3.

Experiment	**Aq. ph. [g]**	**Gas [g]**	**Coke [g]**	**Oil [g]**	**Y_{Gas} [%]**	**Y_{Coke} [%][a]**	**Y_{Oil} [%][a]**	**Y_{Total} [%]**
P3.280.2.H2O.0	1.9448	0.14	0.2561	0.1346	n/a	24.40	12.82	41.19
P3.380.2.H2O.1	2.0550	1.29	0.1452	0.1756	104.88	13.96	16.88	58.75
P3.280.6.H2O.1	2.4959	1.10	0.0922	0.2087	91.67	8.87	20.07	62.85
P3.380.6.H20.0	2.4743	0.20	0.2433	0.2506	n/a	23.17 (+5.80)	23.87 (-0.58)	52.45
P3.380.6.H20.0.R1	1.7982	0.13	0.1204	0.2603	n/a	11.58 (-5.80)	25.03 (+0.58)	38.42
P3.330.4.H2O.0,5	2.2058	0.66	0.0770	0.2143	108.20	7.41	20.61	51.59

[a] Deviation from the mean for bio-oil and coke yields for each replica (R) in the experimental series was calculated.

The yields of bio-oil, coke, and gas obtained in Pilot Series 3 are illustrated in Figure 4.5-c.

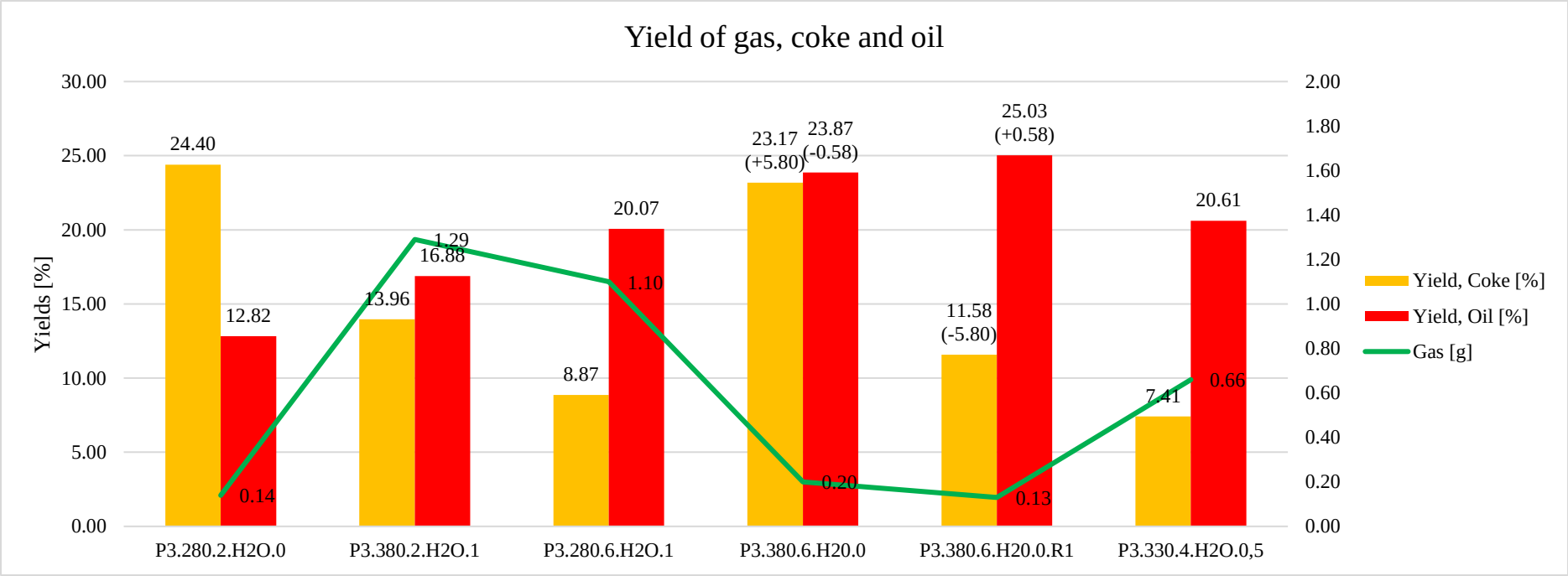

Figure 4.5-c: Yields of HTL products from Pilot Series 3. Deviation from the mean for bio-oil and coke yields for each replica (R) are included, in brackets.

4.5.3 MULTIVARIATE ANALYSIS

Principal component analysis (PCA) and partial least squares regression (PLSR) were conducted on the HTL samples of gas, coke, and bio-oil from Pilot Series 3. Figure 4.5-d shows a biplot from the PCA analysis of all objects, variables, and responses in Pilot Series 3, including cross-terms of the variables.

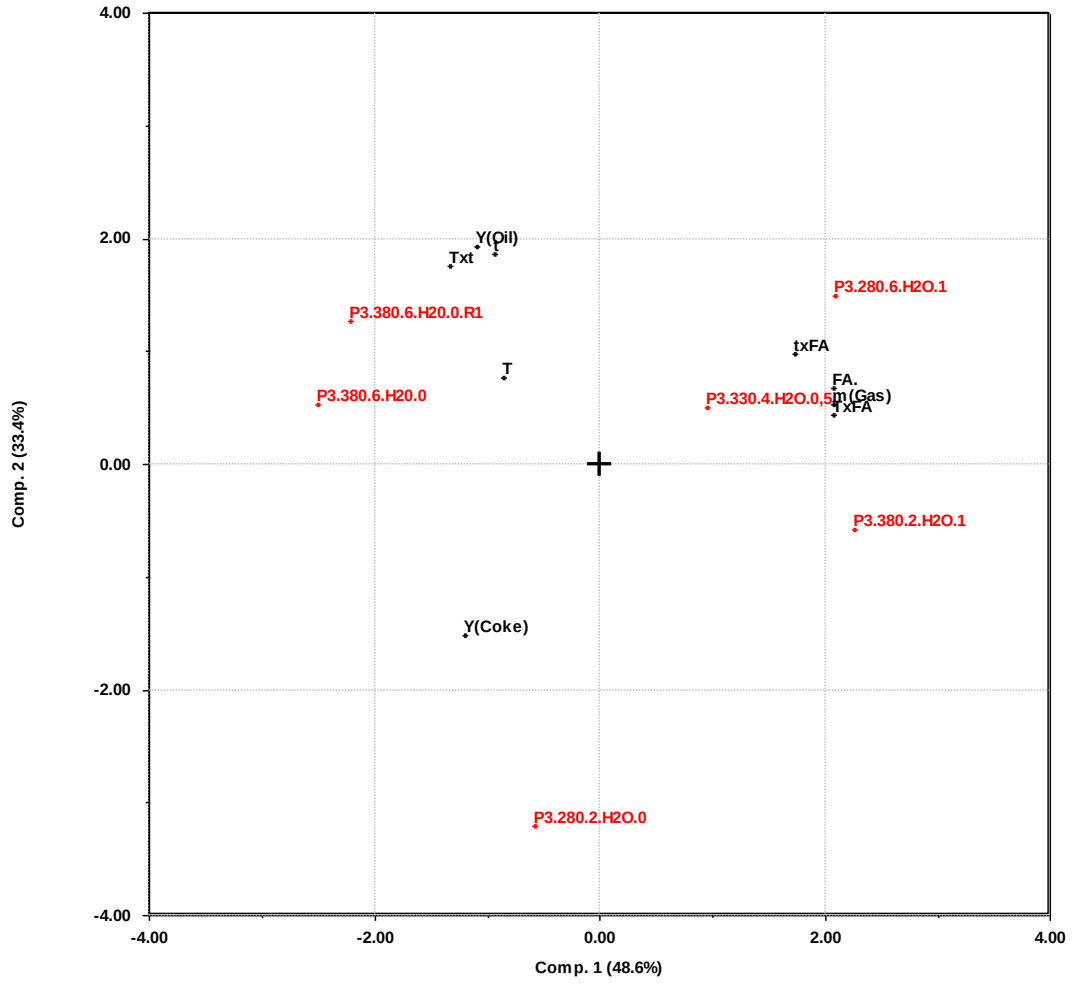

Figure 4.5-d: Biplot from the PCA analysis of all objects, variables, responses in Pilot Series 3. In addition, the plot shows the effect of interaction between the variables (factors) in the form of cross-terms: Txt (temperature x time); TxFA (temperature x formic acid); txFA (time x formic acid).

Two PLS plots were conducted for the bio-oil samples, as the predicted regression equations based on each of these PLS plots were considered representative, in terms of bio-oil yield. The PLS plot for the PLSR of bio-oil samples are shown in Figure 4.5-e and 4.5-f. The PLS plots for coke and gas are presented in Figure C.3-a and Figure C.3-b, respectively, in Appendix C.

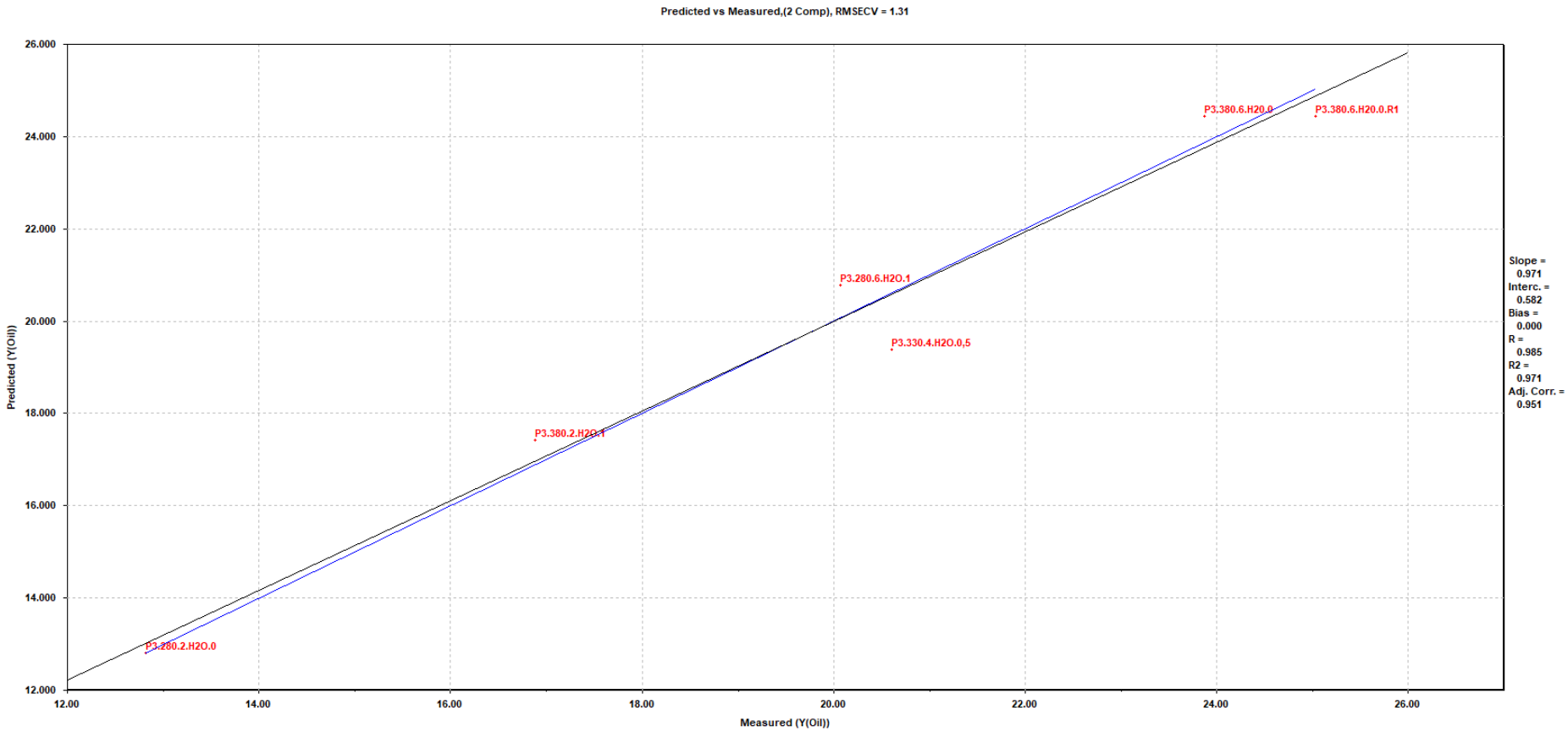

Figure 4.5-e: PLS plot of predicted vs measured values for all bio-oil yields in Pilot Series 3.

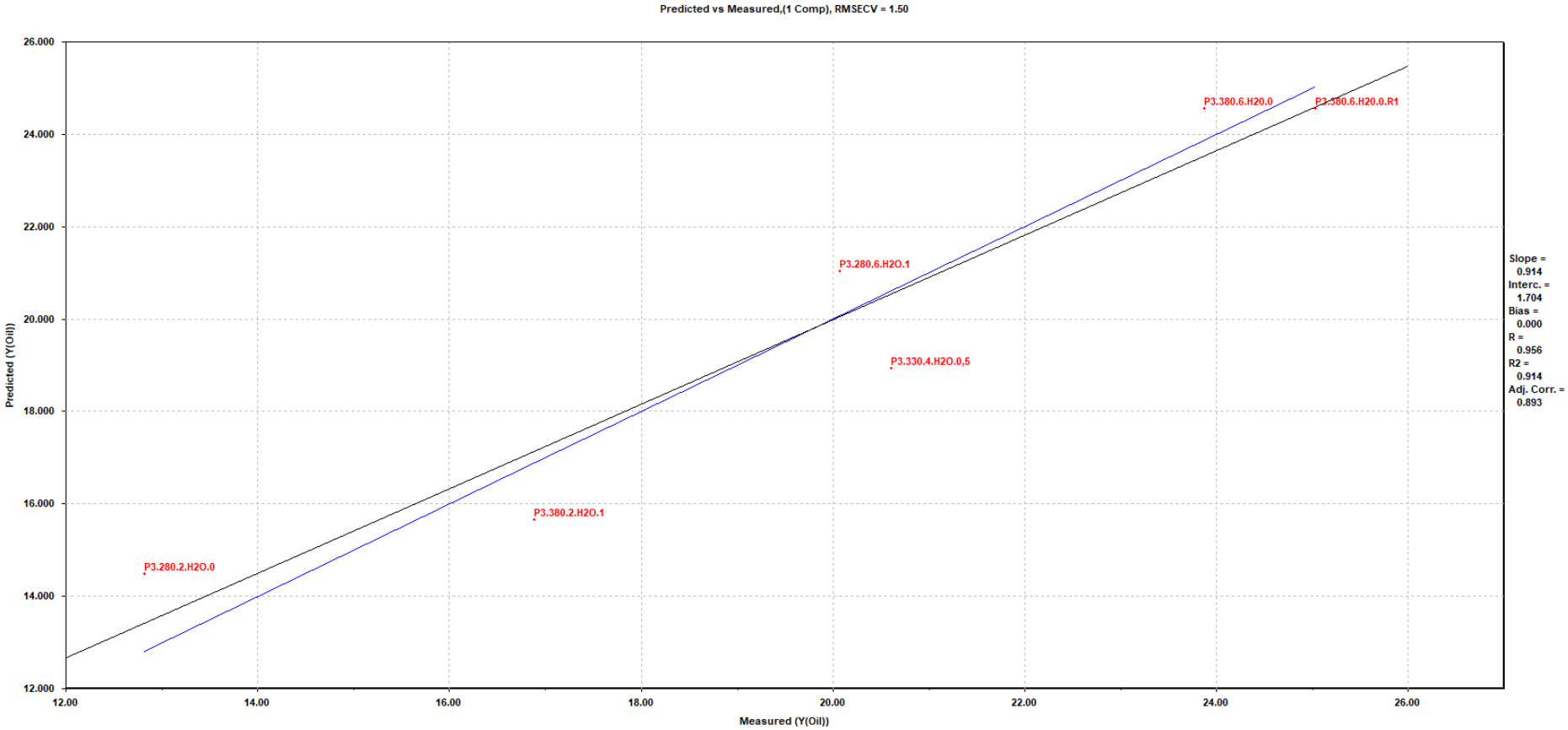

Figure 4.5-f: PLS plot of predicted vs measured values for all bio-oil yields in Pilot Series 3.

Table 4.5-3 shows the correlation coefficients for the predicted regression equations from partial least square regression (PLSR) analysis, based on the PLS model for bio-oil, coke, and gas yields (Table 4.5-4).

Table 4.5-3: Correlation coefficients to the responses from PLS analysis of Pilot Series 3.

Respons	R	R^2
Y_{Oil}	0.985	0.971
	0.956	0.914
Y_{Coke}	0.842	0.709
m_{Gas}	0.996	0.992

Table 4.5-4: Equations to PLS model for the responses from PLS analysis of Pilot Series 3.

Respons	Coeff.	T	t	FA.	Txt	TxFA	txFA
Y_{Oil}	0.19	0.33	0.42	0.13	0.45	-	-
	2.48	-	-	-	0.96	-	-
Y_{Coke}	3.76	-	-	-0.88	-0.45	-	-
m_{Gas}	0.31	-	-	-	-	1.00	-

4.5.4 GC-MS

Table 4.5-5 gives an overview of the compounds identified in the chromatograms of the bio-oil experiments in P3. A cross (X) represents the presence of the associated compounds, identified by use of NIST database, based on GC-peak. Two crosses are used in the case of two peaks for isomeric compounds. For convenience, the isomers are illustrated in cis-configuration in all the GC-chromatograms.

The semi-quantitative analysis of the GC-chromatograms for the oil-samples, based on area under the peaks, are shown in Table C.4-2 (Appendix C) and presented in Figure 4.5-g and 4.5-h. Figure 4.3-i shows the chromatogram for the bio-oil experiment P3.280.2.H2O.0. The peaks analyzed are numbered with the corresponding compound inserted directly into the chromatogram. The compounds were sketched using ChemDraw 21.0.0.

Table 4.5-5: Overview of identified components for Soxhlet extracts and bio-oils produced from HTL in Pilot Series 3.

Designation	Formula	SE 1[a]	SE 2[b]	P3.280.2.H2O.0	P3.380.2.H2O.1	P3.280.6.H2O.1	P3.380.6.H20.0	P3.380.6.H20.0.R1	P3.330.4.H2O.0,5
N-Trimethylsilyl-2-pyrrolidinone	**C7H15NOSi**						X	X	
Pentanoic acid, 4-oxo-, trimethylsilyl ester	**C8H16O3Si**			X					
Butanedioic acid, bis(trimethylsilyl)ester	**C10H22O4Si2**			X		X			
3-Ethylphenol, trimethylsilyl ether	**C11H18OSi**				X		X	X	X
Butanedioic acid, methyl-, bis(trimethylsilyl) ester	**C11H24O4Si2**			X					
L-proline, 5-oxo-1-(trimethylsilyl)-,trimethylsilyl ester	**C11H23NO3Si2**			X		X			
Glycerol, tris(trimethylsilyl) ether	**C12H32O3Si3**	X	X			X			X
4-Hydroxyphenylethanol, di-TMS	**C14H26O2Si2**								X
Tetradecanoic acid, trimethylsilyl ester	**C17H36O2Si**	X	X	X	X	X	X	X	X
Ethyl 9-hexadecenoate	**C18H43O2**	X	X						
Palmitelaidic acid, trimethylsilyl ester	**C19H38O2Si**			X	X	X			X
9-Hexadecenoic acid, trimethylsilyl ester	**C19H40O2Si**	X	X						
Hexadecanoic acid, trimethylsilyl ester	**C19H40O2Si**	X	X	X	X	X	X	X	X
9,12-Octadecadienoic acid *(Z,Z)*-, trimethylsilyl ester	**C21H40O2Si**	X	X						
Octadecanoic acid, trimethylsilyl ester	**C21H44O2Si**								X
Arachidonic acid, trimethylsilyl ester	**C23H40O2Si**	X	X						
***cis*-5,8,11,14,17-Eicosapentaenoic acid, trimethylsilyl ester**	**C23H38O2Si**	X	X						
Hexadecanoic acid, 2,3-bis[(trimethylsilyl)oxy]propyl ester	**C25H54O4Si2**	X	X	X	X	X	X	X	X
Octadecanoic acid, 2,3-bis[(trimethylsilyl)oxy]propyl ester	**C27H58O4Si2**			X					

[a,b] SE1 and SE2 stand for Soxhlet extract 1 and 2, respectively.

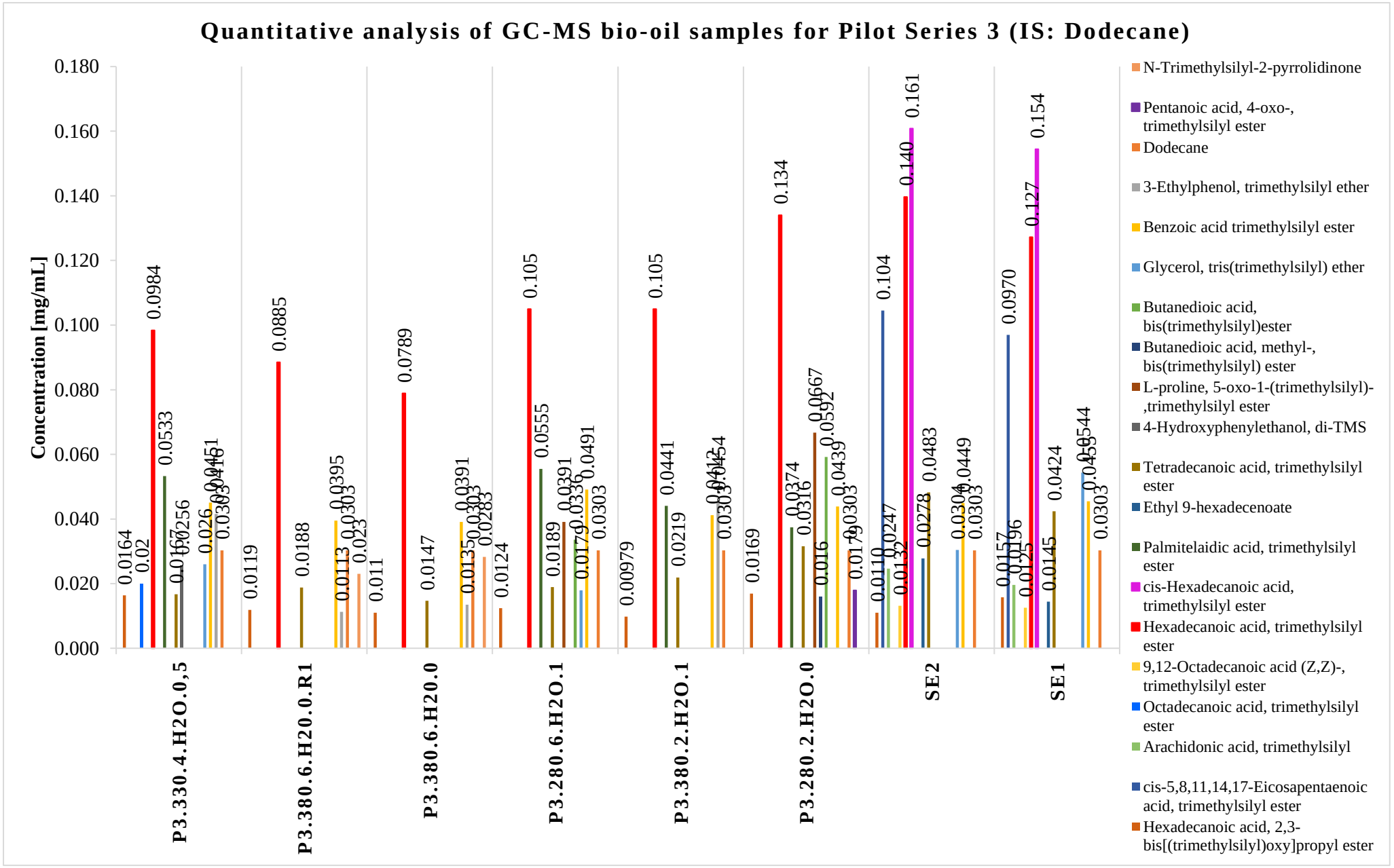

Figure 4.5-g: Semi-quantitative analysis of GC-MS bio-oil samples for Pilot Series 2, relative to dodecane as internal standard

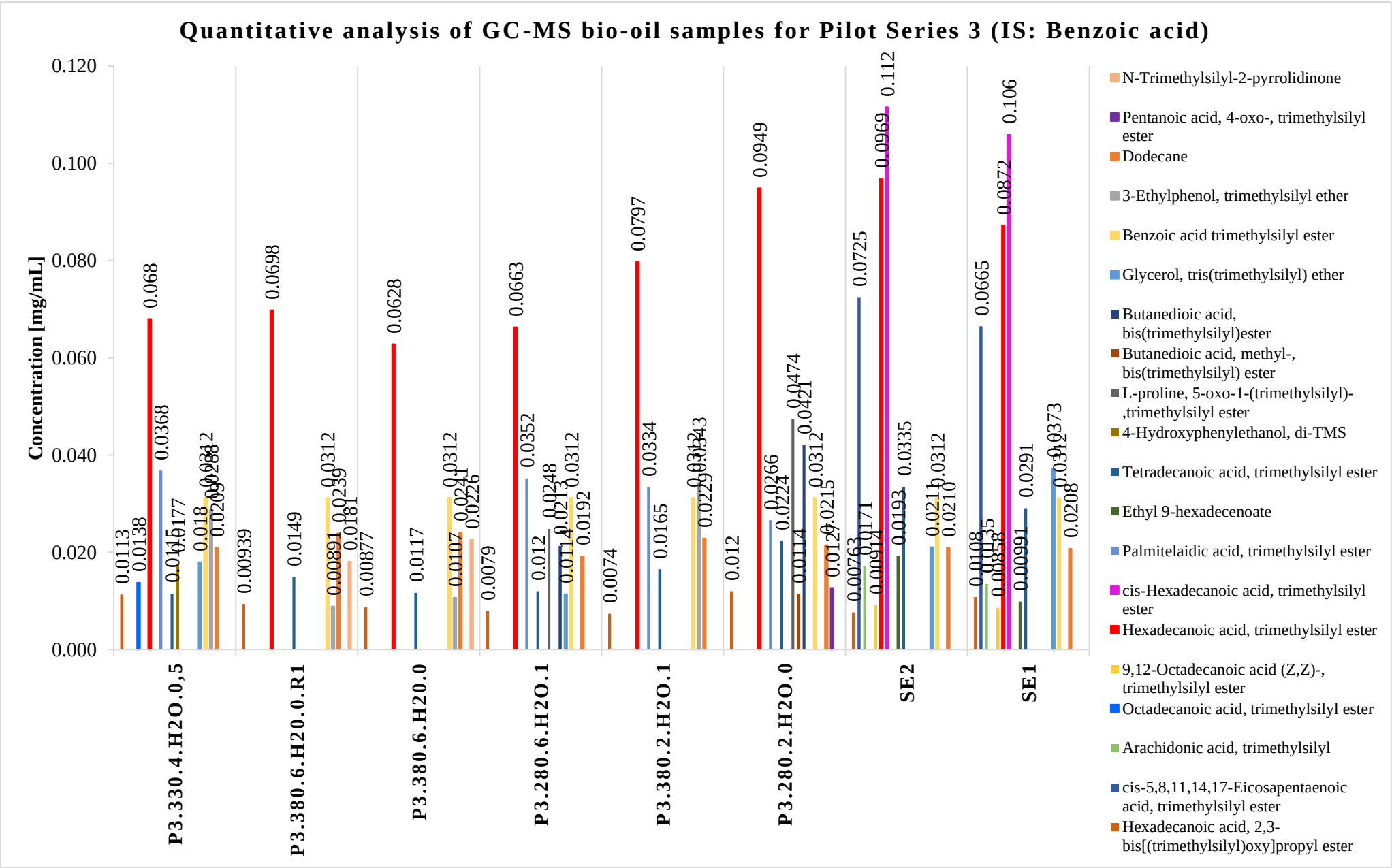

Figure 4.5-h: Semi-quantitative analysis of GC-MS bio-oil samples for Pilot Series 2, relative to benzoic acid as internal standard

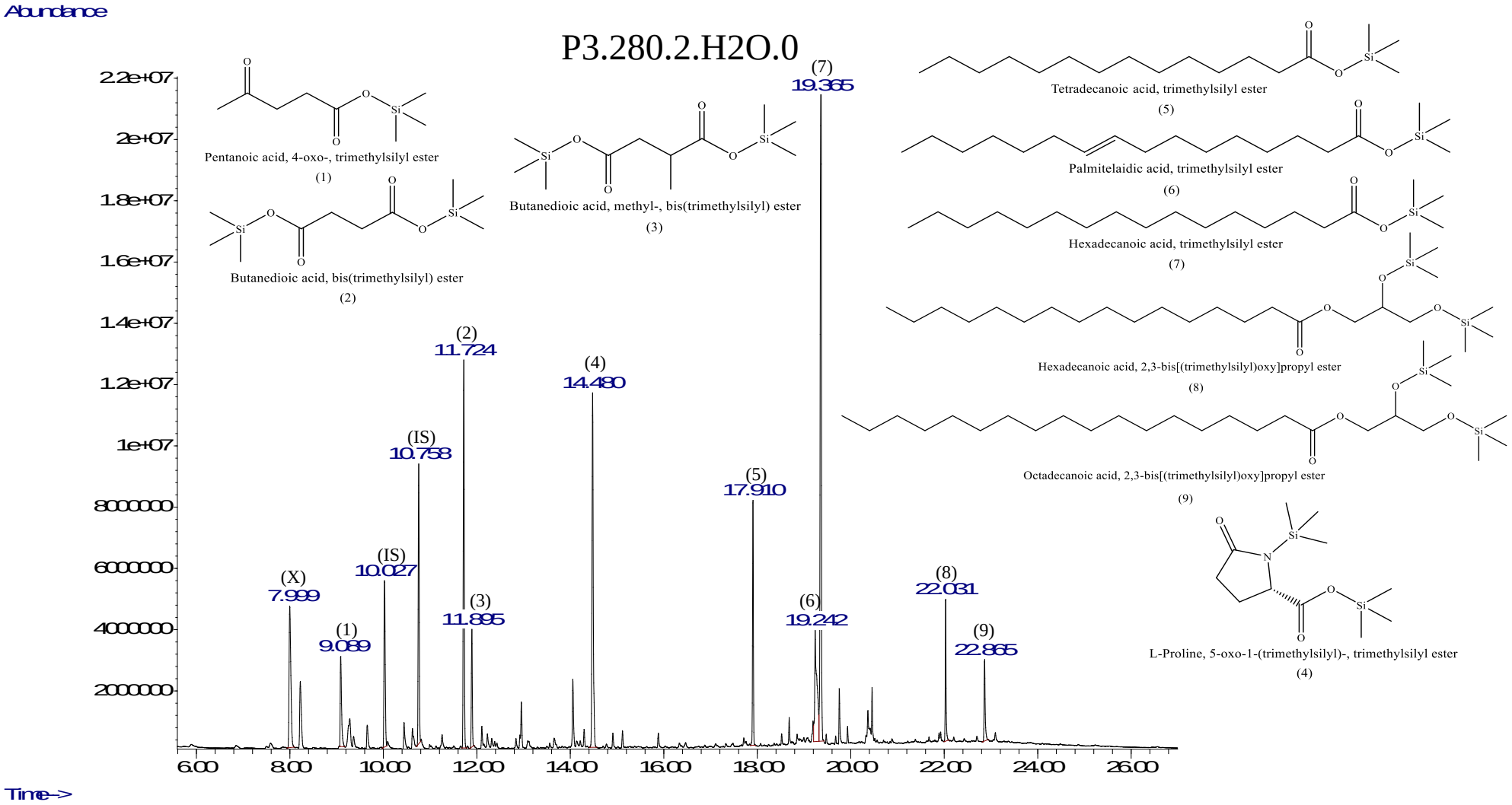

Figure 4.5-i: GC-MS chromatogram of bio-oil experiment P3.280.2.H2O.0. Dodecane and benzoic acid were used as internal standards (IS). (X) marks unidentified peaks.

4.5.6 FT-IR

IR analysis was performed to determine the presence of some of the characteristic functional groups found for bio-oil samples in Pilot Series 3. IR-spectra of the coke samples are included in Appendix C but were only used for comparison of coke samples. Table 4.5-6 shows theoretical and observed infrared absorption frequencies of functional groups from the IR-spectra for the bio-oils samples in Pilot Series 3. The collection of the IR spectra can be found in Appendix C.

Table 4.5-6: IR – analysis for bio-oils in Pilot Series 3

		Functional groups							
		Alkanes				**Alkenes**	**Alcohols**		**Carboxylic acids**
		***sp*³ C-H stretch**	**-CH_2 bend**	**-CH_3 bend**	**Long-chain band**	**C=C stretch**	**C-O stretch**	**O-H stretch (H-bonded)**	**C=O stretch**
Experiments	**Theoretic value[a] [cm^{-1}]**	3000-2850 (s)	1450 (m)	1375 (m)	720 (s)	1680-1600 (m-w)	1260-1000 (s)	3400-3200 (m)	1725-1700 (s)
P3.280.2.H2O.0	**Observed value [cm^{-1}]**	2922.06 (s) and 2852.35 (m)	1456.82 (m)	1377.26 (m)	721.71 (m)		1207.12 (m)		1707.97 (s)
P3.380.2.H2O.1	**Observed value [cm^{-1}]**	2922.65 (s) and 2852.79 (m)	1456.38 (m)	1377.40 (m)	721.76 (m)	1662.58 (s)	1266.88 (m)	3205.75 (w)	1700.97 (s)
P3.280.6.H2O.1	**Observed value [cm-1]**	2923.05 (s) and 2852.93 (m)	1455.45 (m)	1378.35 (m)	721.54 (m)	1653.49 (s)	1225.03 (m)	3235.51 (w)	1699.88 (s)
P3.380.6.H20.0	**Observed value [cm^{-1}]**	2922.51 (s) and 2852.70 (s)	1456.02 (s)	1376.11 (m)	721.76 (m)	1672.19 (s)	1239.69 (m)	3196.34 (w)	
P3.380.6.H20.0.R1	**Observed value [cm^{-1}]**	2922.53 (s) and 2852.75 (s)	1456.19 (s)	1376.14 (m)	721.85 (m)	1673.19 (s)	1239.37 (m)	3197.91 (w)	
P3.330.4.H2O.0,5	**Observed value [cm^{-1}]**	2919.42 (s) and 2850.38 (s)	1456.39 (s)	1377.02 (m)	720.77 (m)	1662.67 (m) and 1637.94 (m)	1269.15 (m)	3299.93 (w)	

[a] Based on an infrared spectral correlation chart from *"Introduction to spectroscopy"* by Pavia et al. [86, p. 29].

5.0 DISCUSSION

5.1 PROXIMATE ANALYSIS

Table 4.1-1 shows that the results for TS, VS, and Wv are approximately the same for both feedstock batches. The small variation in total solids, together with organic and inorganic dry matter, suggests that the batches of feedstocks are relatively homogeneous in terms of moisture, volatile matter, total solids, and ash content. However, proximate analysis is only used as an estimate, due to its low accuracy. Thus, further analysis is necessary to confirm this indication and to investigate if the same applies in terms of elemental composition between the batches of feedstock and within each batch of feedstock. The average amount of total

solids for Feedstock 1 and 2 is 26.12% and 25.94%, respectively. This means that approximately 2.96 g of the 4 g of feedstock added to the reactor in each HTL workup, is expected to consist of water.

5.2 Pilot Series 1

5.2.1 Effect of reaction conditions on HTL yields

Except for the outlier, the bio-oil yields are relatively similar in yields across the experimental series, with a yield range of 37.66-45.97% (Table 4.2-1). This suggests that a change of one or more of the selected reaction parameters (temperature, holding time, catalyst, and formic acid), only has a small influence on the oil yield. The average bio-oil yield achieved for this series is 41.65%. The largest bio-oil yield (45.97%) was achieved for the experiment with a temperature of 280℃, a 6-hour holding time, without catalyst, and with the addition of formic acid. Experiments performed at high temperatures seem to result in slightly lower bio-oil yields, as the three bio-oil samples with the highest oil yield were conducted at low temperatures (280℃), as shown in Figure 4.2-e. Furthermore, two out of the three bio-oils have a 6-hour holding time and are without a catalyst, which might suggest that holding time and catalyst have a slight positive and negative correlation, respectively, with the bio-oil yield. The two center value experiments in this pilot series achieved the lowest oil yields of 37.66% and 38.55%. The operational parameter for these two experiments differs only in the presence and absence of the KOH catalyst. With these observations in mind, this suggests that the addition of catalyst in the form of 1M KOH solution is not efficient in terms of bio-oil yield for this type of feedstock. The effect of formic acid on bio-oil yield seems to be either positive or non-correlated, as the highest bio-oil yield was achieved with the addition of formic acid. Compared to the results of bio-oil yields, the amounts of coke and gas vary significantly between the different experiments. In terms of coke yield, there seems to be no certain pattern in accordance with the selected reaction conditions. The highest yield of coke was achieved for the second replica of the outlier, experiment P1.280.2.H2O.0.R2, with a yield of 16.32%. However, this replica differs considerably in terms of the yield of coke from the first replica (P1.280.2.H2O.0.R1) of 12.54%. Both center value experiments in this pilot series achieved the lowest yields of coke, in which both generated approximately 1.50% coke each. A clear correlation is observed between the amount of formic acid added and the amount of biogas produced in the HTL. The greatest yields of gas were achieved in the experiments with 1 mL formic acid added to the reactor. These experiments achieved a mean yield of approximately 1.11 g gas, while the experiments without the addition of formic acid achieved a mean yield of 0.11 g. The yield of gas products seems to be almost independent of the other reaction conditions (temperature, holding time, and catalyst). Similarly, the yield values for the aqueous phase seem to be largely a function of the input of water.

The overall low mass balance ranging from 49.32% to 68.90% (Table 4.2-1), which includes all HTL products, suggests that there is a consequential and repetitive sample loss during the experimental workup protocol. Complete extraction of the aqueous phase from solvent was not practically feasible with this method, as the aqueous phase adhered to the glass equipment. The water residues were dried from the solvent with drying salt. Thus, the significant weight loss is explicitly from water. The workup process includes the removal of the solvent under reduced pressure, using a rotary evaporator. This also might have

contributed to some loss of the most volatile products during evaporation. In addition, some sample loss of coke was detected during the extraction of coke from the batch reactor, as some of the coke was particularly attached to the sides and bottom of the reactor. However, these weight losses are considered less significant compared to the loss of water during HTL workup.

Deviation from the mean for bio-oil and coke yields, by comparison of respective replica experiments, indicates good reproducibility with a variation of less than $\pm$ 2.0% for both oil and coke yields. With this in mind, the results of HTL products are considered acceptable. The influence of the operational parameters on bio-oil, coke, and gas yields, were further analyzed with help of PCA and PLSR.

5.2.2 MULTIVARIATE ANALYSIS

The biplot for the two principal components (Comp.1 and Comp.2) together explains 59.8% of the total variation in the HTL products (Figure 4.2-f). The holding time lies closer to the origin of the coordination system of the biplot, compared to the other variables, which suggests that it has a smaller impact on the responses (bio-oil, coke, and gas). Temperature shows a clear negative correlation with the bio-oil yield, which confirms the observations based on the HTL results in the previous subchapter 5.2.1, where the three highest bio-oil yields were obtained at low temperatures. The biplot suggests that the addition of catalyst, including the combination of catalyst and formic acid (Cat.xFA), has a negative impact on the bio-oil yield. In addition, the biplot also indicates that bio-oil yield is unaffected by the addition of formic acid. However, the combination of holding time and formic acid (txFa) seems to have a slight positive effect on the bio-oil yield. In summary, the biplot indicates that bio-oil production is favored for experiments with low temperatures, high holding time, with formic acid, and without the addition of an alkali (KOH) catalytic solution. This represents the operational parameter for experiment P1.280.6.H2O.1, which achieved the highest bio-oil yield in this pilot series. The biplot also indicates that there is no significant correlation between oil yield and the other responses (coke and gas). However, there seems to be a negative correlation between the production of gas and coke. In terms of the production of coke, it appears to be unaffected by temperature, and negatively correlated with the addition of formic acid. These observations are almost the opposite for gas, which corroborates the observation that gas and coke production is negatively correlated with each other. The biplot shows a clear positive correlation between the addition of formic acid (FA) and the production of the gas, which again supports the assumption that all the formic acid ends up in the gaseous products during HTL. There seems to be a similar positive correlation between the yield of gas and the cross-term TxFA, which suggests that high temperature combined with formic acid has a positive effect on the gas yield.

The biplot shows a correlation between the replica experiments, which strengthens the assumption of acceptable reproducibility for P1. This is also reasonable as the parallel experiments are affected by the same reaction conditions.

The regression equation for bio-oil yield fits the interpretations from the PCA plot and shows that temperature, along with cross-terms txFa and Cat.xFa, affects the bio-oil yield (Table 4.2-3). The predicted regression equation for coke yields, suggests that catalyst and formic acid, including the two cross-terms txCat. and Cat.xFA, affects the bio-oil yield. However, the

correlation coefficient for oil and coke yield is relatively low in value, and, thus, the fit line is not as accurate. On the other hand, the predicted regression equation for gas yield is very representative, based on the high correlation coefficient. As for the yield of gas, the regression equations comply with the assumption that the addition of formic acid increases the yield.

Based on these observations and results, it is worth testing the HTL production of bio-oil at lower temperatures and without catalyst, for comparison. It is worth including formic acid yet again to confirm the indication that formic acid, together with holding time, has a positive effect on bio-oil yields.

5.2.3 ELEMENTAL ANALYSIS

The completeness of the HTL conversion can be estimated by the comparison of the elemental composition of the feedstock with the elemental composition of the bio-oil and solid by-product (coke). During HTL, the biomass undergoes hydrodeoxygenation, which means the simultaneous removal of oxygen and the addition of hydrogen to form water as a by-product. The Van Krevelen diagram for the bio-oils shows that the oils achieved substantially lower H/C and O/C ratios, compared to the initial feedstock (Figure 4.2-h and Figure 4-2-i). Thus, the substantial drop in these two ratios of the bio-oils suggests that efficient hydrodeoxygenation takes place during HTL conversion of the feedstock. Figure 4.2-h shows that the bio-oil experiments performed at low temperatures obtained a slightly higher O/C ratio, which agrees with the observation done by Paulsen (2019) and Ødegaard (2019), where higher temperatures resulted in a lower O/C ratio of the bio-oils. One experiment (P1.380.2.H2O.1) clearly deviates from this trend and from the rest of the bio-oils. This experiment differs considerably from its parallel in terms of the H/C ratio (1.04 vs. 1.87). There is also a noticeable difference in O/C values (0.11 vs. 0.16) between the two parallels. The lower hydrogen content and higher oxygen content for this bio-oil sample most likely results from technical difficulties in the calibration of the H-value for the EA instrument. New oil samples had to be prepared and run again for some of the bio-oil experiments, as the first ones obtained an inordinately low H content and, subsequently, a higher content of O. Thus, this experiment is considered an outlier. Figure 4.2-i illustrates that the bio-oils with formic acid generally obtain a slightly higher H/C ratio, compared to the bio-oils without formic acid. This makes sense as the formic acid works as a hydrogen donor and, thus, helps with creating a reducing environment. Overall, the figures show that the bio-oils are clustered together within a small area with a H/C range of about 1.40 to 2.00 and an O/C ratio of about 0.07 to 0.15. This again indicates that the different reaction parameters have only a small effect on the bio-oil composition. This is also confirmed by the similarity in higher heating values (HVV), shown in Table 4.2-4. These bio-oils obtained an average profile for HHV of 35.66%, while the estimated HHV for the feedstock was just 7.65%. This shows that HTL conversion of wet feedstock leads to energy-dense biofuels.

5.2.4 GC-MS

The GC-MS analysis for this pilot series shows that the different bio-oil samples comprise similar compounds, while the abundance varies according to the reaction conditions. Figure 4.2-j shows a chromatogram of bio-oil experiment P1.280.2.H2O.0, to illustrate the main components found in the bio-oils. According to GC-MS analysis, all the bio-oil samples are

mainly comprised of long-chain fatty acids and glycerol. Table 4.2-5 gives an overview of the bio-oil constituents identified within the detection limit. The GC-MS analysis shows that glycerol was only detected for the bio-oils with low and center value temperatures, and not at 380℃. The semi-quantitative analysis, shown in Figure 4.2-k and Figure 4.2-l, was calculated using dodecane and benzoic acid, respectively, as internal standards. The data gives a clear indication that hexadecanoic acid trimethylsilyl ester is the prominent constituent, and in the highest abundance, in almost all the bio-oil samples. The two center value experiments obtained the highest concentration of this fatty acid, in almost equal quantities, relative to dodecane as the internal standard (Figure 4.2-k). This semi-quantitative analysis differs slightly from the semi-quantitative analysis done with benzoic acid as IS. With benzoic acid as the internal standard, the highest concentration of hexadecanoic acid trimethylsilyl ester was achieved for the bio-oil conducted at high temperature, maximum holding time, without catalyst, and without the addition of formic acid. The disagreement in the results concludes that the semi-quantitative analysis can to some degree be used for comparison but does not give a reliable quantification of constituents in oil samples.

5.2.5 FT-IR

Due to the complexity of the oil and coke samples, the IR spectra are difficult to interpret. Table 4.2-6 shows the detected functional groups in IR-analysis for bio-oils in P1.

The broad peak found near 3400-3300 cm^{-1} appears to be the hydrogen-bonded O-H band for either alcohol or phenol. The C-O stretch near 1300-1000 cm^{-1} confirms the presence of alcohol in the oil samples. The C-O-H bending is often obscured by the H-C-H bending vibrations to yield some broad and weak peaks in the 1440-1220 cm^{-1} region [87]. These broad peaks are difficult to observe because they often appear under the more strongly absorbing CH_3 bending vibrations at 1375 cm^{-1} (Figure 4.2-m). The peak near 1650 cm^{-1} indicates the presence of a C=C alkene stretch. The double bond is confirmed by consulting the C-H region; aliphatic sp^3 C-H absorption occurs at a frequency less than 3000 cm^{-1} (3000-2840 cm^{-1}) [87]. Methyl (CH_3) and methylene (CH_2) groups have a characteristic bending absorption peak at approximately 1375 and 1465 cm^{-1}, respectively. The bending rocking motion associated with four or more CH_2 groups in an open chain occurs at about 720 cm^{-1} (called a *long-chain band*) [87]. Based on the GC-MS analysis, we would expect a strong absorption peak for the carbonyl (C=O) group for the fatty acids near 1730-1700 cm^{-1}. Some of the oil samples show a weak band in this area, however, none of these bio-oils have the characteristic C=O absorption feature of the strong C=O band.

5.3 PILOT SERIES 2

5.3.1 EFFECT OF REACTION CONDITIONS ON HTL YIELDS

Experiment P2.280.6.H2O.0 is considered an outlier and, therefore, is not included in any of the quantitative analyses in Pilot Series 2. Similarly to Pilot Series 1, the bio-oil yields are relatively comparable in yields across this experimental series, with a yield range of 36.36-58.64% (Table 4.3-1), which suggests that the reaction parameters (temperature, holding time, and formic acid), only has a small effect on the oil yield. The average bio-oil yield achieved for this series is 45.86%. This shows that the oils obtained a slightly higher oil yield compared

to Pilot Series 1, with an average increase of 4.21%. The highest bio-oil yield of 58.64% was achieved for the replica of the experiment with a temperature of 220℃, a 2-hour holding time, and with the addition of formic acid. The two parallels of this experiment achieved the highest oil yields but varied noticeably in yields of 49.75% vs. 58.64%. A dark green color in the diluted oil phase was observed, during HTL workup, for both oil samples with this set of experimental conditions. The green color suggests incomplete conversion of the biomass, which again is most likely a result of too low temperature in combination with minimum holding time. The coke also obtained a mix of grey and green colored parts, while the aqueous phase was unclear and muddy with dark particles. A thin film was formed on the surface of the oil samples, during the drying of the bio-oil with nitrogen gas, which caused insufficient drying of the bio-oils. The oil samples had to be dried with N_2 gas for 5 days, to remove the remaining solvent. Thus, the yields from these bio-oils might not reflect a high-quality bio-oil. In terms of coke yield, there seems to be no certain pattern in accordance with the selected reaction conditions. The lowest yield of coke was achieved for the replica of the outlier, experiment P2.280.6.H2O.0.R1, with a yield of 12.51%, while the highest coke yield of 29.73% was achieved for experiment P2.220.2.H2O.0. Compared to the results for bio-oil and coke yields, the amounts of gas vary significantly between the different experiments. A clear correlation is observed between the amount of formic acid added and the amount of biogas produced in the HTL (Figure 4.3-b). The greatest yields of gas were achieved in the experiments with 1 mL formic acid added to the reactor. These experiments achieved a mean yield of approximately 0.78 g gas, while the experiments without the addition of formic acid achieved a mean yield of 0.07 g. The two experiments where the HTL conversion was considered uncomplete, due to too low temperature and holding time, also obtained a smaller amount of gas compared to the other experiments with formic acid. The yield of gas products seems to be almost independent of the other reaction conditions (temperature, and holding time). Similarly to P1, the input of water seems to be the prominent factor in the yield values for the aqueous phase.

The relatively low mass balance ranging from 30.80 to 68.23% (Table 4.3-1) is in accordance with the results from P1, where it was suggested that water was the major component in sample loss during the experimental workup protocol. The deviation from the mean for the parallels of bio-oil and coke indicates good reproducibility with a variation of less than ± 5.0%.

5.3.2 MULTIVARIATE ANALYSIS

Experiment P2.280.6.H2O.0 is considered an outlier (Figure B.2-1, Appendix B) and is not included in the multivariate analysis of the HTL products. The two principal components (Comp.1 and Comp.2) combined explain 74.1% of the total variation in the HTL products. The biplot shows a clear division between the HTL products with formic acid and the HTL products without formic acids. The biplot also indicates that experiments with the same holding time have a greater similarity with each other, compared to samples with similar temperatures. There seems to be a correlation between the replica samples performed, which suggests sufficient reproducibility. This is also reasonable as the parallel experiments are affected by the same reaction conditions. The temperature does not seem to have a significant effect on the oil yield but does seem to have a negative correlation yield of coke in the samples. This is the opposite of the results from Pilot Series 1, where the temperature had a

negative effect on oil yield and an insignificant effect on coke yield. Pilot Series 2 has another temperature range, and this is most likely the main reason why the temperature dependence is different for the pilot series. The biplot shows a strong positive correlation between the yields of oil and formic acid, which was non-correlated for the results from Pilot Series 1. Pilot Series 1 and 2 have in common that they show a clear correlation between the addition of formic acid (FA) and the production of gas.

5.3.3 ELEMENTAL ANALYSIS

Similar to Pilot Series 1, the Van Krevelen diagram for the bio-oils in Pilot Series 2 shows that the oils achieved substantially lower H/C and O/C ratios, compared to the initial feedstock (Figure 4.3-e and Figure 4-3-f). This again suggests that efficient hydrodeoxygenation takes place during HTL conversion of the feedstock. Figure 4.2-h shows that the elemental composition is relatively unaffected by a temperature change from 220℃ to 280℃. Figure 4.3-f illustrates that the bio-oils in this series are also relatively unaffected by the addition of formic acid. This conflicts with the statement that formic acid works as a hydrogen donor. Overall, the figures show that the bio-oils are clustered together within a small area with a H/C range of about 1.40 to 1.80 and an O/C ratio of about 0.07 to 0.17. This again indicates that the different reaction parameters have only a small effect on the bio-oil composition.

This is also confirmed by the similarity in higher heating values (HHV), shown in Table 4.2-4. These bio-oils obtained an average profile for HHV of 33.12%. This differs considerably from the calculated HHV for the feedstock in Pilot Series 1 (7.65%). This indicates that HTL conversion of the feedstock results in energy-dense biofuels and suggests that experiments with low temperature and holding time are adequate, in terms of the quality of the bio-oils.

5.3.4 GC-MS

The GC-MS analysis for this pilot series shows similar oil products as in P1 and suggests that the abundance of these constituents varies according to the reaction conditions. Figure 4.3-i shows a chromatogram of bio-oil experiment P2.220.2.H2O.0, to illustrate the main components found in the bio-oils. According to GC-MS analysis, all the bio-oil samples are mainly comprised of long-chain fatty acids, glycerol, and aromatic heterocyclic compounds. Table 4.3-5 shows that several compounds are obtained in all bio-oils samples, with 9-hexadecenoic acid trimethylsilyl ester and hexadecanoic acid trimethylsilyl ester as the two prominent constituents, in terms of abundance, in almost all the bio-oil samples. More glycerol was obtained in these experiments compared to the bio-oil samples in P1, which suggests that lower temperatures promote the production of this compound. The highest concentration of hexadecanoic acid trimethylsilyl ester was achieved for the bio-oil conducted at low temperature, minimum holding time, and with the addition of formic acid (Figure 4.3-g and Figure 4.3-h). This is one of the parallels in the experimental series, where the HTL conversion was considered incomplete. The large quantity of this long-chain fatty acid suggests that the reaction conditions for these experiments might after all be suitable to produce biofuels from the algal feedstock.

5.3.5 FT-IR

Table 4.3-6 shows theoretical and observed infrared absorption frequencies of functional groups from the IR-spectra for the bio-oils samples in Pilot Series 2. The IR-spectra for the bio-oils are very similar to the IR-spectra for the oils in Pilot Series 1, which again indicates that they contain similar compounds. Some of the oil samples show a weak band near 1730-1700 cm^{-1}, however, none of these bio-oils have the characteristic C=O absorption feature of the strong C=O band.

5.4 PILOT SERIES 3

5.4.1 SOXHLET EXTRACTION

The quantitative data from the two parallel experiments of Soxhlet extraction are used for the comparison of lipid recovery, including recovery of water and feedstock residues. The two parallel Soxhlet extractions obtained a similar yield of Soxhlet extract (lipids) of 22.78 wt.% and 22.97 wt.%. Similarly, the water recovery for these two extractions were also comparable in yields (61.48% and 65.67%). However, the yield of feedstock residues obtained in the two Soxhlet extractions was noticeable different in comparison (30.58 % vs. 39.58%). The first Soxhlet extraction experiment obtained an unfeasible mass balance of 111.20%, which is most likely due to errors in weight measurements during the experimental workup, while the second extraction experiment obtained an excellent mass balance of 98.06%. However, the second Soxhlet extraction was considered incomplete and, thus, might have obtained a similar mass balance if it had been completed. Therefore, the quantitative results from these Soxhlet extractions are considered unreliable, and additional Soxhlet extractions should be conducted to investigate these results further. However, the qualitative results can still be used for comparisons of compositional differences between HTL products from untreated feedstock and feedstock residues from Soxhlet extraction, in addition to differences between the latter materials.

Figure 4.4-a shows the main compounds identified in GC-MS of Soxhlet extract 1, from the first Soxhlet extraction. The GC-MS of the two Soxhlet extracts shows similarities in compound composition compared to the HTL bio-oils obtained in Pilot Series 1 and 2. This suggests that the two methods are comparable in terms of product composition and that Soxhlet extraction and HTL could be used almost interchangeably. This should further be confirmed by elemental analysis of the Soxhlet extracts for comparison with the HTL bio-oils, in terms of elemental composition and higher heating values.

5.4.2 EFFECT OF REACTION CONDITIONS ON HTL YIELDS

The results from Pilot Series 3 (Table 4.5-2) show noticeably lower yields of bio-oils, compared to the yields in Pilot Series 1 and 2. This makes sense as most of the fatty acids and other liquid components, which readily convert to bio-oil, were extracted from the feedstock during Soxhlet extraction. This pilot series obtained a yield range of just 12.82-25.03% for bio-oil. In contrast to the other two pilot series, the results show a clear positive correlation between the oil yield and the two variables: temperature and time. The two experiments with the highest yields are conducted at high temperatures and high holding time, while the lowest bio-oil yields were achieved at low temperatures and low holding time. Both the center value

experiment and the experiment with a low temperature and high holding time obtained mean values in this experimental series. The coke yield of the experiment with all low levels of HTL conditions was higher than that of oil yield. This might have resulted from incomplete conversion of algal feedstock to bio-oil, mainly due to the low temperature and holding time, which leads to residues of feedstock in the coke. The same trend for the yield of gas products, as for the other pilot series, is observed in this series. Clearly, the amount of gas produced is closely related to the amount of formic acid added. The deviation from mean values between parallels shows good reproducibility with regard to oil yield.

5.4.3 MULTIVARIATE ANALYSIS

The two principal components (Comp.1 and Comp.2) combined explain 82.0% of the total variation in the HTL-products. The biplot shows a strong positive correlation between oil yield, holding time, and cross-term Txt, which suggests that time is the dominating reaction parameter in this series, in terms of bio-oil production. The biplot also indicates a positive correlation between bio-oil yield and temperature. The bio-oil yield seems to be nearly unaffected by the addition of formic acid. The coke yield seems to be anticorrelated to the addition of formic acid, while unaffected by the two other responses (temperature and time). The biplot confirms the clear positive correlation between the amount of gas produced and the amount of formic acid added. Otherwise, the gas yield seems to be unaffected by the other individual responses. However, there seems to be a strong positive correlation between the amount of gas produced and the cross-terms, associated with formic acid, TxFA, and txFA. Thus, high temperature and holding time, in combination with the addition of formic acid, seem to promote the production of gaseous products.

5.4.4 GC-MS

Figure 4.5-i shows a chromatogram of bio-oil experiment P3.280.2.H2O.0, to illustrate the main components found in the bio-oils. The GC-MS analysis shows that the bio-oils are mostly comprised of long-chain fatty acids, glycerol, and aromatic heterocyclic compounds. Table 4.5-5 shows that several compounds are obtained in all bio-oils samples, with hexadecanoic acid trimethylsilyl ester as the prominent constituent, in terms of abundance, in almost all the bio-oil samples. The highest concentration of hexadecanoic acid trimethylsilyl ester was achieved for the bio-oil conducted at high temperature, minimum holding time, and without the addition of formic acid (Figure 4.5-g and Figure 4.5-h). This bio-oil achieved a similar concentration of hexadecanoic acid trimethylsilyl ester as that obtained in the two Soxhlet extracts.

5.4.5 FT-IR

Table 4.5-6 shows theoretical and observed infrared absorption frequencies of functional groups from the IR-spectra for the bio-oils samples in Pilot Series 3. The IR-spectra for the bio-oils are very similar to the IR-spectra for the oils found in the other pilot series, which again indicates that they contain similar compounds. In addition, a strong absorption peak for the carbonyl (C=O) group for the fatty acids was observed near 1730-1700 cm^{-1} for some of the oil samples.

6.0 CONCLUSION

The objective of this thesis focuses on the production and application of bio-oil from HTL.

The data obtained from Pilot Series 1 and 2 shows that oil yields were almost unaffected by the HTL-conditions. In P1, the largest bio-oil yield (45.97%) was achieved for the experiment with a temperature of 280℃, a 6-hour holding time, without catalyst, and with the addition of formic acid. In this series, lower temperatures seem to result in slightly higher bio-oil yields, based on the HTL results and multivariant analysis. Holding time also seems to have a slight positive correlation, while catalyst seems to have a negative impact on the bio-oil yield. The bio-oil yield also seems to be independent of the addition of formic acid. The low mass balance of the HTL products resulted from a consequential and repetitive weight loss of water during the experimental workup protocol. In summary, this pilot series suggests that bio-oil production is favored for experiments with low temperatures, high holding time, with formic acid, and without the addition of alkali (KOH) catalytic solution. Similarly to Pilot Series 1, the bio-oil yields are relatively comparable in yields across Pilot Series 2, which suggests that a reduction of temperature does not have a significant effect on the bio-oil yields. This also applies to the other reaction parameters (holding time and formic acid). The highest bio-oil yield of 58.64% was achieved for the replica of the experiment with a temperature of 220℃, a 2-hour holding time, and with the addition of formic acid. However, this experiment was somewhat difficult to dry during HTL workup, which might be the result why it obtained a higher yield compared to its parallel (49.75%). The Van Krevelen diagram for Pilot Series 1 and 2 indicates that the different reaction parameters only have a small effect on the bio-oil composition. The bio-oils in Pilot Series 1 and 2 obtained an average HHV of 35.66% and 33.12%, respectively.

A noticeably lower yield of bio-oils was obtained in Pilot Series 3, compared to the yields in Pilot Series 1 and 2. This makes sense as most of the fatty acids and other liquid components, which readily convert to bio-oil, were extracted from the feedstock during Soxhlet extraction. The highest bio-oil yield of 25.03% was achieved for the replica of the experiment with a temperature of 380℃, a 6-hour holding time, and without the addition of formic acid. In contrast to the other pilot series, the results show a clear positive correlation between the oil yield and the two variables: temperature and time. A clear correlation between the amount of formic acid added and the amount of biogas produced in the HTL is observed in all the pilot series.

According to GC-MS analysis, the bio-oils in the three pilot series are mainly comprised of long-chain fatty acids, glycerol, and aromatic heterocyclic compounds, with abundances that vary according to the reaction conditions. The main compounds identified in GC-MS of the two Soxhlet extracts shows similarities in compound composition compared to the HTL bio-oils obtained in the pilot series. Based on the results obtained, the two methods are comparable in terms of product yield and composition. However, the Soxhlet extraction is a more time laboring process that requires relatively large amounts solvent. Thus, HTL is the preferred method for the HTL conversion of wet algal feedstock to liquid biofuels.

7.0 FURTHER WORK

This chapter presents some of the proposals to further work that can be interesting to investigate with this type of feedstock and HTL conversion to produce liquid biofuels.

- Further analysis of the feedstock should be conducted to confirm whether the batches of feedstocks are homogeneous in terms of elemental composition, and to investigate if the same applies in terms of elemental composition within each batch of feedstock.
- Additional HTL experiments should be conducted on bio-oil experiments that obtained the highest bio-oil yield in each of the pilot series, to investigate their reproducibility and, thus, their reliability in terms of yield.
- The quantitative results of the Soxhlet extractions were considered unreliable, and additional Soxhlet extractions should be conducted to investigate these results further.
- Elemental analysis of Soxhlet extracts and HTL bio-oils should be conducted for elemental comparison of HTL and Soxhlet extraction as feasible methods for production of biofuels.

BIBLIOGRAPHY

[1] X. Zhao *et al.*, "Biomass-based chemical looping technologies: The good, the bad and the future," *Energy and Environmental Science*, vol. 10, no. 9. Royal Society of Chemistry, pp. 1885–1910, Sep. 01, 2017, doi: 10.1039/c6ee03718f.

[2] D. Xu, G. Lin, S. Guo, S. Wang, Y. Guo, and Z. Jing, "Catalytic hydrothermal liquefaction of algae and upgrading of biocrude: A critical review," *Renewable and Sustainable Energy Reviews*, vol. 97. Elsevier Ltd, pp. 103–118, Dec. 01, 2018, doi: 10.1016/j.rser.2018.08.042.

[3] S. R. Medipally, F. M. Yusoff, S. Banerjee, and M. Shariff, "Microalgae as sustainable renewable energy feedstock for biofuel production," *BioMed Research International*, vol. 2015. Hindawi Publishing Corporation, 2015, doi: 10.1155/2015/519513.

[4] Y. Guo, T. Yeh, W. Song, D. Xu, and S. Wang, "A review of bio-oil production from hydrothermal liquefaction of algae," *Renewable and Sustainable Energy Reviews*, vol. 48. pp. 776–790, 2015, doi: 10.1016/j.rser.2015.04.049.

[5] A. Bahadar and M. Bilal Khan, "Progress in energy from microalgae: A review," *Renewable and Sustainable Energy Reviews*, vol. 27. Elsevier Ltd, pp. 128–148, 2013, doi: 10.1016/j.rser.2013.06.029.

[6] D. López Barreiro, B. R. Gómez, F. Ronsse, U. Hornung, A. Kruse, and W. Prins, "Heterogeneous catalytic upgrading of biocrude oil produced by hydrothermal liquefaction of microalgae: State of the art and own experiments," *Fuel Process. Technol.*, vol. 148, pp. 117–127, 2016, doi: 10.1016/j.fuproc.2016.02.034.

[7] S. Xiu and A. Shahbazi, "Bio-oil production and upgrading research: A review," *Renewable and Sustainable Energy Reviews*, vol. 16, no. 7. pp. 4406–4414, Sep. 2012, doi: 10.1016/j.rser.2012.04.028.

[8] W. Wang, M. Zhou, and D. Yuan, "Carbon dioxide capture in amorphous porous organic polymers," *Journal of Materials Chemistry A*, vol. 5, no. 4. pp. 1334–1347, 2017, doi: 10.1039/c6ta09234a.

[9] A. Modak and S. Jana, "Advancement in porous adsorbents for post-combustion CO2 capture," *Microporous and Mesoporous Materials*, vol. 276. Elsevier B.V., pp. 107–132, Mar. 01, 2019, doi: 10.1016/j.micromeso.2018.09.018.

[10] R. Rebecca Lindsey, "Climate Change: Atmospheric Carbon Dioxide | NOAA Climate.gov," *Climate.gov*, pp. 1–5, 2020, Accessed: Dec. 08, 2020. [Online]. Available: https://www.climate.gov/news-features/understanding-climate/climate-change-atmospheric-carbon-dioxide.

[11] I. P. on C. C. (IPCC), "AR6 Climate Change 2022: Mitigation of Climate Change," 2022. Accessed: May 27, 2022. [Online]. Available: https://www.ipcc.ch/report/sixth-assessment-report-working-group-3/.

[12] M. I. Khan, J. H. Shin, and J. D. Kim, "The promising future of microalgae: Current status, challenges, and optimization of a sustainable and renewable industry for biofuels, feed, and other products," *Microbial Cell Factories*, vol. 17, no. 1. BioMed Central Ltd., Mar. 05, 2018, doi: 10.1186/s12934-018-0879-x.

[13] D. Hone, "The Paris Agreement," in *Putting the Genie Back*, 2017, pp. 121–159.

[14] C. A. Horowitz, "Paris Agreement," *Int. Leg. Mater.*, vol. 55, no. 4, pp. 740–755, 2016, doi: 10.1017/s0020782900004253.

[15] M. Hannon, J. Gimpel, M. Tran, B. Rasala, and S. Mayfield, “Biofuels from algae: Challenges and potential,” *Biofuels*, vol. 1, no. 5, pp. 763–784, Sep. 2010, doi: 10.4155/bfs.10.44.

[16] O. M. Adeniyi, U. Azimov, and A. Burluka, “Algae biofuel: Current status and future applications,” *Renewable and Sustainable Energy Reviews*, vol. 90. Elsevier Ltd, pp. 316–335, Jul. 01, 2018, doi: 10.1016/j.rser.2018.03.067.

[17] P. McKendry, “Energy production from biomass (part 1): Overview of biomass,” *Bioresour. Technol.*, vol. 83, no. 1, pp. 37–46, 2002, doi: 10.1016/S0960-8524(01)00118-3.

[18] A. R. K. Gollakota, N. Kishore, and S. Gu, “A review on hydrothermal liquefaction of biomass,” *Renew. Sustain. Energy Rev.*, vol. 81, pp. 1378–1392, Jan. 2018, doi: 10.1016/J.RSER.2017.05.178.

[19] G. Trif-Tordai and I. Ionel, “Waste Biomass as Alternative Bio-Fuel - Co-Firing versus Direct Combustion,” in *Alternative Fuel*, InTech, 2011.

[20] S. van Loo and J. Koppejan, *The handbook of biomass combustion and co-firing*. Taylor and Francis, 2012.

[21] S. Nanda, R. Rana, P. K. Sarangi, A. K. Dalai, and J. A. Kozinski, “A broad introduction to first-, second-, and third-generation biofuels,” in *Recent Advancements in Biofuels and Bioenergy Utilization*, Springer Singapore, 2018, pp. 1–25.

[22] S. A. Haryanto and Y. S. Pradana, “Hydrothermal liquefaction of low-lipid microalgae Tetraselmis chuii: Effect of temperature and reaction time,” in *AIP Conference Proceedings*, Sep. 2021, vol. 2370, no. 1, p. 080003, doi: 10.1063/5.0062474.

[23] M. R. Brown and S. I. Blackburn, “Biofuels from microalgae,” in *Sustainable Energy Solutions in Agriculture*, vol. 0, no. 0, Biotechnol Prog, 2014, pp. 277–321.

[24] T. Suganya, M. Varman, H. H. Masjuki, and S. Renganathan, “Macroalgae and microalgae as a potential source for commercial applications along with biofuels production: A biorefinery approach,” *Renewable and Sustainable Energy Reviews*, vol. 55. Elsevier Ltd, pp. 909–941, Mar. 01, 2016, doi: 10.1016/j.rser.2015.11.026.

[25] L. Gouveia and A. C. Oliveira, “Microalgae as a raw material for biofuels production,” *J. Ind. Microbiol. Biotechnol.*, vol. 36, no. 2, pp. 269–274, Feb. 2009, doi: 10.1007/s10295-008-0495-6.

[26] Y. Tang, J. N. Rosenberg, M. J. Betenbaugh, and F. Wang, “Optimization of one-step in situ transesterification method for accurate quantification of epa in nannochloropsis gaditana,” *Appl. Sci.*, vol. 6, no. 11, 2016, doi: 10.3390/app6110343.

[27] P. J. Valdez, M. C. Nelson, H. Y. Wang, X. N. Lin, and P. E. Savage, “Hydrothermal liquefaction of Nannochloropsis sp.: Systematic study of process variables and analysis of the product fractions,” *Biomass and Bioenergy*, vol. 46, pp. 317–331, 2012, doi: 10.1016/j.biombioe.2012.08.009.

[28] P. T. Pienkos and A. Darzins, “The promise and challenges of microalgal-derived biofuels,” *Biofuels, Bioprod. Biorefining*, vol. 3, no. 4, pp. 431–440, Jul. 2009, doi: 10.1002/bbb.159.

[29] Y. Chisti, “Biodiesel from microalgae,” *Biotechnology Advances*, vol. 25, no. 3. Elsevier, pp. 294–306, May 01, 2007, doi: 10.1016/j.biotechadv.2007.02.001.

[30] B. Wiyarno, M. Mel, and R. M. Yunus, “OIL ALGAE EXTRACTION FROM NANNOCHLOROPSIS SP: A STUDY OF SOXHLET EXTRACTION AND ULTRASONIC ASSISTED EXTRACTION Biofuel and Bioenergy View project Biomass and Sugar Content View project OIL ALGAE EXTRACTION FROM NANNOCHLOROPSIS SP: A STUDY OF SOXHLET EXTRA,” 2010. [Online]. Available:

https://www.researchgate.net/publication/270049419.

[31] H. D. Goff and Q. Guo, “Chapter 1: The Role of Hydrocolloids in the Development of Food Structure,” in *Food Chemistry, Function and Analysis*, vol. 2020-Janua, no. 18, Royal Society of Chemistry, 2020, pp. 3–28.

[32] A. Hallmann, “Algae Biotechnology – Green Cell-Factories on the Rise,” *Curr. Biotechnol.*, vol. 4, no. 4, pp. 389–415, Nov. 2015, doi: 10.2174/2211550105666151107001338.

[33] S. P. M. Ventura *et al.*, “Extraction of value-added compounds from microalgae,” in *Microalgae-Based Biofuels and Bioproducts: From Feedstock Cultivation to End-Products*, Elsevier Inc., 2017, pp. 461–483.

[34] B. Sialve, N. Bernet, and O. Bernard, “Anaerobic digestion of microalgae as a necessary step to make microalgal biodiesel sustainable,” *Biotechnology Advances*, vol. 27, no. 4. Biotechnol Adv, pp. 409–416, Jul. 2009, doi: 10.1016/j.biotechadv.2009.03.001.

[35] Z. Wang, “Reaction mechanisms of hydrothermal liquefaction of model,” 2011.

[36] C. Prestigiacomo *et al.*, “Sewage sludge as cheap alternative to microalgae as feedstock of catalytic hydrothermal liquefaction processes,” *J. Supercrit. Fluids*, vol. 143, pp. 251–258, Jan. 2019, doi: 10.1016/J.SUPFLU.2018.08.019.

[37] P. J. Valdez, M. C. Nelson, H. Y. Wang, X. N. Lin, and P. E. Savage, “Hydrothermal liquefaction of Nannochloropsis sp.: Systematic study of process variables and analysis of the product fractions,” *Biomass and Bioenergy*, vol. 46, pp. 317–331, Nov. 2012, doi: 10.1016/j.biombioe.2012.08.009.

[38] P. Biller, B. K. Sharma, B. Kunwar, and A. B. Ross, “Hydroprocessing of bio-crude from continuous hydrothermal liquefaction of microalgae,” *Fuel*, vol. 159, pp. 197–205, 2015, doi: 10.1016/j.fuel.2015.06.077.

[39] U. Jena, K. C. Das, and J. R. Kastner, “Comparison of the effects of Na2CO3, Ca3(PO4)2, and NiO catalysts on the thermochemical liquefaction of microalga Spirulina platensis,” *Appl. Energy*, vol. 98, pp. 368–375, 2012, doi: 10.1016/j.apenergy.2012.03.056.

[40] C. C. Xu *et al.*, “Hydrothermal Liquefaction of Biomass in Hot-Compressed Water, Alcohols, and Alcohol-Water Co-solvents for Biocrude Production,” 2014, pp. 171–187.

[41] M. Saber, B. Nakhshiniev, and K. Yoshikawa, “A review of production and upgrading of algal bio-oil,” *Renewable and Sustainable Energy Reviews*, vol. 58. pp. 918–930, 2016, doi: 10.1016/j.rser.2015.12.342.

[42] S. S. Toor, L. Rosendahl, and A. Rudolf, “Hydrothermal liquefaction of biomass: A review of subcritical water technologies,” *Energy*, vol. 36, no. 5. Elsevier Ltd, pp. 2328–2342, 2011, doi: 10.1016/j.energy.2011.03.013.

[43] W. Yang, X. Li, Z. Li, C. Tong, and L. Feng, “Understanding low-lipid algae hydrothermal liquefaction characteristics and pathways through hydrothermal liquefaction of algal major components: Crude polysaccharides, crude proteins and their binary mixtures,” *Bioresour. Technol.*, vol. 196, pp. 99–108, Nov. 2015, doi: 10.1016/j.biortech.2015.07.020.

[44] P. Biller, B. K. Sharma, B. Kunwar, and A. B. Ross, “Hydroprocessing of bio-crude from continuous hydrothermal liquefaction of microalgae,” *Fuel*, vol. 159, pp. 197–205, Jul. 2015, doi: 10.1016/j.fuel.2015.06.077.

[45] M. Kleinert and T. Barth, “Towards a lignincellulosic biorefinery: Direct one-step conversion of lignin to hydrogen-enriched biofuel,” *Energy and Fuels*, vol. 22, no. 2, pp. 1371–1379, 2008, doi: 10.1021/ef700631w.

[46] C. Løhre, H. V. Halleraker, and T. Barth, “Composition of lignin-to-liquid solvolysis oils from

lignin extracted in a semi-continuous organosolv process," *Int. J. Mol. Sci.*, vol. 18, no. 1, Jan. 2017, doi: 10.3390/ijms18010225.

[47] P. A. Marrone *et al.*, "Bench-Scale Evaluation of Hydrothermal Processing Technology for Conversion of Wastewater Solids to Fuels," *Water Environ. Res.*, vol. 90, no. 4, pp. 329–342, Apr. 2018, doi: 10.2175/106143017X15131012152861.

[48] M. Paulsen, "Hydrotermisk omdanning av biorest fra biogassanlegget i Rådalen og analysering av produkter ved EA, GC-MS, IR og SPE," no. November, p. 154, 2019, Accessed: Oct. 15, 2020. [Online]. Available: http://bora.uib.no/handle/1956/21232.

[49] M. L. Ødegaard, "Hydrotermisk omdanning av biorest fra Bergen biogassanlegg og analyse av produkt ved EA, GC-MS, IR og NMR," p. 135, Dec. 2019, Accessed: Jun. 08, 2020. [Online]. Available: http://hdl.handle.net/1956/21231.

[50] M. I. Khan, J. H. Shin, and J. D. Kim, "The promising future of microalgae: Current status, challenges, and optimization of a sustainable and renewable industry for biofuels, feed, and other products," *Microbial Cell Factories*, vol. 17, no. 1. BioMed Central Ltd., Mar. 05, 2018, doi: 10.1186/s12934-018-0879-x.

[51] M. J. Scholz *et al.*, "Ultrastructure and composition of the Nannochloropsis gaditana cell wall," *Eukaryot. Cell*, vol. 13, no. 11, pp. 1450–1464, Nov. 2014, doi: 10.1128/EC.00183-14.

[52] J. H. Janssen, R. H. Wijffels, and M. J. Barbosa, "Lipid production in nannochloropsis gaditana during nitrogen starvation," *Biology (Basel).*, vol. 8, no. 1, 2019, doi: 10.3390/biology8010005.

[53] T. M. Brown, P. Duan, and P. E. Savage, "Hydrothermal liquefaction and gasification of Nannochloropsis sp.," in *Energy and Fuels*, 2010, vol. 24, no. 6, pp. 3639–3646, doi: 10.1021/ef100203u.

[54] H. Li *et al.*, "Conversion efficiency and oil quality of low-lipid high-protein and high-lipid low-protein microalgae via hydrothermal liquefaction," *Bioresour. Technol.*, vol. 154, pp. 322–329, 2014, doi: 10.1016/j.biortech.2013.12.074.

[55] S. He, M. Zhao, J. Wang, Z. Cheng, B. Yan, and G. Chen, "Hydrothermal liquefaction of low-lipid algae Nannochloropsis sp. and Sargassum sp.: Effect of feedstock composition and temperature," *Sci. Total Environ.*, vol. 712, p. 135677, Apr. 2020, doi: 10.1016/j.scitotenv.2019.135677.

[56] I. Megía-Hervás *et al.*, "Scale-up cultivation of Phaeodactylum tricornutum to produce biocrude by hydrothermal liquefaction," *Processes*, vol. 8, no. 9, Sep. 2020, doi: 10.3390/pr8091072.

[57] V. Martin-Jézéquel and B. Tesson, "3 Phaeodactylum tricornutum polymorphism : an overview," in *Advances in Algal Cell Biology*, DE GRUYTER, 2013, pp. 43–80.

[58] J. Antony, "Full Factorial Designs," in *Design of Experiments for Engineers and Scientists*, Elsevier, 2014, pp. 63–85.

[59] M. Paulsen, "Hydrotermisk omdanning av biorest fra biogassanlegget i Rådalen og analysering av produkter ved EA, GC-MS, IR og SPE," no. November, p. 154, 2019, [Online]. Available: http://hdl.handle.net/1956/21232.

[60] Parr Instrument Company, "Stirred Reactors and Pressure Vessels," *Parr Instrum. Co.*, 2020, Accessed: Jun. 13, 2021. [Online]. Available: https://www.parrinst.com/download/38230/.

[61] H. V. Halleraker, S. Ghoreishi, and T. Barth, "Investigating reaction pathways for formic acid and lignin at HTL conditions using 13C-labeled formic acid and 13C NMR," *Results Chem.*, vol. 2, p. 100019, Jan. 2020, doi: 10.1016/j.rechem.2019.100019.

[62] C. Løhre, H. V. Halleraker, and T. Barth, "Composition of lignin-to-liquid solvolysis oils from

lignin extracted in a semi-continuous organosolv process," *Int. J. Mol. Sci.*, vol. 18, no. 1, Jan. 2017, doi: 10.3390/ijms18010225.

[63] M. L. Ødegaard, "Hydrotermisk omdanning av biorest fra Bergen biogassanlegg og analyse av produkt ved EA, GC-MS, IR og NMR," p. 135, 2019, Accessed: Oct. 15, 2020. [Online]. Available: http://bora.uib.no/handle/1956/21231.

[64] I. T. Jollife and J. Cadima, "Principal component analysis: A review and recent developments," *Philosophical Transactions of the Royal Society A: Mathematical, Physical and Engineering Sciences*, vol. 374, no. 2065. The Royal Society Publishing, Apr. 13, 2016, doi: 10.1098/rsta.2015.0202.

[65] J. Zakaria, "A Step-by-step explanation of Principal Component Analysis (PCA)," *Built In*. pp. 1–13, 2021, Accessed: Jun. 02, 2022. [Online]. Available: https://builtin.com/data-science/step-step-explanation-principal-component-analysis.

[66] "A practical guide for getting the most out of Principal Component Analysis. | Towards Data Science." https://towardsdatascience.com/what-are-pca-loadings-and-biplots-9a7897f2e559 (accessed Jun. 09, 2022).

[67] Y. Xia, "Correlation and association analyses in microbiome study integrating multiomics in health and disease," in *Progress in Molecular Biology and Translational Science*, vol. 171, Academic Press, 2020, pp. 309–491.

[68] L. Wang and C. L. Weller, "Recent advances in extraction of nutraceuticals from plants," *Trends in Food Science and Technology*, vol. 17, no. 6. pp. 300–312, 2006, doi: 10.1016/j.tifs.2005.12.004.

[69] A. Guldhe, B. Singh, F. A. Ansari, Y. Sharma, and F. Bux, "Extraction and Conversion of Microalgal Lipids," 2016, pp. 91–110.

[70] P. Manirakiza, A. Covaci, and P. Schepens, "Comparative Study on Total Lipid Determination using Soxhlet, Roese-Gottlieb, Bligh & Dyer, and Modified Bligh & Dyer Extraction Methods," *J. Food Compos. Anal.*, vol. 14, no. 1, pp. 93–100, Feb. 2001, doi: 10.1006/jfca.2000.0972.

[71] "2019/12/9 Solvent Physical Properties," p. 2019, 2019, Accessed: Jun. 10, 2022. [Online]. Available: https://people.chem.umass.edu/xray/solvent.html.

[72] S. A. Channiwala and P. P. Parikh, "A unified correlation for estimating HHV of solid, liquid and gaseous fuels," *Fuel*, vol. 81, no. 8, pp. 1051–1063, May 2002, doi: 10.1016/S0016-2361(01)00131-4.

[73] "Elemental analyzers for solid fuel analysis - Elementar." https://www.elementar.com/en/applications/energy/coal-coke-biomass (accessed Sep. 02, 2021).

[74] "manual_vario el_e." https://studylib.net/doc/18608820/manual_vario-el_e. (accessed Sep. 02, 2021).

[75] L. Smart, *Separation, purification and identification*, vol. 40, no. 07. Royal Society of Chemistry, 2007.

[76] P. Mercer and R. E. Armenta, "Developments in oil extraction from microalgae," *European Journal of Lipid Science and Technology*, vol. 113, no. 5. pp. 539–547, May 2011, doi: 10.1002/ejlt.201000455.

[77] H. J. Hübschmann, *Handbook of GC/MS: Fundamentals and Applications*. Wiley, 2008.

[78] J. Mohrig, D. Alberg, G. Hofmeister, P. Schatz, and C. Hammond, "Laboratory Techniques in Organic Chemistry," *Chem. Eng. News Arch.*, vol. 54, no. 22, p. 28, 1976, doi: 10.1021/cen-

v054n022.p028.

[79] I. Martínez-Castro, J. Sanz, and M. V. Dabrio, “CHROMATOGRAPHY | Gas Chromatography,” in *Encyclopedia of Food Sciences and Nutrition*, no. November, Berlin, Heidelberg: Springer, Berlin, Heidelberg, 2003, pp. 1280–1288.

[80] E. de Hoffmann, *Mass spectrometry : principles and applications*. 2007.

[81] H. J. Cleaves, “GC/MS,” in *Encyclopedia of Astrobiology*, Springer, Berlin, Heidelberg, 2015, pp. 924–924.

[82] V. Ruiz-Hernández, M. J. Roca, M. Egea-Cortines, and J. Weiss, “A comparison of semi-quantitative methods suitable for establishing volatile profiles,” *Plant Methods*, vol. 14, no. 1, pp. 1–15, Aug. 2018, doi: 10.1186/s13007-018-0335-2.

[83] Shimadzu, “2. Analysis Results : SHIMADZU (Shimadzu Corporation).” https://www.shimadzu.com/an/service-support/technical-support/analysis-basics/fundamentals/results.html (accessed Apr. 13, 2021).

[84] T. Theophanides, “Introduction to Infrared Spectroscopy,” in *Infrared Spectroscopy - Materials Science, Engineering and Technology*, IntechOpen, 2012.

[85] “FTIR Spectroscopy,” in *Encyclopedia of Biophysics*, 2013, pp. 854–854.

[86] P. Lampman, K. Vyvyan, D. L. Pavia, and G. S. Kriz, *Spectroscopy 4th Ed*. Cengage Learning, 2008.

[87] D. L. Pavia, *Introduction to spectroscopy*, 5th ed., vol. XVII. Stamford, Conn: Cengage Learning, 2015.

APPENDICES

APPENDIX A – PILOT SERIES 1

A.1 PROXIMATE ANALYSIS: TS, VS, AND WV

Table A.1-1: Workup of proximate analysis of Feedstock 1 and 2.

	Feedstock 1		Feedstock 2	
Parallel no.	**1**	**2**	**1**	**2**
Feedstock [g]	8.0803	8.3613	7.3250	7.1457
TS [g]	2.1113	2.1827	1.9126	1.8415
Wv [g]	1.8829	1.9455	n/a	n/a
Inorganic (dw.) [g]	0.2284	0.2372	n/a	n/a

A.2 HTL

Table A.2-1: HTL workup for Pilot Series 1.

Experiment	Feedstock [g]	TS[a] [g]	Wv[b] [g]	Inorganic (dw.) [g]	Water [g]	KOH [g]	Formic acid [g]	Total [g]
P1.280.2. H2O.0	4.04	1.06	0.941	0.0593	2.01	0.00	0.00	6.05
P1.280.2. H2O.0.R1	4.00	1.04	0.931	0.0686	2.01	0.00	0.00	6.01
P1.280.2. H2O.0.R2	4.03	1.05	0.938	0.0616	2.00	0.00	0.00	6.03
P1.380.2. H2O.1	4.02	1.05	0.936	0.0639	1.01	0.00	1.22	6.25
P1.280.6. H2O.1	4.02	1.05	0.936	0.0639	1.01	0.00	1.22	6.25
P1.280.6. H2O.1.R1	4.01	1.05	0.934	0.0663	1.02	0.00	1.22	6.25
P1.380.6. H2O.0	4.01	1.05	0.934	0.0663	1.99	0.00	0.00	6.00
P1.330.4. H2O.0,5	4.01	1.05	0.934	0.0663	1.51	0.00	0.61	6.13
P1.280.2. KOH.1	4.01	1.05	0.934	0.0663	0.00	1.04	1.22	6.27
P1.380.2. KOH.1	4.01	1.05	0.934	0.0663	0.00	1.01	1.22	6.24
P1.380.2. KOH.0	4.02	1.05	0.936	0.0639	1.01	1.03	0.00	6.06
P1.280.6. KOH.0	4.02	1.05	0.936	0.0639	1.00	1.02	0.00	6.04
P1.380.6. KOH.1	4.00	1.04	0.931	0.0686	0.00	1.01	1.22	6.23
P1.330.4. KOH.0,5	4.01	1.05	0.934	0.0663	0.52	1.01	0.61	6.15

[a, b] Based on average TS [%] and average Wv [%] value calculated in proximate analysis for "Feedstock 1", as this algal biomass was used as feedstock in P1. See Table 4.1-1.

A.3 PRINCIPAL COMPONENT ANALYSIS AND REGRESSION

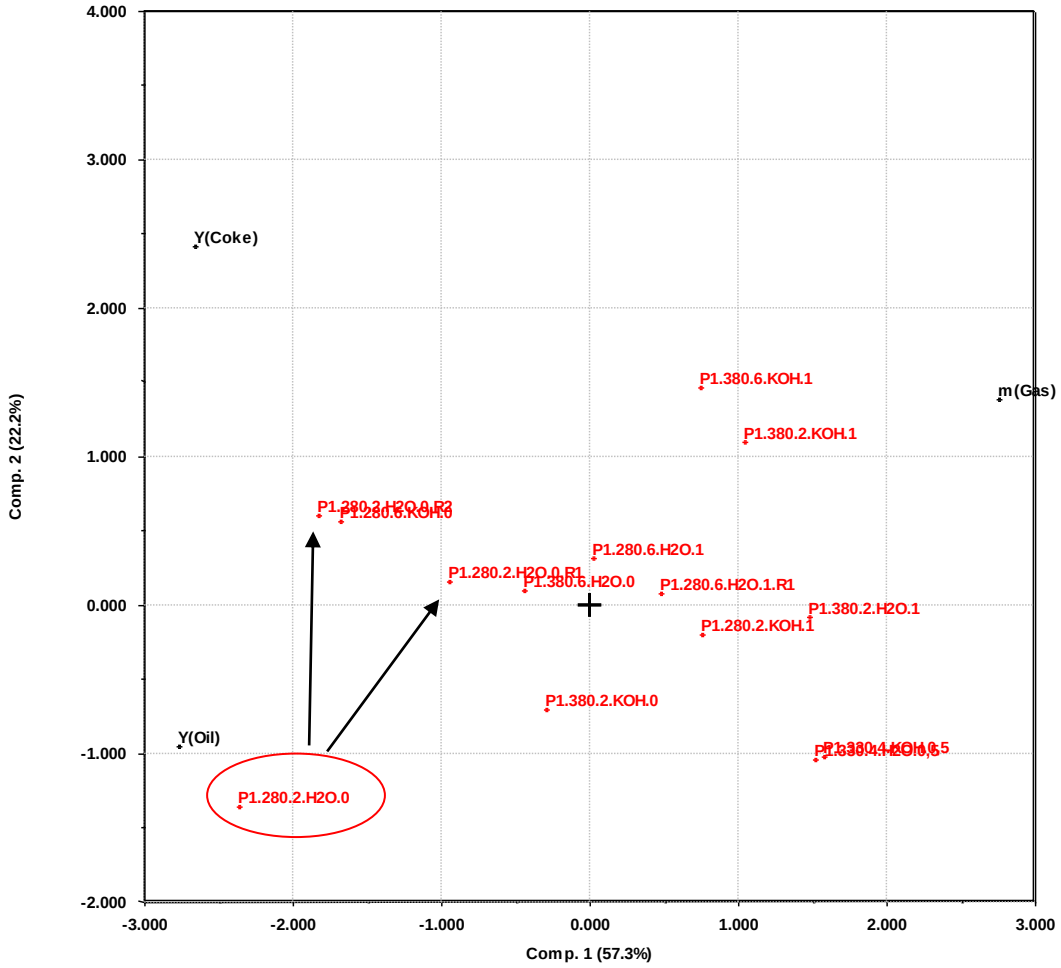

Figure A.3-a: Detection of outliers in Pilot Series 1. The red circle marks the outlier, and the associated arrows points at its replica.

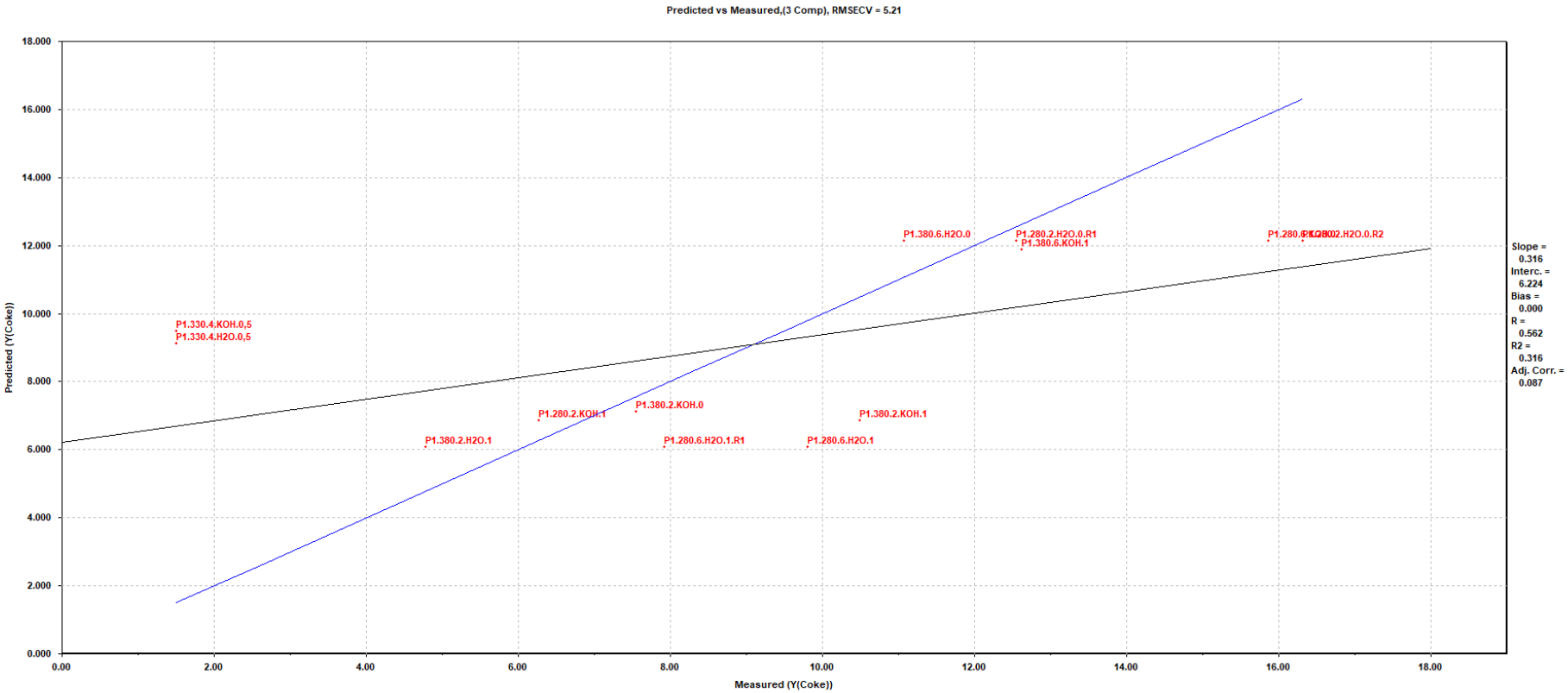

Figure A.3-b: PLS plot of predicted vs measured values for coke yields in Pilot Series 1. All experiments, except P1.280.2.H2O.0.

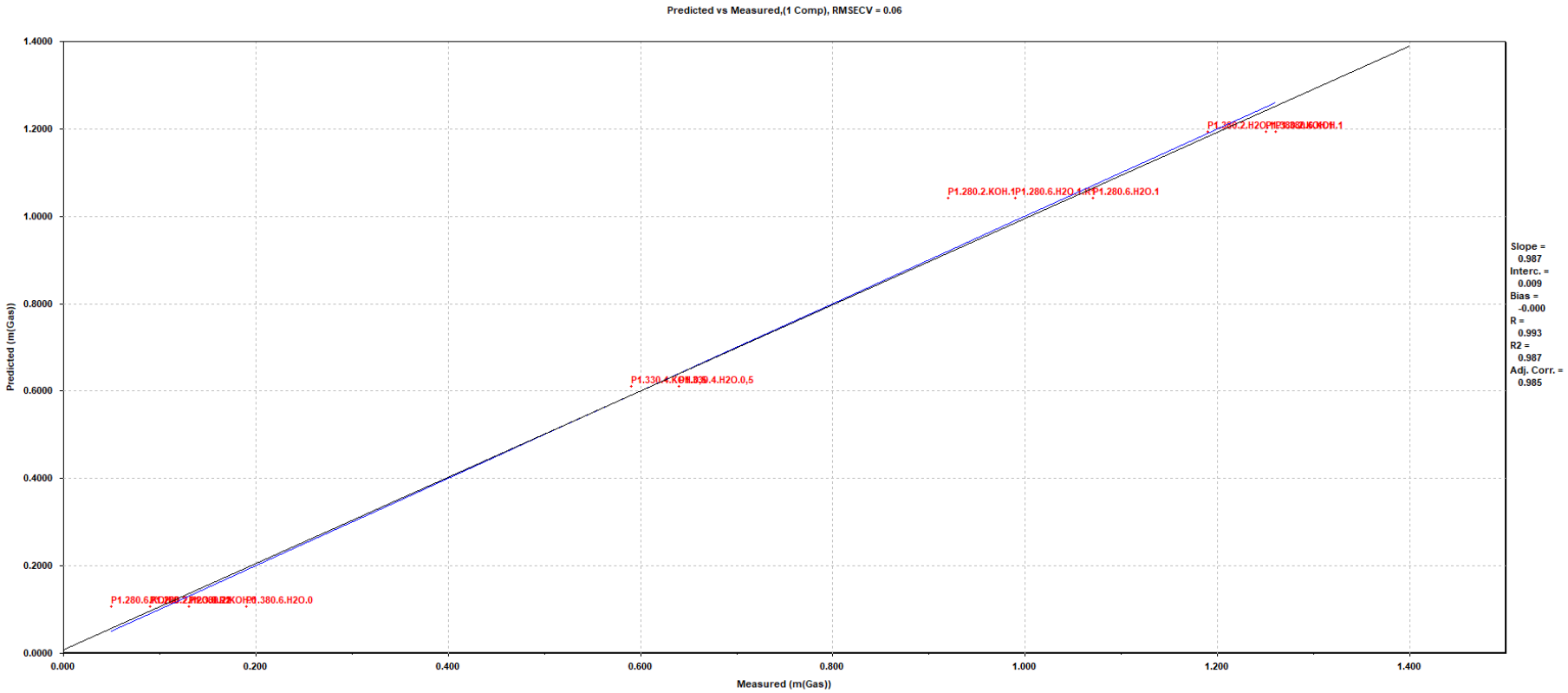

Figure A.3-c: PLS plot of predicted vs measured values for gas yields in Pilot Series 1. All experiments, except P1.280.2.H2O.0.

A.4 ELEMENTAL ANALYSIS

Table A.4-1: Rawdata from EA of bio-oil and feedstock samples in Pilot Series 1.

Sample	% Weight						Oil [g]	Feedstock [g]
	N	C	S	H	Ash	O		
P1.280.2.H2O.0-oil	6.00	70.29	0.03	10.05	0.00	13.63	0.58	4.04
	6.10	70.53	0.02	9.58	0.00	13.76	0.58	4.04
P1.380.2.H2O.1-oil	5.06	72.75	0.04	6.33	0.00	15.82	0.43	4.02
	5.38	72.77	0.13	11.44	0.00	10.28	0.43	4.02
P1.280.6.H2O.1-oil	5.73	71.71	0.08	11.10	0.00	11.38	0.48	4.02
	5.98	71.75	0.15	10.90	0.00	11.23	0.48	4.02
P1.380.6.H2O.0-oil	5.22	76.02	0.18	9.91	0.00	8.67	0.42	4.01
	5.36	75.96	0.19	10.01	0.00	8.48	0.42	4.01
P1.330.4.H2O.0,5-oil	5.13	73.43	0.14	10.99	0.00	10.31	0.40	4.01
	5.29	73.45	0.21	10.58	0.00	10.47	0.40	4.01
P1.280.2.KOH.1-oil	7.81	70.33	0.05	9.82	0.00	11.98	0.44	4.01
	5.57	70.59	0.17	9.57	0.00	14.10	0.44	4.01
P1.380.2.KOH.1-oil	5.42	73.57	0.09	10.41	0.00	10.51	0.41	4.01
	5.35	73.61	0.12	10.80	0.00	10.13	0.41	4.01
P1.380.2.KOH.0-oil	5.58	75.63	0.17	9.81	0.00	8.81	0.44	4.02
	5.41	75.54	0.13	10.05	0.00	8.87	0.44	4.02
P1.280.6.KOH.0-oil	5.34	75.57	0.10	10.17	0.00	8.82	0.46	4.02
	7.47	73.48	0.03	9.30	0.00	9.72	0.46	4.02
P1.380.6.KOH.1-oil	5.96	73.67	0.12	10.31	0.00	9.95	0.41	4.00
	6.20	73.73	0.20	9.52	0.00	10.34	0.41	4.00
P1.330.4.KOH.0,5-oil	4.93	73.53	0.10	10.52	0.00	10.92	0.39	4.01
	4.98	73.49	0.14	10.95	0.00	10.44	0.39	4.01
P1.280.2.H2O.0.R1-oil	-	-	-	-	-	-	-	-
	7.25	72.12	0.10	8.78	0.00	11.74	0.44	4.00
P1.280.6.H2O.1.R1-oil	5.55	71.22	0.15	10.36	0.00	12.72	0.46	4.01
	5.69	71.16	0.19	10.77	0.00	12.19	0.46	4.01
P1.280.2.H2O.0.R2-oil	6.28	72.30	0.16	9.83	0.00	11.43	0.48	4.03
	6.24	72.83	0.17	9.60	0.00	11.16	0.48	4.03
P1 - Feedstock	2.48	13.99	0.20	9.26	0.00	74.07	0.00	0.00
	-	-	-	-	-	-	-	-

Table A.4-2: Calculated molar ratios for H/C, O/C, N/C and (O+N)/C for bio-oil and feedstock samples in Pilot Series 1.

	Moles/100 g					Molar ratios				Mean				Deviation of mean			
Sample	**N**	**C**	**S**	**H**	**O**	**H/C**	**O/C**	**N/C**	**(O+N)\C**	**H/C**	**O/C**	**N/C**	**(O+N)\C**	**H/C**	**O/C**	**N/C**	**(O+N)/C**
P1.280.2.H2O.0-oil	0.43	5.85	0.00	9.97	0.85	1.70	0.15	0.07	0.22	1.66	0.15	0.07	0.22	0.04	0.00	0.00	0.00
	0.44	5.87	0.00	9.50	0.86	1.62	0.15	0.07	0.22					-0.04	0.00	0.00	0.00
P1.380.2.H2O.1-oil	0.36	6.06	0.00	6.28	0.99	1.04	0.16	0.06	0.22	1.46	0.13	0.06	0.20	-0.42	0.03	0.00	0.03
	0.38	6.06	0.00	11.35	0.64	1.87	0.11	0.06	0.17					0.42	-0.03	0.00	-0.03
P1.280.6.H2O.1-oil	0.41	5.97	0.00	11.01	0.71	1.84	0.12	0.07	0.19	1.83	0.12	0.07	0.19	0.02	0.00	0.00	0.00
	0.43	5.97	0.00	10.81	0.70	1.81	0.12	0.07	0.19					-0.02	0.00	0.00	0.00
P1.380.6.H2O.0-oil	0.37	6.33	0.01	9.83	0.54	1.55	0.09	0.06	0.14	1.56	0.08	0.06	0.14	-0.01	0.00	0.00	0.00
	0.38	6.33	0.01	9.93	0.53	1.57	0.08	0.06	0.14					0.01	0.00	0.00	0.00
P1.330.4.H2O.0,5-oil	0.37	6.11	0.00	10.90	0.64	1.78	0.11	0.06	0.17	1.75	0.11	0.06	0.17	0.03	0.00	0.00	0.00
	0.38	6.12	0.01	10.50	0.65	1.72	0.11	0.06	0.17					-0.03	0.00	0.00	0.00
P1.280.2.KOH.1-oil	0.56	5.86	0.00	9.75	0.75	1.66	0.13	0.10	0.22	1.64	0.14	0.08	0.22	0.02	-0.01	0.01	0.00
	0.40	5.88	0.01	9.50	0.88	1.62	0.15	0.07	0.22					-0.02	0.01	-0.01	0.00
P1.380.2.KOH.1-oil	0.39	6.13	0.00	10.33	0.66	1.69	0.11	0.06	0.17	1.72	0.11	0.06	0.17	-0.03	0.00	0.00	0.00
	0.38	6.13	0.00	10.71	0.63	1.75	0.10	0.06	0.17					0.03	0.00	0.00	0.00
P1.380.2.KOH.0-oil	0.40	6.30	0.01	9.74	0.55	1.55	0.09	0.06	0.15	1.57	0.09	0.06	0.15	-0.02	0.00	0.00	0.00
	0.39	6.29	0.00	9.97	0.55	1.58	0.09	0.06	0.15					0.02	0.00	0.00	0.00
P1.280.6.KOH.0-oil	0.38	6.29	0.00	10.08	0.55	1.60	0.09	0.06	0.15	1.55	0.09	0.07	0.17	0.05	-0.01	-0.01	-0.02
	0.53	6.12	0.00	9.22	0.61	1.51	0.10	0.09	0.19					-0.05	0.01	0.01	0.02
P1.380.6.KOH.1-oil	0.43	6.13	0.00	10.22	0.62	1.67	0.10	0.07	0.17	1.60	0.10	0.07	0.17	0.06	0.00	0.00	0.00
	0.44	6.14	0.01	9.45	0.65	1.54	0.11	0.07	0.18					-0.06	0.00	0.00	0.00
P1.330.4.KOH.0,5-oil	0.35	6.12	0.00	10.43	0.68	1.70	0.11	0.06	0.17	1.74	0.11	0.06	0.17	-0.04	0.00	0.00	0.00
	0.36	6.12	0.00	10.86	0.65	1.77	0.11	0.06	0.16					0.04	0.00	0.00	0.00

Table A.4-2: Calculated molar ratios for H/C, O/C, N/C and (O+N)/C for bio-oil and feedstock samples in Pilot Series 1. Continued.

	Moles/100 g					Molar ratios				Mean				Deviation of mean			
Sample	**N**	**C**	**S**	**H**	**O**	**H/C**	**O/C**	**N/C**	**(O+N)\C**	**H/C**	**O/C**	**N/C**	**(O+N)\C**	**H/C**	**O/C**	**N/C**	**(O+N)/C**
P1.280.2.H2O.0.R1-oil	-	-	-	-	-	-	-	-	-	-	-	-	-	-	-	-	-
	0.52	6.00	0.00	8.71	0.73	1.45	0.12	0.09	0.21					-	-	-	-
P1.280.6.H2O.1.R1-oil	0.40	5.93	0.00	10.28	0.79	1.73	0.13	0.07	0.20	1.77	0.13	0.07	0.20	-0.03	0.00	0.00	0.00
	0.41	5.92	0.01	10.68	0.76	1.80	0.13	0.07	0.20					0.03	0.00	0.00	0.00
P1.280.2.H2O.0.R2-oil	0.45	6.02	0.01	9.75	0.71	1.62	0.12	0.07	0.19	1.59	0.12	0.07	0.19	0.02	0.00	0.00	0.00
	0.45	6.06	0.01	9.52	0.70	1.57	0.12	0.07	0.19					-0.02	0.00	0.00	0.00
P1 - Feedstock	0.18	1.16	0.01	9.19	4.63	7.89	3.97	0.15	4.13	-	-	-	-	-	-	-	-
	-	-	-	-	-	-	-	-	-					-	-	-	-

A.5 GAS CHROMATOGRAPHY-MASS SPECTROMETRY

Table A.5-1: Preparation of GC-MS, Pilot series 1

	Experiment	P1.280.2.H2O.0	P1.380.2.H2O.1	P1.280.6.H2O.1	P1.380.6.H2O.0	P1.330.4.H2O.0,5	P1.280.2.KOH.1	P1.380.2.KOH.1
Preparation of Solvent A1	**Benzoic acid [g]**	0.2297	0.2297	0.2297	0.2297	0.2297	0.2297	0.2297
	Dodecane [mL]	0.300	0.300	0.300	0.300	0.300	0.300	0.300
	EtOAc [mL]	100	100	100	100	100	100	100
	Benzoic acid [mg/mL]	2.30	2.30	2.30	2.30	2.30	2.30	2.30
	Dodecane [mg/mL]	2.25	2.25	2.25	2.25	2.25	2.25	2.25
Preparation of Solvent A2	**Solvent A [mL]**	3.50	3.50	3.50	3.50	3.50	3.50	3.50
	EtOAc [mL]	100	100	100	100	100	100	100
	Benzoic acid [mg/mL]	0.0804	0.0804	0.0804	0.0804	0.0804	0.0804	0.0804
	Dodecane [mg/mL]	0.0788	0.0788	0.0788	0.0788	0.0788	0.0788	0.0788
Preparation of Oil solution	**Oil sample [mg]**	7.5	7.6	7.6	7.7	7.5	7.7	7.6
	Solvent A2 [mL]	3.00	3.00	3.00	3.00	3.00	3.00	3.00
	Oil [mg/mL]	2.5	2.5	2.5	2.6	2.5	2.6	2.5
	Benzoic acid [mg/mL]	0.0804	0.0804	0.0804	0.0804	0.0804	0.0804	0.0804
	Dodecane [mg/mL]	0.0788	0.0788	0.0788	0.0788	0.0788	0.0788	0.0788
Preparation of Derivatized oil solution	**Oil solution [mL]**	1.00	1.00	1.00	1.00	1.00	1.00	1.00
	Pyridine [mL]	0.150	0.150	0.150	0.150	0.150	0.150	0.150
	BSTFA [mL]	0.150	0.150	0.150	0.150	0.150	0.150	0.150
	Oil [mg/mL]	1.9	2.0	2.0	2.0	1.9	2.0	2.0
	Benzoic acid [mg/mL]	0.0618	0.0618	0.0618	0.0618	0.0618	0.0618	0.0618
	Dodecane [mg/mL]	0.0606	0.0606	0.0606	0.0606	0.0606	0.0606	0.0606
Preparation of GC-MS Oil sample	**Derivatized oil solution [mL]**	0.700	0.700	0.700	0.700	0.700	0.700	0.700
	Pentane [mL]	0.700	0.700	0.700	0.700	0.700	0.700	0.700
	Oil [mg/mL]	0.96	0.97	0.97	0.99	0.96	0.99	0.97
	Benzoic acid [mg/mL]	0.0309	0.0309	0.0309	0.0309	0.0309	0.0309	0.0309
	Dodecane [mg/mL]	0.0303	0.0303	0.0303	0.0303	0.0303	0.0303	0.0303

Table A.5-1: Preparation of GC-MS, Pilot series 1. Table continued.

	Experiment	P1.380.2.KOH.0	P1.280.6.KOH.0	P1.380.6.KOH.1	P1.330.4.KOH.0,5	P1.280.2.H2O.0.R1	P1.280.6.H2O.1.R1	IS
Preparation of Solvent A1	**Benzoic acid [g]**	0.2297	0.2297	0.2297	0.2297	0.2297	0.2297	0.2297
	Dodecane [mL]	0.300	0.300	0.300	0.300	0.300	0.300	0.300
	EtOAc [mL]	100	100	100	100	100	100	100
	Benzoic acid [mg/mL]	2.30	2.30	2.30	2.30	2.30	2.30	2.30
	Dodecane [mg/mL]	2.25	2.25	2.25	2.25	2.25	2.25	2.25
Preparation of Solvent A2	**Solvent A [mL]**	3.50	3.50	3.50	3.50	3.50	3.50	3.50
	EtOAc [mL]	100	100	100	100	100	100	100
	Benzoic acid [mg/mL]	0.0804	0.0804	0.0804	0.0804	0.0804	0.0804	0.0804
	Dodecane [mg/mL]	0.0788	0.0788	0.0788	0.0788	0.0788	0.0788	0.0788
Preparation of Oil solution	**Oil sample [mg]**	7.6	7.5	7.8	7.6	7.7	7.7	n/a
	Solvent A2 [mL]	3.00	3.00	3.00	3.00	3.00	3.00	3.00
	Oil [mg/mL]	2.5	2.5	2.6	2.5	2.6	2.6	n/a
	Benzoic acid [mg/mL]	0.0804	0.0804	0.0804	0.0804	0.0804	0.0804	n/a
	Dodecane [mg/mL]	0.0788	0.0788	0.0788	0.0788	0.0788	0.0788	0.0788
Preparation of Derivatized oil solution	**Oil solution [mL]**	1.00	1.00	1.00	1.00	1.00	1.00	1.00
	Pyridine [mL]	0.150	0.150	0.150	0.150	0.150	0.150	0.150
	BSTFA [mL]	0.150	0.150	0.150	0.150	0.150	0.150	0.150
	Oil [mg/mL]	2.0	1.9	2.0	2.0	2.0	2.0	n/a
	Benzoic acid [mg/mL]	0.0618	0.0618	0.0618	0.0618	0.0618	0.0618	0.0618
	Dodecane [mg/mL]	0.0606	0.0606	0.0606	0.0606	0.0606	0.0606	0.0606
Preparation of GC-MS Oil sample	**Derivatized oil solution [mL]**	0.700	0.700	0.700	0.700	0.700	0.700	0.700
	Pentane [mL]	0.700	0.700	0.700	0.700	0.700	0.700	0.700
	Oil [mg/mL]	0.97	0.96	1.00	0.97	0.99	0.99	n/a
	Benzoic acid [mg/mL]	0.0309	0.0309	0.0309	0.0309	0.0309	0.0309	0.0309
	Dodecane [mg/mL]	0.0303	0.0303	0.0303	0.0303	0.0303	0.0303	0.0303

Table A.5-2: Semi-quantitative analysis of GC-MS bio-oil samples for Pilot Series 1.

	Designation	**Dodecane**	**3-Ethylphenol, trimethyl silyl ether**	**Benzoic acid trimethyl silyl ester**	**Glycerol, tris(trimethyl silyl) ether**	**Silane, (dodecyloxy)trimethyl-**	**Tetradecanoic acid, trimethyl silyl ester**	**9-Hexadecenoic acid, trimethyl silyl ester**	**9-Hexadecenoic acid, trimethyl silyl ester**	**Hexadecanoic acid, trimethyl silyl ester**	**Octadecanoic acid, trimethyl silyl ester**	**N,N-Dimethyl dodecanamide**	**Octadecanamide, N-butyl-**	**Hexadecanoic acid, 2,3-bis[(trimethylsilyl)oxy]propyl ester**
	Formula	**C12H26**	**C11H18OSi**	**C1014O2Si**	**C12H32O3Si3**	**C15H34OSi**	**C17H36O2Si**	**C19H38O2Si**	**C19H38O2Si**	**C19H40O2Si**	**C21H44O2Si**	**C14H29NO**	**C22H45NO**	**C25H54O4Si2**
P1.280.2.H2O.0	**Ret. [min]**	10.118		10.851	11.342		17.987	19.299	19.325	19.421				22.084
	Peak area	73828186		140377855	279635085		48095714	200734211	43434007	243657768				27043947
	C_A [mg/mL] (IS:1)[a]	0.0303		0.0576	0.115		0.0197	0.0824	0.0178	0.100				0.0111
	C_A [mg/mL] (IS: 2)[b]	0.0163		0.0309	0.0616		0.0106	0.0442	0.00957	0.0537				0.00596
P1.280.2.H2O.0.R1	**Ret. [min]**	10.118		10.850	11.337	15.001	17.986	19.300	19.329	19.424				
	Peak area	79584315		149365612	147940914	52394602	77996838	264855390	67909743	332883833				
	C_A [mg/mL] (IS:1)[a]	0.0303		0.0568	0.0563	0.0199	0.0297	0.101	0.0258	0.127				
	C_A [mg/mL] (IS: 2)[b]	0.0165		0.0309	0.0306	0.0108	0.0161	0.0548	0.0141	0.0689				
P1.380.2.H2O.1	**Ret. [min]**	10.118	10.729	10.851		15.001	17.987	19.297	19.326	19.429	20.518	20.614		
	Peak area	74097579	45705358	148893715		43023382	68301296	60834307	89752715	429910854	110375785	41750828		
	C_A [mg/mL] (IS:1)[a]	0.0303	0.0187	0.0609		0.0176	0.0279	0.0249	0.0367	0.176	0.0451	0.0171		
	C_A [mg/mL] (IS: 2)[b]	0.0154	0.00949	0.0309		0.00893	0.0142	0.0126	0.0186	0.0893	0.0229	0.00867		
P1.280.6.H2O.1	**Ret. [min]**	10.118		10.850	11.337	15.000	17.987			19.428	20.517			
	Peak area	65967371		138265671	120317850	36278465	59052199			438428109	110071340			
	C_A [mg/mL] (IS:1)[a]	0.0303		0.0635	0.0552	0.0167	0.0271			0.201	0.0505			
	C_A [mg/mL] (IS: 2)[b]	0.0148		0.0309	0.0269	0.00811	0.0132			0.0980	0.0246			

[a, b] Based on the relationship between the peak area ratio and concentration ratio of the target component and IS (1: Dodecane, 2: Benzoic acid) in the chromatogram.

Table A.5-2: Semi-quantitative analysis of GC-MS bio-oil samples for Pilot Series 1. Table continued.

	Designation	**Dodecane**	**3-Ethylphenol, trimethylsilyl ether**	**Benzoic acid trimethylsilyl ester**	**Glycerol, tris(trimethylsilyl) ether**	**Silane, (dodecyloxy)trimethyl-**	**Tetradecanoic acid, trimethylsilyl ester**	**9-Hexadecenoic acid, trimethylsilyl ester**	**9-Hexadecenoic acid, trimethylsilyl ester**	**Hexadecanoic acid, trimethylsilyl ester**	**Octadecanoic acid, trimethylsilyl ester**	**N,N-Dimethyl dodecanamide**	**Octadecanamide, N-butyl-**	**Hexadecanoic acid, 2,3-bis[(trimethylsilyl)oxy]propyl ester**
	Formula	**C12H26**	**C11H18OSi**	**C1014O2Si**	**C12H32O3Si3**	**C15H34OSi**	**C17H36O2Si**	**C19H38O2Si**	**C19H38O2Si**	**C19H40O2Si**	**C21H44O2Si**	**C14H29NO**	**C22H45NO**	**C25H54O4Si2**
P1.280.6.H2O.1.R1	**Ret. [min]**	10.117		10.849	11.336		17.987	19.297	19.327	19.426				
	Peak area	71136333		144291220	125332401		80759167	168564909	129667828	422795152				
	C_A [mg/mL] (IS:1)[a]	0.0303		0.0614	0.0534		0.0344	0.0718	0.0552	0.180				
	C_A [mg/mL] (IS: 2)[b]	0.0152		0.0309	0.0269		0.0173	0.0361	0.0278	0.0906				
P1.380.6.H2O.0	**Ret. [min]**	10.118		10.850		15.000	17.988			19.430	20.520			
	Peak area	82461684		138671662		35788699	85215217			518665131	153729502			
	C_A [mg/mL] (IS:1)[a]	0.0303		0.0509		0.0131	0.0313			0.191	0.0565			
	C_A [mg/mL] (IS: 2)[b]	0.0184		0.0309		0.00798	0.0190			0.116	0.0343			
P1.330.4.H2O.0,5	**Ret. [min]**	10.118	10.729	10.850	11.336	15.001	17.988	19.295	19.325	19.430	20.518	20.615		
	Peak area	71638228	53127201	144909281	84287888	33277631	78695944	75692017	83180976	515325063	142287351	85134339		
	C_A [mg/mL] (IS:1)[a]	0.0303	0.0225	0.0613	0.0356	0.0141	0.0333	0.0320	0.0352	0.218	0.0602	0.0360		
	C_A [mg/mL] (IS: 2)[b]	0.0153	0.0113	0.0309	0.0180	0.00710	0.0168	0.0162	0.0177	0.110	0.0304	0.0182		
P1.280.2.KOH.1	**Ret. [min]**	10.118		10.850	11.337	15.001		19.300	19.327	19.426				
	Peak area	65271291		139312995	128696073	47020638		258692929	88701645	380696723				
	C_A [mg/mL] (IS:1)[a]	0.0303		0.0646	0.0597	0.0218		0.120	0.0412	0.177				
	C_A [mg/mL] (IS: 2)[b]	0.0145		0.0309	0.0286	0.0104		0.0574	0.0197	0.0845				

[a, b] Based on the relationship between the peak area ratio and concentration ratio of the target component and IS (1: Dodecane, 2: Benzoic acid) in the chromatogram.

Table A-5.2: Semi-quantitative analysis of GC-MS bio-oil samples for Pilot Series 1. Table continued.

	Designation	Dodecane	3-Ethylphenol, trimethylsilyl ether	Benzoic acid trimethylsilyl ester	Glycerol, tris(trimethylsilyl) ether	Silane, (dodecyloxy)trimethyl-	Tetradecanoic acid, trimethylsilyl ester	9-Hexadecenoic acid, trimethylsilyl ester	9-Hexadecenoic acid, trimethylsilyl ester	Hexadecanoic acid, trimethylsilyl ester	Octadecanoic acid, trimethylsilyl ester	N,N-Dimethyldodecanamide	Octadecanamide, N-butyl-	Hexadecanoic acid, 2,3-bis[(trimethylsilyl)oxy]propyl ester
	Formula	**C12H26**	**C11H18OSi**	**C1014O2Si**	**C12H32O3Si3**	**C15H34OSi**	**C17H36O2Si**	**C19H38O2Si**	**C19H38O2Si**	**C19H40O2Si**	**C21H44O2Si**	**C14H29NO**	**C22H45NO**	**C25H54O4Si2**
P1.380.2.KOH.1	**Ret. [min]**	10.117		10.850		15.001	17.987	19.296	19.327	19.426	20.517	20.614		
	Peak area	83596374		144070007		33062990	81064531	81269585	184207199	394143006	98506295	37210758		
	C_A [mg/mL] (IS:1)[a]	0.0303		0.0522		0.0120	0.0294	0.0294	0.0667	0.143	0.0357	0.0135		
	C_A [mg/mL] (IS: 2)[b]	0.0179		0.0309		0.00710	0.0174	0.0174	0.0395	0.0846	0.0211	0.00799		
P1.380.2.KOH.0	**Ret. [min]**	10.117	10.729	10.851			17.987	19.296	19.328	19.427	30.518	20.614		
	Peak area	79059361	50928168	153375561			73790308	118132168	148368988	403554498	92294673	55346552		
	C_A [mg/mL] (IS:1)[a]	0.0303	0.0195	0.0588			0.0283	0.0453	0.0568	0.155	0.0354	0.0212		
	C_A [mg/mL] (IS: 2)[b]	0.0159	0.0103	0.0309			0.0149	0.0238	0.0299	0.0814	0.0186	0.0112		
P1.280.6.KOH.0	**Ret. [min]**	10.117		10.850	11.337		17.987	19.297	19.326	19.421		20.612	21.279	
	Peak area	81267320		150381630	137365546		55951477	149719684	106657727	282651850		41426546	34451785	
	C_A [mg/mL] (IS:1)[a]	0.0303		0.0560	0.0512		0.0209	0.0558	0.0398	0.105		0.0154	0.0128	
	C_A [mg/mL] (IS: 2)[b]	0.0167		0.0309	0.0282		0.0115	0.0308	0.0219	0.0581		0.00852	0.00708	
P1.380.6.KOH.1	**Ret. [min]**	10.117	10.729	10.849			17.986		19.325	19.427	20.518	20.614		
	Peak area	84555773	53717582	143987919			76584607		150206024	452519685	124655627	55485370		
	C_A [mg/mL] (IS:1)[a]	0.0303	0.0192	0.0516			0.0274		0.0538	0.162	0.0447	0.0199		
	C_A [mg/mL] (IS: 2)[b]	0.0182	0.0115	0.0309			0.0164		0.0323	0.0972	0.0268	0.0119		

[a, b] Based on the relationship between the peak area ratio and concentration ratio of the target component and IS (1: Dodecane, 2: Benzoic acid) in the chromatogram.

Table A.5-2: Semi-quantitative analysis of GC-MS bio-oil samples for Pilot Series 1. Table continued.

	Designation	**Dodecane**	**3-Ethylphenol, trimethyl silyl ether**	**Benzoic acid trimethyl silyl ester**	**Glycerol, tris(trimethyl silyl) ether**	**Silane, (dodecyloxy)trimethyl-**	**Tetradecanoic acid, trimethyl silyl ester**	**9-Hexadecenoic acid, trimethyl silyl ester**	**9-Hexadecenoic acid, trimethyl silyl ester**	**Hexadecanoic acid, trimethyl silyl ester**	**Octadecanoic acid, trimethyl silyl ester**	**N,N-Dimethyl dodecanamide**	**Octadecanamide, N-butyl-**	**Hexadecanoic acid, 2,3-bis[(trimethylsilyl)oxy]propyl ester**
	Formula	**C12H26**	**C11H18OSi**	**C1014O2Si**	**C12H32O3Si3**	**C15H34OSi**	**C17H36O2Si**	**C19H38O2Si**	**C19H38O2Si**	**C19H40O2Si**	**C21H44O2Si**	**C14H29NO**	**C22H45NO**	**C25H54O4Si2**
P1.330.4.KOH.0,5	**Ret. [min]**	10.117	10.729	10.850	11.335		17.987	19.296	19.326	19.432	20.517	20.615		
	Peak area	77904020	58969023	156583688	45544792		93760141	105897098	109064714	565948351	147284342	86949383		
	C_A [mg/mL] (IS:1)[a]	0.0303	0.0229	0.0609	0.0177		0.0365	0.0412	0.0424	0.220	0.0573	0.0338		
	C_A [mg/mL] (IS: 2)[b]	0.0154	0.0116	0.0309	0.00899		0.0185	0.0209	0.0215	0.1118	0.0291	0.0172		

[a, b] Based on the relationship between the peak area ratio and concentration ratio of the target component and IS (1: Dodecane, 2: Benzoic acid) in the chromatogram.

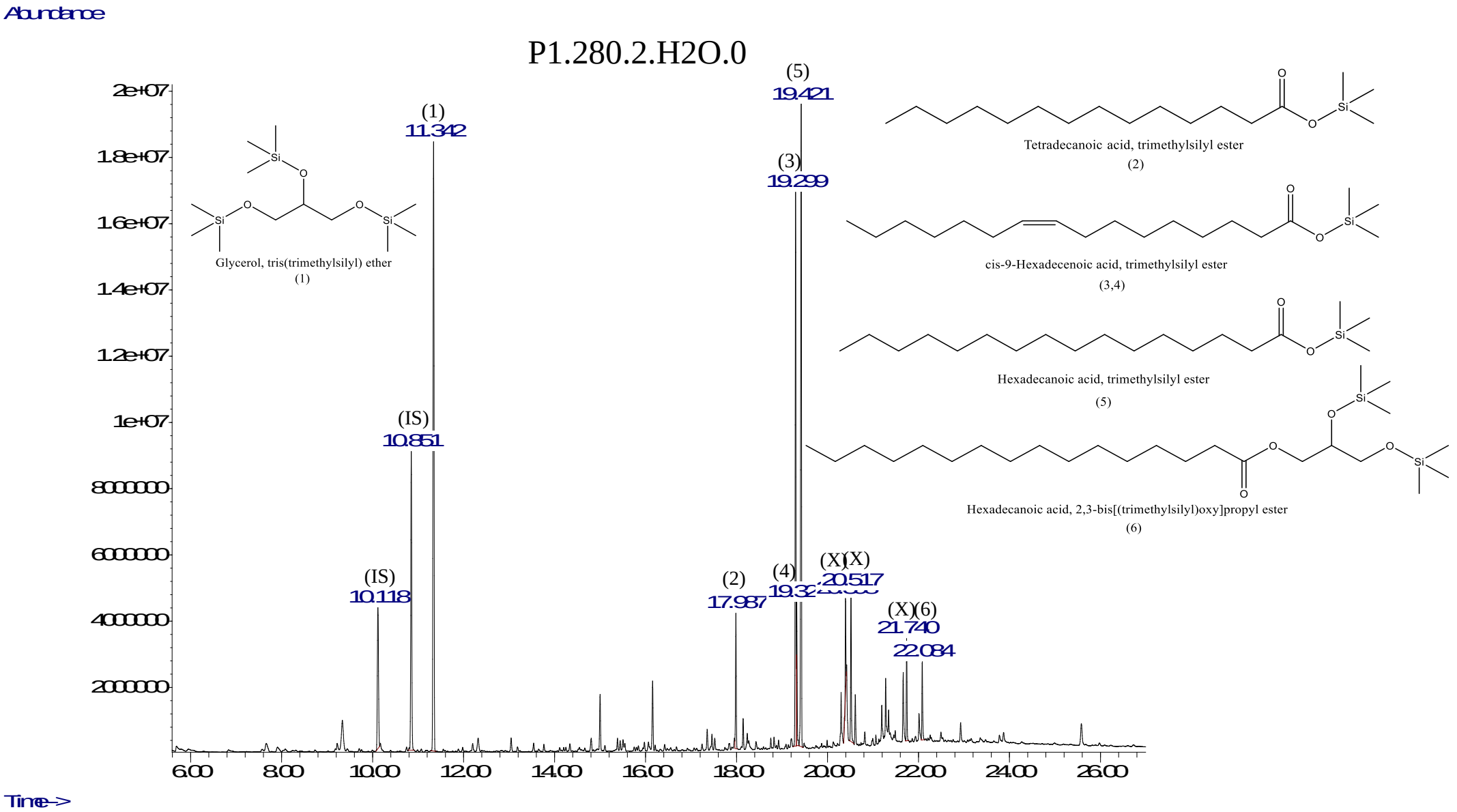
Abundance
P1.280.2.H2O.0
(1)
11.342
(IS)
10.851
(IS)
10.118
(2)
17.987
(3)
19.299
(4)
19.32
(5)
19.421
(X)
20.517
(X)
(X)
21.740
(6)
22.084
2e+07
1.8e+07
1.6e+07
1.4e+07
1.2e+07
1e+07
8000000
6000000
4000000
2000000
6.00
8.00
10.00
12.00
14.00
16.00
18.00
20.00
22.00
24.00
26.00
Time->
Glycerol, tris(trimethylsilyl) ether
(1)
Tetradecanoic acid, trimethylsilyl ester
(2)
cis-9-Hexadecenoic acid, trimethylsilyl ester
(3,4)
Hexadecanoic acid, trimethylsilyl ester
(5)
Hexadecanoic acid, 2,3-bis[(trimethylsilyl)oxy]propyl ester
(6)

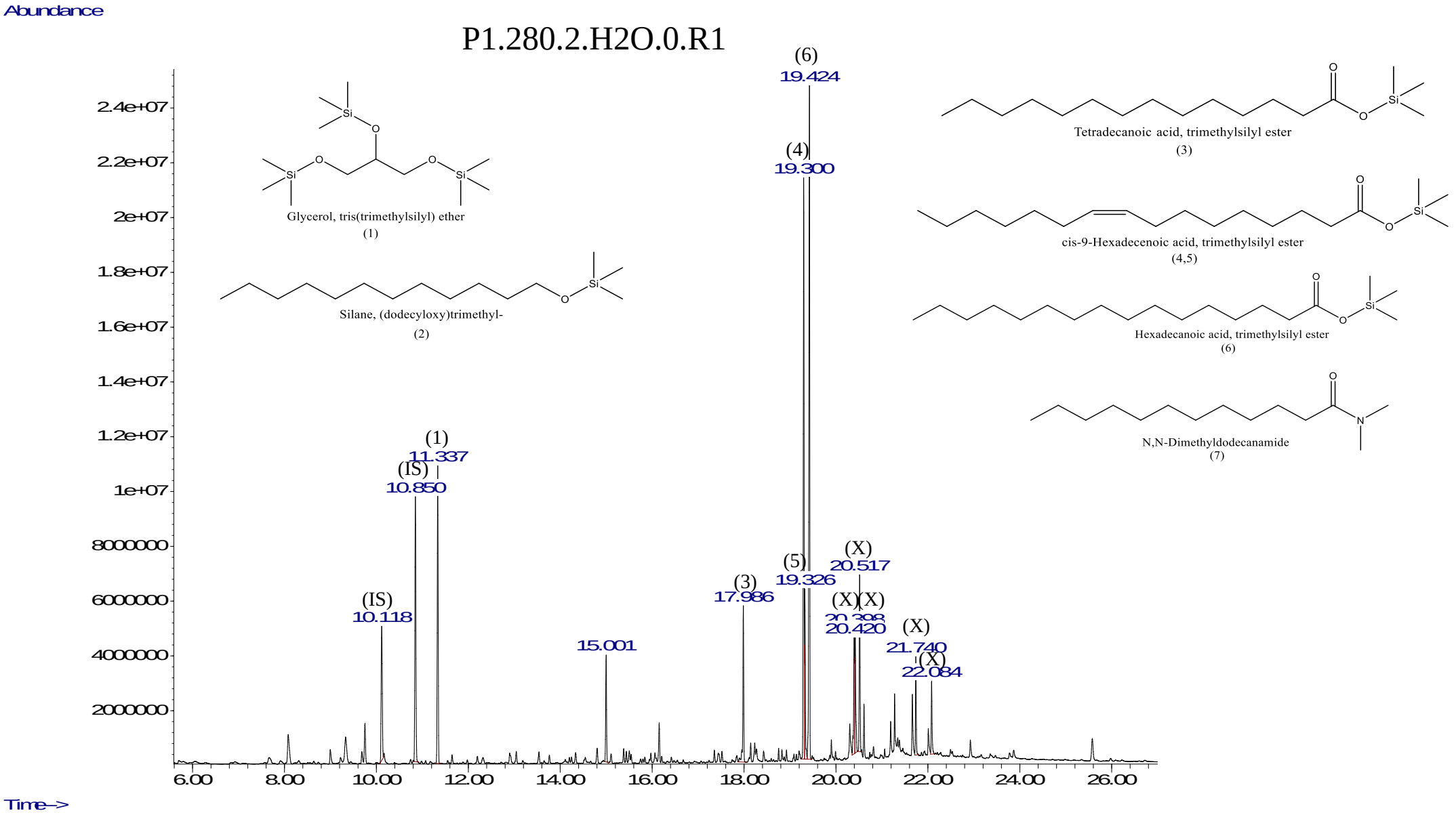
Abundance
P1.280.2.H2O.0.R1
(6)
19.424
(4)
19.300
(1)
11.337
(IS)
10.850
(IS)
10.118
15.001
(3)
17.986
(5)
19.326
(X)
20.517
(X)
20.420
(X)
21.740
(X)
22.084
2.4e+07
2.2e+07
2e+07
1.8e+07
1.6e+07
1.4e+07
1.2e+07
1e+07
8000000
6000000
4000000
2000000
6.00
8.00
10.00
12.00
14.00
16.00
18.00
20.00
22.00
24.00
26.00
Time-->
Glycerol, tris(trimethylsilyl) ether
(1)
Silane, (dodecyloxy)trimethyl-
(2)
Tetradecanoic acid, trimethylsilyl ester
(3)
cis-9-Hexadecenoic acid, trimethylsilyl ester
(4,5)
Hexadecanoic acid, trimethylsilyl ester
(6)
N,N-Dimethyldodecanamide
(7)

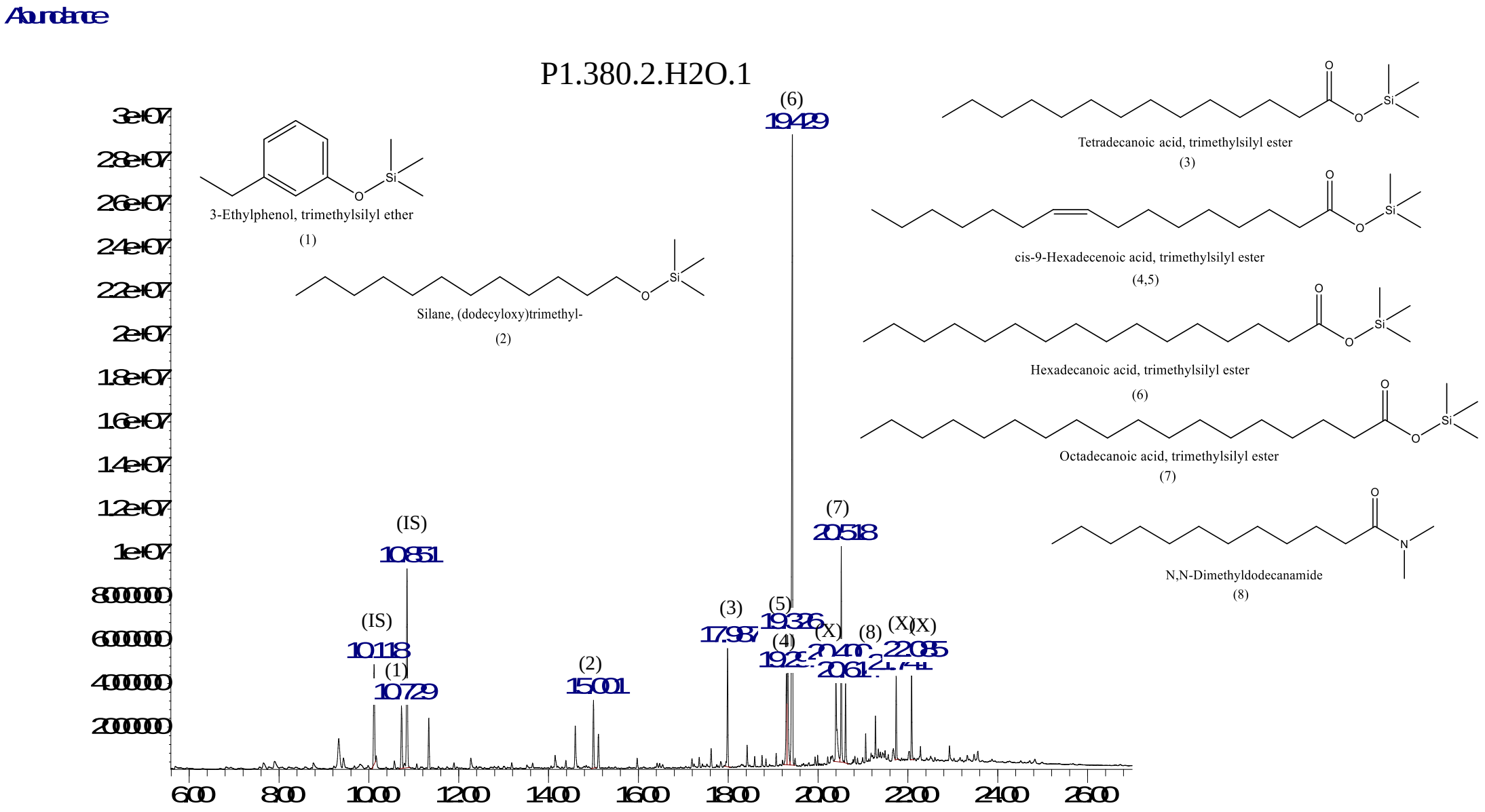
Abundance
P1.380.2.H2O.1
3-Ethylphenol, trimethylsilyl ether
(1)
Silane, (dodecyloxy)trimethyl-
(2)
Tetradecanoic acid, trimethylsilyl ester
(3)
cis-9-Hexadecenoic acid, trimethylsilyl ester
(4,5)
Hexadecanoic acid, trimethylsilyl ester
(6)
Octadecanoic acid, trimethylsilyl ester
(7)
N,N-Dimethyldodecanamide
(8)
(IS)
10851
(IS)
10118
(1)
10729
(2)
15001
(3)
17987
(5)
19336
(4)
(6)
19429
(X)
(7)
20518
(8)
(X)
(X)
22085
3e+07
2.8e+07
2.6e+07
2.4e+07
2.2e+07
2e+07
1.8e+07
1.6e+07
1.4e+07
1.2e+07
1e+07
800000
600000
400000
200000
600
800
1000
1200
1400
1600
1800
2000
2200
2400
2600
Time=>

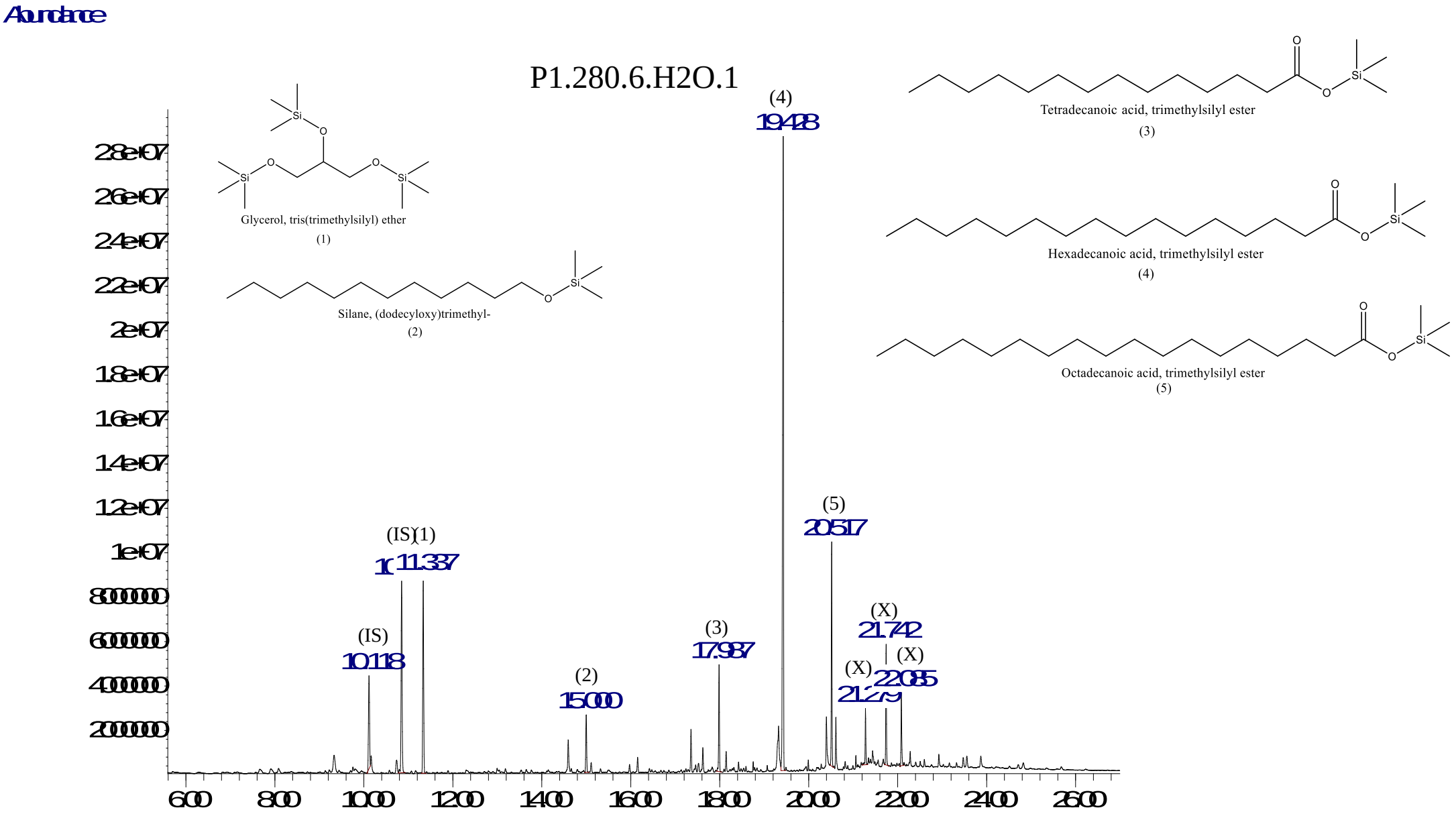
Abundance
P1.280.6.H2O.1
Glycerol, tris(trimethylsilyl) ether
(1)
Silane, (dodecyloxy)trimethyl-
(2)
Tetradecanoic acid, trimethylsilyl ester
(3)
Hexadecanoic acid, trimethylsilyl ester
(4)
Octadecanoic acid, trimethylsilyl ester
(5)
(4)
19.428
(5)
20.517
(IS)(1)
11.337
(IS)
10.118
(2)
15.000
(3)
17.987
(X)
21.742
(X)
22.085
(X)
21.279
2.8e+07
2.6e+07
2.4e+07
2.2e+07
2e+07
1.8e+07
1.6e+07
1.4e+07
1.2e+07
1e+07
8000000
6000000
4000000
2000000
600
800
1000
1200
1400
1600
1800
2000
2200
2400
2600
Time->
113

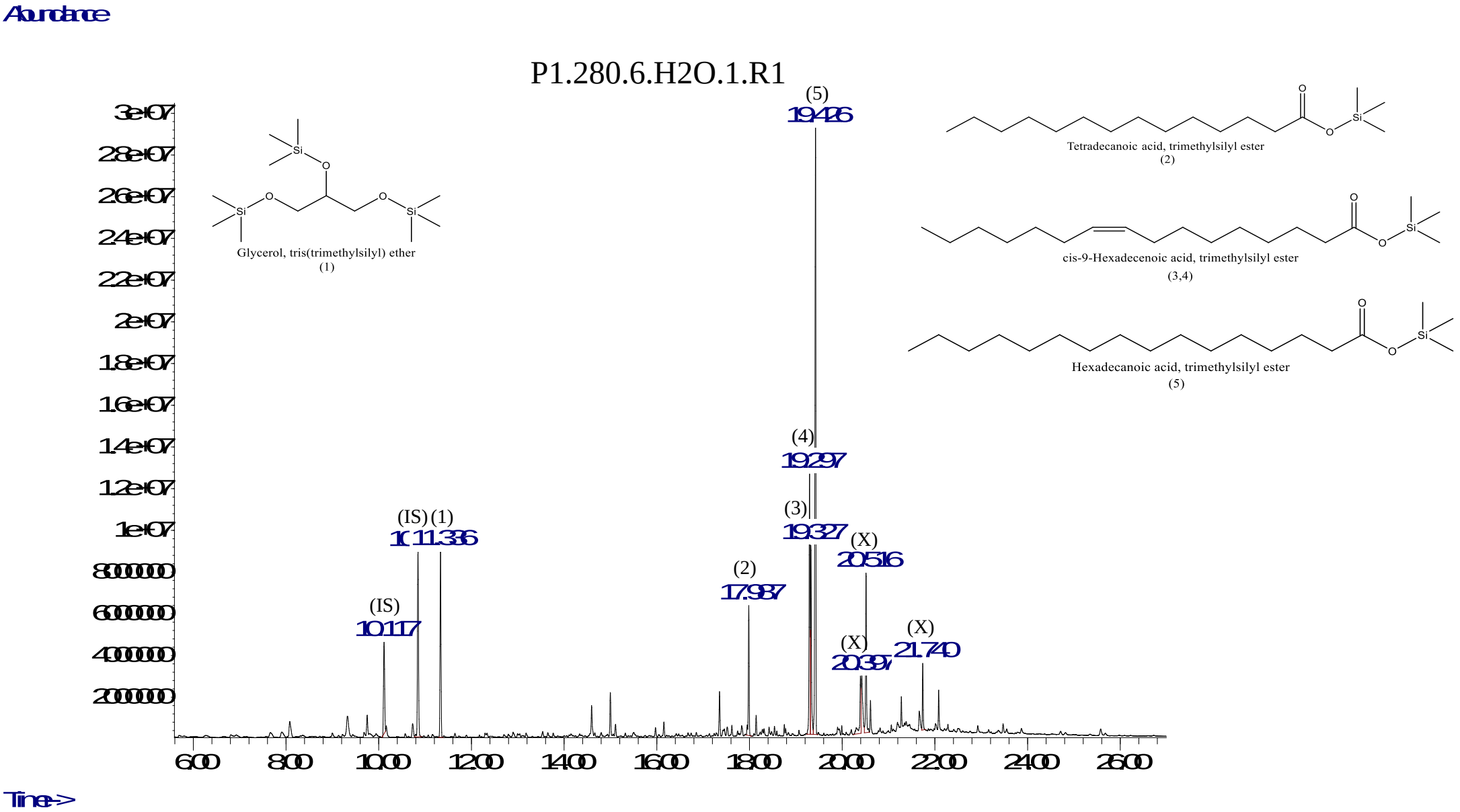
Abundance
P1.280.6.H2O.1.R1
Glycerol, tris(trimethylsilyl) ether
(1)
Tetradecanoic acid, trimethylsilyl ester
(2)
cis-9-Hexadecenoic acid, trimethylsilyl ester
(3,4)
Hexadecanoic acid, trimethylsilyl ester
(5)
(5)
19.426
(4)
19.297
(3)
19.327
(X)
20.516
(2)
17.987
(IS)
10.117
(IS) (1)
11.336
(X)
20.397
(X)
21.740
3e+07
2.8e+07
2.6e+07
2.4e+07
2.2e+07
2e+07
1.8e+07
1.6e+07
1.4e+07
1.2e+07
1e+07
8000000
6000000
4000000
2000000
600
800
1000
1200
1400
1600
1800
2000
2200
2400
2600
Time->
Si
O

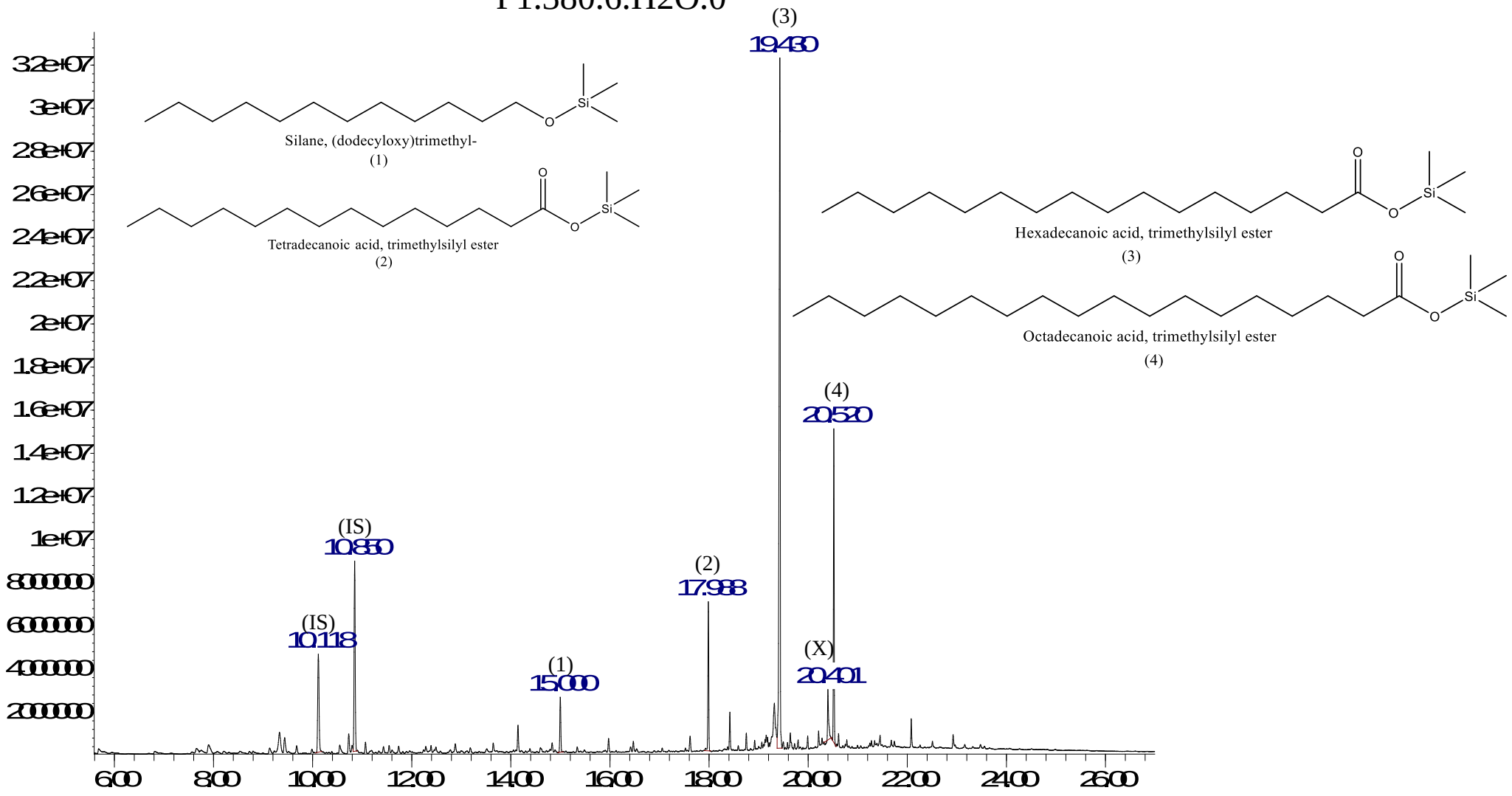
Abundance
P1.380.6.H2O.0
(3)
19.430
Silane, (dodecyloxy)trimethyl-
(1)
Tetradecanoic acid, trimethylsilyl ester
(2)
Hexadecanoic acid, trimethylsilyl ester
(3)
Octadecanoic acid, trimethylsilyl ester
(4)
(4)
20.520
(IS)
10.850
(2)
17.983
(IS)
10.118
(X)
20.401
(1)
15.000
3.2e+07
3e+07
2.8e+07
2.6e+07
2.4e+07
2.2e+07
2e+07
1.8e+07
1.6e+07
1.4e+07
1.2e+07
1e+07
8000000
6000000
4000000
2000000
6.00
8.00
10.00
12.00
14.00
16.00
18.00
20.00
22.00
24.00
26.00
Time->
O
Si

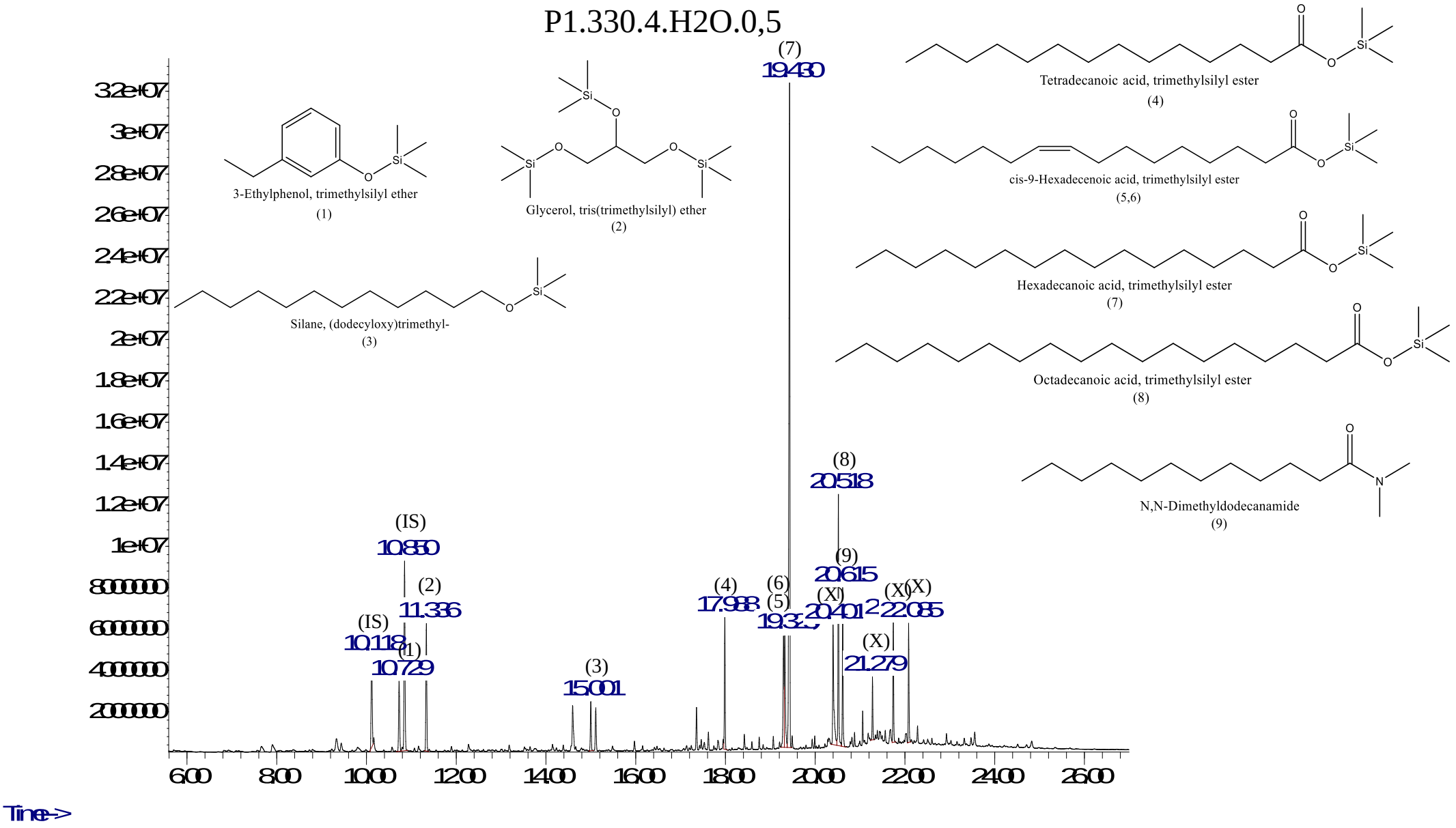
Abundance
P1.330.4.H2O.0,5
3-Ethylphenol, trimethylsilyl ether
(1)
Glycerol, tris(trimethylsilyl) ether
(2)
Silane, (dodecyloxy)trimethyl-
(3)
Tetradecanoic acid, trimethylsilyl ester
(4)
cis-9-Hexadecenoic acid, trimethylsilyl ester
(5,6)
Hexadecanoic acid, trimethylsilyl ester
(7)
Octadecanoic acid, trimethylsilyl ester
(8)
N,N-Dimethyldodecanamide
(9)
(IS)
10.850
(2)
11.336
(IS)
10.118
(1)
10.729
(3)
15.001
(4)
17.988
(6)
(5)
19.327
(7)
19.430
(X)
20.401
(8)
20.518
(9)
20.615
(X)
(X)
21.279
(X)
22.085
3.2e+07
3e+07
2.8e+07
2.6e+07
2.4e+07
2.2e+07
2e+07
1.8e+07
1.6e+07
1.4e+07
1.2e+07
1e+07
800000
600000
400000
200000
600
800
1000
1200
1400
1600
1800
2000
2200
2400
2600
Time->
116

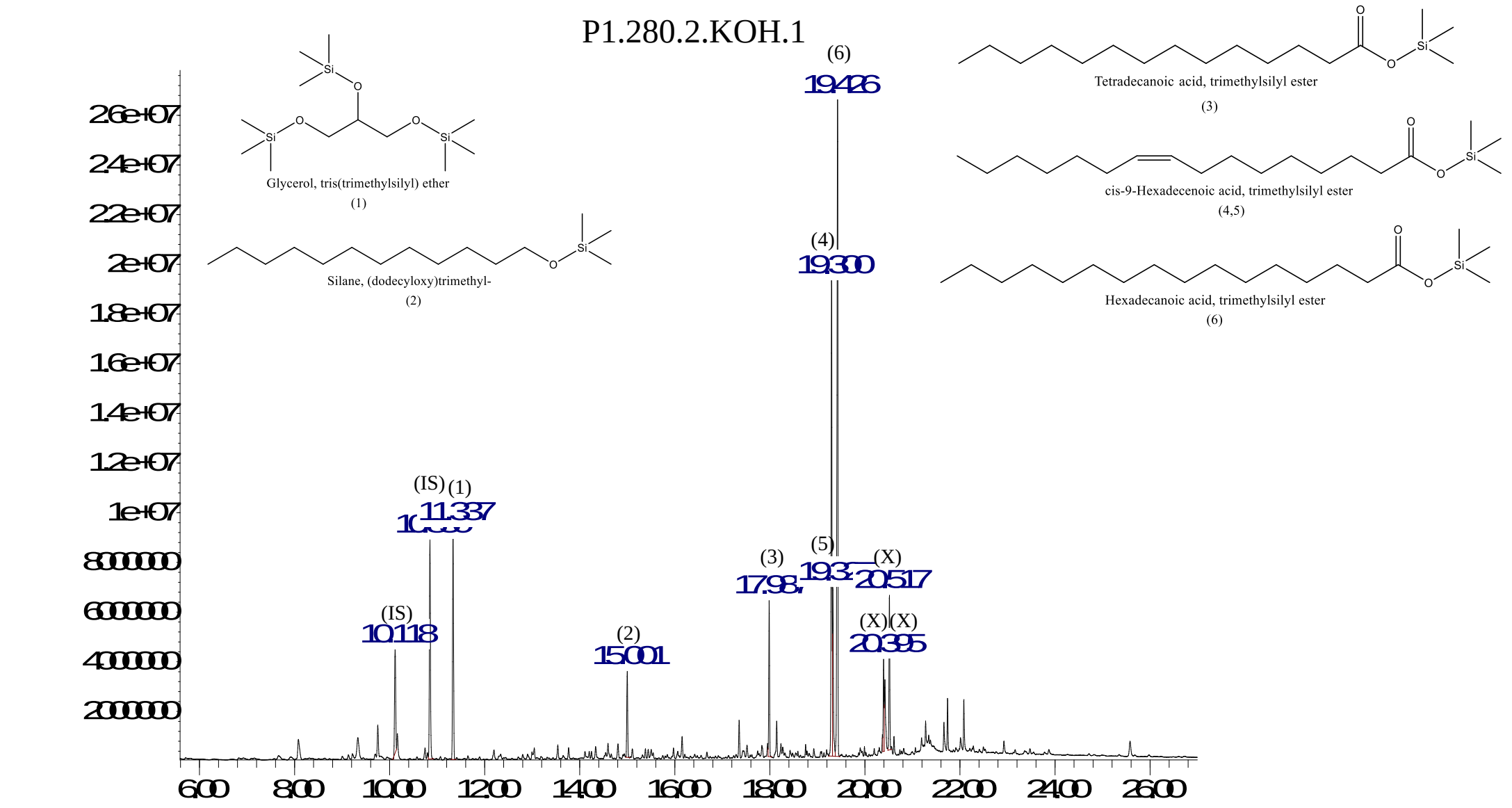
Abundance
P1.280.2.KOH.1
(6)
19.426
(4)
19.300
(5)
19.357
(3)
17.987
(X)
20.517
(X)(X)
20.395
(IS)
10.118
(IS)
(1)
11.337
(2)
15.001
2.6e+07
2.4e+07
2.2e+07
2e+07
1.8e+07
1.6e+07
1.4e+07
1.2e+07
1e+07
800000
600000
400000
200000
600
800
1000
1200
1400
1600
1800
2000
2200
2400
2600
Time->
Glycerol, tris(trimethylsilyl) ether
(1)
Silane, (dodecyloxy)trimethyl-
(2)
Tetradecanoic acid, trimethylsilyl ester
(3)
cis-9-Hexadecenoic acid, trimethylsilyl ester
(4,5)
Hexadecanoic acid, trimethylsilyl ester
(6)

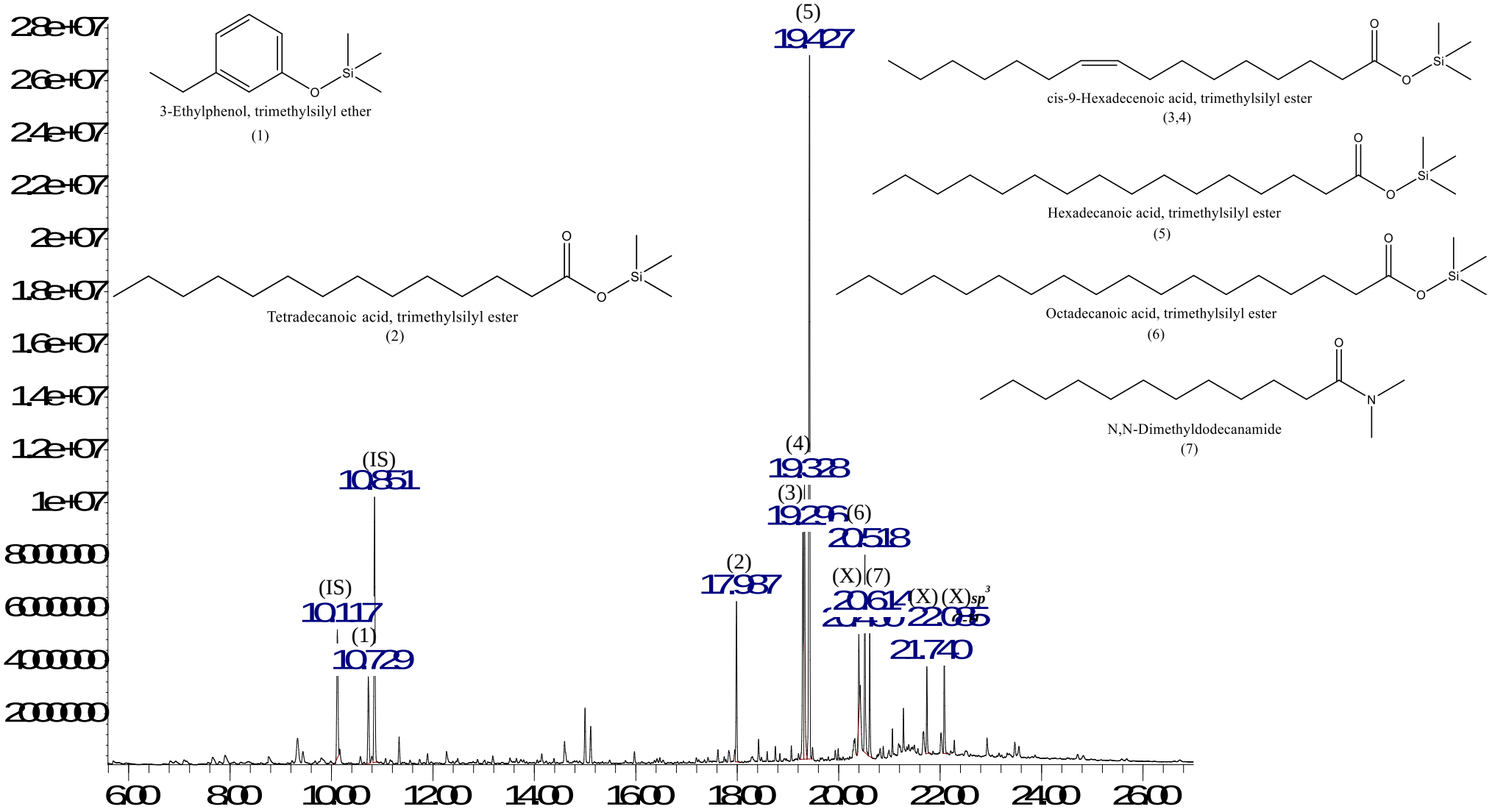
Abundance
P1.380.2.KOH.1
2.8e+07
2.6e+07
2.4e+07
2.2e+07
2e+07
1.8e+07
1.6e+07
1.4e+07
1.2e+07
1e+07
800000
600000
400000
200000
3-Ethylphenol, trimethylsilyl ether
(1)
Tetradecanoic acid, trimethylsilyl ester
(2)
(5)
19.427
cis-9-Hexadecenoic acid, trimethylsilyl ester
(3,4)
Hexadecanoic acid, trimethylsilyl ester
(5)
Octadecanoic acid, trimethylsilyl ester
(6)
N,N-Dimethyldodecanamide
(7)
(IS)
10.851
(4)
19.328
(3)
19.296
(6)
20.518
(2)
17.987
(X)
(7)
20.614
(X)
(X)
sp3
22.085
21.740
(IS)
10.117
(1)
10.729
600
800
1000
1200
1400
1600
1800
2000
2200
2400
2600
Time->
118

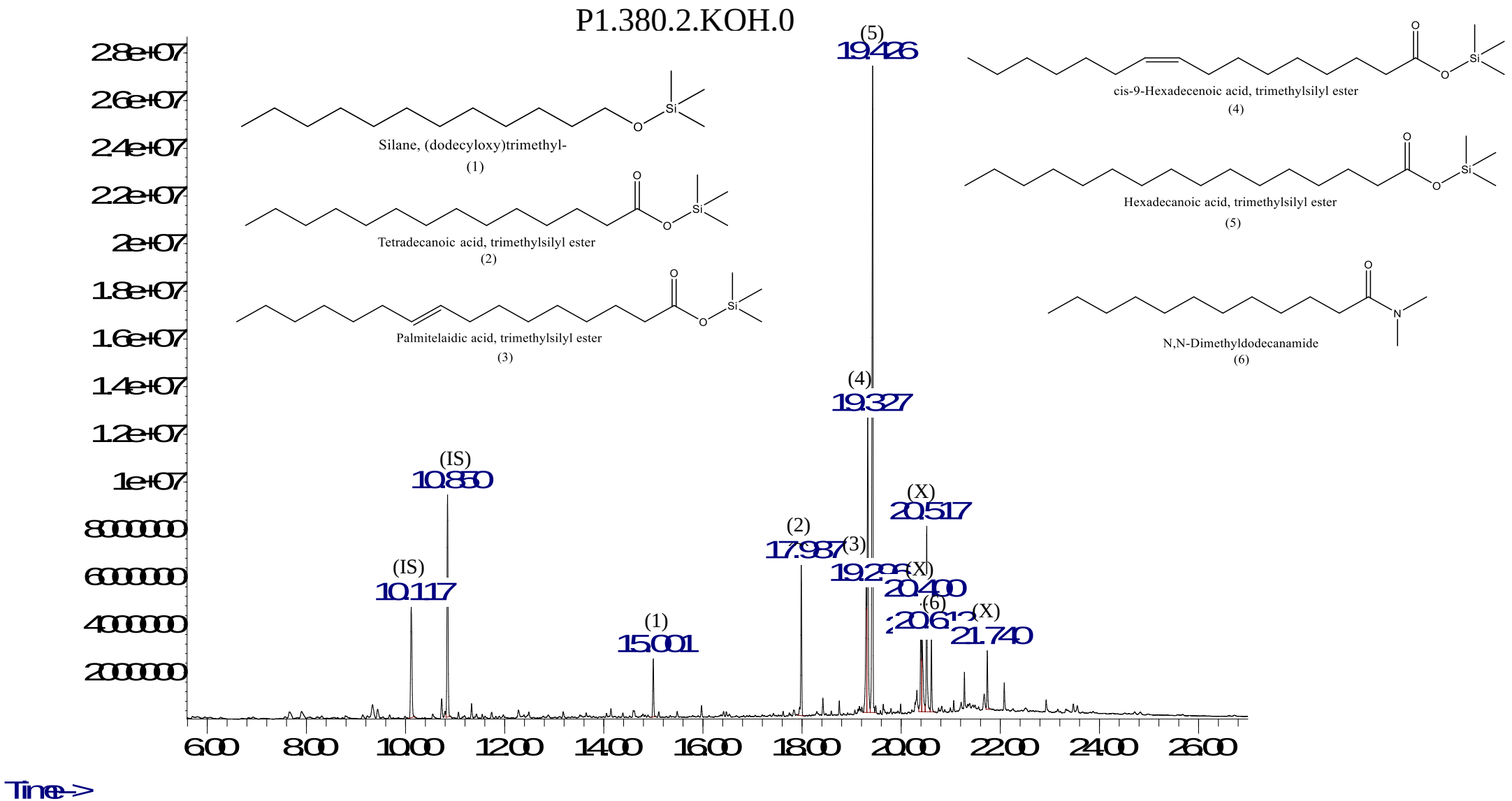
Abundance
P1.380.2.KOH.0
Silane, (dodecyloxy)trimethyl-
(1)
Tetradecanoic acid, trimethylsilyl ester
(2)
Palmitelaidic acid, trimethylsilyl ester
(3)
cis-9-Hexadecenoic acid, trimethylsilyl ester
(4)
Hexadecanoic acid, trimethylsilyl ester
(5)
N,N-Dimethyldodecanamide
(6)
(IS)
10.830
(IS)
10.117
(1)
15.001
(2)
17.987
(3)
19.296
(4)
19.327
(5)
19.426
(X)
20.517
(X)
20.400
(6)
20.613
(X)
21.740
Time->
28e+07
26e+07
24e+07
22e+07
2e+07
18e+07
16e+07
14e+07
12e+07
1e+07
800000
600000
400000
200000
600
800
1000
1200
1400
1600
1800
2000
2200
2400
2600

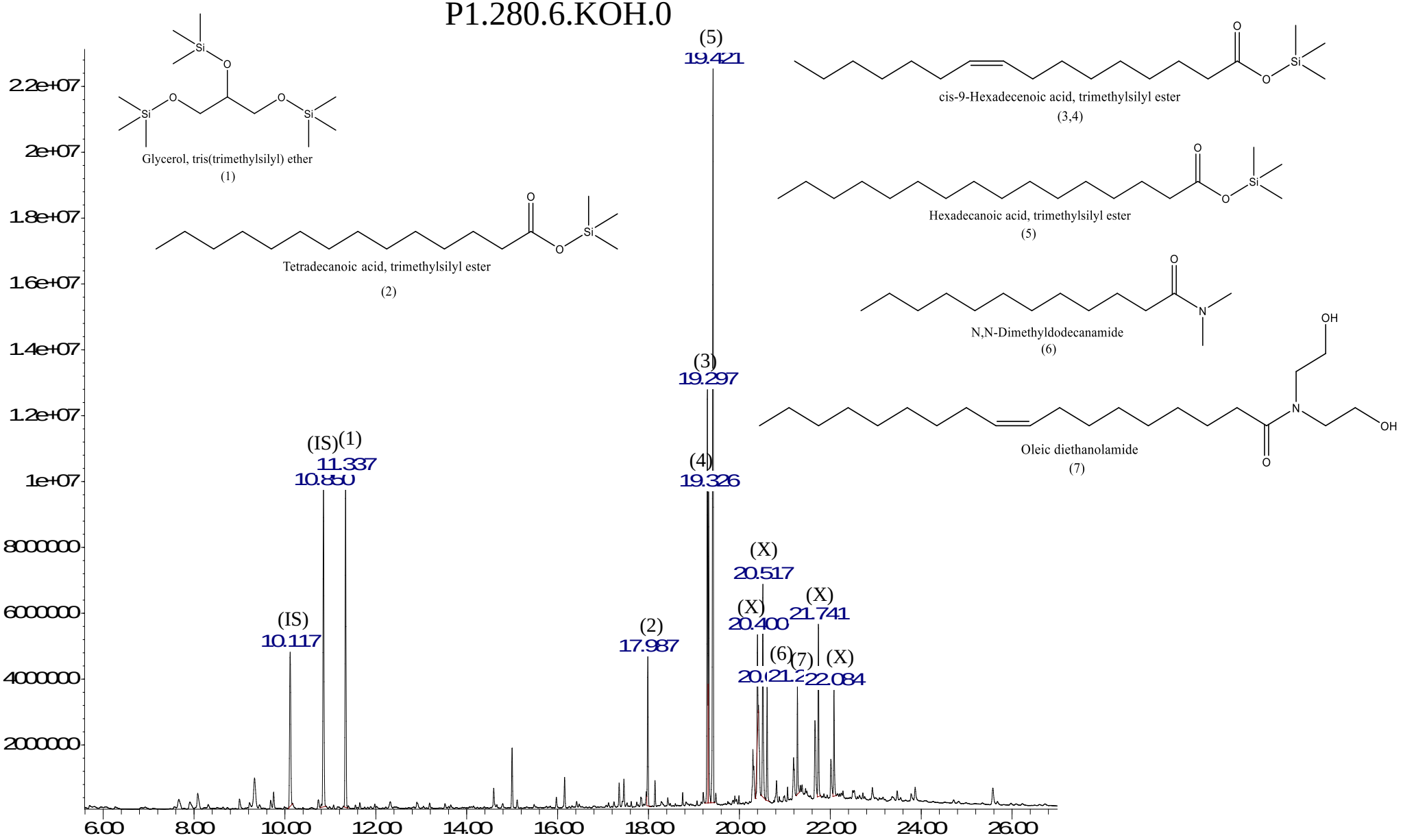
Abundance
P1.280.6.KOH.0
Glycerol, tris(trimethylsilyl) ether
(1)
Tetradecanoic acid, trimethylsilyl ester
(2)
(5)
19.421
cis-9-Hexadecenoic acid, trimethylsilyl ester
(3,4)
Hexadecanoic acid, trimethylsilyl ester
(5)
N,N-Dimethyldodecanamide
(6)
Oleic diethanolamide
(7)
(3)
19.297
(4)
19.326
(IS)
10.117
(IS)
10.850
(1)
11.337
(2)
17.987
(X)
20.517
(X)
20.400
(X)
21.741
(6)
(7)
(X)
22.084
2.2e+07
2e+07
1.8e+07
1.6e+07
1.4e+07
1.2e+07
1e+07
8000000
6000000
4000000
2000000
6.00
8.00
10.00
12.00
14.00
16.00
18.00
20.00
22.00
24.00
26.00
Time-->

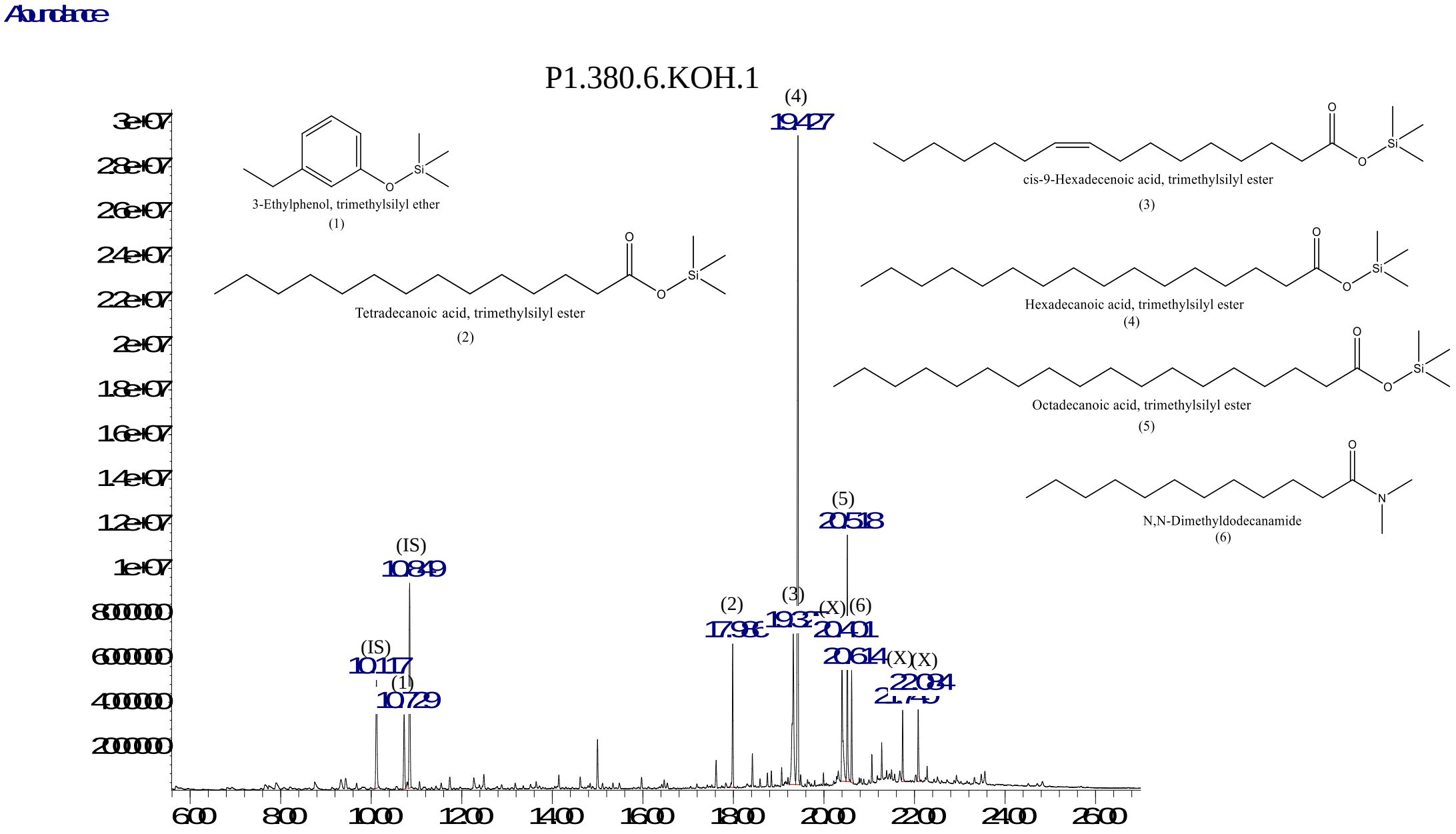
Abundance
P1.380.6.KOH.1
3-Ethylphenol, trimethylsilyl ether
(1)
Tetradecanoic acid, trimethylsilyl ester
(2)
cis-9-Hexadecenoic acid, trimethylsilyl ester
(3)
Hexadecanoic acid, trimethylsilyl ester
(4)
Octadecanoic acid, trimethylsilyl ester
(5)
N,N-Dimethyldodecanamide
(6)
(IS)
(IS)
(1)
(2)
(3)
(4)
(5)
(6)
(X)
(X)
(X)
Time->
600
800
1000
1200
1400
1600
1800
2000
2200
2400
2600

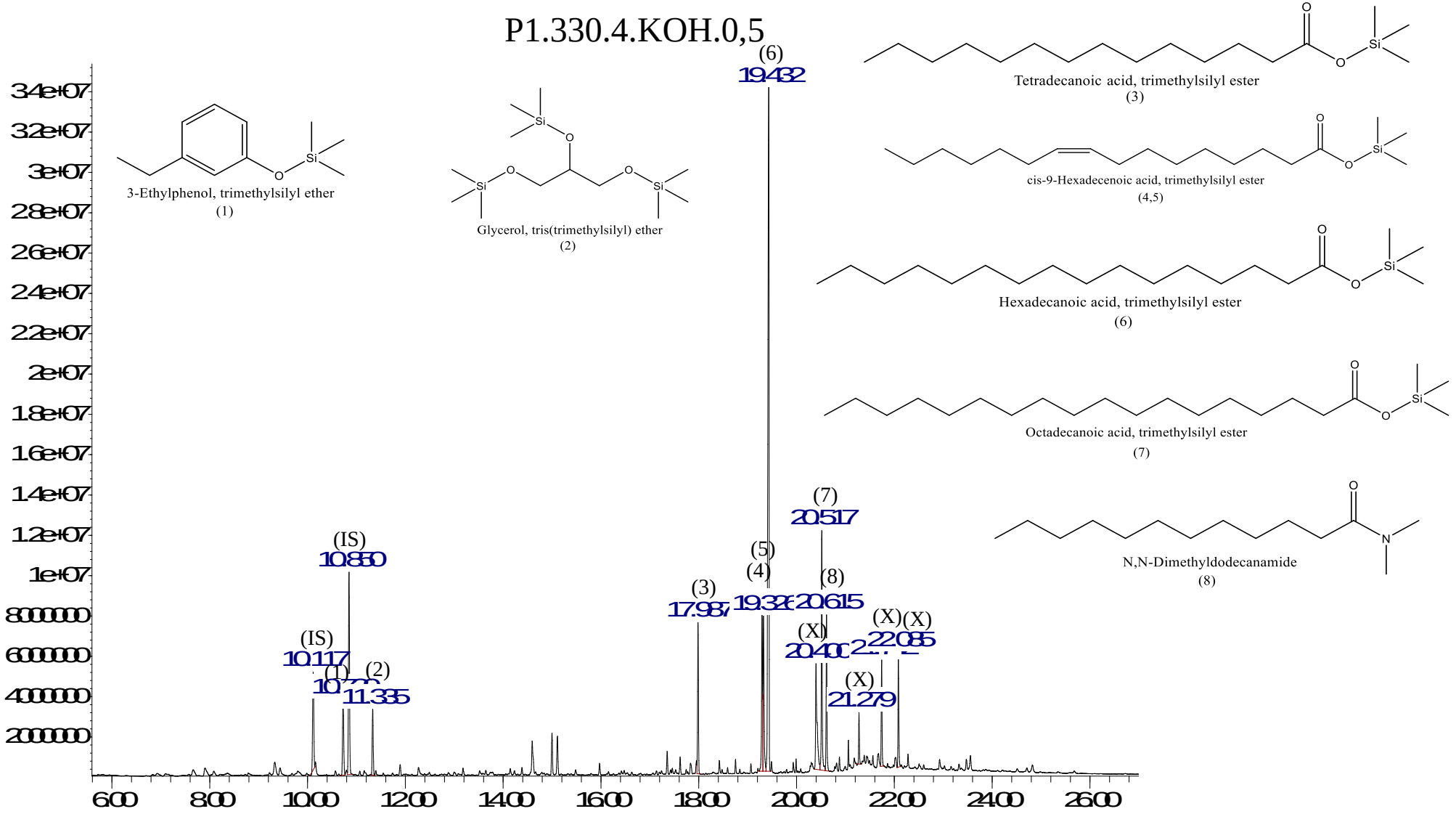
Abundance
P1.330.4.KOH.0,5
3-Ethylphenol, trimethylsilyl ether
(1)
Glycerol, tris(trimethylsilyl) ether
(2)
Tetradecanoic acid, trimethylsilyl ester
(3)
cis-9-Hexadecenoic acid, trimethylsilyl ester
(4,5)
Hexadecanoic acid, trimethylsilyl ester
(6)
Octadecanoic acid, trimethylsilyl ester
(7)
N,N-Dimethyldodecanamide
(8)
(IS)
10.850
(IS)
10.117
(1)
(2)
11.335
(3)
17.987
(4)
(5)
19.432
(6)
19.432
(7)
20.517
(8)
20.615
(X)
20.400
(X)
21.279
(X)
(X)
22.085
34e+07
32e+07
3e+07
28e+07
26e+07
24e+07
22e+07
2e+07
18e+07
16e+07
14e+07
12e+07
1e+07
800000
600000
400000
200000
600
800
1000
1200
1400
1600
1800
2000
2200
2400
2600
Time->
O
Si
N

A.6 INFRARED SPECTROSCOPY

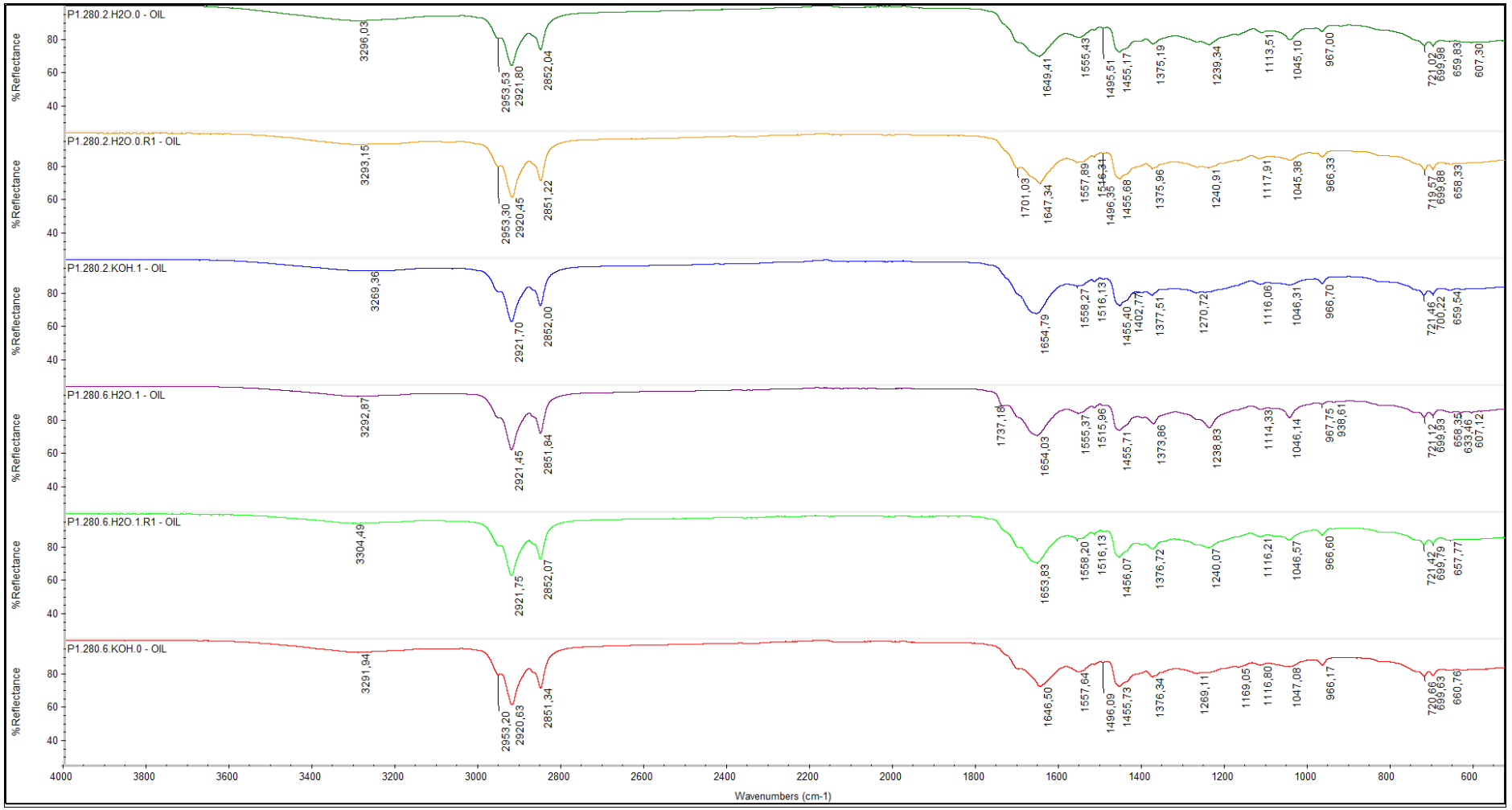

Figure A.6-a: Comparison of the IR spectra for all bio-oil samples in P1 with T=280.

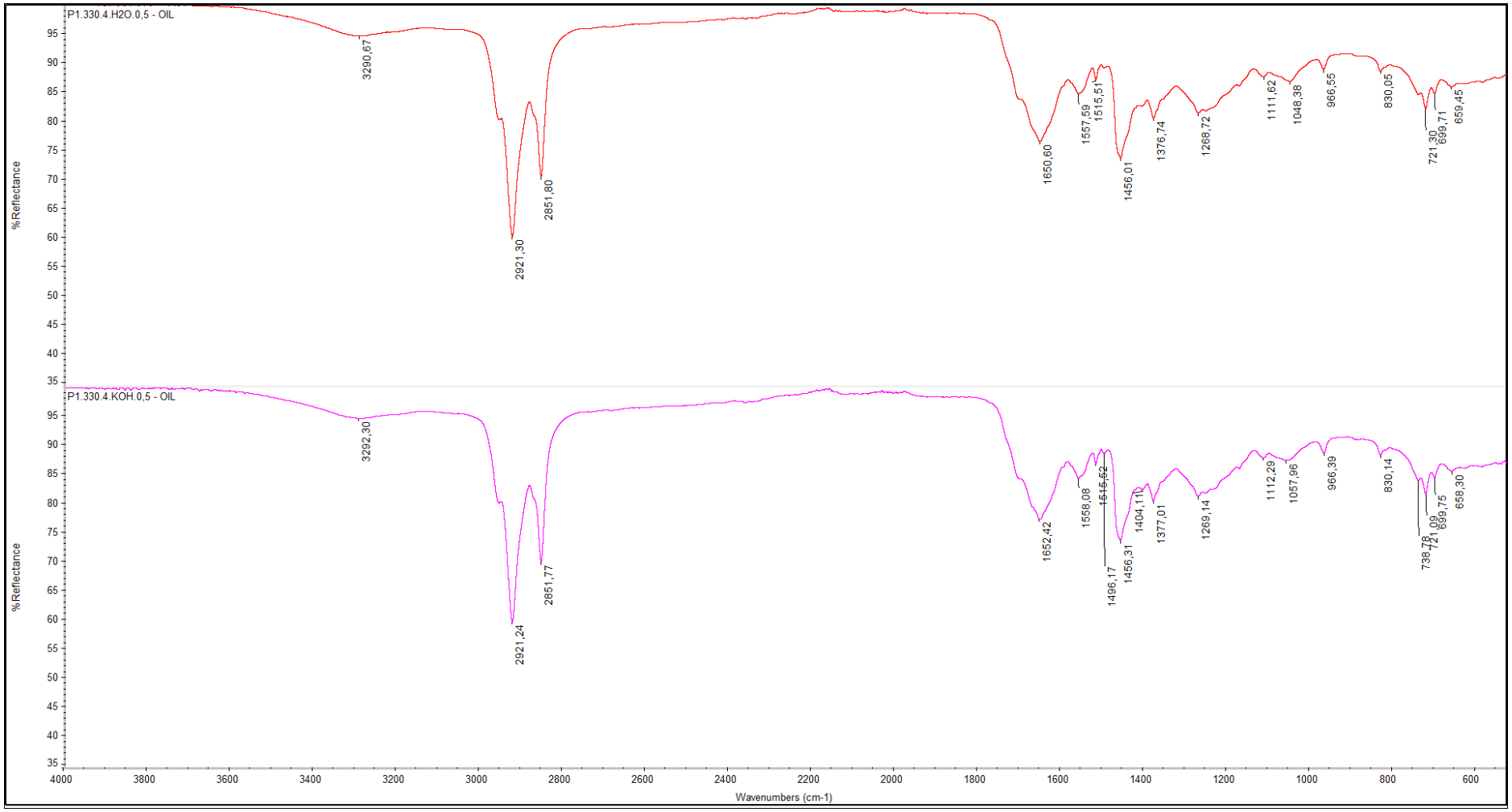

Figure A.6-b: Comparison of the IR spectra for all bio-oil samples in P1 with T=330.

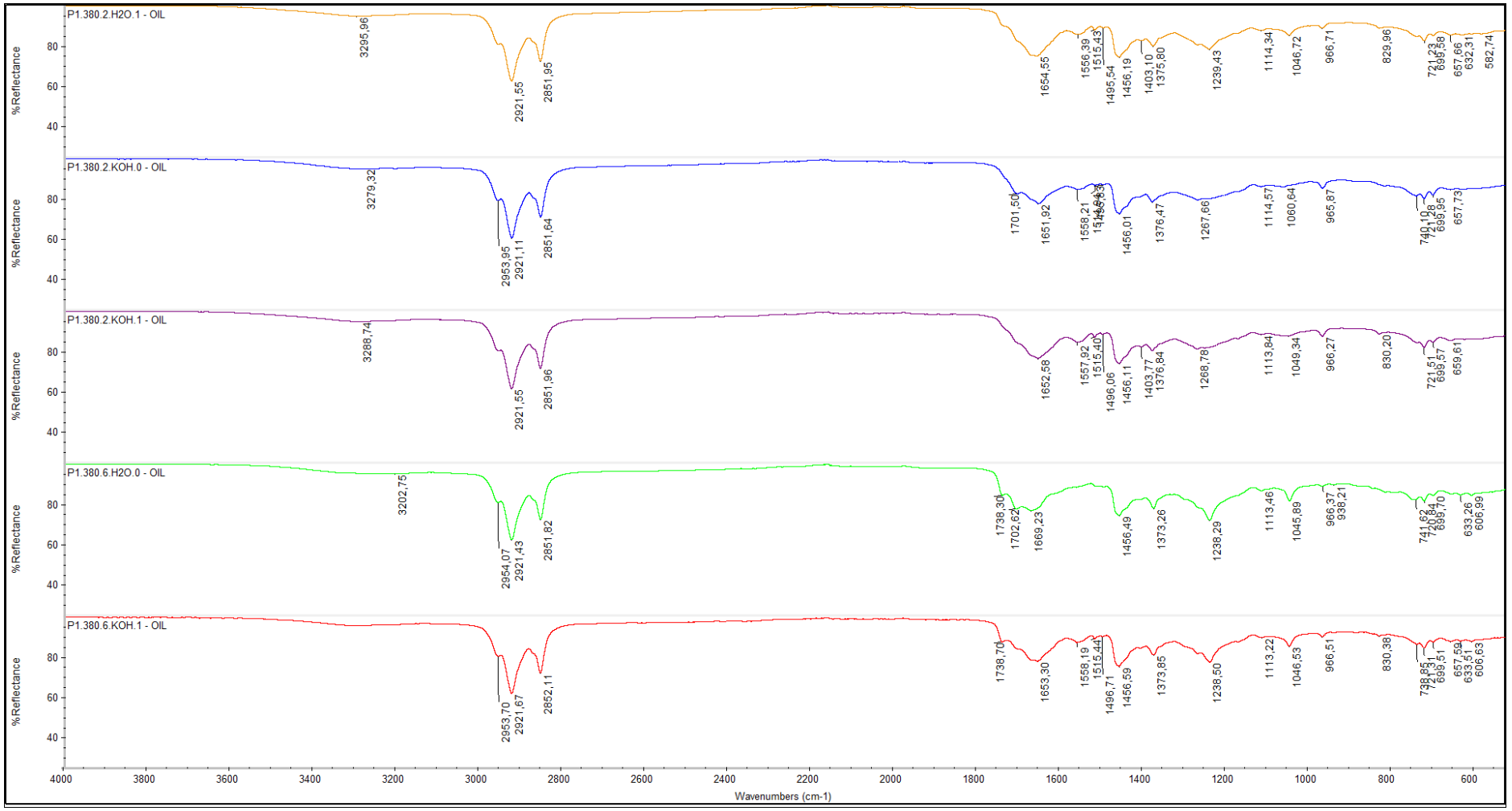

Figure A.6-c: Comparison of the IR spectra for all bio-oil samples in P1 with T=380.

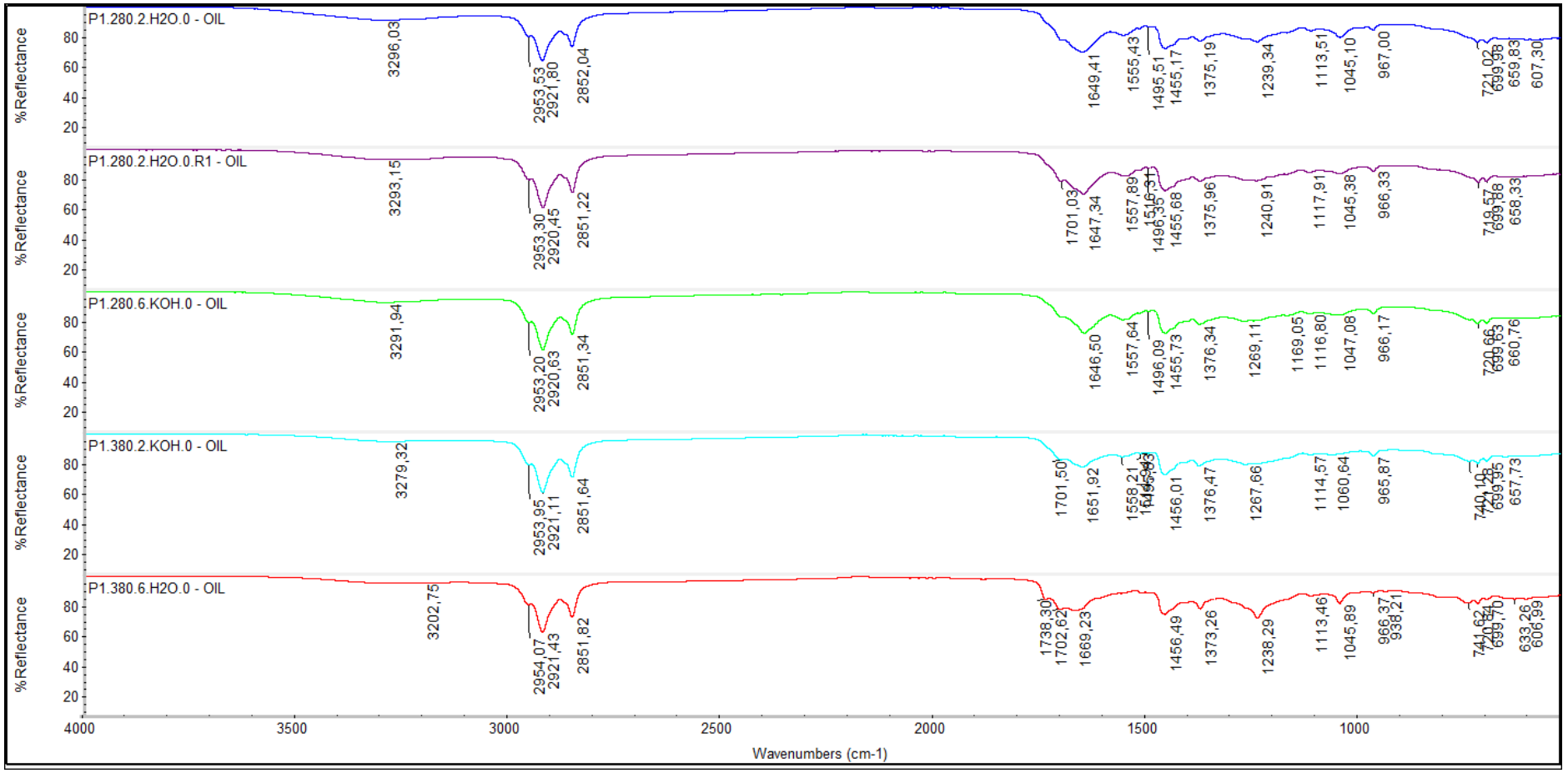

Figure A.6-d: Comparison of the IR spectra for all bio-oil samples in P1 with FA=0.

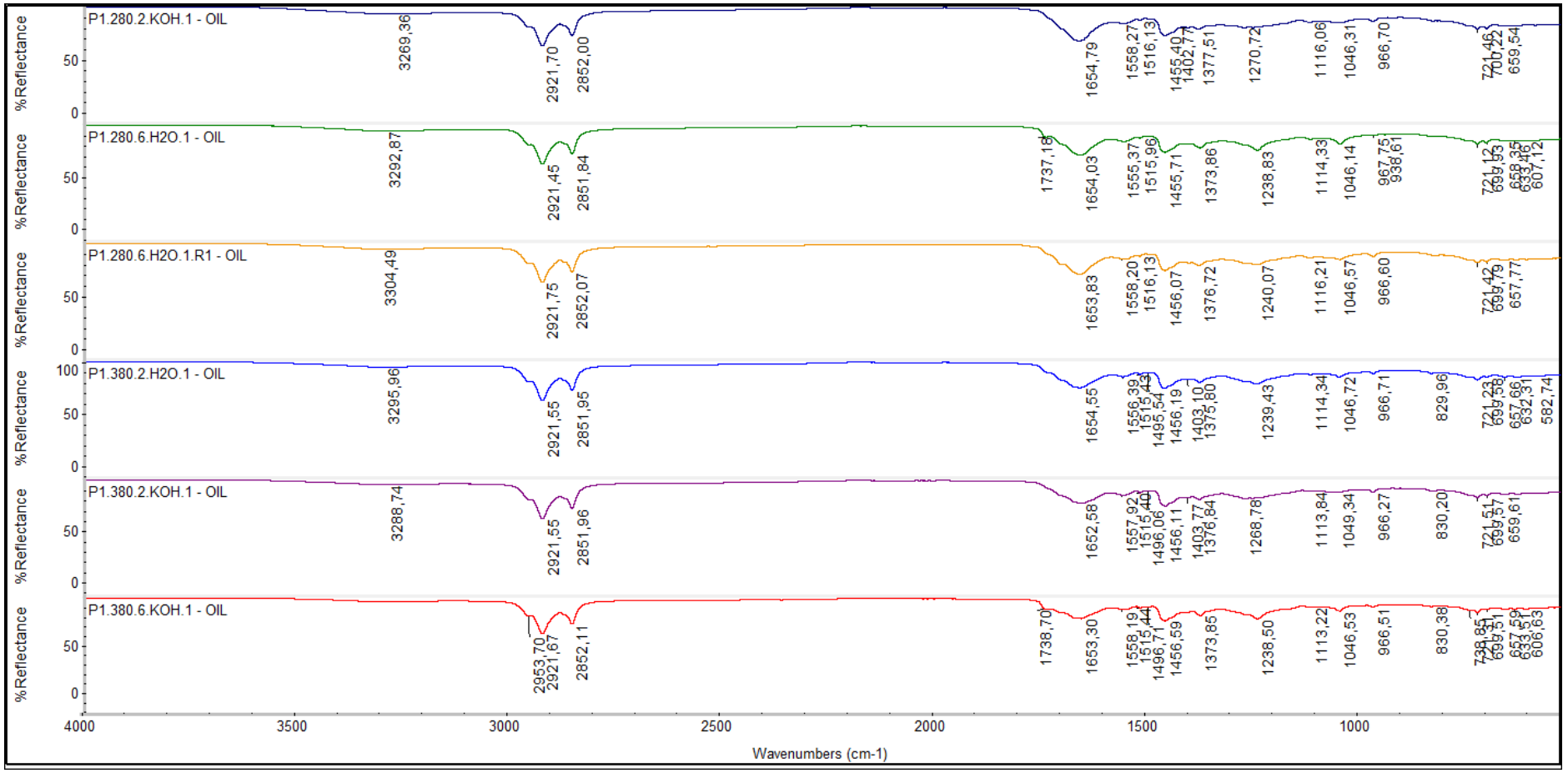

Figure A.6-e: Comparison of the IR spectra for all bio-oil samples in P1 with FA=1.

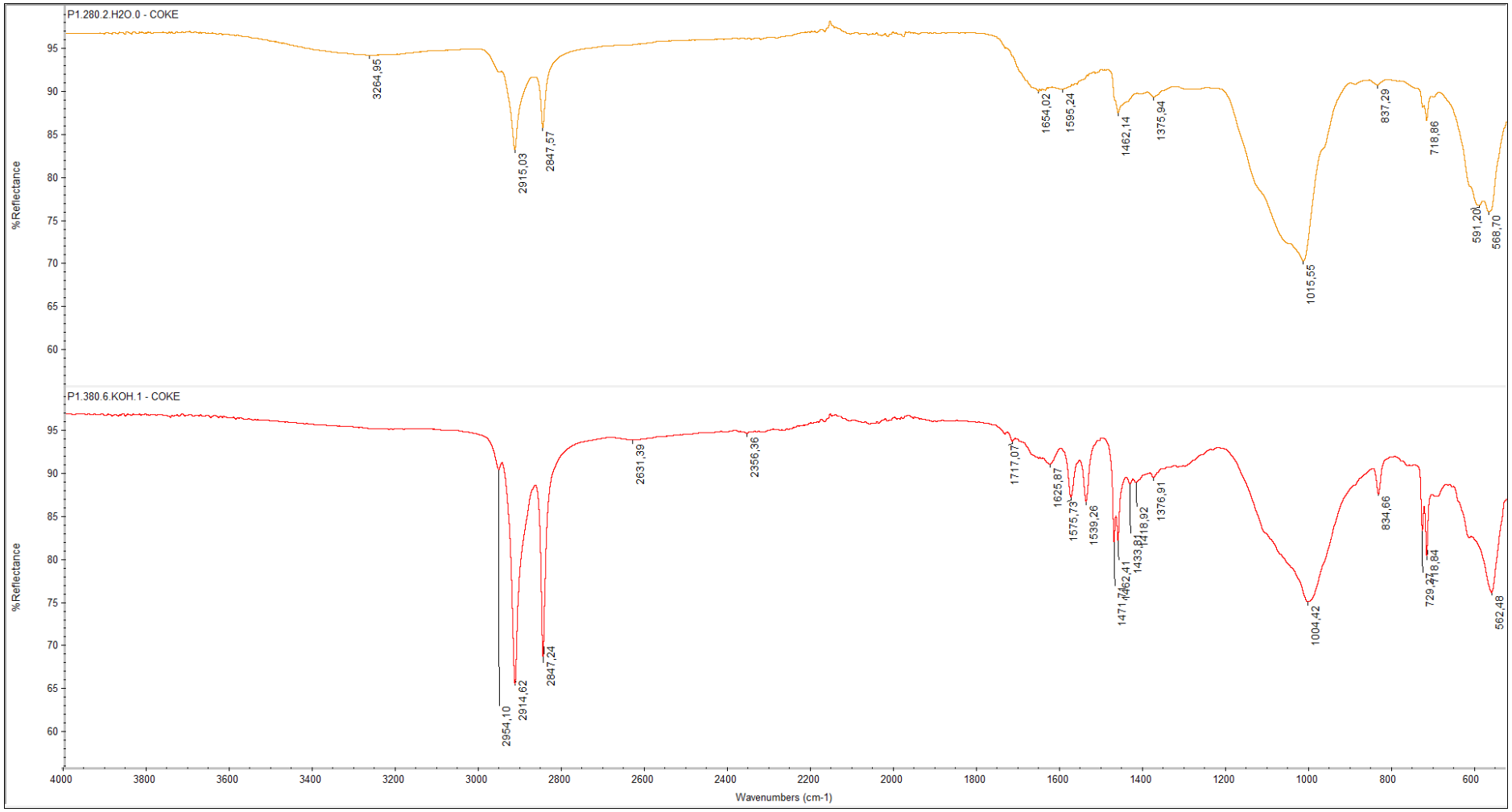

Figure 6.A-f: Comparison of the IR spectra for coke samples in P1 with all high levels [(+)(+)(+)(+)] and all low levels [(-)(-)(-)(-)].

APPENDIX B – PILOT SERIES 2

B.1 HTL

Table B.1-1: HTL workup for Pilot Series 2.

Experiment	Feedstock [g]	TS[a] [g]	Wv[b] [g]	Inorganic (dw.) [g]	Water [g]	Formic acid [g]	Total [g]
P2.220.2.H2O.0	4.01	1.05	0.934	0.0663	2.01	0.00	6.02
P2.280.2.H2O.1	4.03	1.05	0.938	0.0616	1.00	1.22	6.25
P2.220.6.H2O.1	4.01	1.05	0.934	0.0663	1.00	1.22	6.23
P2.280.6.H2O.0	4.02	1.05	0.936	0.0639	2.00	0.00	6.02
P2.280.6.H2O.0.R1	4.01	1.05	0.934	0.0663	2.00	0.00	6.01
P2.220.2.H2O.1	4.03	1.05	0.938	0.0616	1.02	1.22	6.27
P2.220.2.H2O.1.R1	4.01	1.05	0.934	0.0663	1.01	1.22	6.24
P2.280.2.H2O.0	4.03	1.05	0.938	0.0616	2.00	0.00	6.03
P2.220.6.H2O.0	4.03	1.05	0.938	0.0616	1.99	0.00	6.02
P2.280.6.H2O.1	4.01	1.05	0.934	0.0663	1.00	1.22	6.23
P2.250.4.H2O.0	4.01	1.05	0.934	0.0663	2.00	0.00	6.01
P2.250.4.H2O.1	4.02	1.05	0.936	0.0639	1.00	1.22	6.24

[a, b] Based on the average TS [%] and average Wv [%] values calculated in proximate analysis for "Feedstock 1". See Table 4.1-1.

B.2 PRINCIPAL COMPONENT ANALYSIS AND REGRESSION

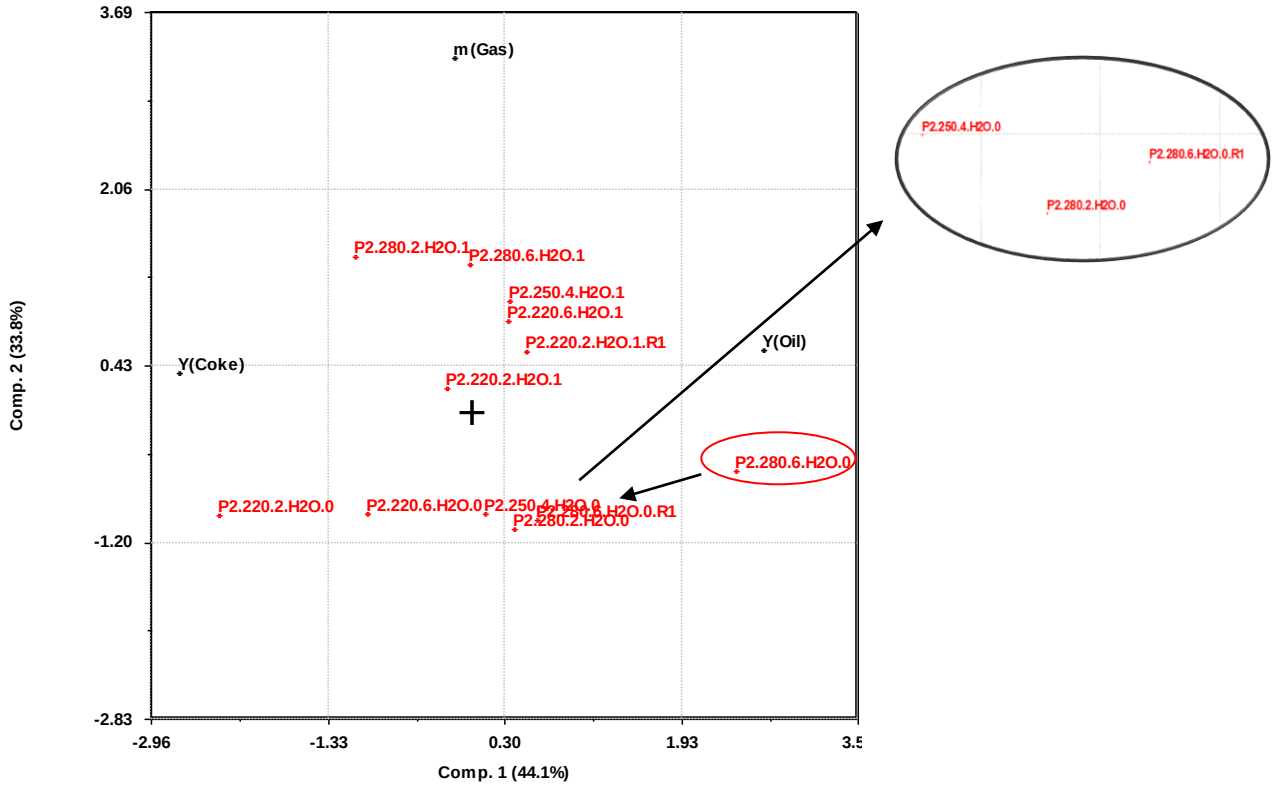

Figure B.2-a: Detection of outliers in Pilot Series 2., with only yield of oil, coke, gas and objects are included. The red circle marks the outlier, and the associated arrow points at its replica.

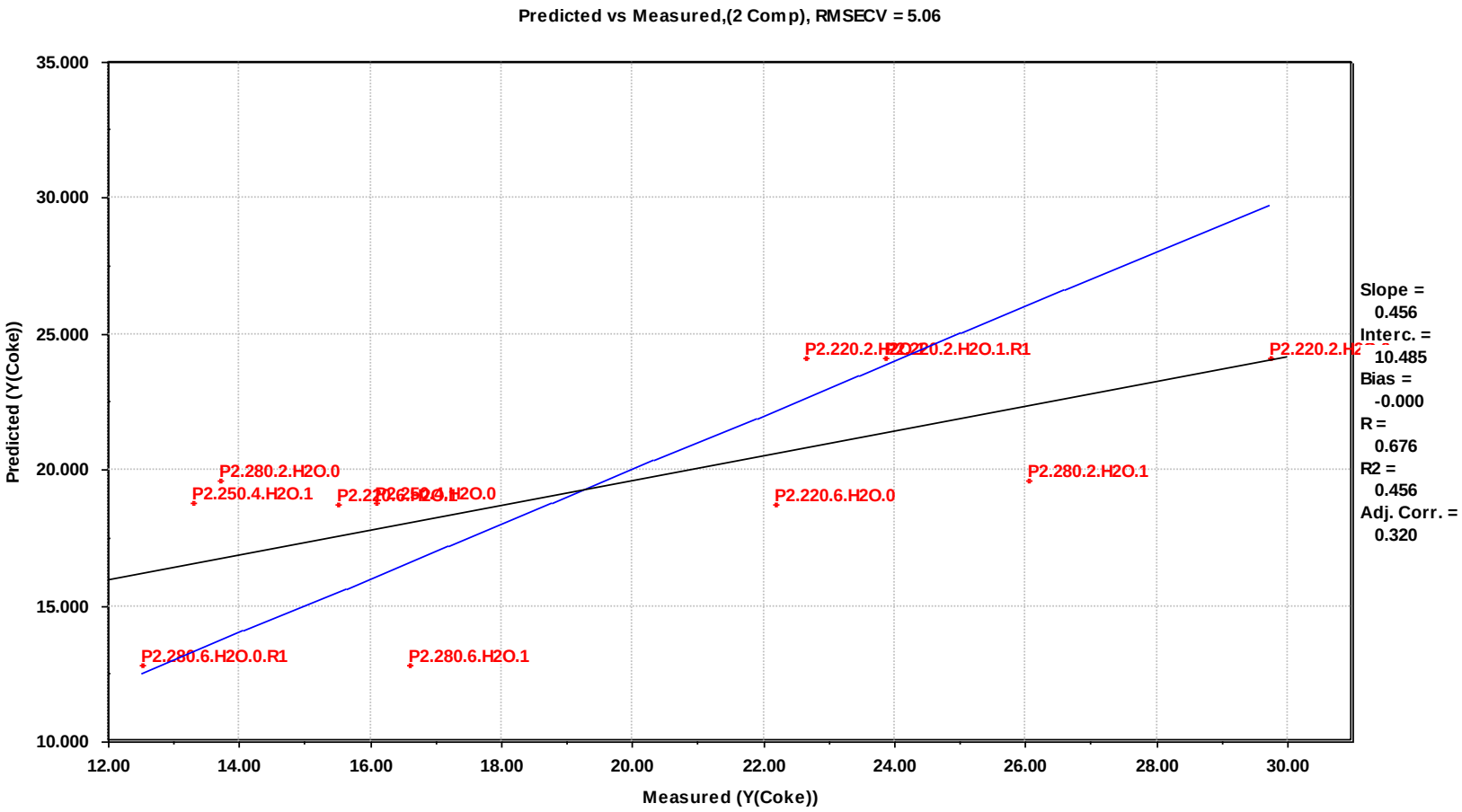

Figure B.2-b: PLS plot of predicted vs measured values for coke yields in Pilot Series 2. All experiments, without outliers.

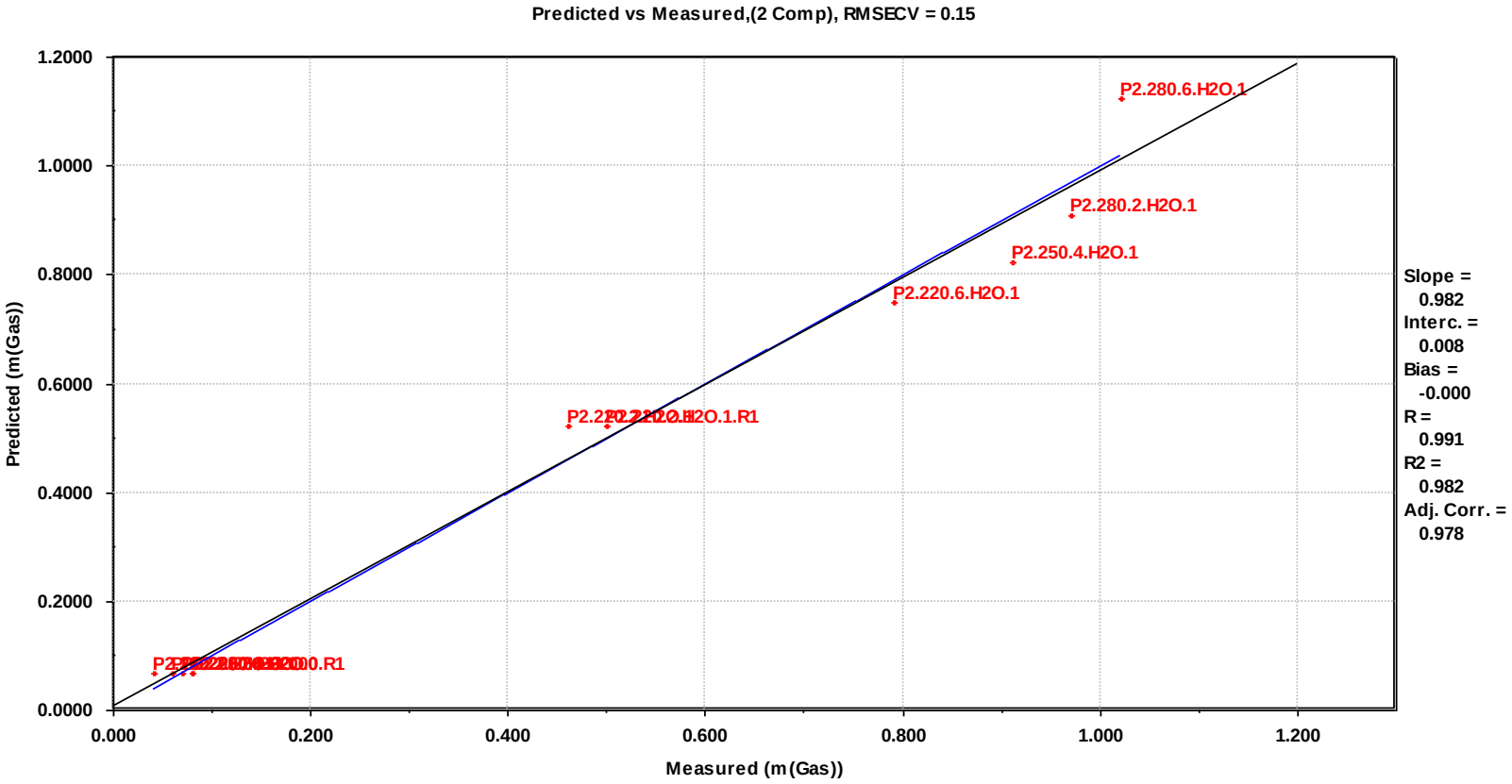

Figure B.2-c: PLS plot of predicted vs measured values for gas yields in Pilot Series 2. All experiments, without outliers.

B.3 ELEMENTAL ANALYSIS

Table B.3-1: Rawdata from EA of bio-oil samples in Pilot Series 2.

	% Weight							
Sample	**N**	**C**	**S**	**H**	**Ash**	**O**	**Oil [g]**	**Feedstock [g]**
P2.220.2.H2O.0	6.53	71.19	0.13	8.62	0.00	13.52	0.38	4.01
	6.66	70.41	0.07	8.63	0.00	14.23	0.38	4.01
P2.280.6.H2O.1	6.73	70.43	0.05	9.67	0.00	13.12	0.47	4.01
	7.14	70.81	0.03	10.31	0.00	11.71	0.47	4.01
P2.220.2.H2O.1	6.86	57.20	0.01	8.17	0.00	27.76	0.52	4.03
	6.83	57.40	0.03	7.48	0.00	28.26	0.52	4.03
P2.280.6.H2O.0	6.73	75.01	0.01	9.42	0.00	8.83	0.66	4.02
	4.03	74.69	0.07	9.22	0.00	11.99	0.66	4.02
P2.280.2.H2O.0	7.54	70.29	0.06	9.05	0.00	13.06	0.47	4.03
	7.26	72.05	0.09	9.79	0.00	10.81	0.47	4.03
P2.250.4.H2O.1	6.14	70.70	0.04	9.38	0.00	13.73	0.47	4.02
	6.50	72.42	0.08	10.70	0.00	10.30	0.47	4.02
P2.280.2.H2O.1	7.30	71.75	0.04	9.69	0.00	11.22	0.48	4.03
	4.74	72.28	0.08	9.39	0.00	13.52	0.48	4.03
P2.220.6.H2O.0	7.54	71.58	0.08	9.53	0.00	11.26	0.43	4.03
	7.32	70.93	0.15	10.26	0.00	11.34	0.43	4.03
P2.250.4.H2O.0	6.16	69.81	0.08	9.81	0.00	14.13	0.47	4.01
	7.60	67.91	0.09	9.42	0.00	14.99	0.47	4.01
P2.220.6.H2O.1	5.99	64.98	0.07	8.92	0.00	20.04	0.49	4.01
	6.08	65.28	0.09	9.09	0.00	19.45	0.49	4.01
P2.280.6.H2O.0.R1	7.40	74.20	0.09	9.32	0.00	8.99	0.48	4.01
	7.22	74.88	0.07	10.36	0.00	7.48	0.48	4.01
P2.220.2.H2O.1.R1	4.79	58.84	0.05	8.81	0.00	27.51	0.61	4.01
	5.65	48.12	0.08	7.78	0.00	38.37	0.61	4.01

Table B.3-2: Calculated molar ratios for H/C, O/C, N/C and (O+N)/C for bio-oil samples in Pilot Series 2.

	Moles/100 g					Molar ratios				Mean				Deviation of mean			
Sample	**N**	**C**	**S**	**H**	**O**	**H/C**	**O/C**	**N/C**	**(O+N)\C**	**H/C**	**O/C**	**N/C**	**(O+N)\C**	**H/C**	**O/C**	**N/C**	**(O+N)/C**
P2.220.2.H2O.0	0.47	5.93	0.00	8.55	0.85	1.44	0.14	0.08	0.22	1.45	0.15	0.08	0.23	-0.01	0.00	0.00	-0.01
	0.48	5.86	0.00	8.56	0.89	1.46	0.15	0.08	0.23					0.01	0.00	0.00	0.01
P2.280.6.H2O.1	0.48	5.86	0.00	9.59	0.82	1.64	0.14	0.08	0.22	1.69	0.13	0.08	0.22	-0.05	0.01	0.00	0.01
	0.51	5.90	0.00	10.23	0.73	1.74	0.12	0.09	0.21					0.05	-0.01	0.00	-0.01
P2.220.2.H2O.1	0.49	4.76	0.00	8.10	1.74	1.70	0.36	0.10	0.47	1.63	0.37	0.10	0.47	0.07	0.00	0.00	0.00
	0.49	4.78	0.00	7.42	1.77	1.55	0.37	0.10	0.47					-0.07	0.00	0.00	0.00
P2.280.6.H2O.0	0.48	6.25	0.00	9.34	0.55	1.50	0.09	0.08	0.17	1.48	0.10	0.06	0.17	0.01	-0.02	0.02	0.00
	0.29	6.22	0.00	9.15	0.75	1.47	0.12	0.05	0.17					-0.01	0.02	-0.02	0.00
P2.280.2.H2O.0	0.54	5.85	0.00	8.98	0.82	1.53	0.14	0.09	0.23	1.58	0.13	0.09	0.22	-0.04	0.01	0.00	0.02
	0.52	6.00	0.00	9.71	0.68	1.62	0.11	0.09	0.20					0.04	-0.01	0.00	-0.02
P2.250.4.H2O.1	0.44	5.89	0.00	9.31	0.86	1.58	0.15	0.07	0.22	1.67	0.13	0.08	0.20	-0.09	0.02	0.00	0.02
	0.46	6.03	0.00	10.62	0.64	1.76	0.11	0.08	0.18					0.09	-0.02	0.00	-0.02
P2.280.2.H2O.1	0.52	5.97	0.00	9.62	0.70	1.61	0.12	0.09	0.20	1.58	0.13	0.07	0.20	0.03	-0.01	0.02	0.00
	0.34	6.02	0.00	9.32	0.84	1.55	0.14	0.06	0.20					-0.03	0.01	-0.02	0.00
P2.220.6.H2O.0	0.54	5.96	0.00	9.46	0.70	1.59	0.12	0.09	0.21	1.66	0.12	0.09	0.21	-0.07	0.00	0.00	0.00
	0.52	5.91	0.00	10.18	0.71	1.72	0.12	0.09	0.21					0.07	0.00	0.00	0.00
P2.250.4.H2O.0	0.44	5.81	0.00	9.74	0.88	1.67	0.15	0.08	0.23	1.66	0.16	0.09	0.24	0.01	-0.01	-0.01	-0.02
	0.54	5.65	0.00	9.35	0.94	1.65	0.17	0.10	0.26					-0.01	0.01	0.01	0.02
P2.220.6.H2O.1	0.43	5.41	0.00	8.85	1.25	1.64	0.23	0.08	0.31	1.65	0.23	0.08	0.31	-0.01	0.00	0.00	0.00
	0.43	5.44	0.00	9.01	1.22	1.66	0.22	0.08	0.30					0.01	0.00	0.00	0.00
P2.280.6.H2O.0.R1	0.53	6.18	0.00	9.25	0.56	1.50	0.09	0.09	0.18	1.57	0.08	0.08	0.17	-0.08	0.01	0.00	0.01
	0.52	6.23	0.00	10.27	0.47	1.65	0.07	0.08	0.16					0.08	-0.01	0.00	-0.01
P2.220.2.H2O.1.R1	0.34	4.90	0.00	8.74	1.72	1.78	0.35	0.07	0.42	1.86	0.47	0.09	0.56	-0.07	-0.12	-0.02	-0.14
	0.40	4.01	0.00	7.72	2.40	1.93	0.60	0.10	0.70					0.07	0.12	0.02	0.14

B.4 GAS CHROMATOGRAPHY – MASS SPECTROMETRY

Table B.4-1: Preparation of GC-MS, Pilot series 2.

	Experiment	P2.220.2.H2O.0	P2.280.6.H2O.1	P2.220.2.H2O.1	P2.280.6.H2O.0	P2.280.2.H2O.0	P2.250.4.H2O.1	P2.280.2.H2O.1
Preparation of Solvent A1	**Benzoic acid [g]**	0.2297	0.2297	0.2297	0.2297	0.2297	0.2297	0.2297
	Dodecane [mL]	0.300	0.300	0.300	0.300	0.300	0.300	0.300
	EtOAc [mL]	100	100	100	100	100	100	100
	Benzoic acid [mg/mL]	2.30	2.30	2.30	2.30	2.30	2.30	2.30
	Dodecane [mg/mL]	2.25	2.25	2.25	2.25	2.25	2.25	2.25
Preparation of Solvent A2	**Solvent A1 [mL]**	3.50	3.50	3.50	3.50	3.50	3.50	3.50
	EtOAc [mL]	100	100	100	100	100	100	100
	Benzoic acid [mg/mL]	0.0804	0.0804	0.0804	0.0804	0.0804	0.0804	0.0804
	Dodecane [mg/mL]	0.0788	0.0788	0.0788	0.0788	0.0788	0.0788	0.0788
Preparation of Oil solution	**Oil sample [mg]**	7.6	7.7	7.5	7.4	7.6	7.6	7.7
	Solvent A2 [mL]	3.00	3.00	3.00	3.00	3.00	3.00	3.00
	Oil [mg/mL]	2.5	2.6	2.5	2.5	2.5	2.5	2.6
	Benzoic acid [mg/mL]	0.0804	0.0804	0.0804	0.0804	0.0804	0.0804	0.0804
	Dodecane [mg/mL]	0.0788	0.0788	0.0788	0.0788	0.0788	0.0788	0.0788
Preparation of Derivatized oil solution	**Oil solution [mL]**	1.00	1.00	1.00	1.00	1.00	1.00	1.00
	Pyridine [mL]	0.150	0.150	0.150	0.150	0.150	0.150	0.150
	BSTFA [mL]	0.150	0.150	0.150	0.150	0.150	0.150	0.150
	Oil [mg/mL]	2.0	2.0	1.9	1.9	2.0	2.0	2.0
	Benzoic acid [mg/mL]	0.0618	0.0618	0.0618	0.0618	0.0618	0.0618	0.0618
	Dodecane [mg/mL]	0.0606	0.0606	0.0606	0.0606	0.0606	0.0606	0.0606
Preparation of GC-MS Oil sample	**Derivatized oil solution [mL]**	0.700	0.700	0.700	0.700	0.700	0.700	0.700
	Pentane [mL]	0.700	0.700	0.700	0.700	0.700	0.700	0.700
	Oil [mg/mL]	0.97	0.99	0.96	0.95	0.97	0.97	0.99
	Benzoic acid [mg/mL]	0.0309	0.0309	0.0309	0.0309	0.0309	0.0309	0.0309
	Dodecane [mg/mL]	0.0303	0.0303	0.0303	0.0303	0.0303	0.0303	0.0303

Table B.4-1: Preparation of GC-MS, Pilot series 2. Table continued.

	Experiment	P2.220.6.H2O.0	P2.250.4.H2O.0	P2.220.6.H2O.1	P2.280.6.H2O.0.R1	P2.220.2.H2O.1.R1	IS
Preparation of Solvent A1	**Benzoic acid [g]**	0.2297	0.2297	0.2297	0.2297	0.2297	0.2297
	Dodecane [mL]	0.300	0.300	0.300	0.300	0.300	0.300
	EtOAc [mL]	100	100	100	100	100	100
	Benzoic acid [mg/mL]	2.30	2.30	2.30	2.30	2.30	2.30
	Dodecane [mg/mL]	2.25	2.25	2.25	2.25	2.25	2.25
Preparation of Solvent A2	**Solvent A1 [mL]**	3.50	3.50	3.50	3.50	3.50	3.50
	EtOAc [mL]	100	100	100	100	100	100
	Benzoic acid [mg/mL]	0.0804	0.0804	0.0804	0.0804	0.0804	0.0804
	Dodecane [mg/mL]	0.0788	0.0788	0.0788	0.0788	0.0788	0.0788
Preparation of Oil solution	**Oil sample [mg]**	7.5	7.7	7.4	7.4	7.5	-
	Solvent A2 [mL]	3.00	3.00	3.00	3.00	3.00	3.00
	Oil [mg/mL]	2.5	2.6	2.5	2.5	2.5	-
	Benzoic acid [mg/mL]	0.0804	0.0804	0.0804	0.0804	0.0804	0.0804
	Dodecane [mg/mL]	0.0788	0.0788	0.0788	0.0788	0.0788	0.0788
Preparation of Derivatized oil solution	**Oil solution [mL]**	1.00	1.00	1.00	1.00	1.00	1.00
	Pyridine [mL]	0.150	0.150	0.150	0.150	0.150	0.150
	BSTFA [mL]	0.150	0.150	0.150	0.150	0.150	0.150
	Oil [mg/mL]	1.9	2.0	1.9	1.9	1.9	-
	Benzoic acid [mg/mL]	0.0618	0.0618	0.0618	0.0618	0.0618	0.0618
	Dodecane [mg/mL]	0.0606	0.0606	0.0606	0.0606	0.0606	0.0606
Preparation of GC-MS Oil sample	**Derivatized oil solution [mL]**	0.700	0.700	0.700	0.700	0.700	0.700
	Pentane [mL]	0.700	0.700	0.700	0.700	0.700	0.700
	Oil [mg/mL]	0.96	0.99	0.95	0.95	0.96	-
	Benzoic acid [mg/mL]	0.0309	0.0309	0.0309	0.0309	0.0309	0.0309
	Dodecane [mg/mL]	0.0303	0.0303	0.0303	0.0303	0.0303	0.0303

Table B.4-2: Semi-quantitative analysis of GC-MS bio-oil samples for Pilot Series 2.

	Designation	**Butanoic acid 2-(trimethylsilyl)oxy-trimethylsilyl ester**	**Dodecane**	**Benzoic acid trimethylsilyl ester**	**Glycerol, tris(trimethylsilyl) ether**	**Butanedioic acid, bis(trimethylsilyl)ester**	**Pyrimidine, 2,4-bis[(trimethylsilyl)oxy]-**	**L-proline, 5-oxo-1-(trimethylsilyl)-,trimethylsilyl ester**	**Silane, (1,2,4,5-cyclohexanetetrayltetraoxy)tetrakis[trimethyl-**	**Tetradecanoic acid, trimethylsilyl ester**	**9-Hexadecenoic acid, trimethylsilyl ester**	**9-Hexadecenoic acid, trimethylsilyl ester**	**Hexadecanoic acid, trimethylsilyl ester**	**9,12-Octadecadienoic acid (Z,Z)-, trimethylsilyl ester**	**Octadecanoic acid, trimethylsilyl ester**	**Pimaric acid TMS**	**cis-5,8,11,14,17-Eicosapentaenoic acid, trimethylsilyl ester**	**Dehydroabietic acid, trimethylsilyl ester**	**Hexadecanoic acid, 2,3-bis[(trimethylsilyl)oxy]propyl ester**
	Formula	**C10H24O3Si2**	**C12H26**	**C1014O2Si**	**C12H32O3Si3**	**C10H22O4Si2**	**C10H20N2O2Si2**	**C11H23NO3Si2**	**C18H44O4Si4**	**C17H36O2Si**	**C19H38O2Si**	**C19H38O2Si**	**C19H40O2Si**	**C21H40O2Si**	**C21H44O2Si**	**C23H38O2Si**	**C23H38O2Si**	**C23H36O2Si**	**C25H54O4Si2**
P2.220.2.H2O.0	**Ret. [min]**		10.038	10.771	11.275		12.119		16.081	17.921	19.252		19.357				21.150		22.037
	Peak area		87162093	14803443	35280950		84092244		95202787	89014085	34452317		32071189				13205257		39660585
	C_A [mg/mL] (IS:1)[a]		0.0303	0.0514	0.123		0.0292		0.0331	0.0309	0.120		0.111				0.0459		0.0138
	C_A [mg/mL] (IS: 2)[b]		0.0182	0.0309	0.0737		0.0176		0.0199	0.0186	0.0720		0.0670				0.0276		0.00828
P2.280.2.H2O.1	**Ret. [min]**		10.037	10.770	11.261					17.921	19.246	19.272	19.376						
	Peak area		80066343	14723265	10303412					93857123	25648640	11569178	34369677						
	C_A [mg/mL] (IS:1)[a]		0.0303	0.0557	0.0390					0.0355	0.0970	0.0438	0.130						
	C_A [mg/mL] (IS: 2)[b]		0.0168	0.0309	0.0216					0.0197	0.0539	0.0243	0.0722						

[a, b] Based on the relationship between the peak area ratio and concentration ratio of the target component and IS (1: Dodecane, 2: Benzoic acid) in the chromatogram.

Table B.4-2: Semi-quantitative analysis of GC-MS bio-oil samples for Pilot Series 2. Table continued.

	Designation	Butanoic acid 2-(trimethylsilyl)oxy-trimethylsilyl ester	Dodecane	Benzoic acid trimethylsilyl ester	Glycerol, tris(trimethylsilyl) ether	Butanedioic acid, bis(trimethylsilyl)ester	Pyrimidine, 2,4-bis[(trimethylsilyl)oxy]-	L-proline, 5-oxo-1-(trimethylsilyl)-,trimethylsilyl ester	Silane, (1,2,4,5-cyclohexanetetrayltetraoxy)tetrakis[trimethyl-	Tetradecanoic acid, trimethylsilyl ester	9-Hexadecenoic acid, trimethylsilyl ester	9-Hexadecenoic acid, trimethylsilyl ester	Hexadecanoic acid, trimethylsilyl ester	9,12-Octadecadienoic acid (Z,Z)-, trimethylsilyl ester	Octadecanoic acid, trimethylsilyl ester	Pimaric acid TMS	cis-5,8,11,14,17-Eicosapentaenoic acid, trimethylsilyl ester	Dehydroabietic acid, trimethylsilyl ester	Hexadecanoic acid, 2,3-bis[(trimethylsilyl)oxy]propyl ester
	Formula	**C10H24O3Si2**	**C12H26**	**C1014O2Si**	**C12H32O3Si3**	**C10H22O4Si2**	**C10H20N2O2Si2**	**C11H23NO3Si2**	**C18H44O4Si4**	**C17H36O2Si**	**C19H38O2Si**	**C19H38O2Si**	**C19H40O2Si**	**C21H40O2Si**	**C21H44O2Si**	**C23H38O2Si**	**C23H38O2Si**	**C23H36O2Si**	**C25H54O4Si2**
P2.220.6.H2O.1	**Ret. [min]**	9.059	10.038	10.771	11.263	11.730	12.117			17.921	19.250	19.274	19.376						
	Peak area	42555766	79842350	14588369	16190724	44427346	33598002			95205863	30011937	95011138	31333957						
	C_A [mg/mL] (IS:1)[a]	0.0161	0.0303	0.0553	0.0614	0.0169	0.0127			0.0361	0.114	0.0360	0.119						
	C_A [mg/mL] (IS: 2)[b]	0.00902	0.0169	0.0309	0.0343	0.00942	0.00712			0.0202	0.0636	0.0201	0.0664						
P2.280.6.H2O.0	**Ret. [min]**		10.038	10.770	11.260					17.919	19.240	19.269	19.368	20.323		20.943		21.292	
	Peak area		86774697	14634840	72258410					44844788	12029747	86645468	22582645	25867407		41536849		72445741	
	C_A [mg/mL] (IS:1)[a]		0.0303	0.0511	0.0252					0.0157	0.0420	0.0302	0.0788	0.00903		0.0145		0.0253	
	C_A [mg/mL] (IS: 2)[b]		0.0183	0.0309	0.0153					0.00948	0.0254	0.0183	0.0477	0.00547		0.00878		0.0153	

[a, b] Based on the relationship between the peak area ratio and concentration ratio of the target component and IS (1: Dodecane, 2: Benzoic acid) in the chromatogram.

Table B.4-2: Semi-quantitative analysis of GC-MS bio-oil samples for Pilot Series 2. Table continued.

	Designation	Butanoic acid 2-(trimethylsilyl)oxy-trimethylsilyl ester	Dodecane	Benzoic acid trimethylsilyl ester	Glycerol, tris(trimethylsilyl) ether	Butanedioic acid, bis(trimethylsilyl)ester	Pyrimidine, 2,4-bis[(trimethylsilyl)oxy]-	L-proline, 5-oxo-1-(trimethylsilyl)-,trimethylsilyl ester	Silane, (1,2,4,5-cyclohexanetetrayltetraoxy)tetrakis[trimethyl-	Tetradecanoic acid, trimethylsilyl ester	9-Hexadecenoic acid, trimethylsilyl ester	9-Hexadecenoic acid, trimethylsilyl ester	Hexadecanoic acid, trimethylsilyl ester	9,12-Octadecadienoic acid (Z,Z)-, trimethylsilyl ester	Octadecanoic acid, trimethylsilyl ester	Pimaric acid TMS	cis-5,8,11,14,17-Eicosapentaenoic acid, trimethylsilyl ester	Dehydroabietic acid, trimethylsilyl ester	Hexadecanoic acid, 2,3-bis[(trimethylsilyl)oxy]propyl ester
	Formula	**C10H24O3Si2**	**C12H26**	**C1014O2Si**	**C12H32O3Si3**	**C10H22O4Si2**	**C10H20N2O2Si2**	**C11H23NO3Si2**	**C18H44O4Si4**	**C17H36O2Si**	**C19H38O2Si**	**C19H38O2Si**	**C19H40O2Si**	**C21H40O2Si**	**C21H44O2Si**	**C23H38O2Si**	**C23H38O2Si**	**C23H36O2Si**	**C25H54O4Si2**
P2.280.6.H2O.0.R1	**Ret. [min]**		10.037	10.771	11.267					17.918	19.240	19.270	19.369						
	Peak area		87940909	15643 2218	22821 4194					61054 626	14153 5471	11597 7346	25054 9000						
	C_A [mg/mL] (IS:1)[a]		0.0303	0.0539	0.0786					0.0210	0.0487	0.0399	0.0863						
	C_A [mg/mL] (IS: 2)[b]		0.0174	0.0309	0.0451					0.0121	0.0280	0.0229	0.0495						
P2.220.2.H2O.1	**Ret. [min]**	9.059	10.038	10.770	11.261	11.731	12.117	14.488		17.921	19.252		19.374				21.148		
	Peak area	43106 723	75928 850	13163 8867	67904 344	48554 465	36890 144	65506 334		91776 337	38306 5079		30440 8116				89465 861		
	C_A [mg/mL] (IS:1)[a]	0.0172	0.0303	0.0525	0.0271	0.0194	0.0147	0.0261		0.0366	0.153		0.121				0.0357		
	C_A [mg/mL] (IS: 2)[b]	0.0101	0.0178	0.0309	0.0160	0.0114	0.00867	0.0154		0.0216	0.0900		0.0715				0.0210		

[a, b] Based on the relationship between the peak area ratio and concentration ratio of the target component and IS (1: Dodecane, 2: Benzoic acid) in the chromatogram.

Table B.4-2: Semi-quantitative analysis of GC-MS bio-oil samples for Pilot Series 2. Table continued.

	Designation	Butanoic acid 2-(trimethylsilyl)oxy-trimethylsilyl ester	Dodecane	Benzoic acid trimethylsilyl ester	Glycerol, tris(trimethylsilyl) ether	Butanedioic acid, bis(trimethylsilyl)ester	Pyrimidine, 2,4-bis[(trimethylsilyl)oxy]-	L-proline, 5-oxo-1-(trimethylsilyl)-,trimethylsilyl ester	Silane, (1,2,4,5-cyclohexanetetrayltetraoxy)tetrakis[trimethyl-	Tetradecanoic acid, trimethylsilyl ester	9-Hexadecenoic acid, trimethylsilyl ester	9-Hexadecenoic acid, trimethylsilyl ester	Hexadecanoic acid, trimethylsilyl ester	9,12-Octadecadienoic acid (Z,Z)-, trimethylsilyl ester	Octadecanoic acid, trimethylsilyl ester	Pimaric acid TMS	cis-5,8,11,14,17-Eicosapentaenoic acid, trimethylsilyl ester	Dehydroabietic acid, trimethylsilyl ester	Hexadecanoic acid, 2,3-bis[(trimethylsilyl)oxy]propyl ester
	Formula	**C10H24O3Si2**	**C12H26**	**C1014O2Si**	**C12H32O3Si3**	**C10H22O4Si2**	**C10H20N2O2Si2**	**C11H23NO3Si2**	**C18H44O4Si4**	**C17H36O2Si**	**C19H38O2Si**	**C19H38O2Si**	**C19H40O2Si**	**C21H40O2Si**	**C21H44O2Si**	**C23H38O2Si**	**C23H38O2Si**	**C23H36O2Si**	**C25H54O4Si2**
P2.220.2.H2O.1.R1	**Ret. [min]**	9.058	10.038	10.770	11.260	11.731	12.116	14.488		17.920	19.249		19.367				21.146		
	Peak area	41928267	84054650	15283703	82397471	71772355	47674294	78865066		80182998	32398 5837		21403 9823				77675224		
	C_A [mg/mL] (IS:1)[a]	0.0151	0.0303	0.0551	0.0297	0.0259	0.0172	0.0284		0.0289	0.117		0.0771				0.0280		
	C_A [mg/mL] (IS: 2)[b]	0.00848	0.0170	0.0309	0.0167	0.0145	0.00965	0.0160		0.0162	0.0655		0.0433				0.0157		
P2.280.2.H2O.0	**Ret. [min]**		10.037	10.771	11.273				16.079	17.919	19.244	19.270	19.370						
	Peak area		84098206	14589 9976	30988 2693				40468607	59172967	21408 8581	59757188	24948 8669						
	C_A [mg/mL] (IS:1)[a]		0.0303	0.0525	0.112				0.0146	0.0213	0.0771	0.0215	0.0899						
	C_A [mg/mL] (IS: 2)[b]		0.0178	0.0309	0.0657				0.00858	0.0125	0.0454	0.0127	0.0529						

[a, b] Based on the relationship between the peak area ratio and concentration ratio of the target component and IS (1: Dodecane, 2: Benzoic acid) in the chromatogram.

Table B.4-2: Semi-quantitative analysis of GC-MS bio-oil samples for Pilot Series 2. Table continued.

	Designation	Butanoic acid 2-(trimethylsilyl)oxy-trimethylsilyl ester	Dodecane	Benzoic acid trimethylsilyl ester	Glycerol, tris(trimethylsilyl) ether	Butanedioic acid, bis(trimethylsilyl)ester	Pyrimidine, 2,4-bis[(trimethylsilyl)oxy]-	L-proline, 5-oxo-1-(trimethylsilyl)-,trimethylsilyl ester	Silane, (1,2,4,5-cyclohexanetetrayltetraoxy)tetrakis[trimethyl-	Tetradecanoic acid, trimethylsilyl ester	9-Hexadecenoic acid, trimethylsilyl ester	9-Hexadecenoic acid, trimethylsilyl ester	Hexadecanoic acid, trimethylsilyl ester	9,12-Octadecadienoic acid (Z,Z)-, trimethylsilyl ester	Octadecanoic acid, trimethylsilyl ester	Pimaric acid TMS	cis-5,8,11,14,17-Eicosapentaenoic acid, trimethylsilyl ester	Dehydroabietic acid, trimethylsilyl ester	Hexadecanoic acid, 2,3-bis[(trimethylsilyl)oxy]propyl ester
	Formula	**C10H24O3Si2**	**C12H26**	**C1014O2Si**	**C12H32O3Si3**	**C10H22O4Si2**	**C10H20N2O2Si2**	**C11H23NO3Si2**	**C18H44O4Si4**	**C17H36O2Si**	**C19H38O2Si**	**C19H38O2Si**	**C19H40O2Si**	**C21H40O2Si**	**C21H44O2Si**	**C23H38O2Si**	**C23H38O2Si**	**C23H36O2Si**	**C25H54O4Si2**
P2.220.6.H2O.0	**Ret. [min]**		10.038	10.770	11.264		12.116			17.920	19.251		19.375				21.146		
	Peak area		84249484	14718560	19125737		36002818			86162807	34117131		31438599				64726863		
	C_A [mg/mL] (IS:1)[a]		0.0303	0.0529	0.0688		0.0129			0.0310	0.123		0.113				0.0233		
	C_A [mg/mL] (IS: 2)[b]		0.0177	0.0309	0.0402		0.00756			0.0181	0.0717		0.0660				0.0136		
P2.280.6.H2O.1	**Ret. [min]**		10.038	10.770	11.263					17.920	19.239	19.270	19.374		20.467				
	Peak area		76536570	13054157	13415633					64649679	88257988	86509567	32622773		90851956				
	C_A [mg/mL] (IS:1)[a]		0.0303	0.0517	0.0531					0.0256	0.0349	0.0342	0.129		0.0360				
	C_A [mg/mL] (IS: 2)[b]		0.0181	0.0309	0.0318					0.0153	0.0209	0.0205	0.0773		0.0215				

[a, b] Based on the relationship between the peak area ratio and concentration ratio of the target component and IS (1: Dodecane, 2: Benzoic acid) in the chromatogram.

Table B.4-2: Semi-quantitative analysis of GC-MS bio-oil samples for Pilot Series 2. Table continued.

	Designation	Butanoic acid 2-(trimethylsilyl)oxy-trimethylsilyl ester	Dodecane	Benzoic acid trimethylsilyl ester	Glycerol, tris(trimethylsilyl) ether	Butanedioic acid, bis(trimethylsilyl)ester	Pyrimidine, 2,4-bis[(trimethylsilyl)oxy]-	L-proline, 5-oxo-1-(trimethylsilyl)-,trimethylsilyl ester	Silane, (1,2,4,5-cyclohexanetetrayltetraoxy)tetrakis[trimethyl-	Tetradecanoic acid, trimethylsilyl ester	9-Hexadecenoic acid, trimethylsilyl ester	9-Hexadecenoic acid, trimethylsilyl ester	Hexadecanoic acid, trimethylsilyl ester	9,12-Octadecadienoic acid (Z,Z)-, trimethylsilyl ester	Octadecanoic acid, trimethylsilyl ester	Pimaric acid TMS	cis-5,8,11,14,17-Eicosapentaenoic acid, trimethylsilyl ester	Dehydroabietic acid, trimethylsilyl ester	Hexadecanoic acid, 2,3-bis[(trimethylsilyl)oxy]propyl ester
	Formula	**C10H24O3Si2**	**C12H26**	**C1014O2Si**	**C12H32O3Si3**	**C10H22O4Si2**	**C10H20N2O2Si2**	**C11H23NO3Si2**	**C18H44O4Si4**	**C17H36O2Si**	**C19H38O2Si**	**C19H38O2Si**	**C19H40O2Si**	**C21H40O2Si**	**C21H44O2Si**	**C23H38O2Si**	**C23H38O2Si**	**C23H36O2Si**	**C25H54O4Si2**
P2.250.4.H2O.0	**Ret. [min]**		10.037	10.770	11.272				16.079	17.919	19.246		19.370						
	Peak area		86819674	15382 9908	30777 0089				42181 393	71170 454	29453 7751		26818 0775						
	C_A [mg/mL] (IS:1)[a]		0.0303	0.0537	0.1074				0.0147	0.0248	0.103		0.0936						
	C_A [mg/mL] (IS: 2)[b]		0.0175	0.0309	0.0619				0.0084 8	0.0143	0.0592		0.0539						
P2.250.4.H2O.1	**Ret. [min]**		10.038	10.770	11.261		17.921				19.246	19.272	19.376						
	Peak area		74384 129	13341 6080	93666 240		87859 667				25076 9231	12301 4593	33492 1834						
	C_A [mg/mL] (IS:1)[a]		0.0303	0.0543	0.0381		0.0358				0.102	0.0501	0.136						
	C_A [mg/mL] (IS: 2)[b]		0.0172	0.0309	0.0217		0.0204				0.0581	0.0285	0.0776						

[a, b] Based on the relationship between the peak area ratio and concentration ratio of the target component and IS (1: Dodecane, 2: Benzoic acid) in the chromatogram.

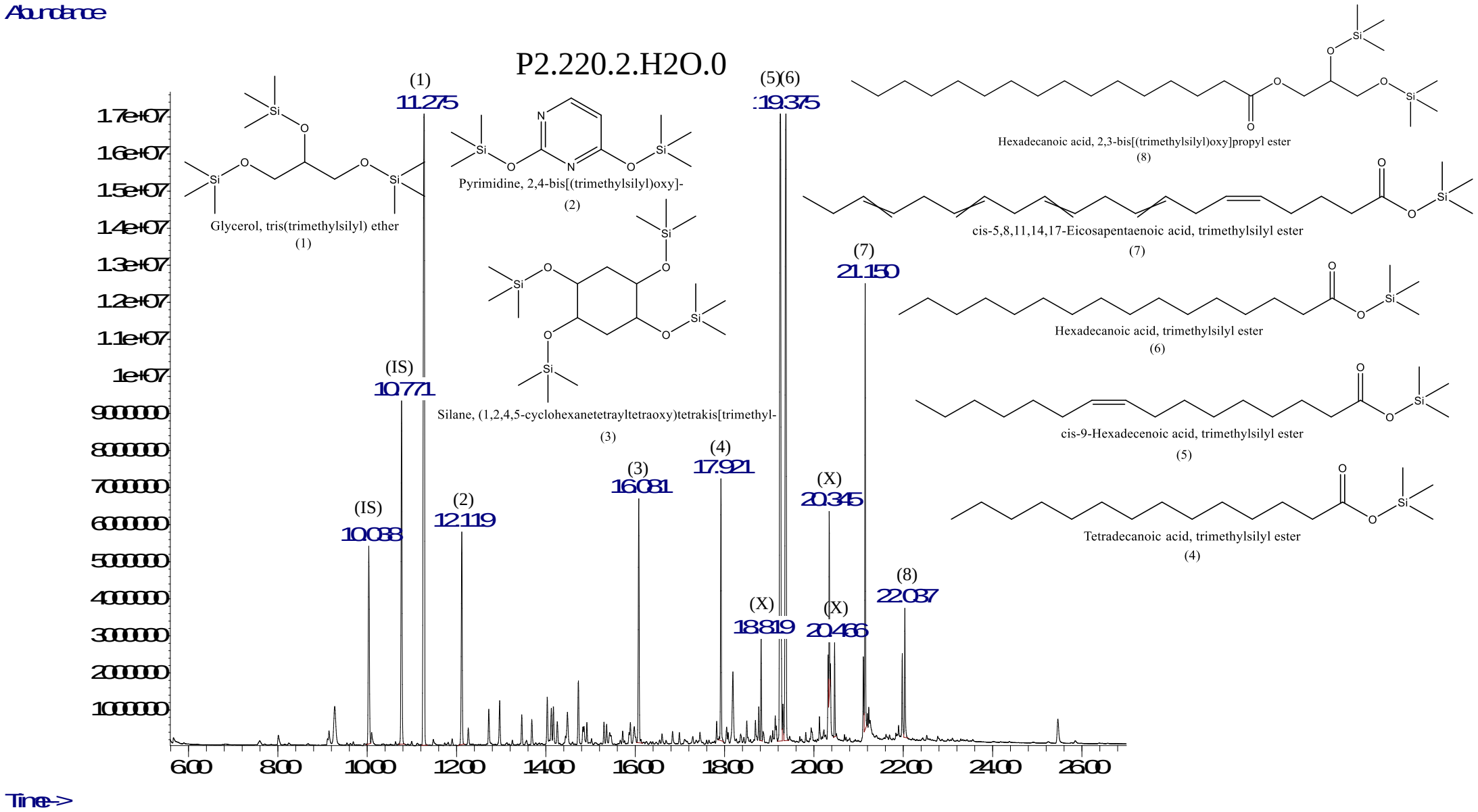
Abundance
P2.220.2.H2O.0
1.7e+07
1.6e+07
1.5e+07
1.4e+07
1.3e+07
1.2e+07
1.1e+07
1e+07
900000
800000
700000
600000
500000
400000
300000
200000
100000
600
800
1000
1200
1400
1600
1800
2000
2200
2400
2600
Time->
(1)
11.275
Glycerol, tris(trimethylsilyl) ether
(1)
Pyrimidine, 2,4-bis[(trimethylsilyl)oxy]-
(2)
Silane, (1,2,4,5-cyclohexanetetrayltetraoxy)tetrakis[trimethyl-
(3)
(IS)
10.771
(IS)
10.088
(2)
12.119
(3)
16.081
(4)
17.921
(5)(6)
19.375
(X)
18.819
(X)
20.466
(7)
21.150
(X)
20.345
(8)
22.037
Hexadecanoic acid, 2,3-bis[(trimethylsilyl)oxy]propyl ester
(8)
cis-5,8,11,14,17-Eicosapentaenoic acid, trimethylsilyl ester
(7)
Hexadecanoic acid, trimethylsilyl ester
(6)
cis-9-Hexadecenoic acid, trimethylsilyl ester
(5)
Tetradecanoic acid, trimethylsilyl ester
(4)

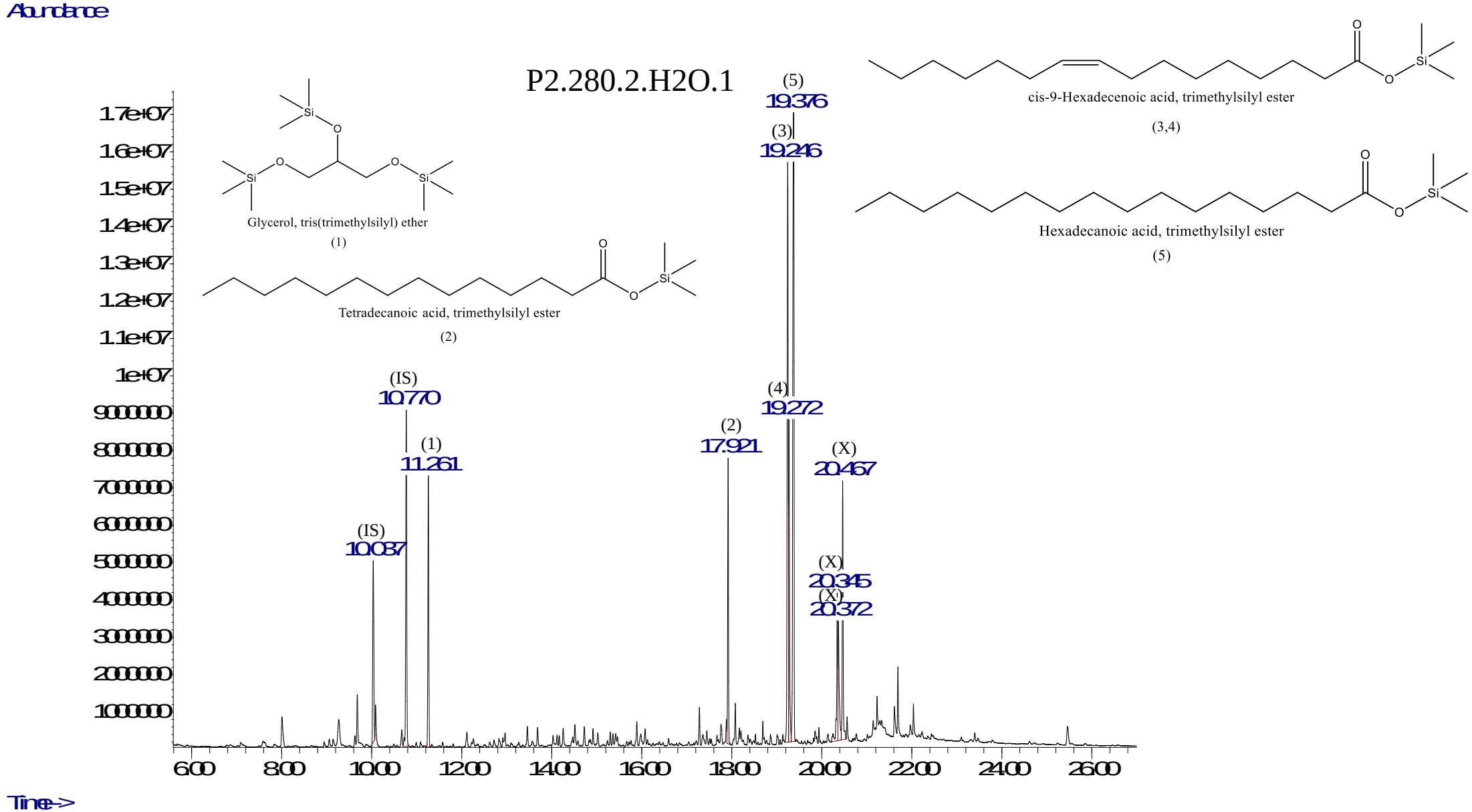
Abundance
P2.280.2.H2O.1
Glycerol, tris(trimethylsilyl) ether
(1)
Tetradecanoic acid, trimethylsilyl ester
(2)
cis-9-Hexadecenoic acid, trimethylsilyl ester
(3,4)
Hexadecanoic acid, trimethylsilyl ester
(5)
(IS) 10.770
(1) 11.261
(IS) 10.037
(2) 17.921
(3) 19.246
(5) 19.376
(4) 19.272
(X) 20.467
(X) 20.345
(X) 20.372
Time->
1.7e+07
1.6e+07
1.5e+07
1.4e+07
1.3e+07
1.2e+07
1.1e+07
1e+07
900000
800000
700000
600000
500000
400000
300000
200000
100000
600
800
1000
1200
1400
1600
1800
2000
2200
2400
2600

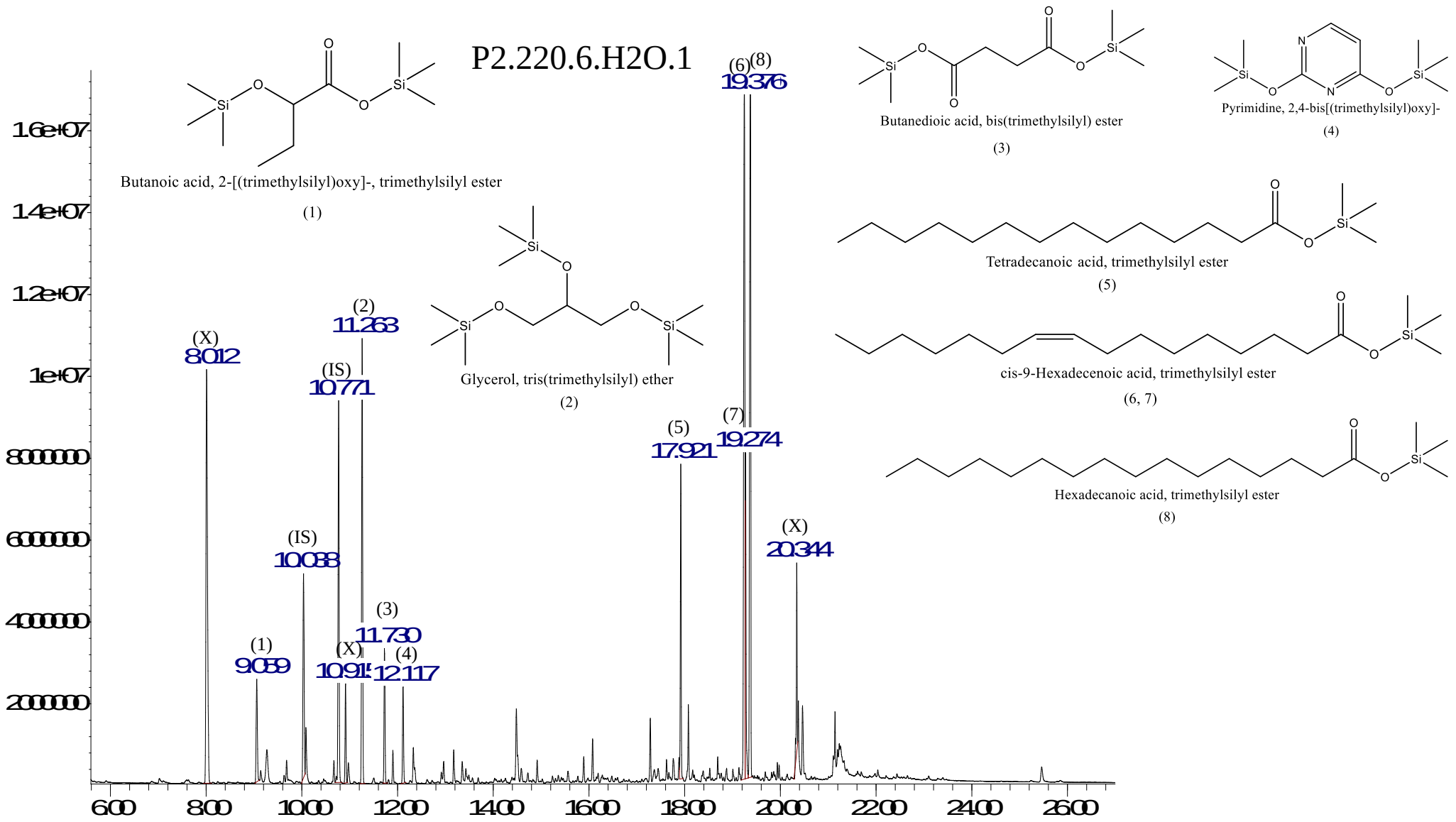
Abundance
P2.220.6.H2O.1
Butanoic acid, 2-[(trimethylsilyl)oxy]-, trimethylsilyl ester
(1)
Glycerol, tris(trimethylsilyl) ether
(2)
Butanedioic acid, bis(trimethylsilyl) ester
(3)
Pyrimidine, 2,4-bis[(trimethylsilyl)oxy]-
(4)
Tetradecanoic acid, trimethylsilyl ester
(5)
cis-9-Hexadecenoic acid, trimethylsilyl ester
(6, 7)
Hexadecanoic acid, trimethylsilyl ester
(8)
(X) 8.012
(1) 9.059
(IS) 10.088
(X) 10.915
(IS) 10.771
(2) 11.263
(3) 11.730
(4) 12.117
(5) 17.921
(6)(8) 19.376
(7) 19.274
(X) 20.344
1.6e+07
1.4e+07
1.2e+07
1e+07
800000
600000
400000
200000
600
800
1000
1200
1400
1600
1800
2000
2200
2400
2600
Time->
Si
O
N

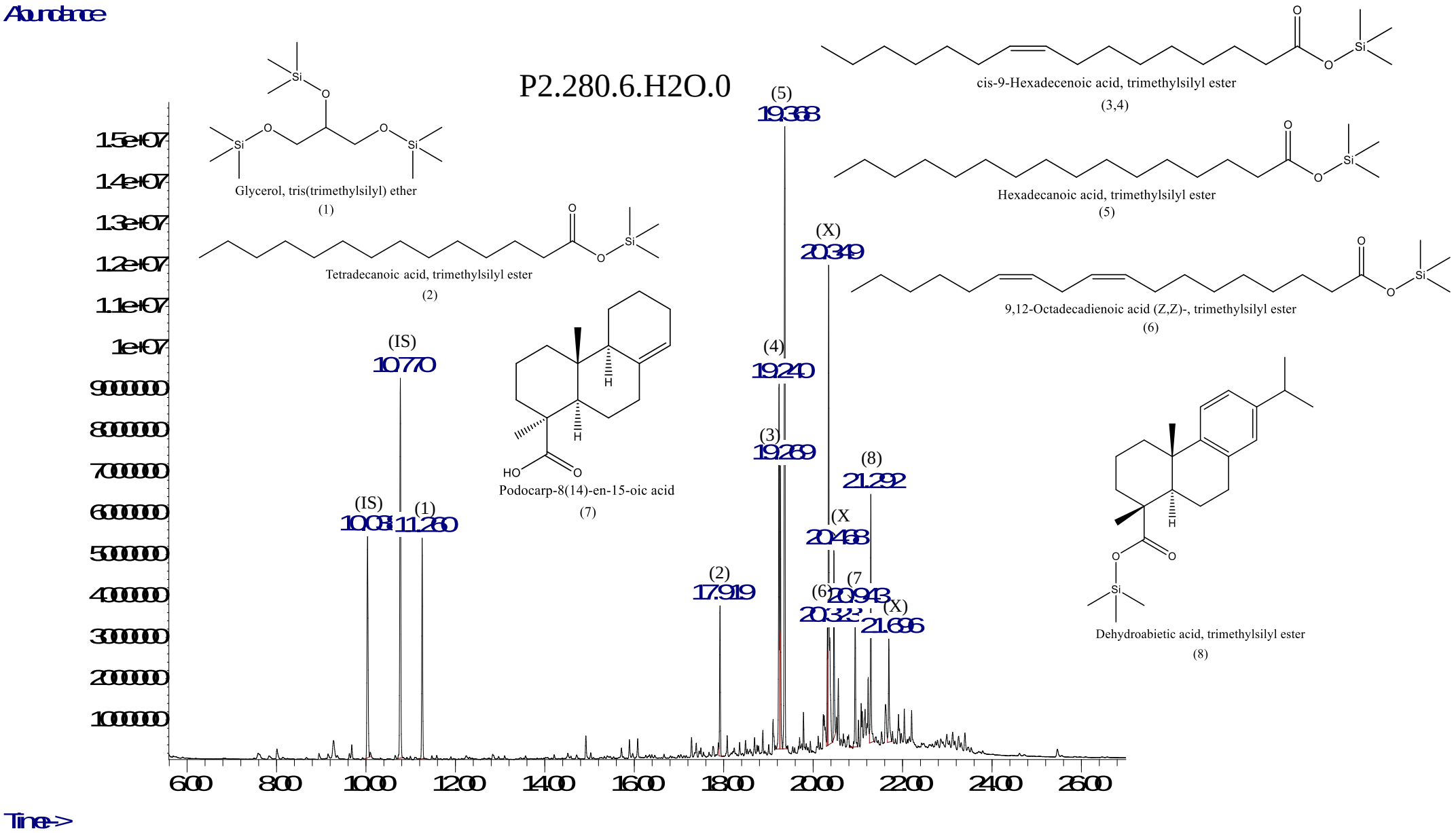
Abundance
P2.280.6.H2O.0
Glycerol, tris(trimethylsilyl) ether
(1)
Tetradecanoic acid, trimethylsilyl ester
(2)
Podocarp-8(14)-en-15-oic acid
(7)
cis-9-Hexadecenoic acid, trimethylsilyl ester
(3,4)
Hexadecanoic acid, trimethylsilyl ester
(5)
9,12-Octadecadienoic acid (Z,Z)-, trimethylsilyl ester
(6)
Dehydroabietic acid, trimethylsilyl ester
(8)
(IS) 10.770
(IS) 10.063
(1) 11.260
(2) 17.919
(3) 19.289
(4) 19.240
(5) 19.368
(X) 20.349
(X 20.468
(6) 20.322
(7 20.943
(X) 21.686
(8) 21.292
1.5e+07
1.4e+07
1.3e+07
1.2e+07
1.1e+07
1e+07
900000
800000
700000
600000
500000
400000
300000
200000
100000
600
800
1000
1200
1400
1600
1800
2000
2200
2400
2600
Time->

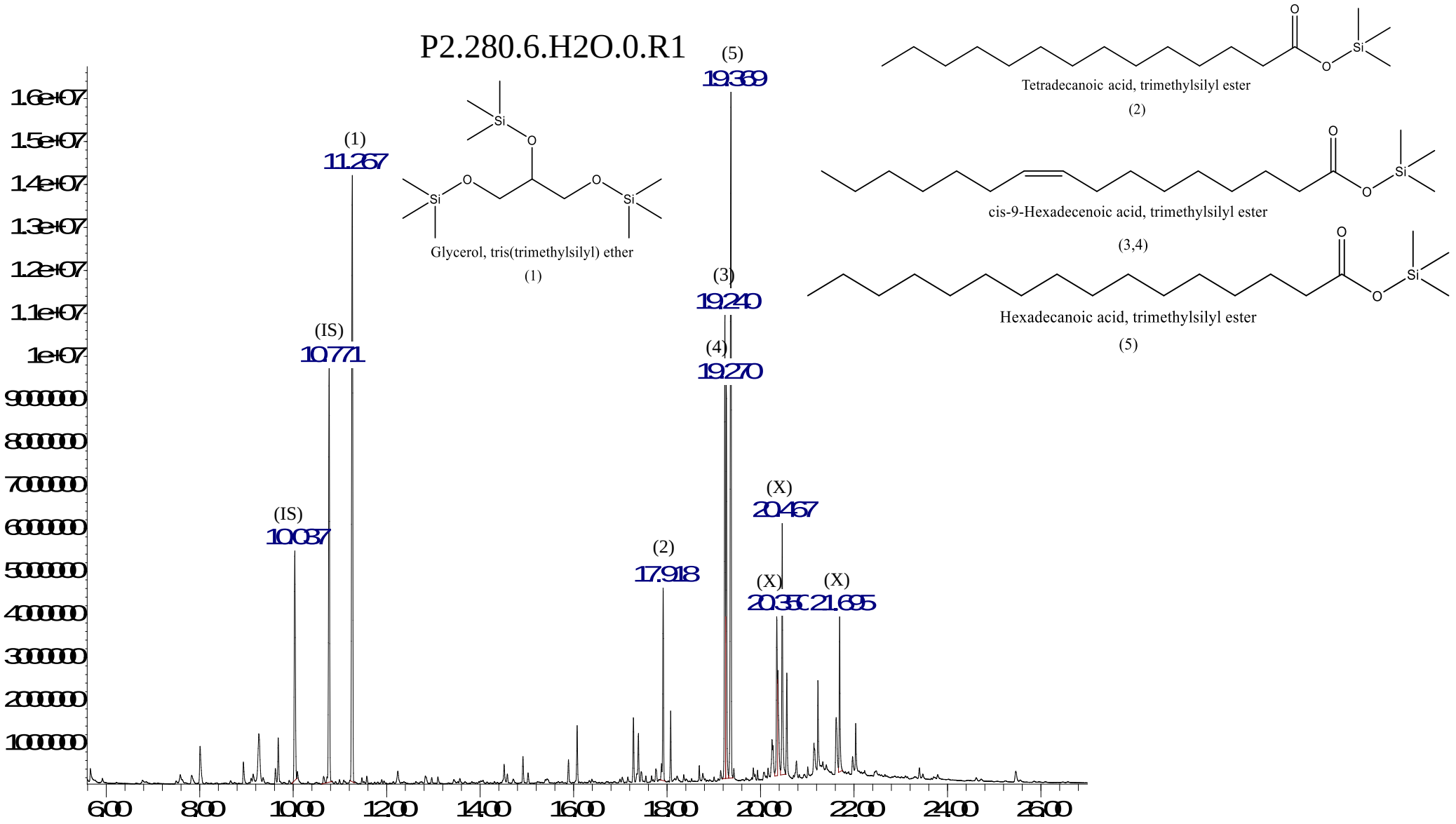
Abundance
P2.280.6.H2O.0.R1
(1)
11.267
(IS)
10.771
(IS)
10.037
(2)
17.918
(3)
19.240
(4)
19.270
(5)
19.389
(X)
20.467
(X)
20.350
(X)
21.695
1.6e+07
1.5e+07
1.4e+07
1.3e+07
1.2e+07
1.1e+07
1e+07
900000
800000
700000
600000
500000
400000
300000
200000
100000
600
800
1000
1200
1400
1600
1800
2000
2200
2400
2600
Time->
Glycerol, tris(trimethylsilyl) ether
(1)
Tetradecanoic acid, trimethylsilyl ester
(2)
cis-9-Hexadecenoic acid, trimethylsilyl ester
(3,4)
Hexadecanoic acid, trimethylsilyl ester
(5)

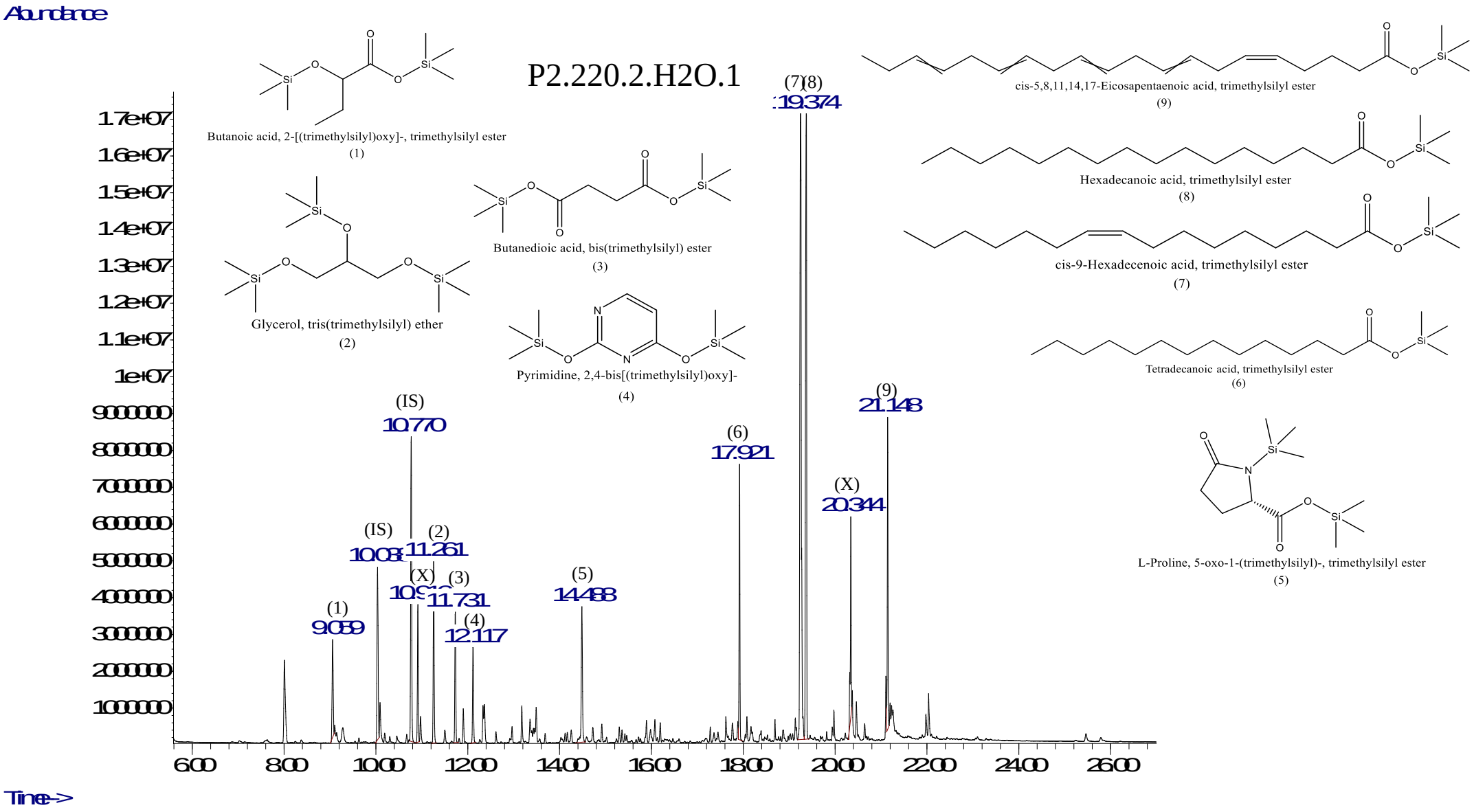
Abundance
P2.220.2.H2O.1
Butanoic acid, 2-[(trimethylsilyl)oxy]-, trimethylsilyl ester
(1)
Glycerol, tris(trimethylsilyl) ether
(2)
Butanedioic acid, bis(trimethylsilyl) ester
(3)
Pyrimidine, 2,4-bis[(trimethylsilyl)oxy]-
(4)
L-Proline, 5-oxo-1-(trimethylsilyl)-, trimethylsilyl ester
(5)
Tetradecanoic acid, trimethylsilyl ester
(6)
cis-9-Hexadecenoic acid, trimethylsilyl ester
(7)
Hexadecanoic acid, trimethylsilyl ester
(8)
cis-5,8,11,14,17-Eicosapentaenoic acid, trimethylsilyl ester
(9)
(IS) 10.770
(IS) 10.038
(2) 11.261
(X) 10.912
(3) 11.731
(4) 12.117
(1) 9.089
(5) 14.488
(6) 17.921
(7)(8) 19.374
(X) 20.344
(9) 21.148
1.7e+07
1.6e+07
1.5e+07
1.4e+07
1.3e+07
1.2e+07
1.1e+07
1e+07
900000
800000
700000
600000
500000
400000
300000
200000
100000
600
800
1000
1200
1400
1600
1800
2000
2200
2400
2600
Time->
148

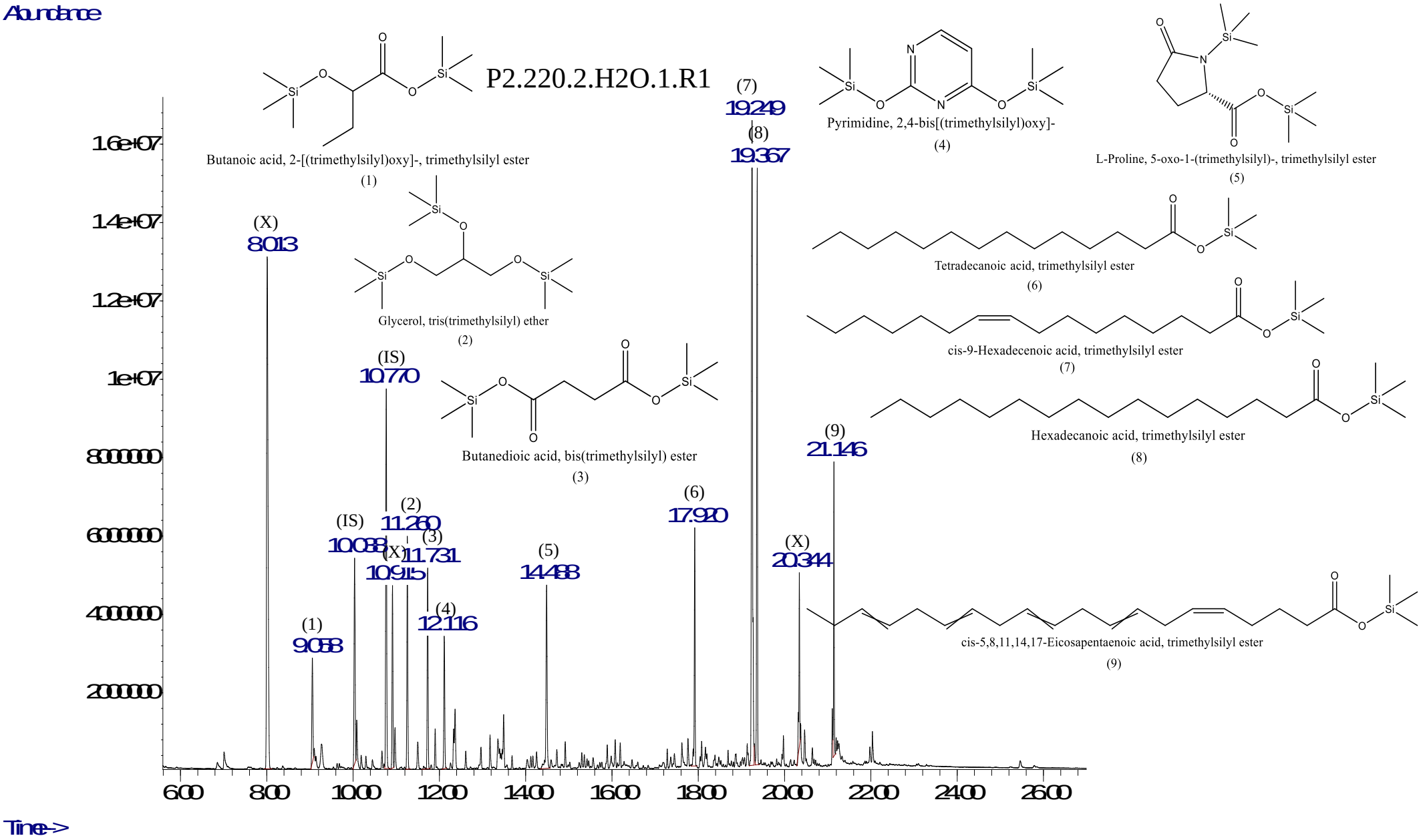
Abundance
P2.220.2.H2O.1.R1
Butanoic acid, 2-[(trimethylsilyl)oxy]-, trimethylsilyl ester
(1)
Glycerol, tris(trimethylsilyl) ether
(2)
Butanedioic acid, bis(trimethylsilyl) ester
(3)
Pyrimidine, 2,4-bis[(trimethylsilyl)oxy]-
(4)
L-Proline, 5-oxo-1-(trimethylsilyl)-, trimethylsilyl ester
(5)
Tetradecanoic acid, trimethylsilyl ester
(6)
cis-9-Hexadecenoic acid, trimethylsilyl ester
(7)
Hexadecanoic acid, trimethylsilyl ester
(8)
cis-5,8,11,14,17-Eicosapentaenoic acid, trimethylsilyl ester
(9)
(X) 8.013
(IS) 10.770
(IS) 10.088
(X) 10.915
(2) 11.260
(3) 11.731
(4) 12.116
(1) 9.058
(5) 14.488
(6) 17.920
(7) 19.249
(8) 19.367
(9) 21.146
(X) 20.344
1.6e+07
1.4e+07
1.2e+07
1e+07
8000000
6000000
4000000
2000000
600
800
1000
1200
1400
1600
1800
2000
2200
2400
2600
Time->
Si
O
N

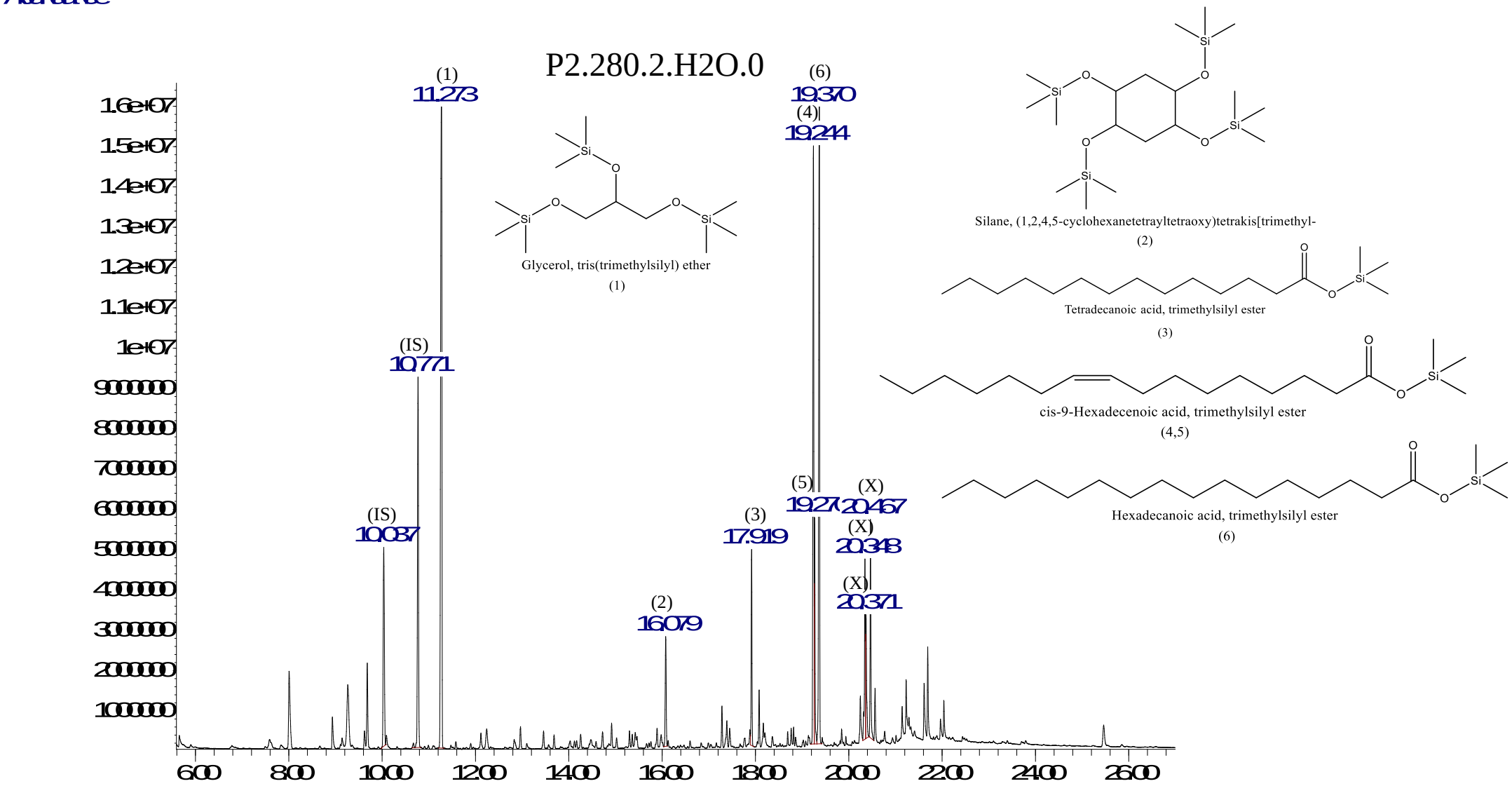
Abundance
P2.280.2.H2O.0
(1)
11.273
(6)
19.370
(4)
19.244
(IS)
10.771
(IS)
10.037
(5)
19.271
(X)
20.467
(3)
17.919
(X)
20.348
(X)
20.371
(2)
16.079
1.6e+07
1.5e+07
1.4e+07
1.3e+07
1.2e+07
1.1e+07
1e+07
900000
800000
700000
600000
500000
400000
300000
200000
100000
600
800
1000
1200
1400
1600
1800
2000
2200
2400
2600
Time->
Glycerol, tris(trimethylsilyl) ether
(1)
Silane, (1,2,4,5-cyclohexanetetrayltetraoxy)tetrakis[trimethyl-
(2)
Tetradecanoic acid, trimethylsilyl ester
(3)
cis-9-Hexadecenoic acid, trimethylsilyl ester
(4,5)
Hexadecanoic acid, trimethylsilyl ester
(6)

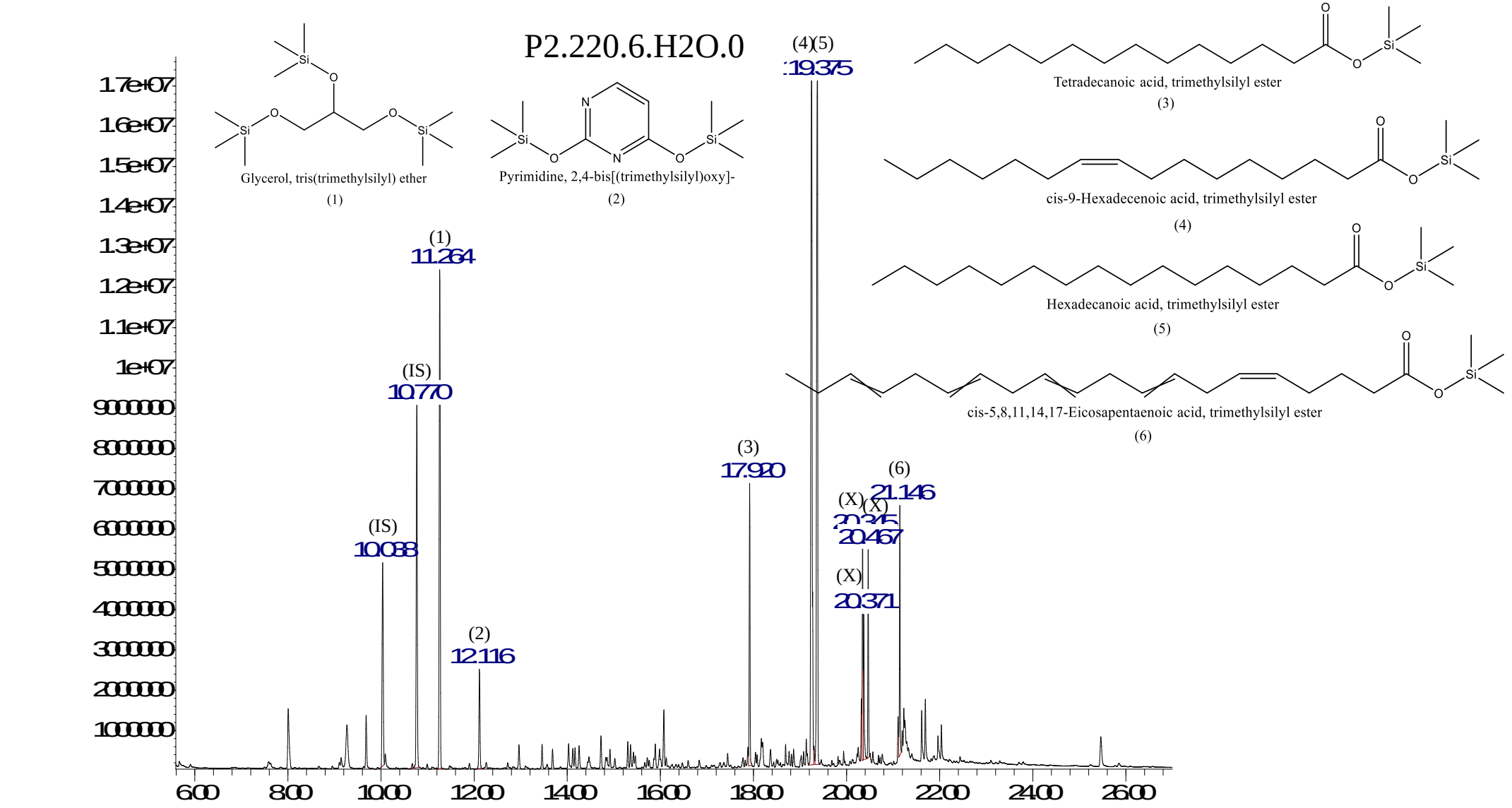
Abundance
P2.220.6.H2O.0
Glycerol, tris(trimethylsilyl) ether
(1)
Pyrimidine, 2,4-bis[(trimethylsilyl)oxy]-
(2)
Tetradecanoic acid, trimethylsilyl ester
(3)
cis-9-Hexadecenoic acid, trimethylsilyl ester
(4)
Hexadecanoic acid, trimethylsilyl ester
(5)
cis-5,8,11,14,17-Eicosapentaenoic acid, trimethylsilyl ester
(6)
(1) 11.264
(IS) 10.770
(IS) 10.038
(2) 12.116
(3) 17.920
(4)(5) 19.375
(X) 20.345
(X) 20.467
(X) 20.371
(6) 21.146
1.7e+07
1.6e+07
1.5e+07
1.4e+07
1.3e+07
1.2e+07
1.1e+07
1e+07
900000
800000
700000
600000
500000
400000
300000
200000
100000
600
800
1000
1200
1400
1600
1800
2000
2200
2400
2600
Time->

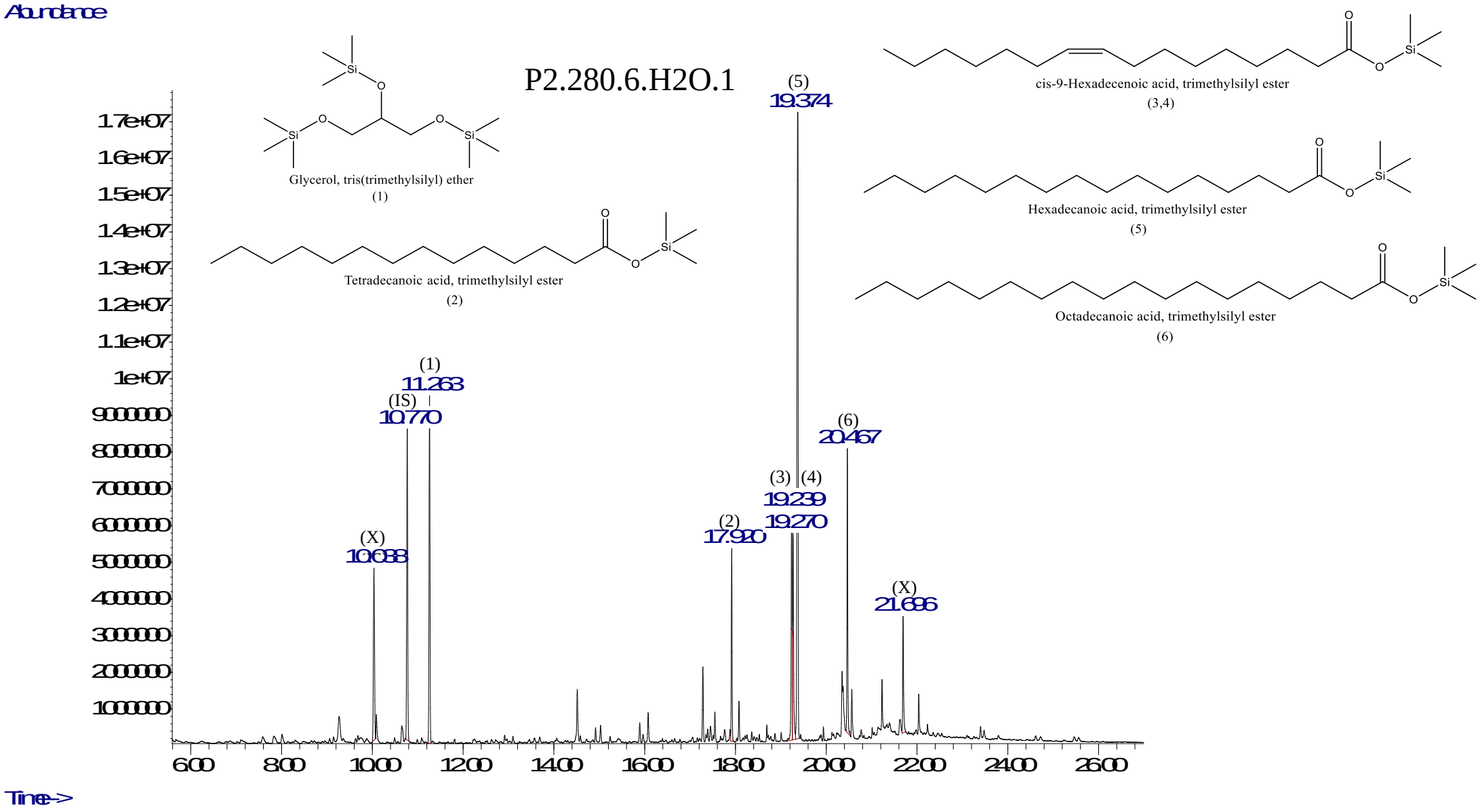
Abundance
P2.280.6.H2O.1
Glycerol, tris(trimethylsilyl) ether
(1)
Tetradecanoic acid, trimethylsilyl ester
(2)
cis-9-Hexadecenoic acid, trimethylsilyl ester
(3,4)
Hexadecanoic acid, trimethylsilyl ester
(5)
Octadecanoic acid, trimethylsilyl ester
(6)
(1) 11.263
(IS) 10.770
(X) 10.688
(2) 17.920
(3) (4) 19.239 19.270
(5) 19.374
(6) 20.467
(X) 21.696
1.7e+07
1.6e+07
1.5e+07
1.4e+07
1.3e+07
1.2e+07
1.1e+07
1e+07
900000
800000
700000
600000
500000
400000
300000
200000
100000
600
800
1000
1200
1400
1600
1800
2000
2200
2400
2600
Time->
Si
O

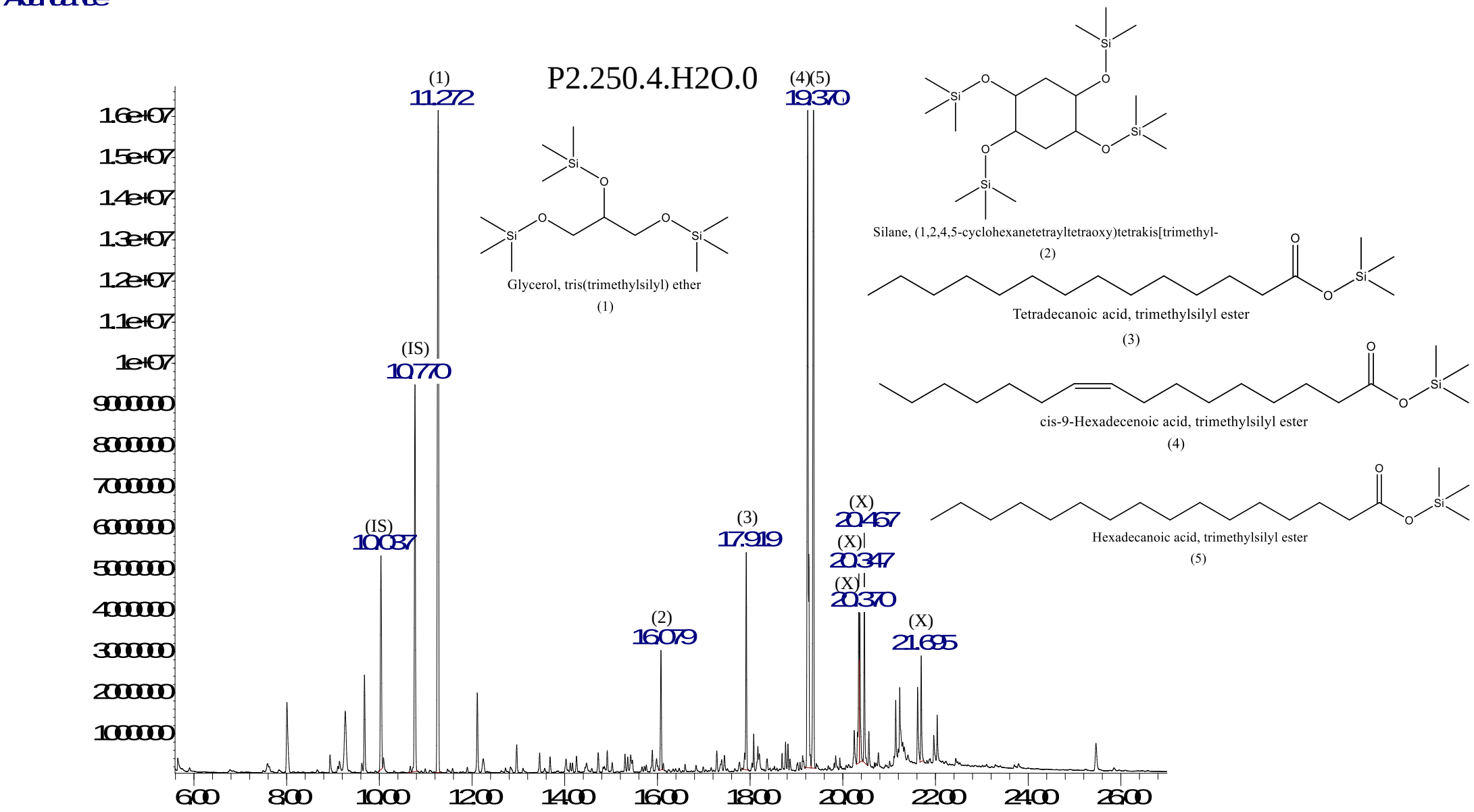
Abundance
P2.250.4.H2O.0
(1)
11.272
(4)(5)
19.370
(IS)
10.770
(IS)
10.037
(3)
17.919
(X)
20.467
(X)
20.347
(X)
20.370
(2)
16.079
(X)
21.695
1.6e+07
1.5e+07
1.4e+07
1.3e+07
1.2e+07
1.1e+07
1e+07
9000000
8000000
7000000
6000000
5000000
4000000
3000000
2000000
1000000
600
800
1000
1200
1400
1600
1800
2000
2200
2400
2600
Time->
Glycerol, tris(trimethylsilyl) ether
(1)
Silane, (1,2,4,5-cyclohexanetetrayltetraoxy)tetrakis[trimethyl-
(2)
Tetradecanoic acid, trimethylsilyl ester
(3)
cis-9-Hexadecenoic acid, trimethylsilyl ester
(4)
Hexadecanoic acid, trimethylsilyl ester
(5)

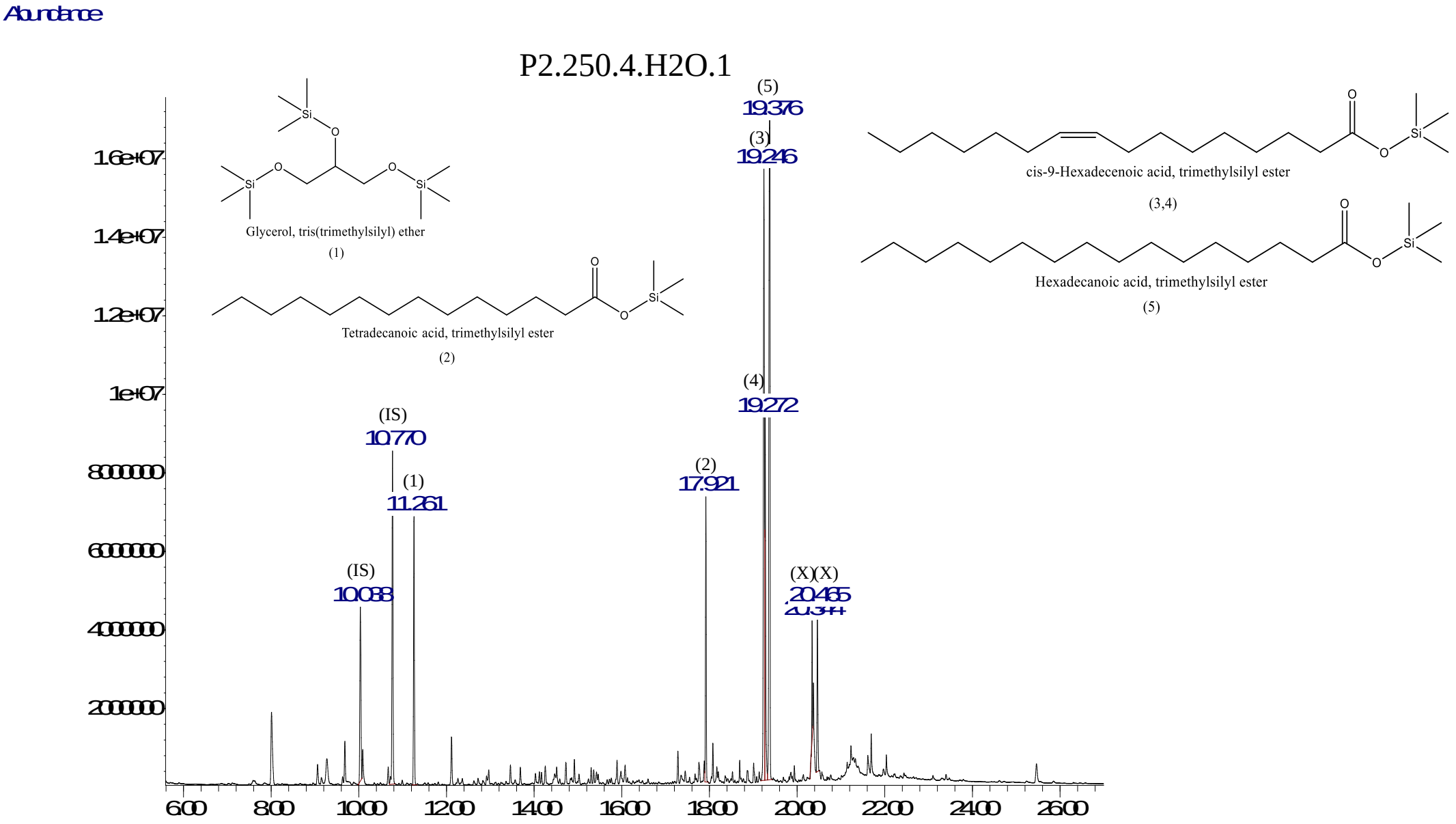
Abundance
P2.250.4.H2O.1
(5)
19.376
(3)
19.246
(4)
19.272
(IS)
10.770
(1)
11.261
(IS)
10.088
(2)
17.921
(X)(X)
20.465
1.6e+07
1.4e+07
1.2e+07
1e+07
800000
600000
400000
200000
600
800
1000
1200
1400
1600
1800
2000
2200
2400
2600
Time->
Glycerol, tris(trimethylsilyl) ether
(1)
Tetradecanoic acid, trimethylsilyl ester
(2)
cis-9-Hexadecenoic acid, trimethylsilyl ester
(3,4)
Hexadecanoic acid, trimethylsilyl ester
(5)

B.5 INFRARED SPECTROSCOPY

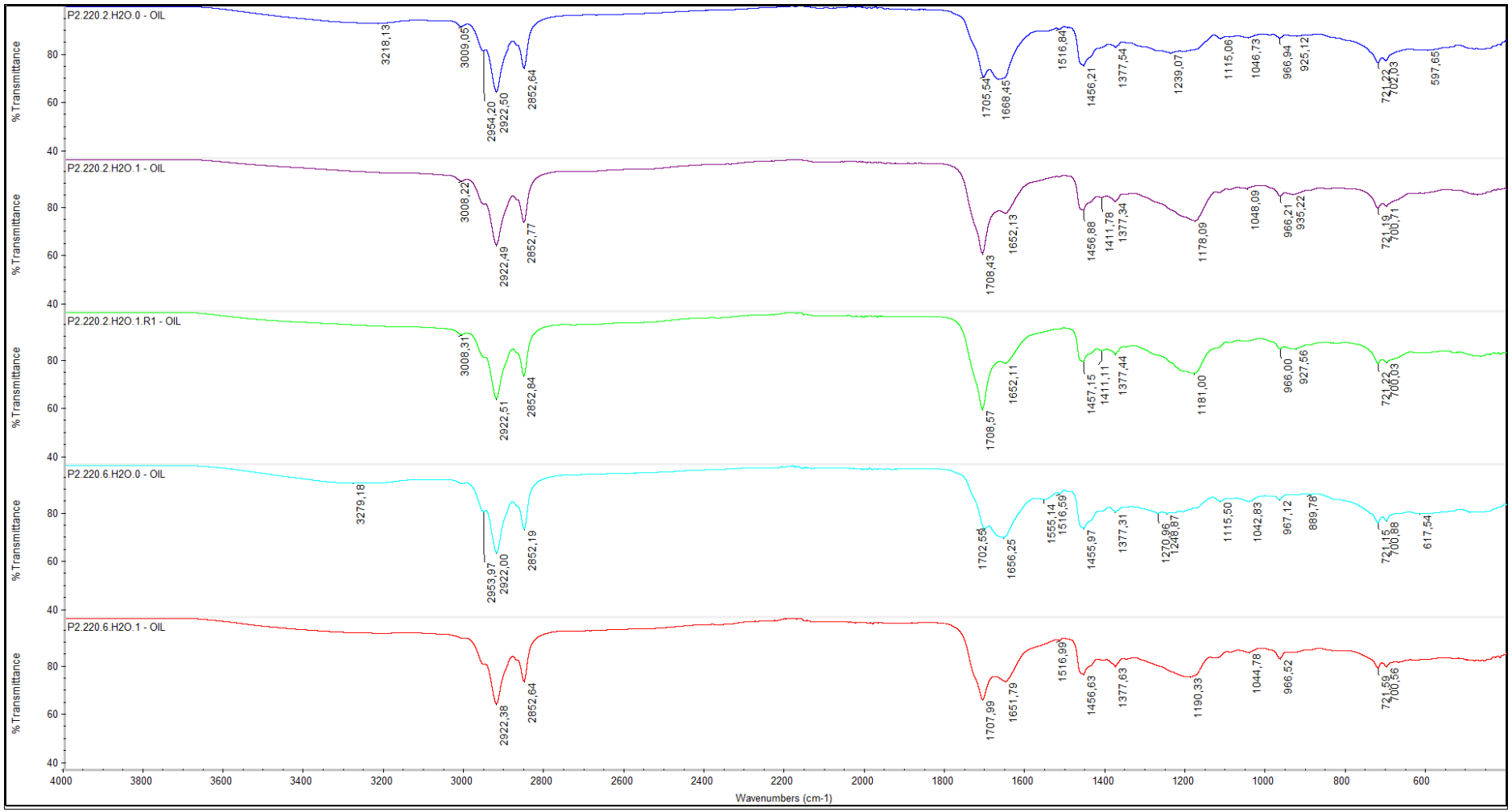

Figure B.5-a: Comparison of the IR spectra for all bio-oil samples in P2 with T=220.

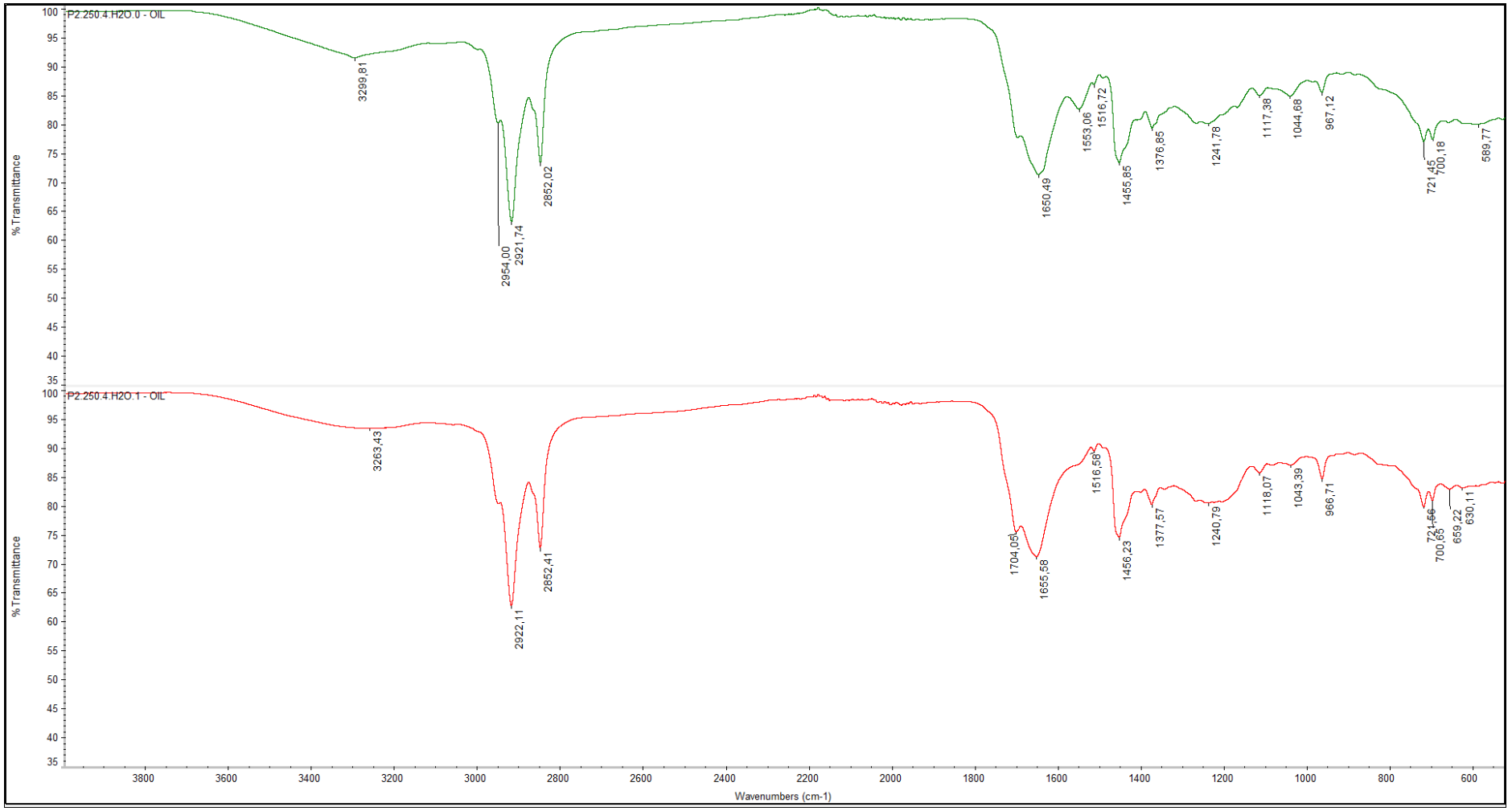

Figure B.5-b: Comparison of the IR spectra for all bio-oil samples in P2 with T=250.

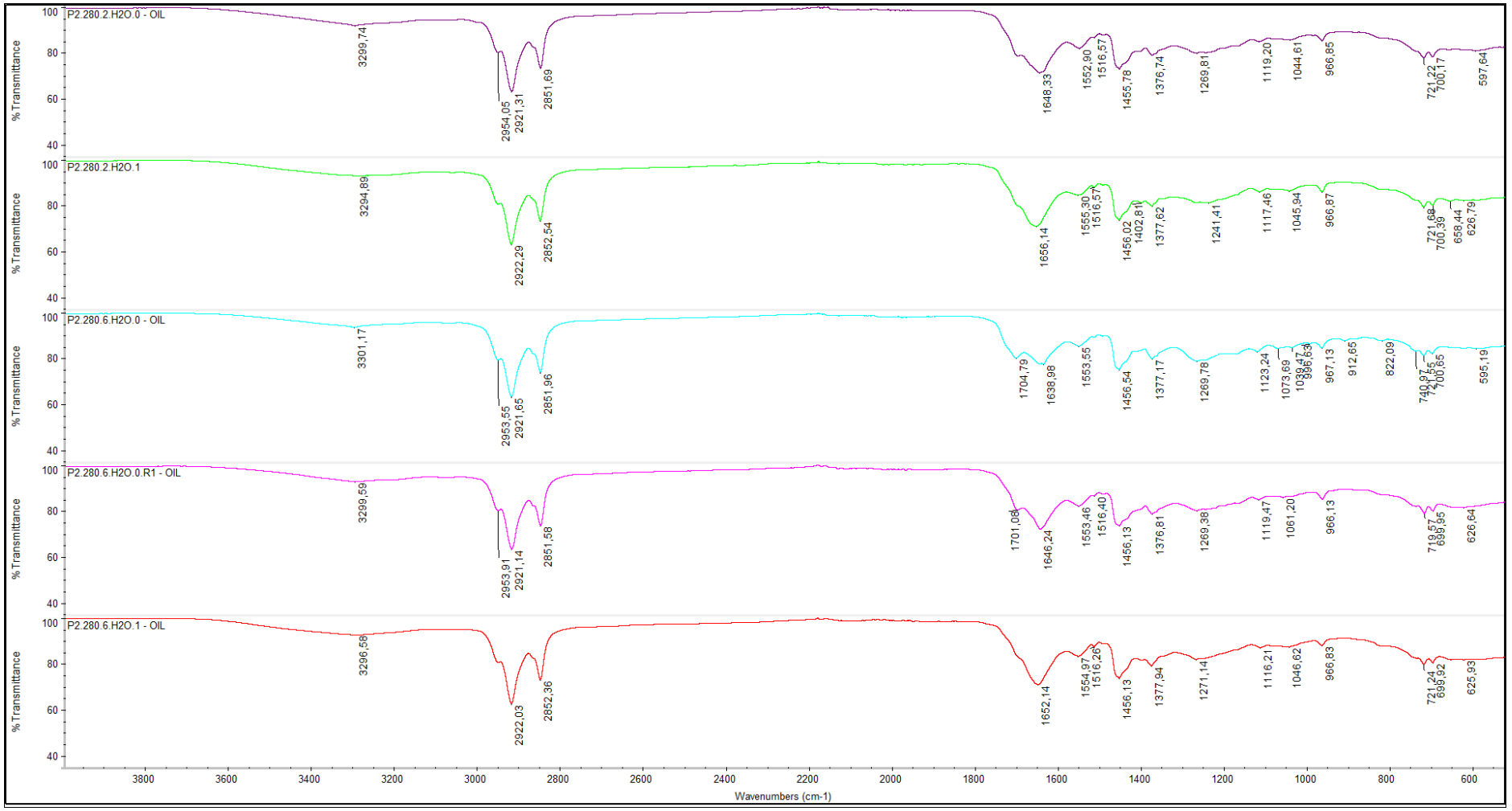

Figure B.5-c: Comparison of the IR spectra for all bio-oil samples in P2 with T=280.

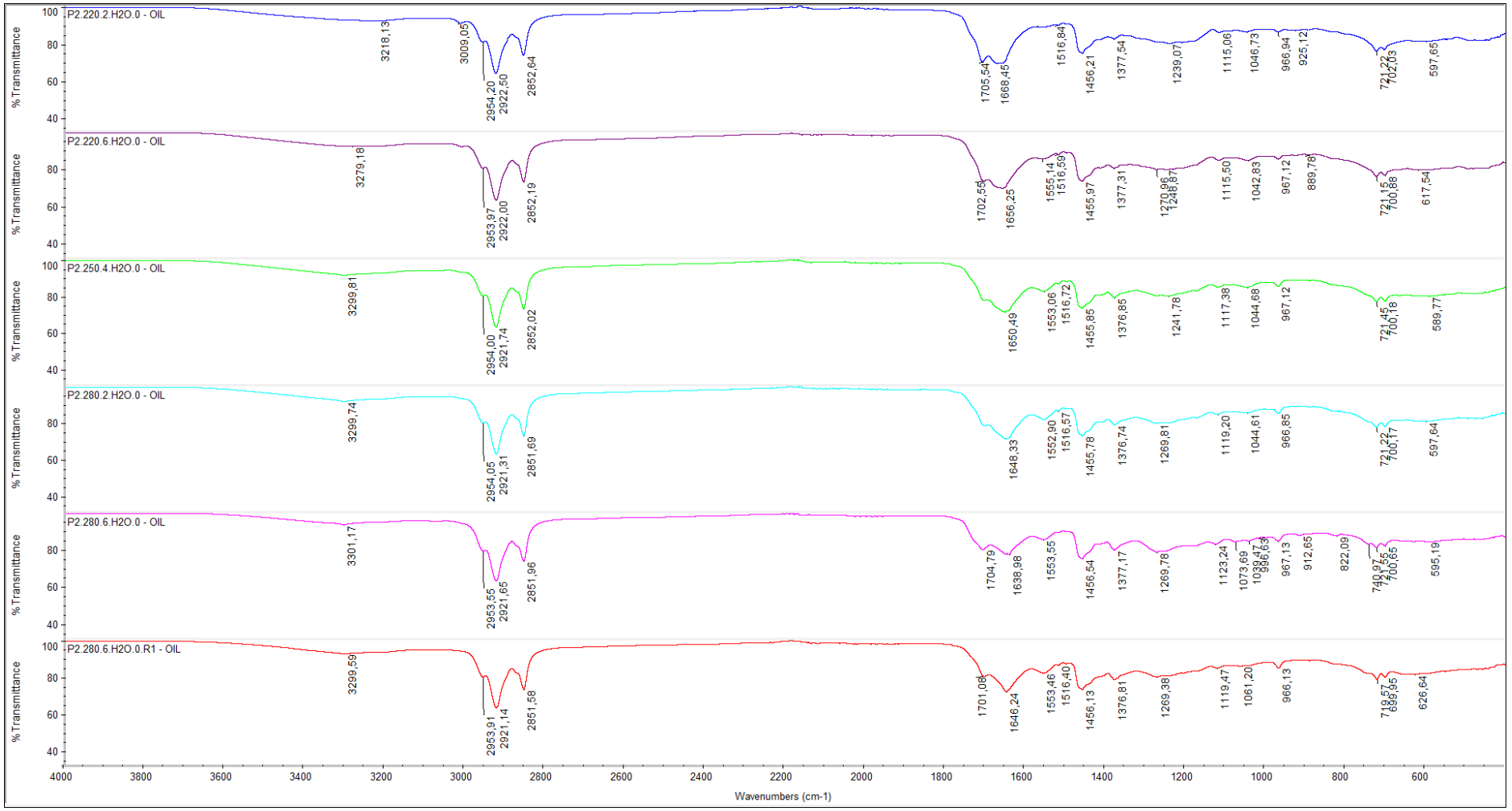

Figure B.5-d: Comparison of the IR spectra for all bio-oil samples in P2 with FA=0.

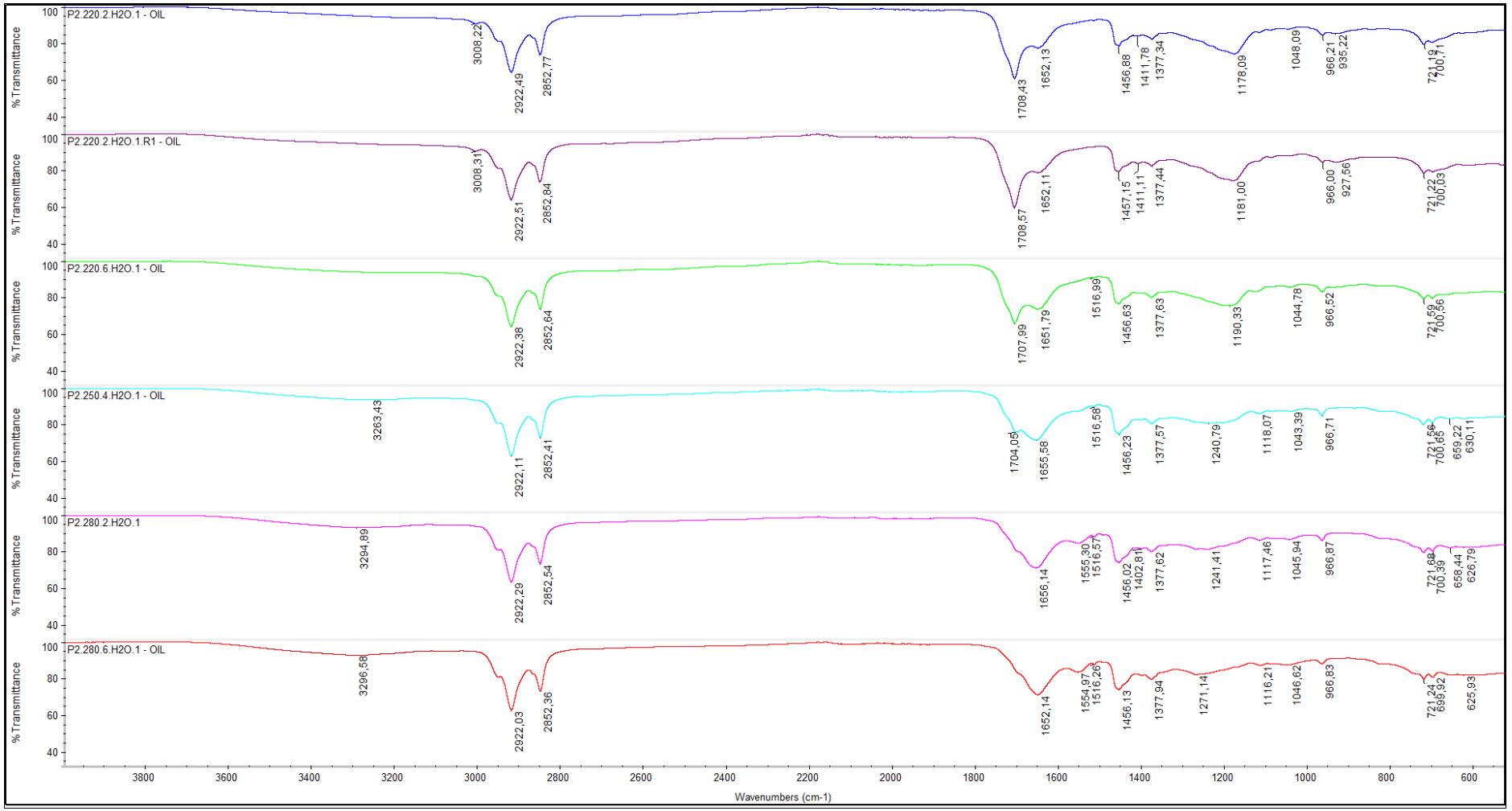

Figure B.5-e: Comparison of the IR spectra for all bio-oil samples in P2 with FA=1.

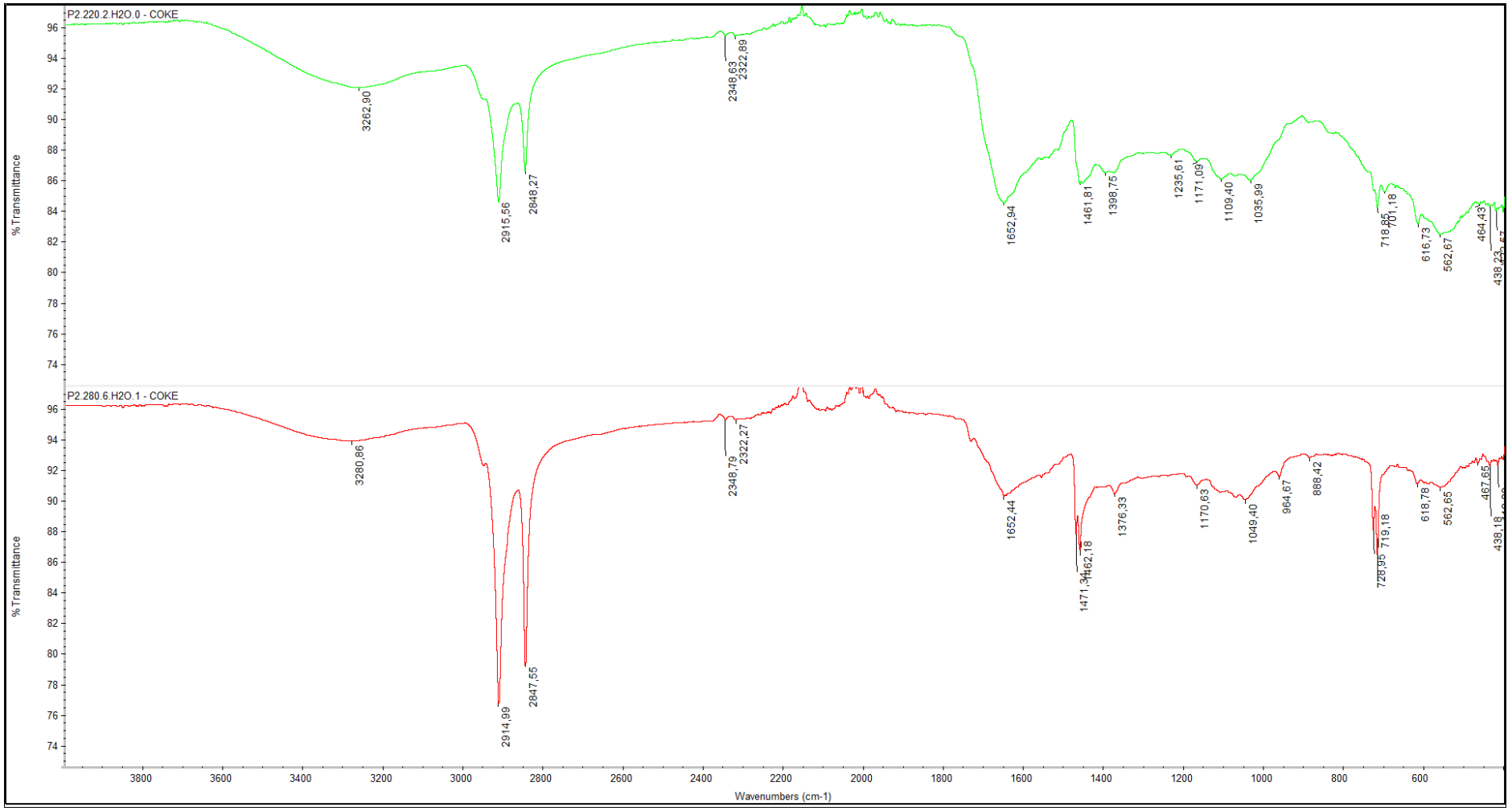

Figure B.5-f: Comparison of the IR spectra for coke samples in P2 with all high levels [(+)(+)(+)] and all low levels [(-)(-)(-)].

APPENDIX C – PILOT SERIES 3

C.1 SOXHLET EXTRACTION

Table C.1-1: Overview of yields from Soxhlet extractions performed on the algal feedstock.

Experiment	1	2
Feedstock [g]	40.1308	40.264
TS MV. [%][a]	26.12	26.12
TS [g]	10.482	10.517
DCM [mL]	500	700
Extraction time [h]	144	258

[a] Based on average TS [%] value calculated in proximate analysis for "Feedstock 1". See Table 4.4-1.

C.2 HTL

Table C.2-1: HTL workup for Pilot Series 3.

Experiment	Feedstock			Wv[b] [g]	Inorganic (dw.) [g]	Water [g]	Formic acid [g]	Total [g]
	Dry feedstock [g]	Water [g]	Total feedstock [g]					
P3.280.2.H2O.0	1.05	2.97	4.02	0.936	0.0638	1.99	0.00	6.01
P3.380.2.H2O.1	1.04	2.97	4.01	0.927	0.0728	1.00	1.23	6.24
P3.280.6.H2O.1	1.04	2.97	4.01	0.927	0.0728	0.99	1.20	6.20
P3.380.6.H20.0	1.05	2.98	4.03	0.936	0.0638	2.01	0.00	6.04
P3.380.6.H20.0.R1	1.04	2.97	4.01	0.927	0.0728	2.00	0.00	6.01
P3.330.4.H2O.0,5	1.04	2.97	4.01	0.927	0.0728	1.50	0.61	6.12

[b] Based on average Wv [%] value calculated in proximate analysis for "Feedstock 1". See Table 4.4-1.

C.3 PRINCIPAL COMPONENT ANALYSIS AND REGRESSION

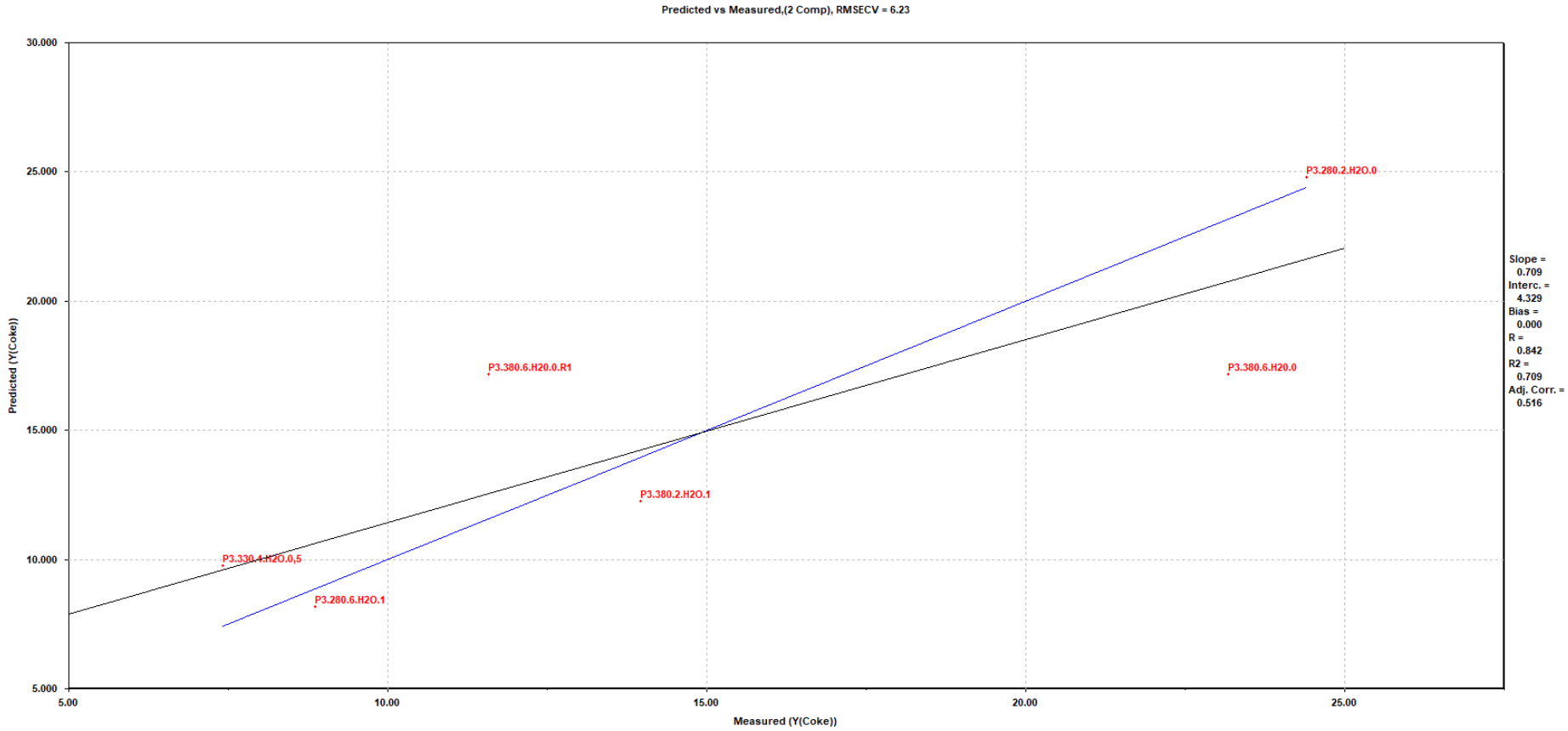

Figure C.3-a: PLS plot of predicted vs measured values for coke yields in Pilot Series 3. All experiments.

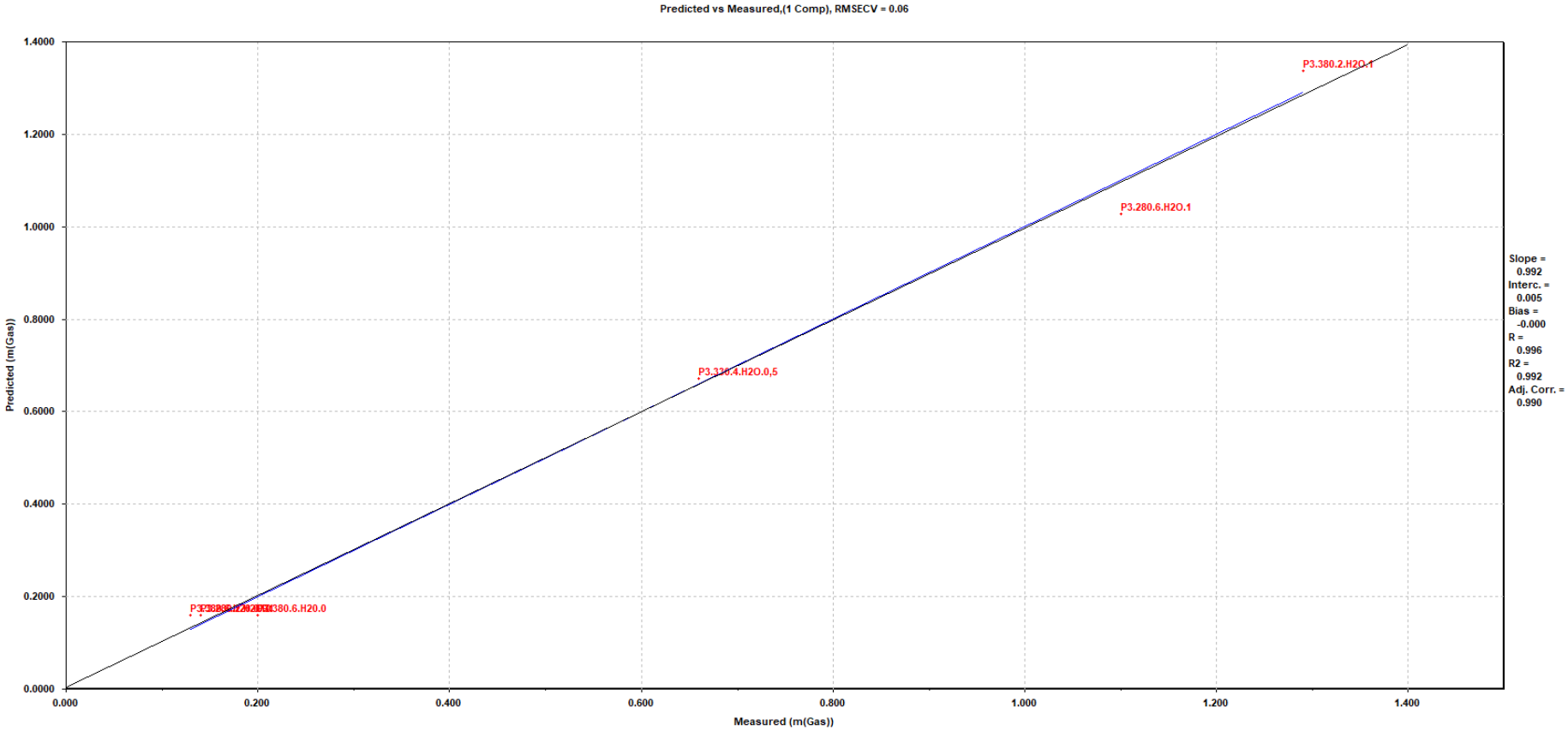

Figure C.3-b: PLS plot of predicted vs measured values for gas yields in Pilot Series 3. All experiments.

C.4 GAS CHROMATOGRAPHY – MASS SPECTROSCOPY

Table C.4-1: Preparation of GC-MS, Pilot series 3.

	Experiment	P3.280.2.H2O.0	P3.380.2.H2O.1	P3.280.6.H2O.1	P3.380.6.H20.0	P3.330.4.H2O.0,5	P3.380.6.H20.0.R1	IS
Preparation of Solvent A1	**Benzoic acid [g]**	0.2315	0.2315	0.2315	0.2315	0.2315	0.2315	0.2315
	Dodecane [mL]	0.300	0.300	0.300	0.300	0.300	0.300	0.300
	EtOAc [mL]	100	100	100	100	100	100	100
	Benzoic acid [mg/mL]	2.32	2.32	2.32	2.32	2.32	2.32	2.32
	Dodecane [mg/mL]	2.25	2.25	2.25	2.25	2.25	2.25	2.25
Preparation of Solvent A2	**Solvent A1 [mL]**	3.50	3.50	3.50	3.50	3.50	3.50	3.50
	EtOAc [mL]	100	100	100	100	100	100	100
	Benzoic acid [mg/mL]	0.0810	0.0810	0.0810	0.0810	0.0810	0.0810	0.0810
	Dodecane [mg/mL]	0.0788	0.0788	0.0788	0.0788	0.0788	0.0788	0.0788
Preparation of Oil solution	**Oil sample [mg]**	7.6	7.6	7.6	7.5	7.5	7.6	-
	Solvent A2 [mL]	3.00	3.00	3.00	3.00	3.00	3.00	3.00
	Oil [mg/mL]	2.5	2.5	2.5	2.5	2.5	2.5	-
	Benzoic acid [mg/mL]	0.0810	0.0810	0.0810	0.0810	0.0810	0.0810	0.0810
	Dodecane [mg/mL]	0.0788	0.0788	0.0788	0.0788	0.0788	0.0788	0.0788
Preparation of Derivatized oil solution	**Oil solution [mL]**	1.00	1.00	1.00	1.00	1.00	1.00	1.00
	Pyridine [mL]	0.150	0.150	0.150	0.150	0.150	0.150	0.150
	BSTFA [mL]	0.150	0.150	0.150	0.150	0.150	0.150	0.150
	Oil [mg/mL]	2.0	2.0	2.0	1.9	1.9	2.0	-
	Benzoic acid [mg/mL]	0.0623	0.0623	0.0623	0.0623	0.0623	0.0623	0.0623
	Dodecane [mg/mL]	0.0606	0.0606	0.0606	0.0606	0.0606	0.0606	0.0606
Preparation of GC-MS Oil sample	**Derivatized oil solution [mL]**	0.700	0.700	0.700	0.700	0.700	0.700	0.700
	Pentane [mL]	0.700	0.700	0.700	0.700	0.700	0.700	0.700
	Oil [mg/mL]	0.97	0.97	0.97	0.96	0.96	0.97	-
	Benzoic acid [mg/mL]	0.0312	0.0312	0.0312	0.0312	0.0312	0.0312	0.0312
	Dodecane [mg/mL]	0.0303	0.0303	0.0303	0.0303	0.0303	0.0303	0.0303

Table C.4-2: Semi-quantitative analysis of GC-MS bio-oil samples for Pilot Series 3.

	Designation	N-Trimethylsilyl-2-pyrrolidinone	Pentanoic acid, 4-oxo-, trimethylsilyl ester	Dodecane	3-Ethylphenol, trimethylsilyl ether	Benzoic acid trimethylsilyl ester	Glycerol, tris(trimethylsilyl) ether	Butanedioic acid, bis(trimethylsilyl)ester	Butanedioic acid, methyl-, bis(trimethylsilyl) ester	L-proline, 5-oxo-1-(trimethylsilyl)-,trimethylsilyl ester	4-Hydroxyphenyl ethanol, di-TMS	Tetradecanoic acid, trimethylsilyl ester	Palmitelaidic acid, trimethylsilyl ester	Hexadecanoic acid, trimethylsilyl ester	Octadecanoic acid, trimethylsilyl ester	Hexadecanoic acid, 2,3-bis[(trimethylsilyl)oxy]propyl ester	Octadecanoic acid, 2,3-bis[(trimethylsilyl)oxy]propyl ester
	Formula	**C7H15NOSi**	**C8H16O3Si**	**C12H26**	**C11H18OSi**	**C1014O2Si**	**C12H32O3Si3**	**C10H22O4Si2**	**C11H24O4Si2**	**C11H23NO3Si2**	**C14H26O2Si2**	**C17H36O2Si**	**C19H38O2Si**	**C19H40O2Si**	**C21H44O2Si**	**C25H54O4Si2**	**C27H58O4Si2**
P3.280.2.H2O.0	**Ret. [min]**		9.089	10.027		10.758		11.724	11.895	14.480		17.910	19.242	19.365		22.031	22.865
	Peak area		57759964	97764439		14160796 4		19118496 8	51580628	21529721 5		10188216 9	12084837 4	43124470 6		54433338	39663146
	C_A [mg/mL] (IS:1)[a]		0.0179	0.0303		0.0439		0.0592	0.0160	0.0667		0.0316	0.0374	0.134		0.0169	0.0123
	C_A [mg/mL] (IS: 2)[b]		0.0127	0.0215		0.0312		0.0421	0.0114	0.0474		0.0224	0.0266	0.0949		0.0120	0.00873
P3.380.2.H2O.1	**Ret. [min]**			10.028	10.638	10.758						17.908	19.242	19.361		22.030	
	Peak area			10386276 5	15568716 4	14143139 9						7498559 3	15137567 7	36152865 8		33577744	
	C_A [mg/mL] (IS:1)[a]			0.0303	0.0454	0.0412						0.0219	0.0441	0.105		0.00979	
	C_A [mg/mL] (IS: 2)[b]			0.0229	0.0343	0.0312						0.0165	0.0334	0.0797		0.00740	
P3.280.6.H2O.1	**Ret. [min]**			10.027		10.757	11.249	11.720		14.475		17.908	19.242	19.357		22.030	
	Peak area			87003014		14107004 6	51485963	96582501		11234093 9		5432566 5	15956432 5	30027580 0		35760378	
	C_A [mg/mL] (IS:1)[a]			0.0303		0.0491	0.0179	0.0336		0.0391		0.0189	0.0555	0.105		0.0124	
	C_A [mg/mL] (IS: 2)[b]			0.0192		0.0312	0.0114	0.0213		0.0248		0.0120	0.0352	0.0663		0.00790	

[a, b] Based on the relationship between the peak area ratio and concentration ratio of the target component and IS (1: Dodecane, 2: Benzoic acid) in the chromatogram.

Table C.4-2: Semi-quantitative analysis of GC-MS bio-oil samples for Pilot Series 3. Table continued.

	Designation	N-Trimethylsilyl-2-pyrrolidinone	Pentanoic acid, 4-oxo-, trimethylsilyl ester	Dodecane	3-Ethylphenol, trimethylsilyl ether	Benzoic acid trimethylsilyl ester	Glycerol, tris(trimethylsilyl) ether	Butanedioic acid, bis(trimethylsilyl)ester	Butanedioic acid, methyl-, bis(trimethylsilyl) ester	L-proline, 5-oxo-1-(trimethylsilyl)-,trimethylsilyl ester	4-Hydroxyphenylethanol, di-TMS	Tetradecanoic acid, trimethylsilyl ester	Palmitelaidic acid, trimethylsilyl ester	Hexadecanoic acid, trimethylsilyl ester	Octadecanoic acid, trimethylsilyl ester	Hexadecanoic acid, 2,3-bis[(trimethylsilyl)oxy] propyl ester	Octadecanoic acid, 2,3-bis[(trimethylsilyl)oxy]propyl ester
	Formula	**C7H15NOSi**	**C8H16O3Si**	**C12H26**	**C11H18OSi**	**C1014O2Si**	**C12H32O3Si3**	**C10H22O4Si2**	**C11H24O4Si2**	**C11H23NO3Si2**	**C14H26O2Si2**	**C17H36O2Si**	**C19H38O2Si**	**C19H40O2Si**	**C21H44O2Si**	**C25H54O4Si2**	**C27H58O4Si2**
P3.380.6.H20.0.R1	**Ret. [min]**	9.247		10.028	10.638	10.758						17.908		19.359		22.030	
	Peak area	83007515		109234467	40765772	14259813 4						67965133		31933744 2		42970812	
	C_A [mg/mL] (IS:1)[a]	0.0230		0.0303	0.0113	0.0395						0.0188		0.0885		0.0119	
	C_A [mg/mL] (IS: 2)[b]	0.0181		0.0239	0.00891	0.0312						0.0149		0.0698		0.00939	
P3.330.4.H2O.0,5	**Ret. [min]**			10.027	10.637	10.758	11.250				15.018	17.908	19.257	19.358	20.458	22.030	
	Peak area			93551483	12852351 5	13925602 2	80309973				79007560	51520309	16460821 8	30382317 1	61807922	50658808	
	C_A [mg/mL] (IS:1)[a]			0.0303	0.0416	0.0451	0.0260				0.0256	0.0167	0.0533	0.0984	0.0200	0.0164	
	C_A [mg/mL] (IS: 2)[b]			0.0209	0.0288	0.0312	0.0180				0.0177	0.0115	0.0368	0.0680	0.0138	0.0113	

[a, b] Based on the relationship between the peak area ratio and concentration ratio of the target component and IS (1: Dodecane, 2: Benzoic acid) in the chromatogram.

Table C.4-2: Semi-quantitative analysis of Soxhlet extract samples from Soxhlet extraction. Table continued.

	Designation	**Dodecane**	**Benzoic acid trimethylsilyl ester**	**Glycerol, tris(trimethylsilyl) ether**	**Tetradecanoic acid, trimethylsilyl ester**	**Ethyl 9-hexadecenoate**	**9-Hexadecanoic acid, trimethylsilyl ester**	**Hexadecanoic acid, trimethylsilyl ester**	**9,12-Octadecanoic acid *(Z,Z)*-, trimethylsilyl ester**	**Arachidonic acid, trimethylsilyl**	***cis*-5,8,11,14,17-Eicosapentaenoic acid, trimethylsilyl ester**	**Hexadecanoic acid, 2,3-bis[(trimethylsilyl)oxy] propyl ester**
	Formula	C12H26	C1014O2Si	C12H32O3Si3	C17H36O2Si	C18H43O2	C19H40O2Si	C19H40O2Si	C21H40O2Si	C23H40O2Si	C23H38O2Si2	C25H54O4Si2
SE1[c]	**Ret. [min]**	10.025	10.754	11.248	17.908	18.866	19.241	19.361	20.312	21.101	21.145	22.029
	Peak area	86002882	129091421	154363913	120364792	41041467	438584485	361292636	35547696	55754930	275433508	44696947
	C_A [mg/mL] (IS:1)[a]	0.0303	0.0455	0.0544	0.0424	0.0145	0.155	0.127	0.0125	0.0196	0.0970	0.0157
	C_A [mg/mL] (IS: 2)[b]	0.0208	0.0312	0.0373	0.0291	0.00991	0.106	0.0872	0.00858	0.0135	0.0665	0.0108
SE2[d]	**Ret. [min]**	10.025	10.754	11.247	17.909	18.558	19.243	19.365	20.311	21.102	21.147	22.029
	Peak area	88460043	131197670	88831489	140922057	81280132	469688860	407833433	38500178	72004142	305198768	32116133
	C_A [mg/mL] (IS:1)[a]	0.0303	0.0449	0.0304	0.0483	0.0278	0.161	0.140	0.0132	0.0247	0.105	0.0110
	C_A [mg/mL] (IS: 2)[b]	0.0210	0.0312	0.0211	0.0335	0.0193	0.112	0.0969	0.00914	0.0171	0.0725	0.00763

[a, b] Based on the relationship between the peak area ratio and concentration ratio of the target component and IS (1: Dodecane, 2: Benzoic acid) in the chromatogram.
[c,d] SE1 and SE2 stand for Soxhlet extract 1 and 2, respectively.

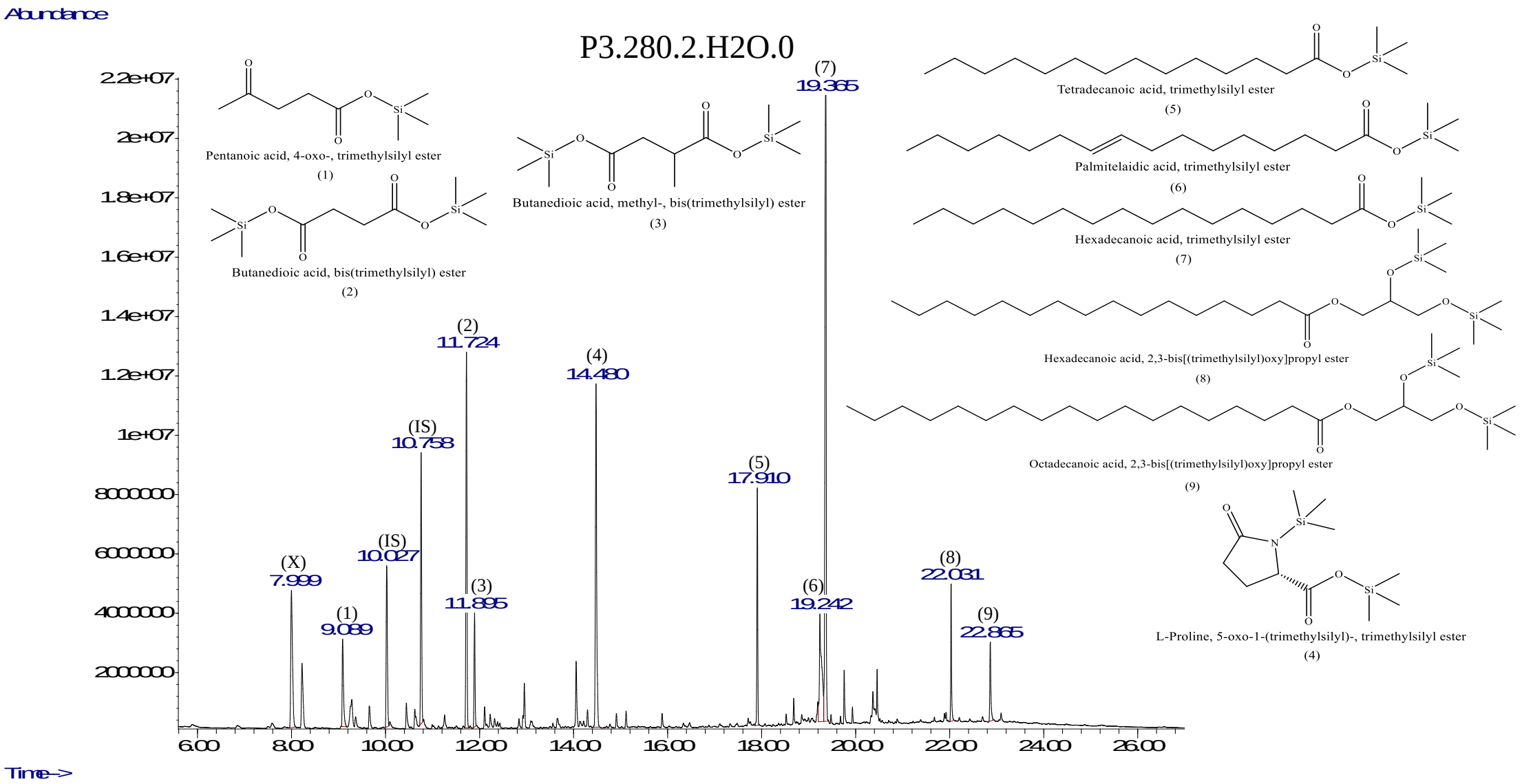
Abundance
P3.280.2.H2O.0
Pentanoic acid, 4-oxo-, trimethylsilyl ester
(1)
Butanedioic acid, bis(trimethylsilyl) ester
(2)
Butanedioic acid, methyl-, bis(trimethylsilyl) ester
(3)
Tetradecanoic acid, trimethylsilyl ester
(5)
Palmitelaidic acid, trimethylsilyl ester
(6)
Hexadecanoic acid, trimethylsilyl ester
(7)
Hexadecanoic acid, 2,3-bis[(trimethylsilyl)oxy]propyl ester
(8)
Octadecanoic acid, 2,3-bis[(trimethylsilyl)oxy]propyl ester
(9)
L-Proline, 5-oxo-1-(trimethylsilyl)-, trimethylsilyl ester
(4)
(X) 7.999
(1) 9.089
(IS) 10.027
(IS) 10.758
(2) 11.724
(3) 11.895
(4) 14.480
(5) 17.910
(6) 19.242
(7) 19.365
(8) 22.031
(9) 22.865
2.2e+07
2e+07
1.8e+07
1.6e+07
1.4e+07
1.2e+07
1e+07
8000000
6000000
4000000
2000000
6.00
8.00
10.00
12.00
14.00
16.00
18.00
20.00
22.00
24.00
26.00
Time-->

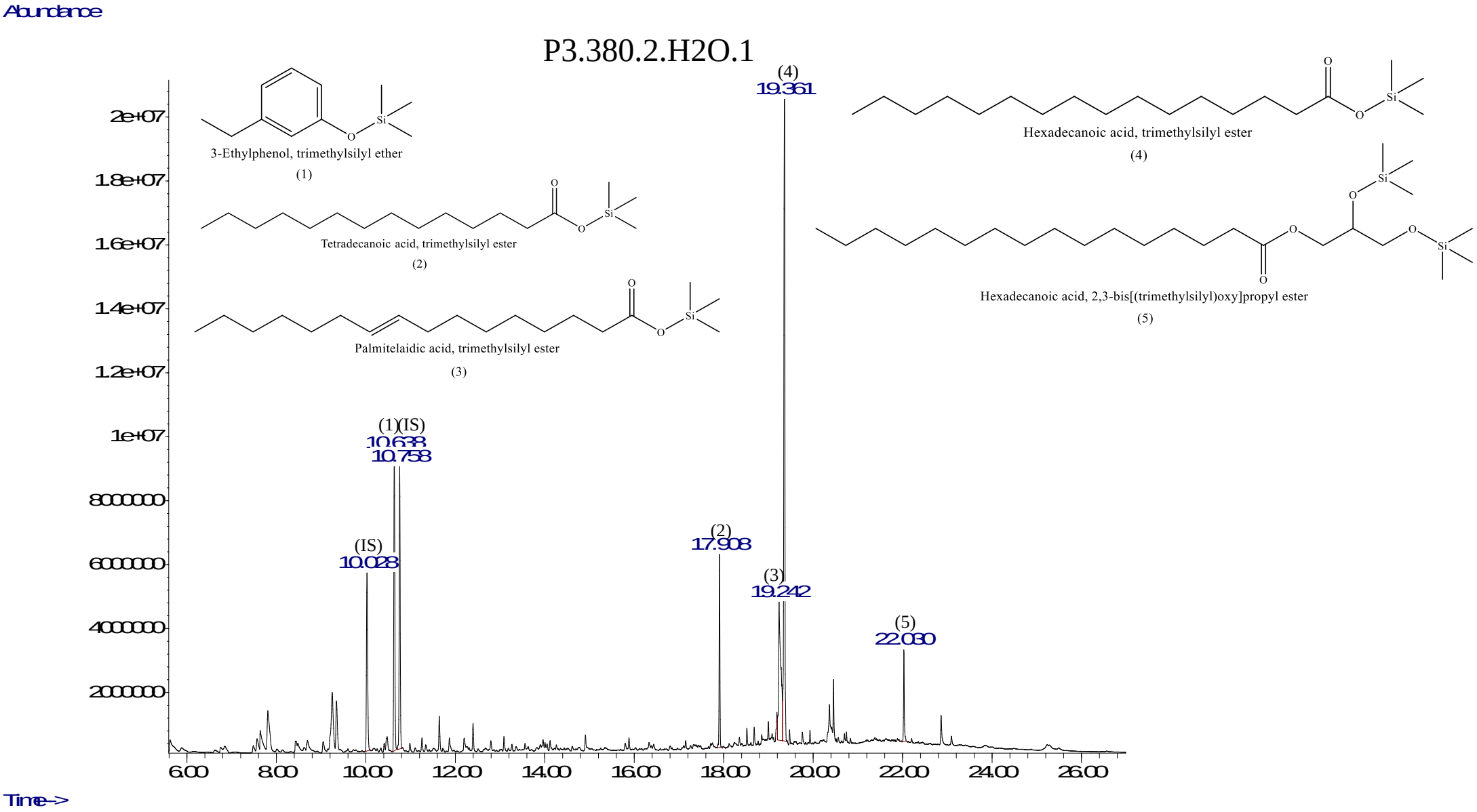
Abundance
P3.380.2.H2O.1
3-Ethylphenol, trimethylsilyl ether
(1)
Tetradecanoic acid, trimethylsilyl ester
(2)
Palmitelaidic acid, trimethylsilyl ester
(3)
(4)
19.361
Hexadecanoic acid, trimethylsilyl ester
(4)
Hexadecanoic acid, 2,3-bis[(trimethylsilyl)oxy]propyl ester
(5)
(1)(IS)
10.638
10.758
(IS)
10.028
(2)
17.908
(3)
19.242
(5)
22.030
2e+07
1.8e+07
1.6e+07
1.4e+07
1.2e+07
1e+07
8000000
6000000
4000000
2000000
6.00
8.00
10.00
12.00
14.00
16.00
18.00
20.00
22.00
24.00
26.00
Time->

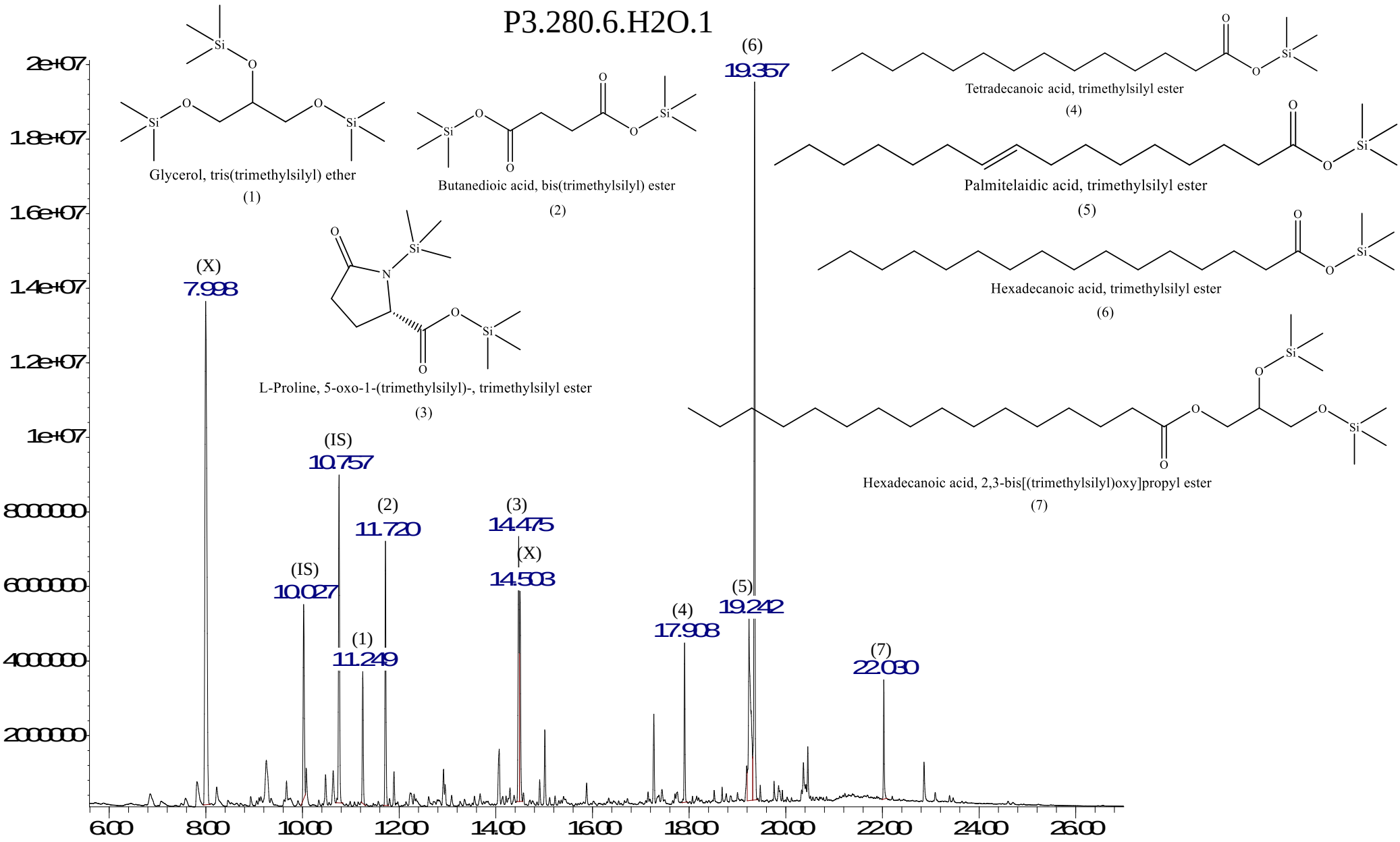
Abundance
P3.280.6.H2O.1
Glycerol, tris(trimethylsilyl) ether
(1)
Butanedioic acid, bis(trimethylsilyl) ester
(2)
L-Proline, 5-oxo-1-(trimethylsilyl)-, trimethylsilyl ester
(3)
Tetradecanoic acid, trimethylsilyl ester
(4)
Palmitelaidic acid, trimethylsilyl ester
(5)
Hexadecanoic acid, trimethylsilyl ester
(6)
Hexadecanoic acid, 2,3-bis[(trimethylsilyl)oxy]propyl ester
(7)
(X) 7.998
(IS) 10.027
(IS) 10.757
(1) 11.249
(2) 11.720
(3) 14.475
(X) 14.503
(4) 17.908
(5) 19.242
(6) 19.357
(7) 22.030
2e+07
1.8e+07
1.6e+07
1.4e+07
1.2e+07
1e+07
800000
600000
400000
200000
6.00
8.00
10.00
12.00
14.00
16.00
18.00
20.00
22.00
24.00
26.00
Time->
170

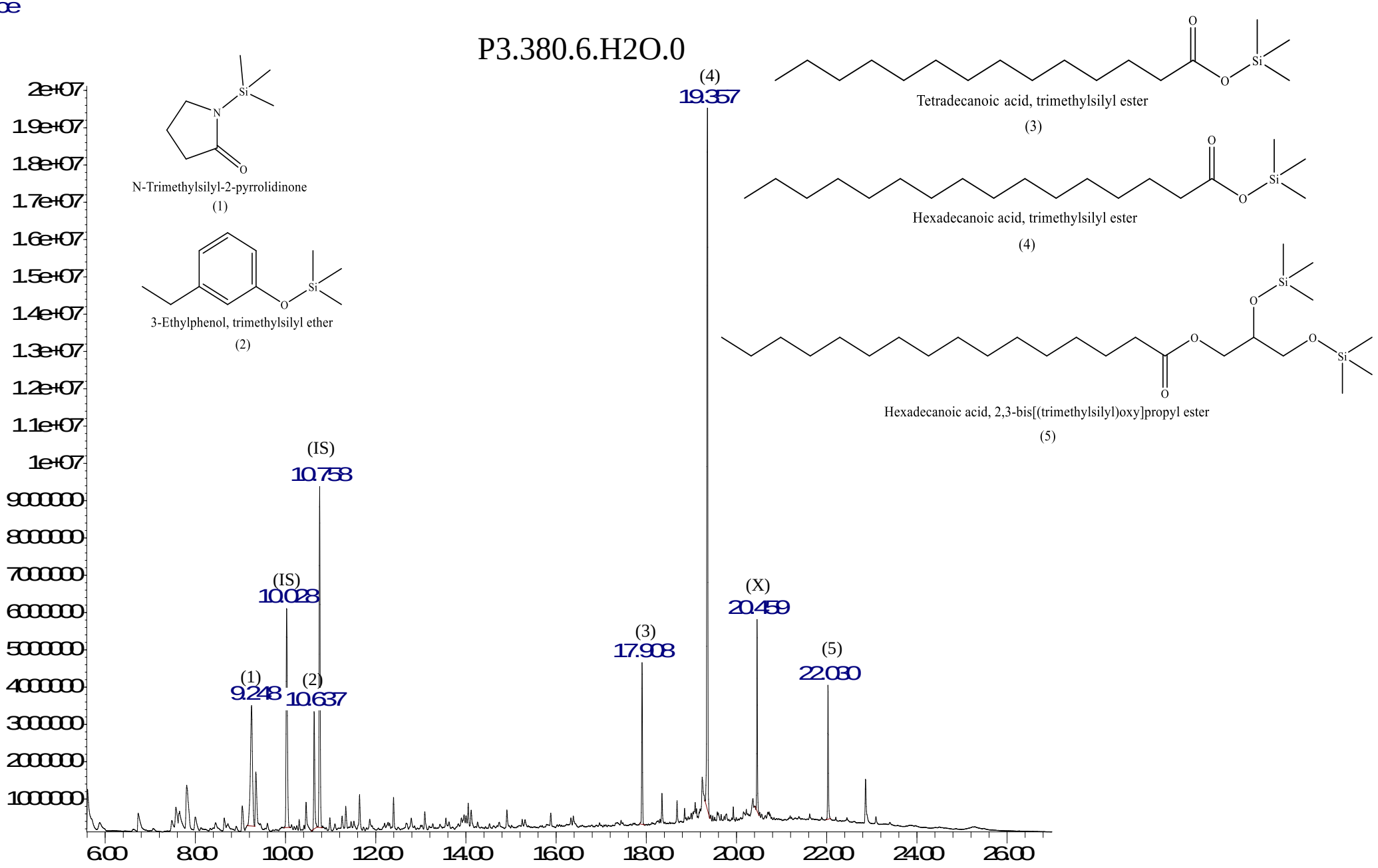
Abundance
P3.380.6.H2O.0
N-Trimethylsilyl-2-pyrrolidinone
(1)
3-Ethylphenol, trimethylsilyl ether
(2)
Tetradecanoic acid, trimethylsilyl ester
(3)
Hexadecanoic acid, trimethylsilyl ester
(4)
Hexadecanoic acid, 2,3-bis[(trimethylsilyl)oxy]propyl ester
(5)
(4)
19.357
(IS)
10.758
(IS)
10.028
(X)
20.459
(3)
17.908
(5)
22.030
(1)
9.248
(2)
10.637
2e+07
1.9e+07
1.8e+07
1.7e+07
1.6e+07
1.5e+07
1.4e+07
1.3e+07
1.2e+07
1.1e+07
1e+07
9000000
8000000
7000000
6000000
5000000
4000000
3000000
2000000
1000000
6.00
8.00
10.00
12.00
14.00
16.00
18.00
20.00
22.00
24.00
26.00
Time-->

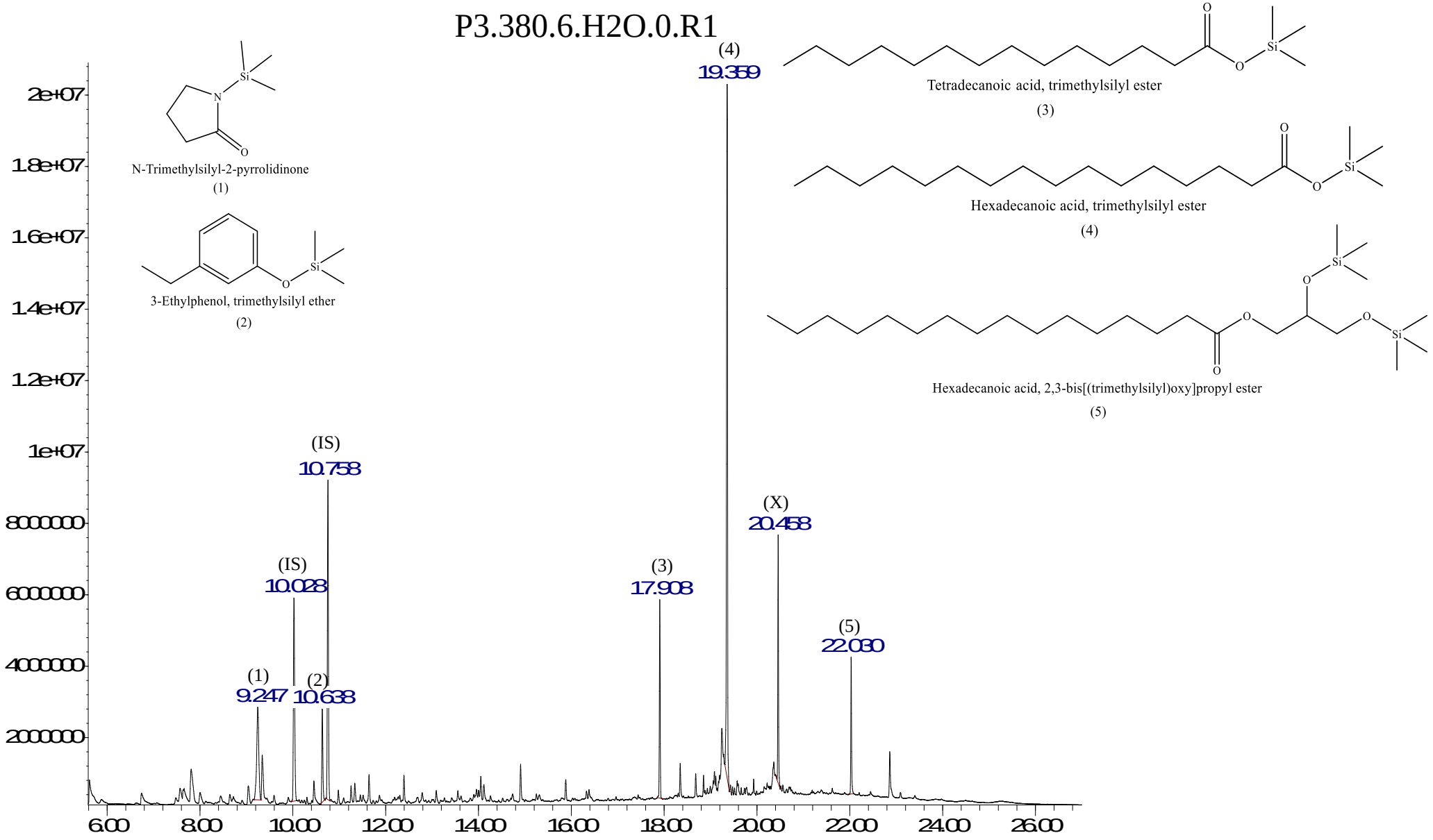
Abundance
P3.380.6.H2O.0.R1
N-Trimethylsilyl-2-pyrrolidinone
(1)
3-Ethylphenol, trimethylsilyl ether
(2)
Tetradecanoic acid, trimethylsilyl ester
(3)
Hexadecanoic acid, trimethylsilyl ester
(4)
Hexadecanoic acid, 2,3-bis[(trimethylsilyl)oxy]propyl ester
(5)
(4)
19.359
(IS)
10.758
(IS)
10.028
(X)
20.458
(3)
17.908
(5)
22.030
(1)
9.247
(2)
10.638
2e+07
1.8e+07
1.6e+07
1.4e+07
1.2e+07
1e+07
8000000
6000000
4000000
2000000
6.00
8.00
10.00
12.00
14.00
16.00
18.00
20.00
22.00
24.00
26.00
Time->

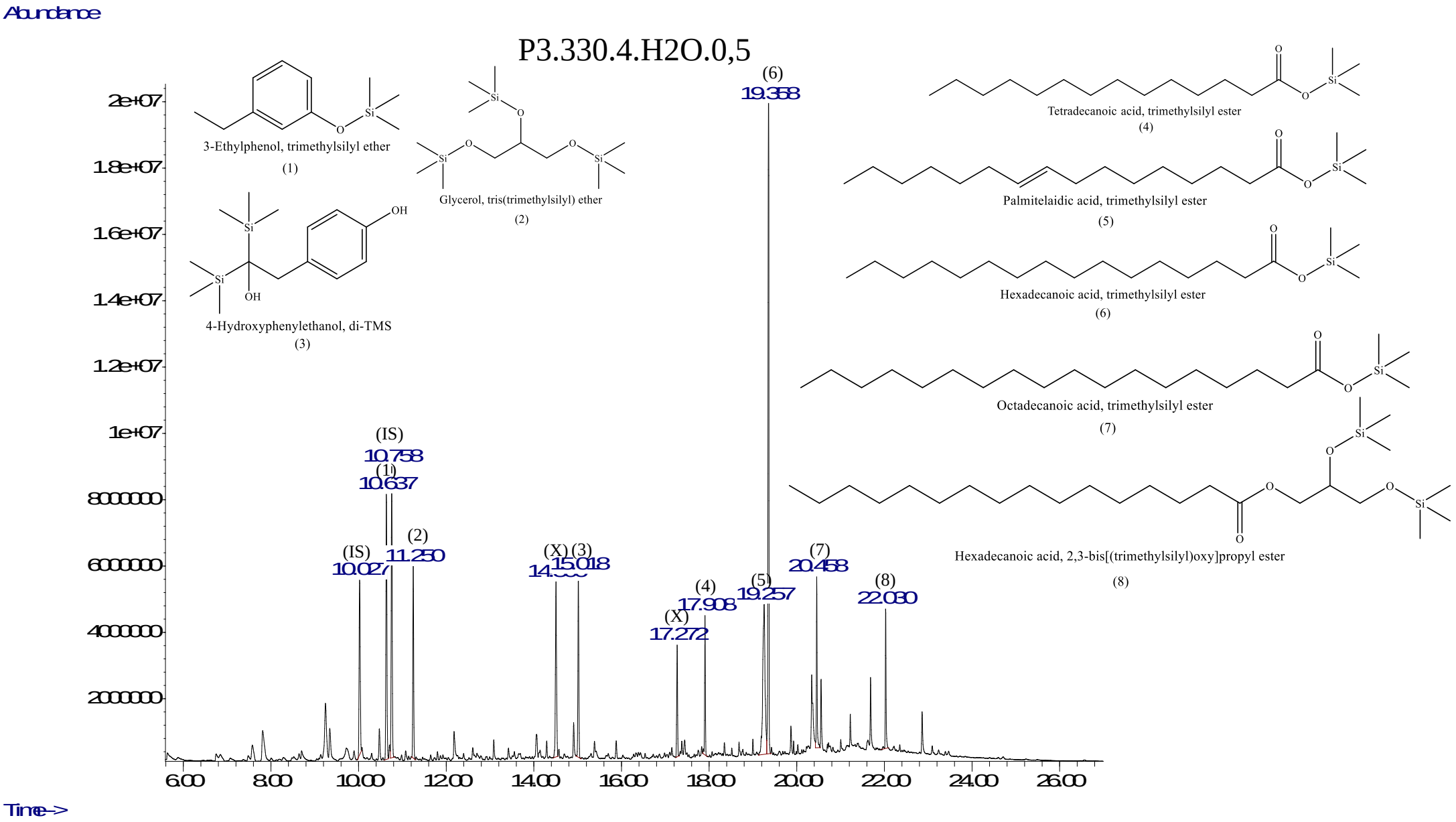
Abundance
P3.330.4.H2O.0,5
3-Ethylphenol, trimethylsilyl ether
(1)
Glycerol, tris(trimethylsilyl) ether
(2)
4-Hydroxyphenylethanol, di-TMS
(3)
Tetradecanoic acid, trimethylsilyl ester
(4)
Palmitelaidic acid, trimethylsilyl ester
(5)
Hexadecanoic acid, trimethylsilyl ester
(6)
Octadecanoic acid, trimethylsilyl ester
(7)
Hexadecanoic acid, 2,3-bis[(trimethylsilyl)oxy]propyl ester
(8)
(IS)
10.758
(1)
10.637
(IS)
10.027
(2)
11.250
(X)
17.272
(4)
17.908
(X) (3)
14.
15.018
(5)
19.257
(6)
19.358
(7)
20.458
(8)
22.080
2e+07
1.8e+07
1.6e+07
1.4e+07
1.2e+07
1e+07
8000000
6000000
4000000
2000000
6.00
8.00
10.00
12.00
14.00
16.00
18.00
20.00
22.00
24.00
26.00
Time->

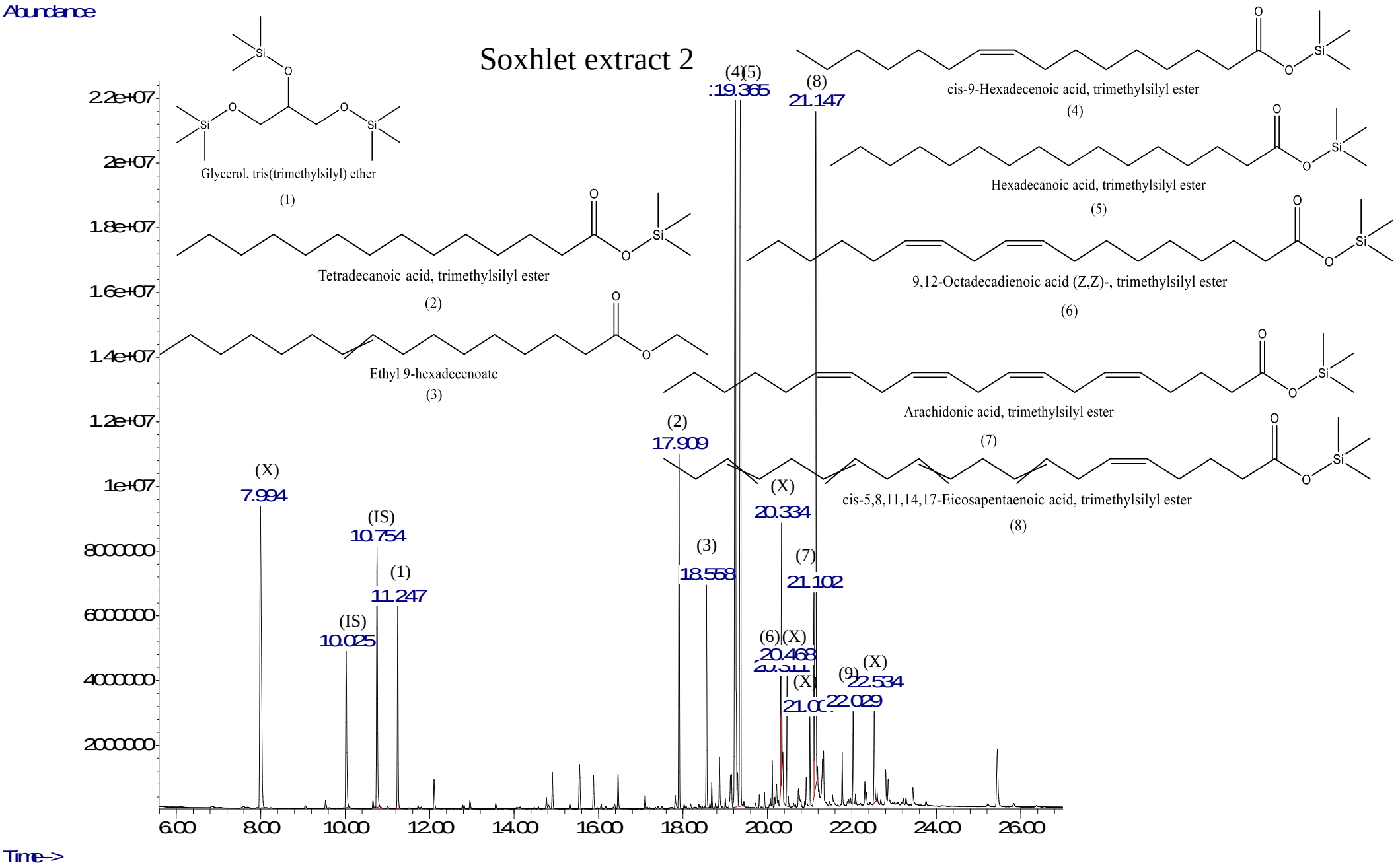
Soxhlet extract 2
Abundance
Time->
Glycerol, tris(trimethylsilyl) ether
(1)
Tetradecanoic acid, trimethylsilyl ester
(2)
Ethyl 9-hexadecenoate
(3)
cis-9-Hexadecenoic acid, trimethylsilyl ester
(4)
Hexadecanoic acid, trimethylsilyl ester
(5)
9,12-Octadecadienoic acid (Z,Z)-, trimethylsilyl ester
(6)
Arachidonic acid, trimethylsilyl ester
(7)
cis-5,8,11,14,17-Eicosapentaenoic acid, trimethylsilyl ester
(8)
(X) 7.994
(IS) 10.754
(IS) 10.025
(1) 11.247
(2) 17.909
(3) 18.558
(4)(5) 19.365
(X) 20.334
(6) 20.468
(7) 21.102
(8) 21.147
(9) 22.534
(X) 22.029
2.2e+07
2e+07
1.8e+07
1.6e+07
1.4e+07
1.2e+07
1e+07
8000000
6000000
4000000
2000000
6.00
8.00
10.00
12.00
14.00
16.00
18.00
20.00
22.00
24.00
26.00

C.5 INFRARED SPECTROSCOPY

Figure C.5-a: Comparison of the IR spectra for Feedstock residue 1 and 2 from Soxhlet extraction.

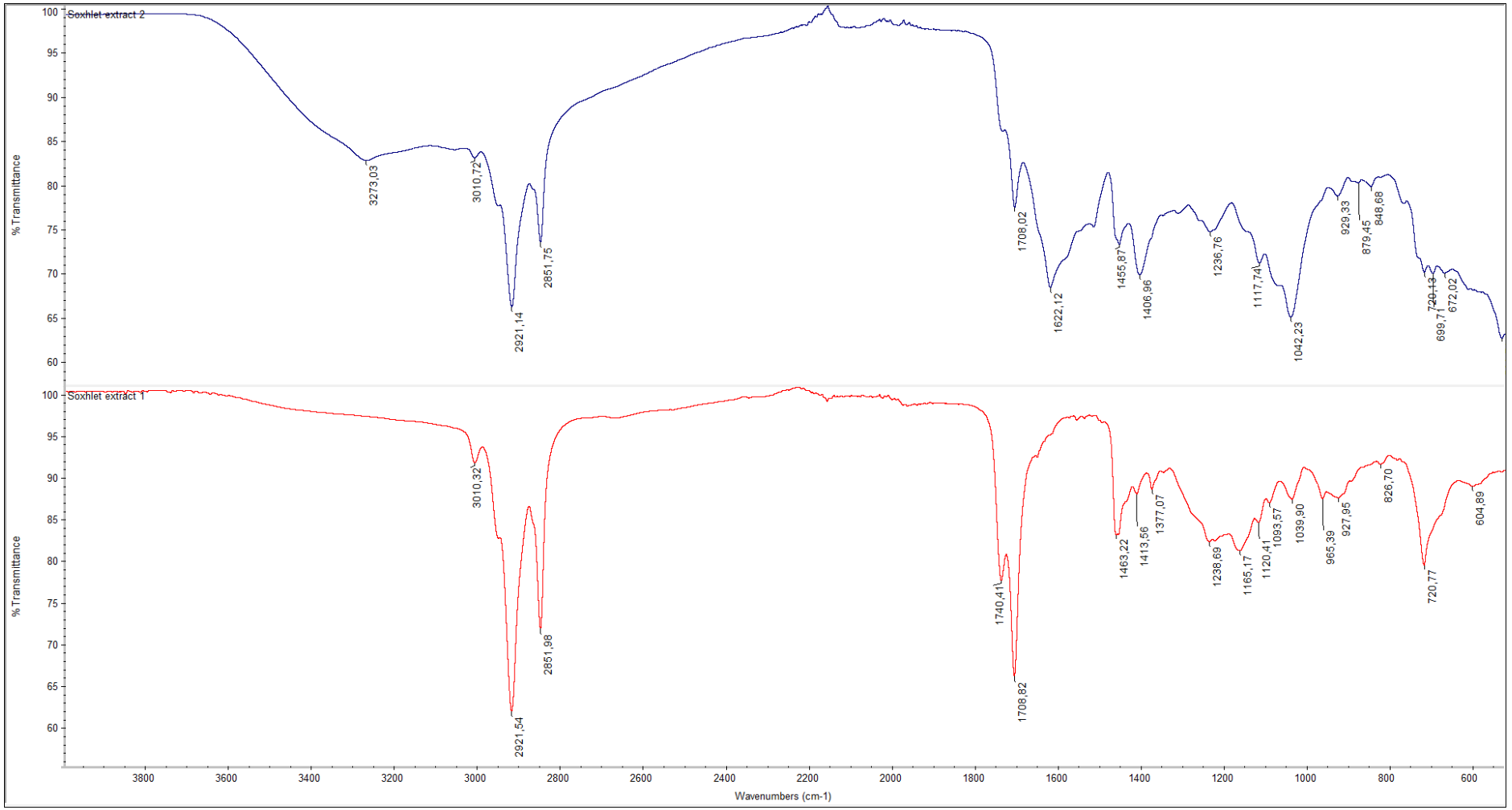

Figure C.5-b: Comparison of the IR spectra for Soxhlet extract 1 and 2 from Soxhlet extraction.

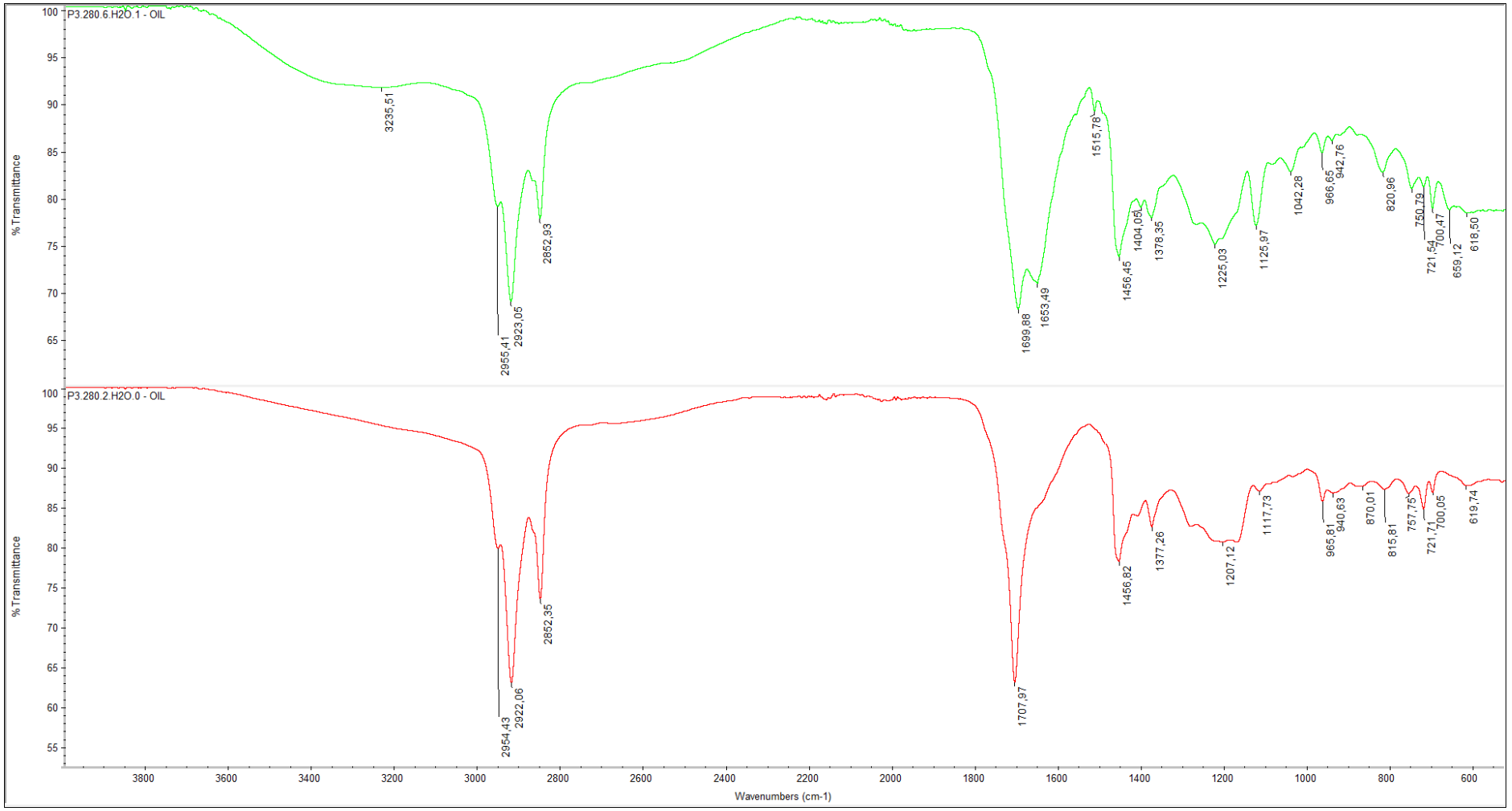

Figure C.5-c: Comparison of the IR spectra for all bio-oil samples in P3 with T=280.

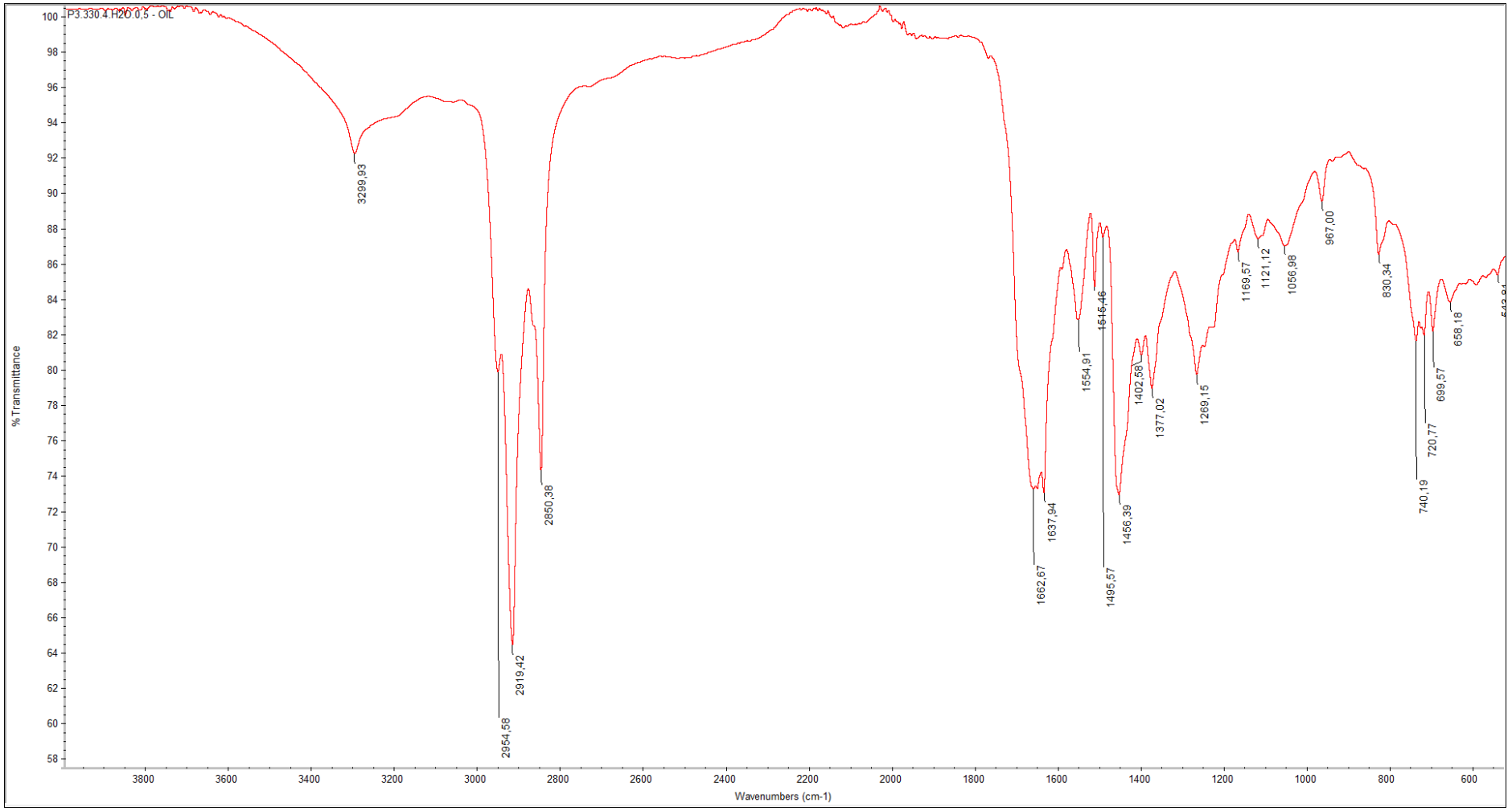

Figure C.5-d: Comparison of the IR spectra for all bio-oil samples P3 with T=250.

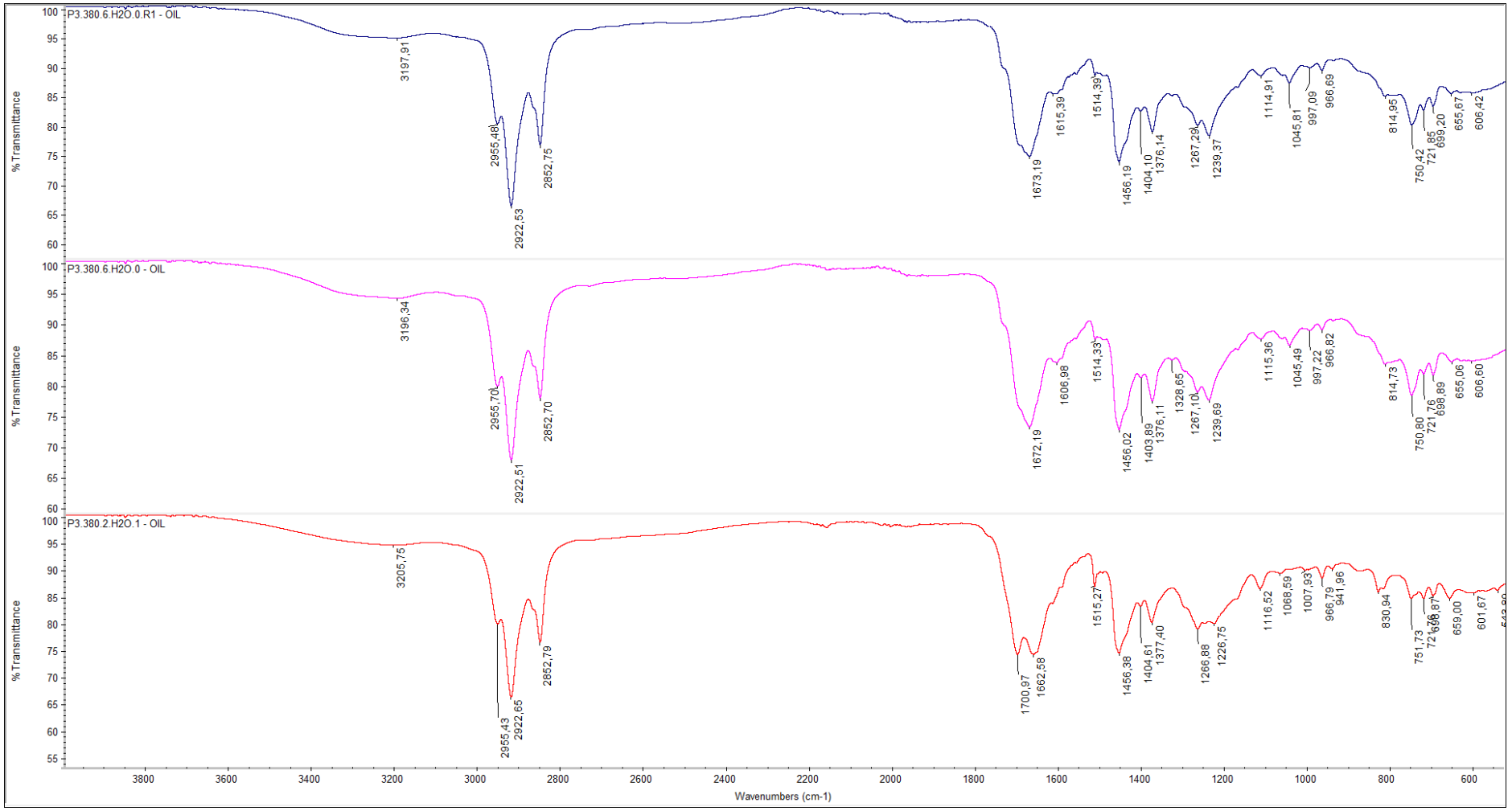

Figure C.5-e: Comparison of the IR spectra for all bio-oil samples in P3 with T=380.

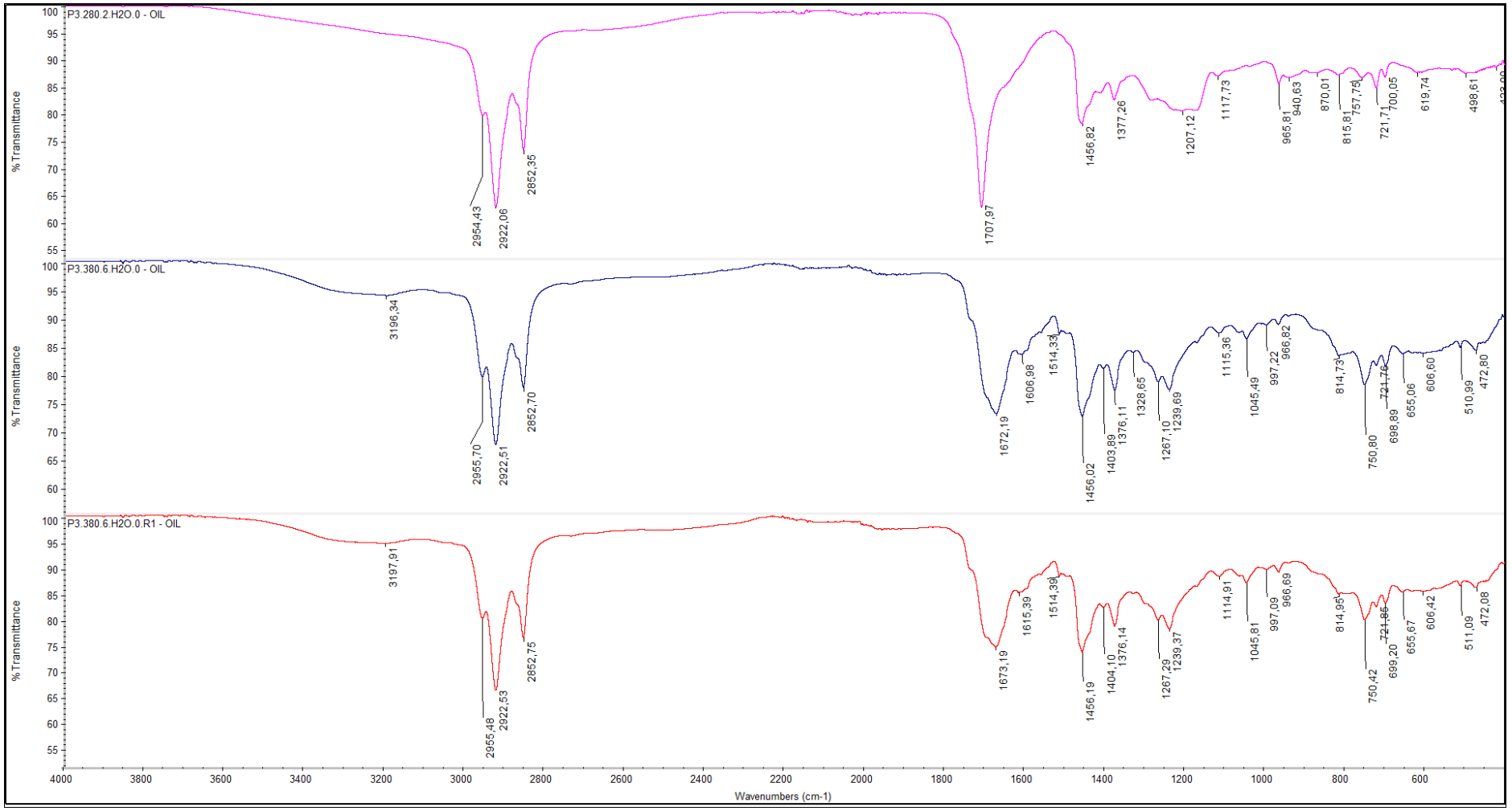

Figure C.5-f: Comparison of the IR spectra for all bio-oil samples in with FA=0.

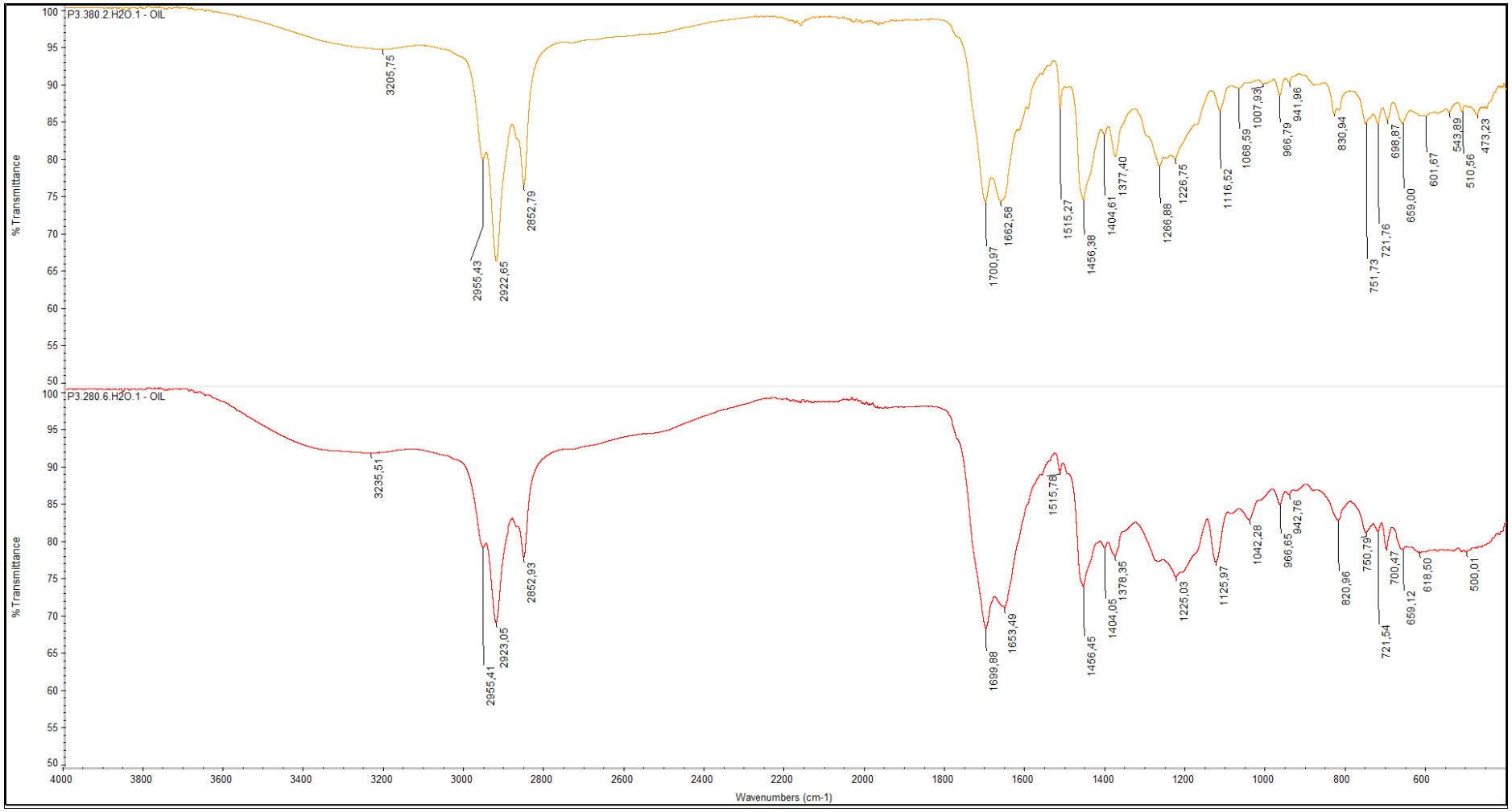

Figure C.5-g: Comparison of the IR spectra for all bio-oil samples in P2 with FA=1.